Synthesis and Coordination Chemistry of Anionic Pnictogenylborane Derivatives

DISSERTATION
ZUR ERLANGUNG DES DOKTORGRADES
DER NATURWISSENSCHAFTEN
(DR. RER. NAT.)
DER FAKULTÄT FÜR CHEMIE UND PHARMAZIE
DER UNIVERSITÄT REGENSBURG

vorgelegt von
Tobias Kahoun
aus Eichstätt
im Jahr 2019

Diese Arbeit wurde angeleitet von Prof. Dr. Manfred Scheer.

Promotionsgesuch eingereicht am: 20. August 2019

Tag der mündlichen Prüfung: 27. September 2019

Vorsitzender: Prof. Dr. Rainer Müller

Prüfungsausschuss: Prof. Dr. Manfred Scheer

Prof. Dr. Arno Pfitzner

Prof. Dr. Frank-Michael Matysik

Universität Regensburg

Eidesstattliche Erklärung

Ich erkläre hiermit an Eides statt, dass ich die vorliegende Arbeit ohne unzulässige Hilfe Dritter und ohne Benutzung anderer als der angegebenen Hilfsmittel angefertigt habe; die aus anderen Quellen direkt oder indirekt übernommenen Daten und Konzepte sind unter Angabe des Literaturzitats gekennzeichnet.

_____

Tobias Kahoun

This thesis was elaborated within the period from January 2016 until August 2019 in the Institute of Inorganic Chemistry at the University of Regensburg, under the supervision of Prof. Dr. Manfred Scheer.

Parts of this work have already been published:

C. Marquardt, T. Kahoun, A. Stauber, G. Balázs, M. Bodensteiner, A. Y. Timoshkin, M. Scheer, *Angew. Chem. Int. Ed.* **2016,** *55*, 14828-14832; *Angew. Chem.* **2016**, *128*, 15048-15052.

There is a theory which states that if ever anyone discovers exactly what the Universe is for and why it is here, it will instantly disappear and be replaced by something even more bizarre and inexplicable.

There is another theory which states that this has already happened.

Dougles Adams

For those who have
the courage and the will
to fight for their goals!

Preface

Some of the presented results have already been published during the preparation of this work (*vide supra*). The relevant content is reprinted with permission of the respective scientific publisher. The corresponding citation and the respective license numbers are given at the beginning of the particular chapter.

At the beginning of each chapter a list of authors is included. Further the contributions of each author are described. Additionally, if some of the presented results have already been partly discussed in other theses, it is stated at the beginning of the respective chapter.

To ensure a uniform design of this work, all chapters are subdivided into “Introduction”, “Results and Discussion”, “Conclusion”, “References” and “Supporting Information”. The subchapter “Supporting Information” is additionally subdivided into “Synthetic Procedures”, “X-ray Diffraction Analysis”, “Solid State Structures”, “Crystallographic Information”, “NMR Spectroscopy” and optionally “Computational Details”.

Furthermore, all chapters have the same text settings and the compound numeration begins anew. Due to different requirements of the journals and different article types, the presentation of figures for single crystal X-ray structures or the “Supporting Information” may differ. In addition, a general introduction is given at the beginning and a comprehensive conclusion of all chapters is presented at the end of this thesis.

Table of Contents

1 Introduction

1.1 Chemistry and Application of 13/15 Compounds

Compounds consisting of triels and pnictogens are also known as 13/15 compounds. The first documented synthesis of such compounds is dated to 1809. The famous scientist Gay-Lussac reported about the obtained ammonia bortrifluoride adduct H_3N-BF_3.[1] Further investigations of such compounds led to the exclusively hydrogen substituted analog of H_3N-BF_3, the ammonia borane H_3N-BH_3, which was firstly isolated in 1955[2] and is currently investigated as potential hydrogen storage material due to its high molecular hydrogen content (~19.6 wt.-%). Subsequent dehydrogenation finally results in the formation of boron nitride (BN) (Scheme 1.1).[3]

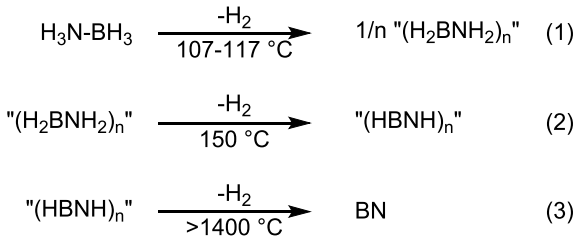

Scheme 1.1. Dehydrogenation of ammonia borane.

Hydration of boron nitride with the aim to obtain ammonia borane proves to be challenging and is part of current research. Recently the groups of *Guo* and *Yu* reported about a viable route for the chemical recycling of metal-B-N containing hydrogen storage materials.[4] Beside pure academical interest boron nitride offers versatile possible applications. Dependent on the modification boron nitride is used as high temperature lubricant, as ceramic linings for rocket engines (α-BN) or abrasive material for industrial processes (β-BN).[5] (The modifications are discussed in detail in the next chapter).

Beside application as hydrogen storage material, ammonia borane also turns out to be a suitable precursor for polymerization. Reactions with transition metal complexes result in catenation of the starting material undergoing a dehydrocoupling reaction, leading to high molecular weight inorganic polymers bearing a boron-nitrogen backbone.[6] Beside nitrogen containing 13/15 adducts also compounds containing heavier group 15 elements are investigated. The phosphorus containing analog of ammonia borane, the phosphine borane H_3P-BH_3, was firstly synthesized in 1966.[7] *Denis et. al* reported about the oligomerization of phosphine borane as well as mono phenyl-substituted derivatives under release of hydrogen, using catalytically amounts of $B(C_6F_5)_3$ (Scheme 1.2).[8]

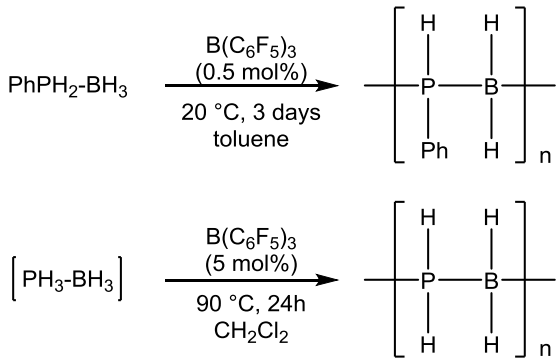

Scheme 1.2. Dehydrocoupling reactions of Phosphinoboranes with catalytical amounts of $B(C_6F_5)_3$.

Overall organosubstituted phosphine boranes are proven to be suitable substrates for transition metal catalyzed polymerization reactions leading to inorganic high molecular weight polymers (M_w = 31.000).[9] Corresponding polymers bearing an arsenic boron backbone are unknown so far. Linear oligomers are limited to cationic compounds of the type $[Me_3N\text{-}BH_2\text{-}AsR_2\text{-}BH_2\text{-}AsR_2\text{-}BH_2\text{-}NMe_3]^+$ (R = H[10], Ph[11]). Beside the pure academical interest, arsenic containing 13/15 adducts also have practical application. *Manasevit* reported about the reaction of $GaEt_3$ with AsH_3 under thermal conditions, leading to formation of GaAs which is used due to its semiconducting properties.[12]

Another very interesting compounds are frustrated Lewis pairs (FLPs). Usually those FLPs reveal a Lewis acid (LA) as well as a Lewis base (LB), in many cases based on group 13 and 15 elements, which are spatially separated. Due to this separation the formation of a typical LA-LB adduct is inhibited. *Stephan et al.* investigated a phosphorus and boron containing FLP resulting in activation of hydrogen under mild conditions (Scheme 1.3).[13]

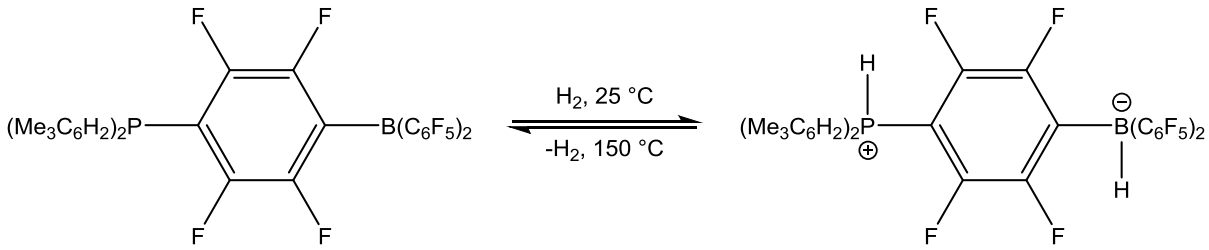

Scheme 1.3. Activation of hydrogen with frustrated Lewis pairs (FLP).

The reaction is reversible and upon heating hydrogen can be released from the zwitterionic product. Offering substrates like CO_2 to such FLPs leads to the activation of the carbon dioxide under formation of the corresponding addition product.[14] Only few years ago successful attempts of hydrogenation of CO_2 using nitrogen-boron based frustrated Lewis pairs have been carried out.[15]

1.2 Comparison of 13/15 compounds with C-C-units

Growing interest in 13/15 compounds is not only caused by their possible applications. A closer look to a carbon-carbon bond in comparison to a group 13-15 bond reveals remarkable structural and chemical similarities as well as differences. One crucial aspect of this relationship is the electronical constellation. While every carbon bears four valence electrons (VE) within a C-C-unit, the distribution in a pncitogen-triel bond is not as equal. Here the group 13 atom contributes three and the group 15 five VE, respectively, never the less leading to a sum of 8 VE in both cases. According to this a C-C- and a 13-15-unit are seen as isoelectronic. The most known modifications of elemental carbon are graphite and diamond. Graphite reveals a two dimensional layer structure, in which each layer is build up by sp^2-hybridised carbon atoms in a hexagonal arrangement. These layers are stacked in a way, so that under each gap within the hexagonal structure a carbon atom of the subjacent layer is located, leading to shifted stacking. The scaffold inside of a diamond reveals a tetrahedral arrangement of sp^3-hybridised carbon atoms. Analog modifications are found for boron nitride (BN) (Figure 1.1).[5]

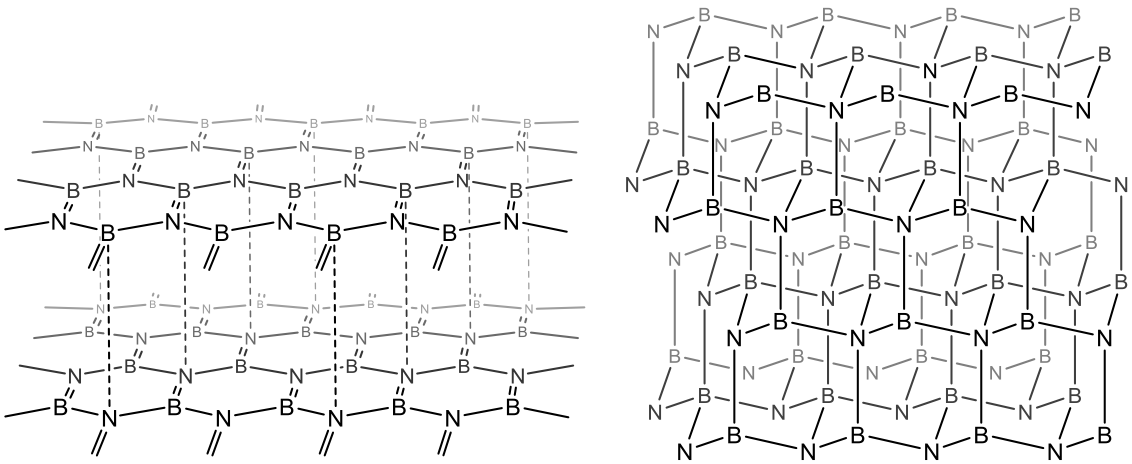

Figure 1.1. Graphite and diamond analog modifications of boron nitride (α-BN and β-BN).

Being the second hardest known material right after diamond itself, β-BN is also known as “inorganic diamond”. Apart from slight deviation between the atomic distances (r_{CC} = 1.54 Å, r_{BN} = 1.56 Å) within the scaffold their structural data are quite similar. Comparable to graphite the α-BN reveals a layer structure as well, but with one crucial difference. Contrary to the carbon analog the layers of the “inorganic graphite” are not shifted but stacked in a way so that above every nitrogen a boron atom is

located and equally the other way round. Never the less the distance between the layers are comparable (d_{CC} = 3.35 Å, d_{BN} = 3.33 Å).

Focusing on common nitrogen boron containing adducts like the ammonia borane, H_3N-BH_3, the structural and electronical analogies to hydrocarbons can be observed further. The arrangement of the substituents as well as the bond length between the CH_3-fragments belonging to an ethane molecule is comparable to the geometry and the distance between NH_3 and BH_3 within the ammonia borane. This similarity applies to the unsaturated derivatives as well as up to borazine often referred as the "inorganic benzene" (Figure 1.2).

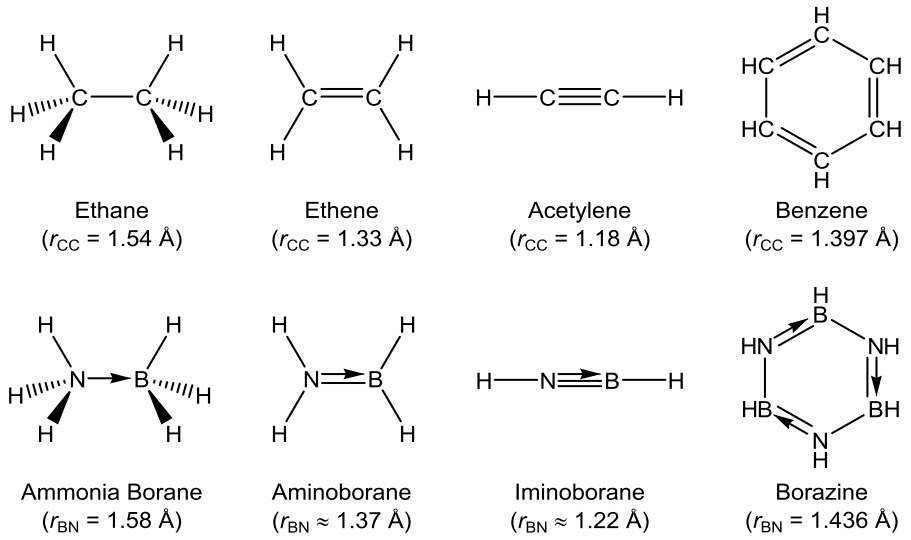

Figure 1.2. Structural comparison between C-C-units and B-N adducts.

In contrast to the homopolar bonding situation within the ethane molecule the unequal VE contribution and different electronegativities within the ammonia borane lead to a polarization of the B-N bond and therefore to different reactivity. Addition reactions towards amino- and iminoborane proceed faster and more predictable than towards the unsaturated hydrocarbon analogs. With focus on the bonding situation between NH_3 and BH_3 another difference can be observed. While the carbon-carbon bond within an ethane molecule can be defined as covalent, calculations reveal that only 0.2 e^- are transferred from nitrogen towards the boron atom within ammonia borane and most electron density remains near to the group 15 element.[16] According to this the B-N-bond is more precisely described as dative interaction. Proceeding to boron adducts with phosphorus, the heavier homolog of nitrogen, the resulting compounds are no longer comparable to ethane or ammonia borane regarding structural and electronical properties. They are isoelectronical to C-Si- and N-Al-units instead.[17] Another crucial aspect is stability. While the B-N compounds shown in Figure 1.2 are accessible under standard conditions, the phosphorus analogs are unknown so far except of

phosphane-borane.[18] Beside stabilization at temperatures below -30 °C also a Lewis base stabilized derivative of the phosphanylborane H_2P-BH_2-NMe_3 is accessible which is discussed in the next chapter.[19] Also the structural differences of the unsaturated derivatives compared to aminoborane and iminoborane, respectively, are apparent (Figure 1.3).[5]

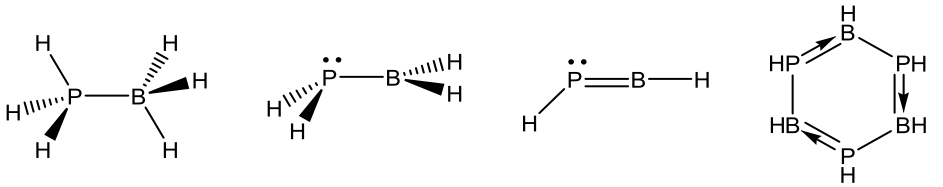

Figure 1.3. Phosphorus containing analog and unsaturated derivatives of presented ammonia borane.

DFT computations reveal that a pyramidal environment of the phosphorus atom in the H_2P-BH_2-unit is energetically favoured. Additionally computations indicate that P-B moieties do not show the same ability to form planar species compared to B-N units leading to the angled shape of phosphino- and phoshiminoborane, respectively. The corresponding arsenic containing derivatives to the compounds shown in Figure 1.3 are solely investigated by theoretical studies[20] except of a Lewis base stabilized derivative of the arsanylborane H_2As-BH_2-NMe_3 which is discussed in the next chapter.[21]

1.3 Chemistry of parent Lewis base stabilized Pnictogenylboranes

Ammonia borane (H_3B-NH_3) is a good accessible and stable chemical which can be handled even without inert gas conditions. The unsaturated derivative, the aminoborane, reveals a decreased stability. Never the less it was possible to isolate and study H_2B-NH_2 under cryogenic conditions.[22] Raising temperature increases the reactivity and leads to catenation. Due to an empty orbital at the boron atom and an accessible lone pair located at the pnictogen atom it tends to undergo a head-to-tail polymerization (Figure 1.4).

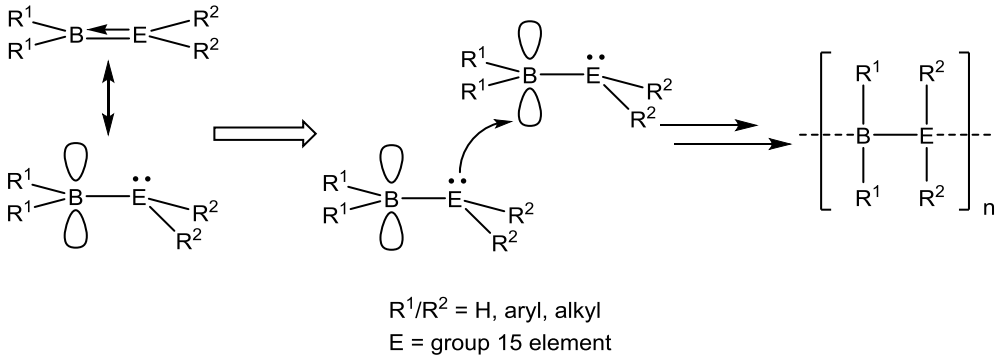

Figure 1.4. Head-to-tail polymerization of pnictogenylborane monomers.

To avoid polymerization, which occurs at temperatures above -30 °C, the stability of aminoborane can be increased by introducing bulky organic substituents on the group 13 and 15 elements.[23] Another possibility is blocking the free orbital on the boron atom and hindering the accessibility of the lone pair (LP) at the pnictogen atom. This can be achieved by coordination of the LP to Lewis acids and coordination of Lewis bases to boron, resulting in compounds even stable at room temperature.[24]

Moving on to phosphorus and arsenic containing analogs the stability decreases even further in comparison to nitrogen containing compounds and their unsaturated derivatives. While the phosphine borane adduct (H_3P-BH_3) is only accessible at low temperatures[18] the investigation of H_3As-BH_3 is limited to theoretical studies.[20] To obtain stable monomeric phosphanylboranes[25] and arsanylboranes,[26] respectively, the introduction of bulky organic substitutents is necessary (**I**).

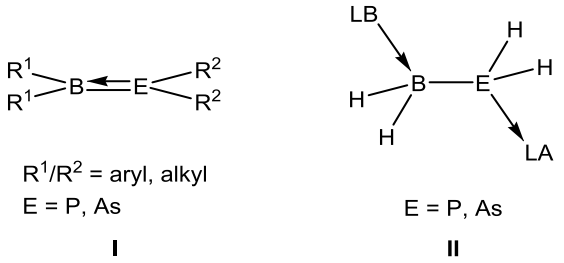

Neither the monomeric hydrogen substituted phosphanyl- nor the arsanylborane are accessible so far. As already mentioned above, coordination of the unsaturated parent compounds towards LAs and coordination of LBs to the boron center leads to stable derivatives which can be handled even at room temperature (**II**).[27] With increasing stability the reactivity of the obtained pnictogenylboranes is lowered due to the fact that the functional groups are sterically shielded or saturated, hampering more detailed investigations of their reactivity. Further development of the synthetic procedure of above mentioned phosphanyl- and arsanylborane (**II**) by the *Scheer* group results in the first Lewis base stabilized phosphanylborane[19] followed by the corresponding arsenic containing analog few years later (Scheme 1.4).[21]

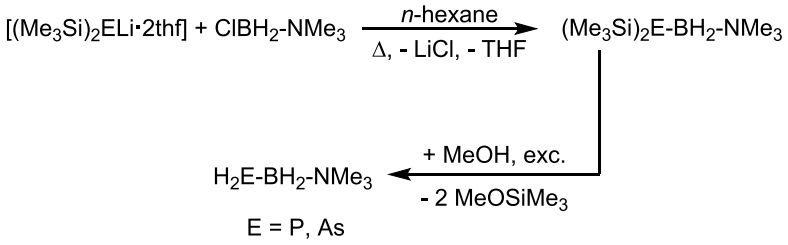

Scheme 1.4. Synthetic pathway of the Lewis base stabilized phosphanyl- and arsanylborane.

Both compounds are stable even at room temperature and offer a terminal phosphine and arsine group, respectively, suitable for versatile chemistry (**III**, Scheme 1.5). Functionalization with organic substituents leads to Lewis base stabilized pnictogenylborane derivatives (**III**) where the phosphorus containing compounds undergo catalyst free oligo- and polymerization at very mild conditions (**IV**, Scheme 1.5). Especially the mono *tert*-butyl substituted phosphanylborane leads to high molecular polymers containing up to 2000 repeating units.[28] Polymerization of phosphanylboranes only occurs when the terminal phosphane group is nucleophilic enough to remove the coordinating LB NMe_3 resulting in a head-to-tail polymerization. Treating the polymer $[^tBuPH\text{-}BH_2]_n$ with even stronger nucleophiles than NMe_3 like NHC (NHC = N-heterocyclic carbene) results in cleavage of phosphorus-boron bonds leading to the monomeric building blocks $^tBuPH\text{-}BH_2$-NHC, stabilized by NHC.[29] Attempts to polymerize corresponding arsanylboranes have not been successful so far despite variation of reaction conditions as well as substitutents.

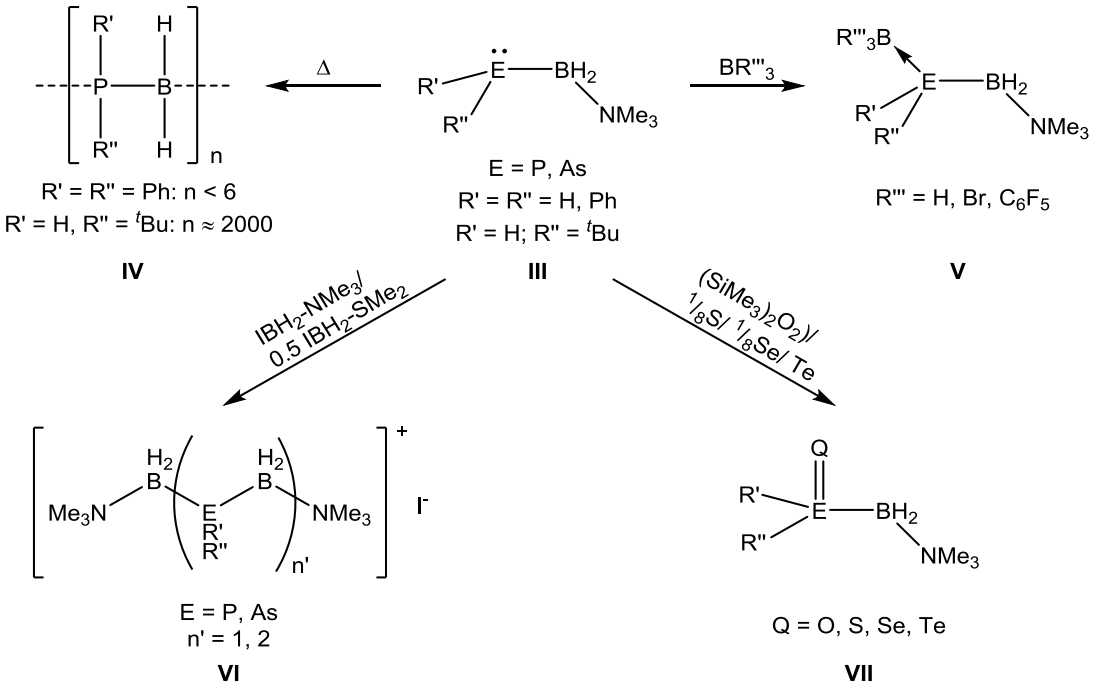

Scheme 1.5. Selected reactions of Lewis base stabilized pnictogenylboranes.

Beside coordination towards boron centered LAs of the type BR_3 (**V**, Scheme 1.5)[11,19,21,30] also cationic compounds, revealing two Lewis base stabilized pnictogenylborane equivalents bridged by a BH_2 group, can be obtained (**VI**, Scheme 1.5).[10,11,31] These compounds are unique for bearing the longest arsenic boron containing linear chain like structure. Reactions of these pnictogenylboranes with elemental chalcogens lead to the corresponding oxidation products proving the suitability for redox-chemistry (**VII**, Scheme 1.5).[11,19,32] Based on the investigations concerning phosphanyl- and arsanylboranes, respectively, also the synthesis of the first LB stabilized parent stibanylborane $H_2Sb\text{-}BH_2\text{-}NMe_3$ was recently published.[33]

Another focus of current investigations is the behavior of Lewis base stabilized pnictogenylboranes in the coordination sphere of transition metal fragments. Reactions of $H_2E\text{-}BH_2\text{-}NMe_3$ (E = P, As) with gold(I) salts lead to 1-dimensional coordination polymers built from a linear chain of gold cations.[34] These compounds reveal luminescence properties in the solid state while solutions does not exhibit any luminescence. Treating $H_2P\text{-}BH_2\text{-}NMe_3$ with [Cp_2Ti(btmsa)] (Cp = cyclopentadienyl, btmsa = bis(trimethylsilyl)acetylene) again reveals the suitability of $H_2P\text{-}BH_2\text{-}NMe_3$ as ligand.[35] At low temperatures the coordination product **VIII** (Scheme 1.6) can be isolated.

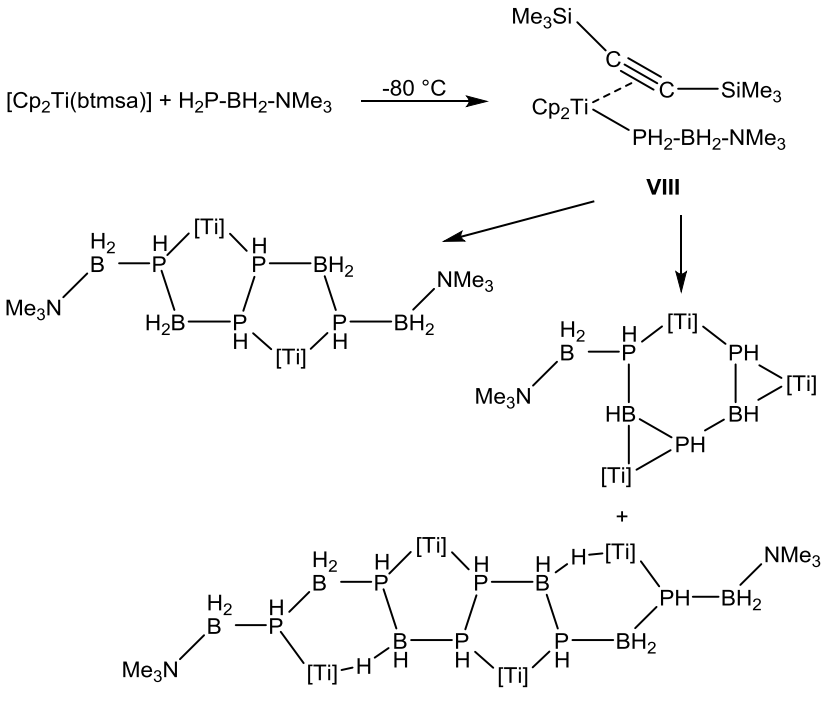

Scheme 1.6. Reaction of $H_2P\text{-}BH_2\text{-}NMe_3$ with [Cp_2Ti(btmsa)].

At temperatures above -80 °C elimination of the trimethylamine and subsequent catenation of the phosphanylborane can be observed. Depending on the reaction conditions oligomers of different length can be stabilized in the coordination sphere of Cp_2Ti fragments (Scheme 1.6).

1.4 References

[1] J. L. Gay-Lussac, J. L. Thénard, *Mem. de. Phys. et de. Chim. de la Soc. d'Arcueil* **1809**, *2*, 210 as cited in V. Jonas, G. Frenking, *J. Chem. Soc., Chem. Commun.* **1994**, 1489-1490.

[2] S. G. Shore, R. W. Parry, *J. Am. Chem. Soc.* **1955**, *77*, 6084-6085.

[3] C. W. Hamilton, R. T. Baker, A. Staubitz, I. Manners, *Chem. Soc. Rev.* **2009**, *38*, 279-293.

[4] Z. Tang, L. Zhang, L. Wan, Z. Huang, H. Liu, Z. Guo, X. Yu, *Int. J. Hydrogen Energ.* **2016**, *41*, 407-412.

[5] A. F. Hollemann, E. Wiberg, *Lehrbuch der Anorganischen Chemie* **2007**, 102. Auflage, Walter de Gruyter Verlag, Berlin, 1111-1124.

[6] M. C. Denney, V. Pons, T. J. Hebden, D. M. Heinekey, K. I. Goldberg, *J. Am. Chem. Soc.* **2006**, *128*, 12048-12049.

[7] R. W. Rudolph, R. W. Parry, C. F. Farran, *Inorg. Chem.* **1966**, *5*, 723-726.

[8] J-M. Denis, H. Forintos, H. Szelke, L. Toupet, T.-N. Pham, P.-J. Madec, A.-C. Gaumont, *Chem. Commun.* **2003**, 54-55.

[9] H. Dorn, R. A. Singh, J. A. Massey, A. J. Lough, I. Manners, *Angew. Chem. Int. Ed.* **1999**, 38, 3321-3323, *Angew. Chem.* **1999**, *111*, 3540-3543.

[10] C. Marquardt, G. Balázs, J. Baumann, A. V. Virovets, M. Scheer, *Chem. Eur. J.* **2017**, *23*, 11423-11429.

[11] O. Hegen, A. V. Virovets, A. Y. Timoshkin, M. Scheer *Chem. Eur. J.* **2018**, *24*, 16521-16525.

[12] H. M. Manasevit, *Appl. Phys. Lett.* **1968**, *12*, 156-159.

[13] G. C. Welch, R. R. S. Juan, J. D. Masuda, D. W. Stephan, *Science* **2006**, *314*, 1124-1126.

[14] Z. Jian, G. Kehr, C. G. Daniliuc, B. Wibbeling, G. Erker, *Dalton Trans.* **2017**, *46*, 11715-11721.

[15] M.-A. Courtemanche, A. P. Pulis, É. Rochette, M.-A. Légaré, D. W. Stephan, F.-G. Fontaine, *Chem. Commun.* **2015**, *51*, 9797-9800.

[16] H. Umeyama, K. Morokuma, *J. Am. Chem. Soc.* **1976**, *98*, 7208-7220.

[17] P. P. Power, *Angew. Chem. Int. Ed.* **1990**, *29*, 449-460; *Angew. Chem.* **1990**, *102*, 527-538.

[18] E. L. Gamble, P. Gilmont, *J. Am. Chem. Soc.* **1940**, *62*, 717-721.

[19] K.-C. Schwan, A. Y. Timoshkin, M. Zabel, M. Scheer, *Chem. Eur. J.* **2006**, *12*, 4900-4908.

[20] a) A. El Guerraze, A. M. El-Nahas, A. Jarid, C. Serrar, H. Anane, M. Esseffar, *Chem. Phys.* **2005**, *313*, 159-168; b) A. Es-sofi, C. Serrar, A. Ouassas, A. Jarid, A. Boutalib, I. Nebot-Gil, F. Thomás, *J. Phys. Chem. A* **2002**, *106*, 9065-9070; c) A. El Guerraze, H. Anane, C. Serrar, A. Es-sofi, A. M. Lamsabhi, A. Jarid, *J. Mol. Struc-Theochem.* **2004**, *709*, 117-122; d) I. V. Alabugin, S. Bresch, M. Manoharan, *J. Phys. Chem. A* **2014**, *118*, 3663-3677.

[21] C. Marquardt, A. Adolf, A. Stauber, M. Bodensteiner, A. V. Virovets, A. Y. Timoshkin, M. Scheer, *Chem. Eur. J.* **2013**, *19*, 11887-11891.

[22] C. T. Kwon, H. A. Jr. McGee, *Inorg. Chem.* **1970**, *9*, 2458-2461.

[23] a) U. Höbel, H. Nöth , H. Prigge, *Chem. Ber.* **1986**, *119*, 325-337; b) A. P. M. Roberson, G. R. Whittell, A. Staubitz, K. Lee, A. J. Lough, I. Manners, *Eur. J. Inorg. Chem.* **2011**, *34*, 5729-2587.

[24] A. C. Malcolm, K. J. Sabourin, R. McDonald, M. J. Ferguson, E. Rivard, *Inorg. Chem.* **2012**, *51*, 12905-12916.

[25] S. J. Geier, T. M. Gilbert, D. W. Stephan, *J. Am. Chem. Soc.* 2008, *130*, 12632-12633; b) S. H. Geier, T. M. Gilbert, D. W. Stephan, *Inorg. Chem.* 2010, *50*, 336; c) S. J. Geiert, T. M. Gilbert, D. W. Stephan, *Inorg. Chem.* **2011**, *50*, 336-244.

[26] M. A. Mardones, A. H. Cowley, L. Contreras, R. A. Jones, C. J. Carrano, *J. Organomet. Chem.* **1993**, *455*, C1-C2.

[27] U. Vogel, P. Hoemensch, K.-C. Schwan, A. Y. Timoshkin, M. Scheer, *Chem. Eur. J.* **2003**, *9*, 515-519.

[28] C. Marquardt, T. Jurca, K.-C. Schwan, A. Stauber, A. V. Virovets, G. R. Whittell, I. Manners, M. Scheer, *Angew. Chem. Int. Ed.* **2015**, *54*, 13782-13786; *Angew. Chem.* **2015**, *127*, 13986-13991.

[29] C. Marquardt, O. Hegen, A. Vogel, A. Stauber, M. Bodensteiner, A. Y. Timoshkin, M. Scheer, *Chem. Eur. J.* **2018**, *24*, 360-363.

[30] C. Marquardt, T. Kahoun, J. Baumann, A. Y. Timoshkin, M. Scheer, *Z. Anorg. Allg. Chem.* **2017**, *643*, 1326-1330.

[31] C. Marquardt, C. Thoms, A. Stauber, G. Balázs, M. Bodensteiner, M. Scheer, *Angew. Chem. Int. Ed.* **2014**, *53*, 3727-3739; *Angew. Chem.* **2014**, *126*, 3801-3804.

[32] C. Marquardt, O. Hegen, T. Kahoun, M. Scheer, *Chem. Eur. J.* **2017**, *23*, 4397-4404.

[33] C. Marquardt, O. Hegen, M. Hautmann, G. Balázs, M. Bodensteienr, A. V. Virovets, A. Y. Timoshkin, M. Scheer, *Angew. Chem. Int. Ed.* **2015**, *54*, 13122-13125; *Angew. Chem.* **2015**, *127*, 13315-13318.

[34] J. Braese, A. Schinabeck, M. Bodensteiner, H. Yersin, A. Y. Timoshkin, M. Scheer, *Chem. Eur. J.* **2018**, *24*, 10073-10077.

[35] C. Thoms, C. Marquardt, A. Y. Timoshkin, M. Bodensteiner, M. Scheer, *Angew. Chem. Int. Ed.* **2013**, *52*, 5150-5154; *Angew. Chem.* **2013**, *125*, 5254-5259.

2 Research Objectives

As an alternative to carbon based organic polymers the catenation of group 13/15 monomers is in the focus of current researches. Additionally to nitrogen and boron, phosphorus and boron containing adducts are revealed to be suitable substrates for polymerization experiments. One key step during the linking of the monomers is the formation of unsaturated E=B units (E = N, P) and the subsequent spontaneous head-to-tail polymerization. There are several different starting points to achieve this. *In situ* generation of the highly reactive molecules via metal catalyzed dehydrocoupling reactions of saturated pnictogen boron adducts is a well established procedure. Since the accessibility of Lewis base stabilized phosphanylboranes an alternative catalyst free route to phosphorus containing inorganic polymers is available. However a weakly coordinating Lewis base, removable by the terminal PR_2 group (R = H, alkyl, aryl), is an inevitable requirement for a successful catenation of such compounds. Trimethylamine (NMe_3) turns out to be a suitable choice as Lewis base. Never the less it proves challenging to conduct the polymerization step by step. Attempts for the polymerization of arsanylboranes are unsuccesfull so far, despite changing reaction conditions. For investigations regarding the nucleophilic attack of ER_2 groups (E = P, As; R = H, alkyl, aryl) towards Lewis base stabilized pnicotgenylboranes and the simultaneous removement of the Lewis base NMe_3 the following tasks arise:

- Reaction of pnictogen based nucleophiles of the type MER_2 (M = alkali metal; E = P, As; R = H, alkyl, aryl) with Lewis base stabilized pnictogenylboranes which should result in the formation of discrete anionic linear entities.
- Investigating the reactivity of the anionic units by subsequent reaction with equivalent amounts of pnictogenylboranes leading to elongation of the 13/15 backbone.

The coordination chemistry of pnictogenylboranes towards transition metal fragments is well investigated. Removing the Lewis base from $R_2E\text{-}BH_2\text{-}NMe_3$ (E = P, As; R = H, alkyl, aryl) by pnictogen based nucleophiles should lead to formation of anionic pnictogenylborane derivatives bearing two terminal ER_2-units (E = P, As; R = H, alkyl, aryl) as functional groups. Researches regarding the coordination behavior and suitability as chelating ligands as well as a linker include:

- Reaction of anionic pnictogenylborane derivatives with transition metal fragments offering at least two coordination sites.
- Reactivity towards Cu(I) cations.

Preface

The following chapter has already been published:
Angew. Chem. Int. Ed. **2016,** *55*, 14828-14832; *Angew. Chem.* **2016**, *128*, 15048-15052.
The article is reprinted with slight modifications with permission of "John Wiley and Sons". License Number: 4639300123902.

Authors

Christian Marquardt, Tobias Kahoun, Andreas Stauber, Gabor Balázs, Michael Bodensteiner , Alexey Y. Timoshkin, Manfred Scheer.

Author contributions

The synthesis and characterization of compounds **2**$(thf)_2$ was performed by Dr. Christian Marquardt. Compound **2**$(thf)_2$ has been reported in his PhD-thesis (Regensburg, **2015**).
The synthesis and characterization of compounds **3**, **4**$(thf)_2$, **5**$(thf)_2$ were performed by Tobias Kahoun. Compound **4**$(thf)_2$ has been reported in his master-thesis (Regensburg, **2015**).
The synthesis and characterization of compound **6** was performed by Dr. Andreas Stauber. Compound **2** was synthesized and characterized by NMR spectroscopy and mass spectrometry by Dr. Andreas Stauber for the first time. Both compounds have been reported in his PhD-thesis (Regensburg, **2014**).

X-ray structural analyses of **2**$(thf)_2$ was performed by Dr. Christian Marquardt and Dr. Alexander V. Virovets.
X-ray structural analyses of **3**, **4**$(thf)_2$, **5**$(thf)_2$ were performed by Tobias Kahoun and Dr. Michael Bodensteiner.
X-ray structural analyses of **6** was performed by Dr. Michael Bodensteiner.

DFT-calculations were performed by Dr. Gábor Balázs (University of Regensburg) and Prof. Dr. Alexey Y. Timoshkin (St. Petersburg State University).
The manuscript (including supporting information, figures, schemes and graphical abstract) was written by Christian Marquardt and Tobias Kahoun

3 Anionic Chains of Parent Pnictogenylboranes

C. Marquardt, T. Kahoun, A. Stauber, G. Balázs, M. Bodensteiner, A. Y. Timoshkin, M. Scheer

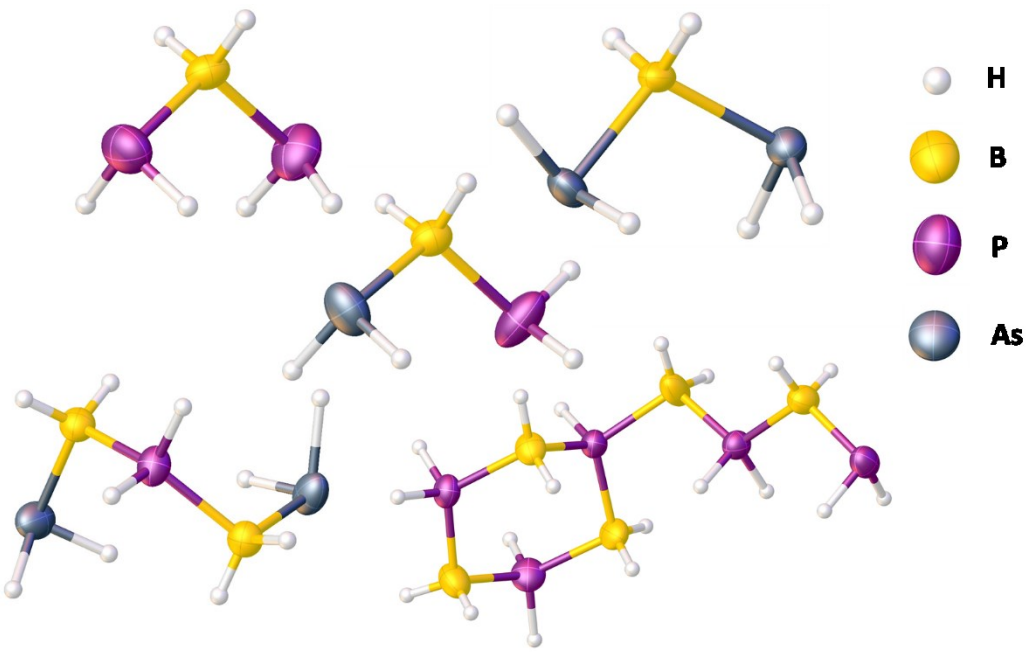

Abstract: We report on the synthesis and structural characterization of unprecedented anionic parent compounds of mixed Group 13/15 elements. The reactions of the pnictogenylboranes H_2E-BH_2-NMe_3 (**1a** = P, **1b** = As) with phosphorus and arsenic centered nucleophiles of the type $[EH_2]^-$ (E = P, As) lead to the formation of compounds of the type $[H_2E$-BH_2-$E'H_2]^-$ (**2**: E = E' = P; **3**: E = E' = As; **4**: E = P, E' = As) containing anionic pnictogen-boron chain-like units. Furthermore, a longer 5-membered chain species $[H_2As$-BH_2-PH_2-BH_2-$AsH_2]^-$ (**5**) and a cyclic compound $[NHC^{dipp}$-H_2B-PH_2-BH_2-$NHC^{dipp}]^+[P_5B_5H_{19}]^-$ (**6**) containing a *n*-butylcyclohexane-like anion were obtained. All the compounds have been characterized by X-ray structure analysis, multinuclear NMR spectroscopy, IR spectroscopy, and mass spectrometry. DFT calculations elucidate their high thermodynamic stability, the charge distribution, and give insight into the reaction pathway.

3.1 Introduction

The interest in the catenation of non-carbon atoms and moieties has increased significantly over the last few years. Current research focuses especially on the catenation of Group 15 elements. Whereas chains of polyphosphines and polyphosphorus anions have already been studied thoroughly in the last few decades,[1] the chemistry of catena-phosphorus cations has been discovered recently and was investigated intensively, for example by the groups Burford[2] and Weigand.[3] The homocatenation of Group 13 elements was explored as well.[4] Moreover, amine- and phosphine-borane adducts gained increasing interest as hydrogen-storage materials as well as precursors for novel inorganic polymers.[5] Polyamino- and polyphosphinoboranes are primarily obtained by dehydrocoupling reactions of the corresponding compounds RR'HE-BH_3 (E = N, P) mediated by metal catalysts and can be viewed as inorganic analogues of organic polymers, such as polyolefins.[5] Recently, a novel non-catalytic addition polymerization of Lewis base stabilized phosphanylborane monomers was achieved.[6] In contrast, only a few short chains of neutral oligophosphinoboranes were characterized by X-ray structure analysis.[7] Compounds containing longer chains were only characterized by spectroscopic methods.[8] In all of the reported compounds the P-B core is protected by organic substituents. We are especially interested in the synthesis and reactivity of parent Group 13/15 compounds containing E-H bonds,[9] a field which is also in the focus of the Rivard group.[10] Recently, we reported the high-yield synthesis of the pnictogenylboranes H_2E-BH_2-NMe_3 (**1a**: E = P; **1b**: E = As),[11] which are excellent building blocks for the formation of oligomeric[12] and polymeric[6] compounds. Moreover, by using them as starting materials we succeeded in the synthesis of novel cationic chains of phosphanyl- and arsanylboranes.[13] The cationic species $[Me_3N\text{-}H_2B\text{-}[PH_2\text{-}BH_2]_n\text{-}NMe_3]^+$ (**I**: n = 1; **II**: n = 2) are thermodynamically sufficiently stable to be isolated, whereas similar compounds containing an anionic P-B-P core are unknown to date.

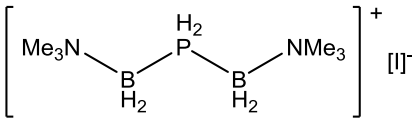

I

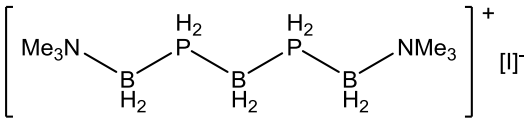

II

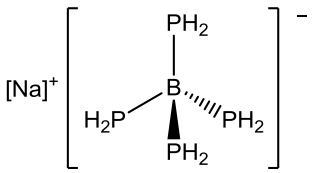

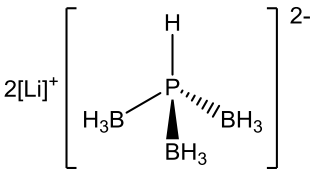

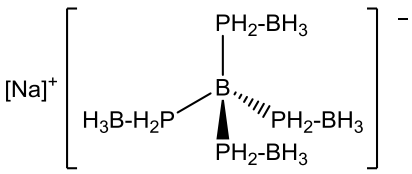

III

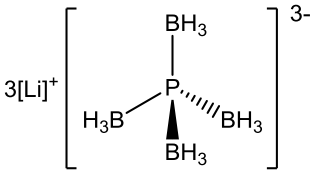

IV

$[M]^+[R_2P\text{-}BH_3]^-$

R = Ph, ^{t}Bu, Me

V

$[M]^+[H_3B\text{-}R_2P\text{-}BH_3]^-$

R = H, Ph

VI

$[R_2P\text{-}BH_2\text{-}PR_2]^-$

$[R_2P\text{-}BH_2\text{-}PR_2\text{-}BH_2\text{-}PR_2]^-$

R = CF_3

VII

In contrast to other cationic[14] and neutral[15] compounds containing a P-B-P backbone,[13] the reported parent anionic species are almost exclusively restricted to branched examples, such as compounds of type **III**[16] and **IV**.[17] Shorter anionic derivatives with BH_3 end groups (type **V**[18] and **VI**)[19] are obtained by the deprotonation of the corresponding phosphine-borane adduct. The only known linear anionic chains contain electron-withdrawing CF_3 groups (type **VII**) to distribute the negative charge appropriately. However, they were only obtained as mixtures and were solely studied by NMR spectroscopy.[20] To our knowledge the only anionic arsenic derivative is the methyl-substituted bis(borane)dimethylarsenide $Na^+[H_3B\text{-}AsMe_2\text{-}BH_3]^-$ (type **VI**).[21] Von Schnering et al. reported on solid-state reactions of BP, BAs, or the elements with potassium at 1000-1100 K leading to the short linear, propadiene analogue Zintl anions $[E\text{-}B\text{-}E]^{3-}$ (E = P, As).[22] However, the quest for alternative solution approaches to linear anionic chains of the parent pnictogneylboranes especially arsenic-rich chains with longer sequences is still open. Herein we present a general synthetic approach and the structural characterization of the first exclusively H-substituted, parent anionic phsphanyl- and arsanylborane chains.

3.2 Results and Discussion

Sonication of a solution of the phosphaynlborane H_2P-BH_2-NMe_3 (**1a**) with one equivalent of $NaPH_2$ in THF leads to the substitution of NMe_3 by PH_2^- and the formation of [Na][H_2P-BH_2-PH_2] (**2**, Scheme 3.1).

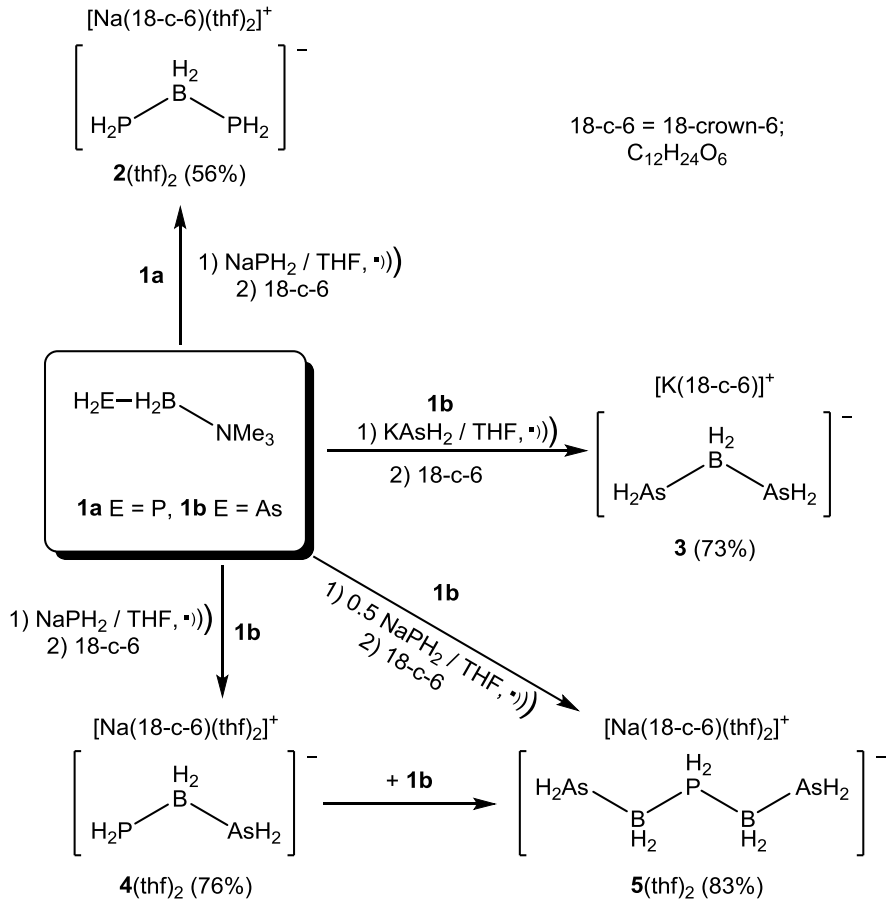

Scheme 3.1. Reaction of **1a** and **1b** with phosphorus and arsenic centered nucleophiles. Isolated yields are given in parentheses.

As arsenides are good nucleophiles as well, $KAsH_2$ was treated with H_2As-BH_2-NMe_3 (**1b**) yielding [K][H_2As-BH_2-AsH_2] (**3**, Scheme 3.1). Treatment of **1b** with $NaPH_2$ selectively yields the mixed chain compound [Na][H_2As-BH_2-PH_2] (**4**, Scheme 3.1).[23] Furthermore, when **1b** is treated with 0.5 equivalents of $NaPH_2$, or another equivalent of **1b** is added to **4**, the longer chain [Na][H_2As-BH_2-PH_2-BH_2-AsH_2] (**5**, Scheme 3.1) is obtained. Unfortunately, **1a**, **2** or **3** cannot be transferred into a similar chain, despite numerous attempts. Compared to the cationic compounds **I** and **II**,[13] the anionic species are much more sensitive and react readily with solvents, such as acetonitrile.

According to ^{31}P and/ or ^{11}B NMR spectroscopy of the crude reaction mixture, **2** and **3** are generated without the formation of side products. In the reaction of **1b** with $NaPH_2$, **4** is also selectively obtained. Only small traces of **5** can be detected as a side product. Compound **5** is obtained selectively when a slight excess of **1b** is used.[24] After addition of 18-crown-6 all the compounds can be isolated as crystalline solids in good to excellent yields (Scheme 3.1).

In the ^{31}P NMR spectrum of **2**$(thf)_2$, a very broad triplet at δ = -175.0 ppm ($^1J_{P,H}$ = 172 Hz) is observed, without further resolved coupling. The ^{11}B NMR spectrum of **2**$(thf)_2$ shows a triplet of triplets at δ = -34.7 ppm ($^1J_{B,P}$ = 26 Hz, $^1J_{B,H}$ = 99 Hz). In the ^{11}B NMR spectrum of **3**, a triplet arises at δ = -34.5 ppm ($^1J_{B,H}$ = 106 Hz). The ^{31}P NMR spectra show a very broad triplet at δ = -174.8 ppm ($^1J_{P,H}$ = 173 Hz) for **4**$(thf)_2$ and at δ = -56.0 ppm ($^1J_{P,H}$ = 307 Hz) for **5**$(thf)_2$. In the ^{11}B NMR spectra, a triplet of doublets can be found at δ = -34.4 ppm ($^1J_{B,P}$ = 27 Hz, $^1J_{B,H}$ = 102 Hz) for **4**$(thf)_2$ and at δ = -37.4 ppm ($^1J_{B,P}$ = 58 Hz, $^1J_{B,H}$ = 105 Hz) for **5**$(thf)_2$.

The X-ray structures of **2**$(thf)_2$, **4**$(thf)_2$ and **5**$(thf)_2$ show the anions without any contacts to the cation. Only in the structure of **3** is the $[H_2As\text{-}BH_2\text{-}AsH_2]^-$ anion in close contact to $[K(18\text{-}c\text{-}6)]^+$. The P-B bond lengths of **2**$(thf)_2$ are at 1.960(3) and 1.963(3) Å slightly shortened as compared to the starting material $H_2P\text{-}BH_2\text{-}NMe_3$ (1.976(2) Å),[9b] but to a lesser extent than in the cationic species $[Me_3N\text{-}BH_2\text{-}PH_2\text{-}BH_2\text{-}NMe_3]^+$ (1.957(3) Å).[13] Compound **3** shows As-B bond lengths with 2.062(2) and 2.069(2) Å, which are again slightly shorter than in $H_2As\text{-}BH_2\text{-}NMe_3$ (2.071(4) Å).[11] The cationic species $[Me_3N\text{-}BH_2\text{-}AsH_2\text{-}BH_2\text{-}NMe_3]^+$ in contrast exhibits slightly elongated As-B bond length (2.076(3)-2.086(3)).[13] The P-B bond length of 4 is 1.975(4) and the As-B bond length 2.050(2) Å.[25] The P-B bond length of **5**$(thf)_2$ is 1.947(3) and the As-B bond length is 2.081(3) Å. Compared to **2** and **3** the P-B bond is shortened, whilst the As-B bond is slightly longer.

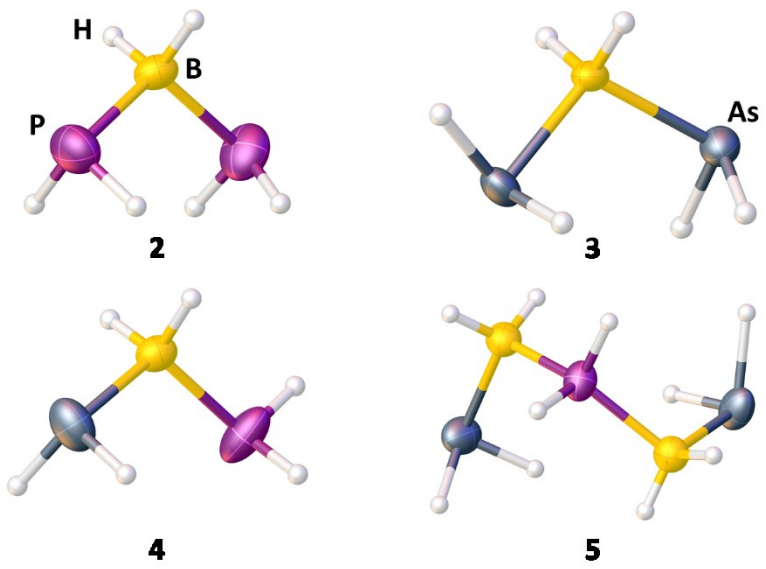

Figure 3.1. Molecular structure of **2**$(thf)_2$, **3**, **4**$(thf)_2$ and **5**$(thf)_2$ in the solid state. Thermal ellipsoids are set at 50% probability. The counter ions are omitted for clarity.

The terminal EH_2 groups show rotational disorder in the solid state for **2**$(thf)_2$ and **3**.[26] In the solid state, the all-antiperiplanar conformation (with respect to the lone pairs) is predominant for **2**$(thf)_2$, whereas **3** favors an all-synclinal conformation (Figure 3.1).[27] Compounds **4**$(thf)_2$ and **5**$(thf)_2$ reveal a mixture of antiperiplanar and synclinal arrangements, resulting in an u-shaped structural motif for **5**$(thf)_2$ (Figure 3.1) similar to the cationic species **II**. This is in good agreement with the calculations for the gas-phase species of Lewis acid/base stabilized pnictogenylboranes, which have shown that the energy differences of different conformations are very small (6-7 kJmol^{-1}).[28]

The natural poplutaion analysis (NPA) reveals that the main part of the negative charge in the chains $[H_2E\text{-}BH_2\text{-}EH_2]^-$ is localized on the B atom (**2**: -0.70e; **3**, **4**: -0.68e) whereas the P and As atoms are almost neutral (-0.06e for P, +0.01e for As in each case). In the longer chain $[H_2As\text{-}BH_2\text{-}PH_2\text{-}BH_2\text{-}AsH_2]^-$ the B atoms also have a negative charge (-0.73e); the As atoms are almost neutral (-0.05e) and the central P atom is positively charged (+0.62e). According to the NPA charge distribution, the anions in **2**-**5** can be best described as boranate anions.

To gain deeper insight into the energetics of the substitution reactions of $H_2P\text{-}BH_2\text{-}NMe_3$ (**1a**) and $H_2As\text{-}BH_2\text{-}NMe_3$ (**1b**), DFT calculations were performed in solutions.[27] Accordingly, the reaction of **1a** with EH_2^- leading to $[H_2P\text{-}BH_2\text{-}EH_2]^-$ is exothermic by -39.4 kJmol^{-1} for E = P and by -42.1 kJmol^{-1} for E = As (Figure 3.2).

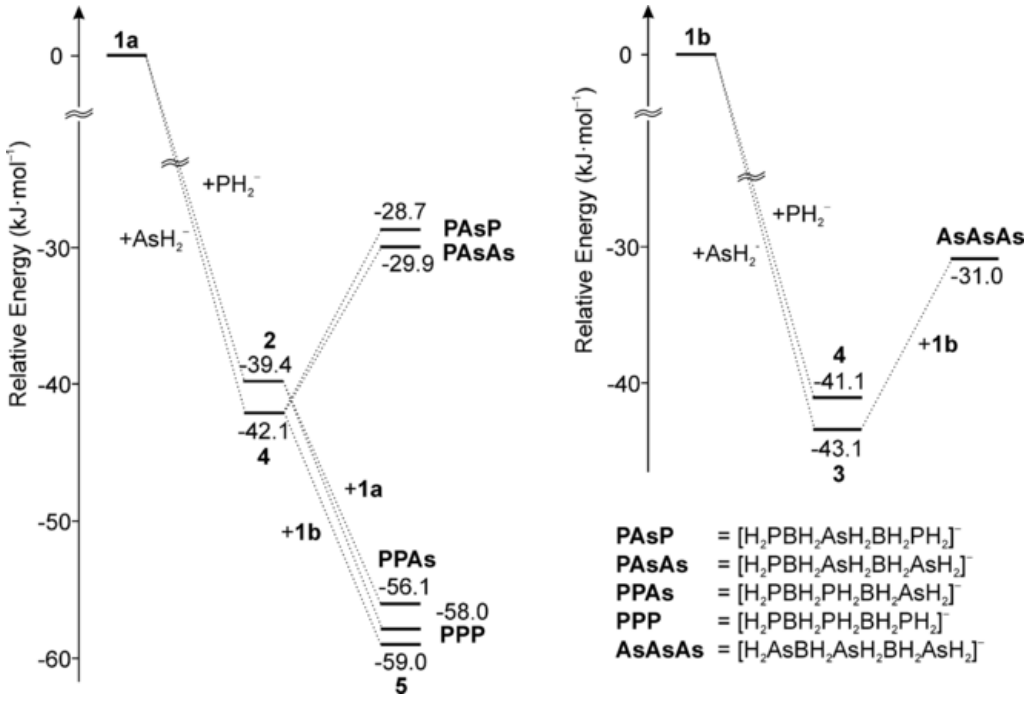

Figure 3.2. Energy profile of the reaction of H_2E-BH_2-NMe_3 (**1a** = P, **1b** = As) with phosphorus- and arsenic-centered nucleophiles. Relative energies calculated at the B3LYP/def2-TZVP level.

Interestingly, the reaction of **1a** or **1b** at the AsH_2 unit of **4** is thermodynamically unfavored, while the reaction at the PH_2 unit is thermodynamically favored (Figure 3.2). Although the reaction of **2** with **1a** or **1b** is predicted to be exothermic, experimentally no reaction was observed. The inspection of the electrostatic potential in **4** shows a light accumulation of negative charge on the phosphorus atom compared to the arsenic atom.

Since N-heterocyclic carbenes (NHCs) are nucleophiles, the reaction of H_2P-BH_2-NMe_3 (**1a**) with NHC^{dipp} was also investigated. At room temperature, no reaction was observed. Refluxing the reactants in toluene affords the mixed ionic Group 13/15 compound **6** (Scheme 3.2) as the only isolated product in minor yields. The formation of 6 is rather unexpected. Probably, during the reaction NMe_3 is eliminated leading to a transient H_2P-BH_2 species that aggregates and in the presence of NHC^{dipp} rearranges to **6**. The formation of the cationic part in **6** may also be a result of the presence of $ClBH_2$-NMe_3 as minor impurities in the starting material.[29]

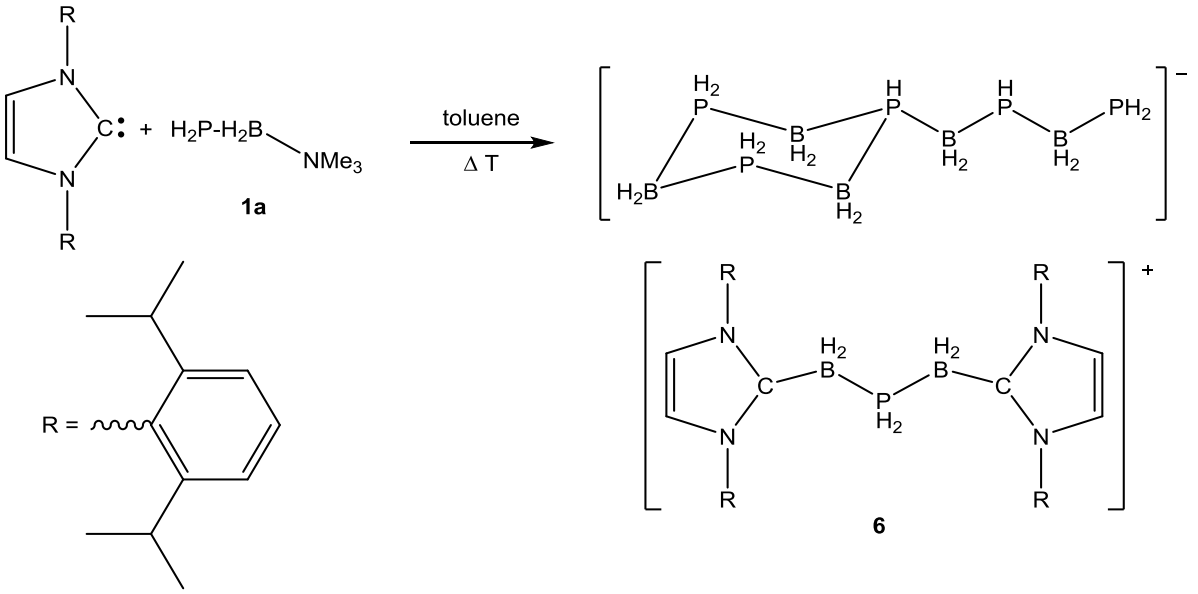

Scheme 3.2. Synthesis of **6**.

DFT computations indicate that gas-phase reactions leading to the contact ion pair **6** are exothermic by -215 and -200 kJmol^{-1} for the reactions 1 and 2, respectively:

$$6\ \mathbf{1a} + 3\ NHC^{dipp} + ClBH_2\text{-}NMe_3 \rightarrow [NHC^{dipp}\text{-}BH_2\text{-}PH_2\text{-}BH_2\text{-}NHC^{dipp}]^+[P_5B_5H_{19}]^- + [NHC^{dipp}H]^+Cl^- + 7\ NMe_3 \quad (1)$$

$$7\ \mathbf{1a} + 2\ NHC^{dipp} \rightarrow [NHC^{dipp}\text{-}BH_2\text{-}PH_2\text{-}BH_2\text{-}NHC^{dipp}]^+[P_5B_5H_{19}]^- + PH_3 + 7\ NMe_3 \quad (2)$$

In the $^{11}B\{^1H\}$ and $^{31}P\{^1H\}$ NMR spectra of **6** an accurate assignment of the signals is not possible because of their broadness and the very complex spin system leading to a superimposed coupling pattern. In the ESI mass spectrum, the molecular ion peak for both the anion $[P_5B_5H_{19}]^-$ (negative mode) and the cation $[NHC^{dipp}\text{-}BH_2\text{-}PH_2\text{-}BH_2\text{-}NHC^{dipp}]^+$ (positive mode) was observed.

The solid-state structure of **6** shows a cation featuring a B-P-B unit that is stabilized by two NHC ligands (Figure 3.3). The anion is a *n*-butylcyclohexane-like unit built up from alternating BH_2 and PH_2 units. The cationic part of **6** reveals P-B bond lengths of 1.929(2) and 1.947(2) Å. Similar B-P bond lengths have been found in the anion of **6** (exocyclic part: 1.927(3) – 1.964(3) Å and within the ring 1.930(3) – 1.952(2) Å). For the neutral cyclic aminoborane tetramer, B-(cyclotriborazanyl)amineborane a related structural motif was recently reported.[30] In contrast to **6** this compound has a NH_2-BH_3 moiety, which is connected to an endocyclic B atom.

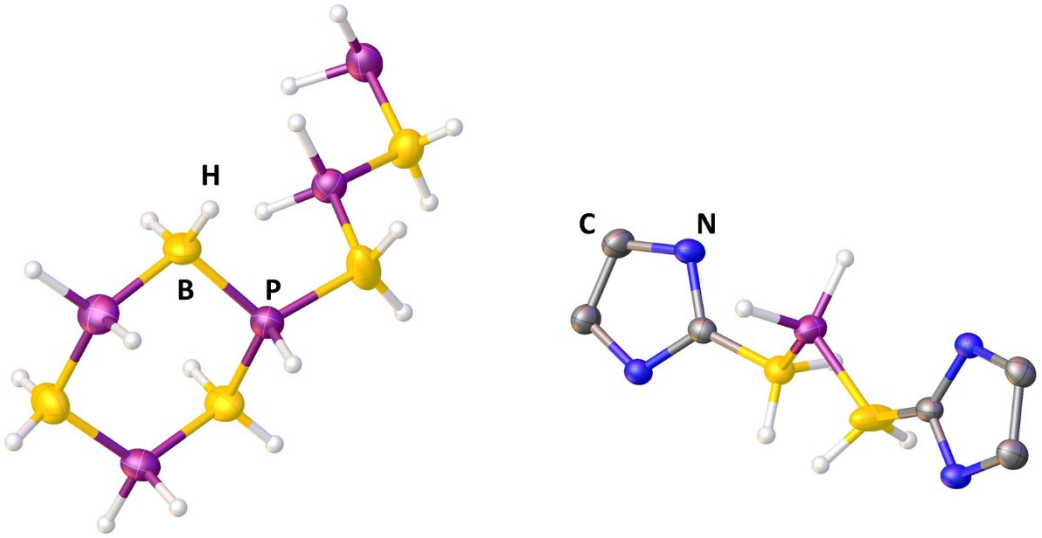

Figure 3.3. Molecular structure of **6** in the solid state. Thermal ellipsoids are set at 50% probability. The hydrogen atoms at the carbon atoms and the dipp groups on the carbenes are omitted for clarity.

3.3 Conclusion

The results show that the parent pnictogenylboranes **1a** and **1b** are valuable starting materials for the generation of mixed anionic Group 13/15 chain compounds. For the first time a rational synthetic approach was achieved for 3- and 5-membered chain compounds, which could be structurally characterized as unprecedented linear, anionic compounds. Furthermore the first examples of parent compounds of anionic arsanylboranes have synthesized. These unique Group 13/15 compounds represent the anionic counterparts of the recently reported cationic species.[13] In comparison to them the compounds **2**-**6** are distinctly more sensitive, but stable under inert conditions. They represent promising starting materials for the preparation of extended mixed Group 13/15 element chain compounds, cycles and polymers.

3.4 References

[1] a) M. Baudler, *Angew. Chem. Int. Ed. Engl.* **1982**, *21*, 492-512; *Angew. Chem.* **1982**, *94*, 520-539; b) M. Baudler, *Angew. Chem. Int. Ed. Engl.* **1987**, *26*, 419-441; *Angew. Chem.* **1987**, *99*, 429-451; c) M. Baudler, K. Glinka, *Chem. Rev.* **1993**, *93*, 1623-1667; d) M. Baudler, K. Glinka, *Chem. Rev.* **1994**, *94*, 1273-1297; e) H. G. von Schnering, W. Hönle, *Chem. Rev.* **1988**, *88*, 243-273; f) R. Wolf, S. Gomes-Ruiz, J. Reinhold, W. Boehlmann, E. Hey-Hawkins, *Inorg. Chem.* **2006**, *45*, 9107-9113; g) R. Wolf. E. Hey-Hawkins, *Z. Anorg. Allg. Chem.* **2006**, *632*, 727-734; h) R. Wolf, E. Hey-Hawkins, *Chem. Commun.* **2004**, 2626-2627; i) R. Wolf, A. Schisler, P. Loennecke, C. Jones, E. Hey-Hawkins, *Eur. J. Inorg. Chem.* **2004**, 3277-3286; j) I. Jevtovikj, P. Könnecke, E. Hey-Hawkins, *Chem. Commun.* **2013**, *49*, 7355-7357.

[2] a) C. A. Dyker, N. Burford, *Chem. Asian J.* **2008**, *3*, 28–36; b) A. P. M. Robertson, P. A. Gray, N. Burford, *Angew. Chem. Int. Ed.* **2014**, *53*, 6050-6069; *Angew. Chem.* 2014, *126*, 6162-6182; c) S. S. Chitnis, E. MacDonald, N. Burford, U. Werner-Zwanziger, R. McDonald, *Chem. Commun.* **2012**, *48*, 7359-7361; d) Y.-Y. Carpenter, C. A. Dyker, N. Burford, M. D. Lumsden, A. Decken, *J. Am. Chem. Soc.* **2008**, *130*, 15732-15741; e) J. J. Weigand, N. Burford, A. Decken, *Eur. J. Inorg. Chem.* **2007**, 4868-4872; f) S. D. Riegel, N. Burford, M. D. Lumsden, A. Decken, *Chem. Commun.* **2007**, 4668-4670; g) C. A. Dyker, S. D. Riegel, N. Burford, M. D. Lumsden, A. Decken, *J. Am. Chem. Soc.* **2007**, *129*, 7464-7474; h) C. A. Dyker, N. Burford, M. D. Lumsden, A. Decken, *J. Am. Chem. Soc.* 2006, *128*, 9632-9633; i) N. Burford, C. A. Dyker, M. Lumsden, A. Decken, *Angew. Chem. Int. Ed.* **2005**, *44*, 6196-6199; *Angew. Chem.* **2005**, *117*, 6352-6355; j) N. Burford, C. A. Dyker, A. Decken, *Angew. Chem. Int. Ed.* **2005**, 44, 2364-2367; *Angew. Chem.* **2005**, *117*, 2416-2419.

[3] a) M. Donath, M. Bodensteiner, J. J. Weigand, *Chem. Eur. J.* **2014**, *20*, 17306-17310; b) M. H. Holthausen, J. J. Weigand, Chem. Soc. Rev. 2014, 43, 6639-6657; c) K.-O. Feldmann, J. J. Weigand, *Angew. Chem. Int. Ed.* **2012**, *51*, 7545-7549; *Angew. Chem.* **2012**, *124*, 7663-7667; d) M. Donath, E. Conrad, P. Jerabek, G. Frenking, R. Fröhlich, N. Burford, J. J. Weigand, *Angew. Chem. Int. Ed.* **2012**, *51*, 2964-2967; *Angew. Chem.* **2012**, *124*, 3018-3021; e) J. J.Weigand, N. Burford, M. D. Lumsden, A. Decken, *Angew. Chem. Int. Ed.* **2006**, *45*, 6733-6736; *Angew. Chem.* **2006**, *118*, 6885-6889; f) J. J. Weigand, N. Burford, R. J. Davidson, T. S. Cameron, P. Seelheim, *J. Am. Chem. Soc.* **2009**, *131*, 17943-17953; g) J. J. Weigand, M. Holthausen, *J. Am. Chem. Soc.* **2009**, *131*, 14210–14211; h) J. J. Weigand, M. Holthausen, R. Fröhlich, *Angew. Chem. Int. Ed.* **2009**, *48*, 295-298; *Angew. Chem.* **2009**, *121*, 301-304; i) J. J. Weigand, N. Burford, S. Riegel, A. Decken, *J. Am. Chem. Soc.* **2007**, *129*, 7969-7976.

[4] a) $B_8(NMe_2)_{10}$: K. H. Hermannsdörfer, E. Metejcikova, H. Nöth, *Chem. Ber.* **1970**, *103*, 516-527; b) $B_4(NMe_2)_6$: G. Linti, D. Loderer, H. Nöth, K. Polborn, W. Rattay, *Chem. Ber.* **1994**, *127*, 1909-1922; c) $B_6(NMe_2)_6$: H. Nöth, H. Pommerening, *Angew. Chem. Int. Ed. Engl.* **1980**, *19*, 482-483; *Angew. Chem.* **1980**, *92*, 481-482; d) B_4R_4: H. Braunschweig, Q. Ye, A. Vargas, R. D. Dewhurst, K. Radacki, A. Damme, *Nat. Chem.* **2012**, *4*, 563 -567; e) In_6: M. S. Hill, P. B. Hitchcock, R. Pongtavornoinyo, *Science* **2006**, *311*, 1904-1907.

[5] a) A. Staubitz, A. P. M. Robertson, M. E. Sloan, I. Manners, *Chem. Rev.* **2010**, *110*, 4023-4078; b) A. Staubitz, A. P. M. Robertson, I. Manners, *Chem. Rev.* **2010**, *110*, 4079-4124.

[6] a) C. Marquardt, T. Jurca, K.-C. Schwan, A. Stauber, A. V. Virovets, G. R. Whittell, I. Manners, M. Scheer, *Angew. Chem. Int. Ed.* **2015**, *54*, 13782-13786; *Angew. Chem.* **2015**, *127*, 13986-13991; b) A. Stauber, T. Jurca, C. Marquardt, M. Fleischmann, M. Seidl, G. R. Whittell, I. Manners, M. Scheer, *Eur. J. Inorg. Chem.* **2016**, 2684–2687.

[7] a) B. Kaufmann, H. Nöth, R. T. Paine, K. Polborn, M. Thomann, *Angew. Chem. Int. Ed. Engl.* **1993**, *32*, 1446-1448; *Angew. Chem.* **1993**, *105*, 1534-1536; b) H. V. Rasika Dias, P. P. Power, *J. Am. Chem. Soc.* **1989**, *111*, 144-148; c) H. Dorn, R. A. Singh, J. A. Massey, A. J. Lough, I. Manners, *Angew. Chem. Int. Ed.* **1999**, *38*, 3321-3323; *Angew. Chem.* **1999**, *111*, 3540-3543; d) H. Dorn, R. A. Singh, J. A. Massey, J. M. Nelson, C. A. Jaska, A. J. Lough, I. Manners, *J. Am. Chem. Soc.* **2000**, *122*, 6669-6678; e) M. E. Sloan, T. J. Clark, I. Manners, *Inorg. Chem.* **2009**, *48*, 2429-2435.

[8] T. Oshiki, T. Imamoto, *Bull. Chem. Soc. Jpn.* **1990**, *63*, 2846-2849.

[9] a) U. Vogel, A. Y. Timoshkin, M. Scheer, *Angew. Chem. Int. Ed.* **2001**, *40*, 4409-4412; *Angew. Chem.* **2001**, *113*, 4541-4544; b) K.-C. Schwan, A. Timoshkin, M. Zabel, M. Scheer, *Chem. Eur. J.* **2006**, *12*, 4900–4908; c) U. Vogel, A. Y. Timoshkin, K.-C. Schwan, M. Bodensteiner, M. Scheer, *J. Organomet. Chem.* **2006**, *691*, 4556-4564.

[10] a) E. Rivard, *Chem. Soc. Rev.* **2016**, *45*, 989-1003; b) A. K. Swarnakar, C. Hering-Junghans, K. Nagata, M. J. Ferguson, R. McDonald, N. Tokitoh, E. Rivard, *Angew. Chem. Int. Ed.* **2015**, *54*, 10666-10669; *Angew. Chem.* **2015**, *127*, 10812-10816; c) A. C. Malcolm, K. J. Sabourin, R. McDonald, M. J. Ferguson, E. Rivard, *Inorg. Chem.* **2012**, *51*, 12905-12916.

[11] C. Marquardt, A. Adolf, A. Stauber, M. Bodensteiner, A. V. Virovets, A. Y. Timoshkin, M. Scheer, *Chem. Eur. J.* **2013**, *19*, 11887-11891.

[12] C. Thoms, C. Marquardt, M. Bodensteiner, M. Scheer, *Angew. Chem. Int. Ed.* **2013**, *52*, 5150-5154; *Angew. Chem.* **2013**, *125*, 5254-5259.

[13] C. Marquardt, C. Thoms, A. Stauber, G. Balazs, M. Bodensteiner, M. Scheer, *Angew. Chem. Int. Ed.* **2014**, *53*, 3727-3730; *Angew. Chem.* **2014**, *126*, 3801-3804, and references herein.

[14] a) T. Costa, H. Schmidbaur, *Chem. Ber.* **1982**, *115*, 1374-1378; b) T. Miyazaki, M. Sugawara, H. Danjo, T. Imamoto, *Tetrahedron Lett.* **2004**, *45*, 9341-9344; c) D. R. Martin, C. M. Merkel, J. P. Ruiz, *Inorg. Chim. Acta* **1985**, *100*, 293-297; d) K. Owsianik, R. Chauvin, A. Balińska, M. Wieczorek, M. Cypryk, M. Mikołajczyk, *Organometallics* **2009**, *28*, 4929-4937; e) H. Schmidbaur, T. Wimmer, G. Reber, G. Müller, *Angew. Chem. Int. Ed. Engl.* **1988**, *27*, 1071-1074; *Angew. Chem.* **1988**, *100*, 1135-1138.

[15] B. Kaufmann, R. Jetzfellner, E. Leissring, K. Issleib, H. Noeth, M. Schmidt, *Chem. Ber.* **1997**, *130*, 1677-1692.

[16] a) M. Baudler, C. Block, *Z. Anorg. Allg. Chem.* **1988**, *567*, 7-12; b) M. Baudler, C. Block, H. Budzikiewicz, H. Münster, *Z. Anorg. Allg. Chem.* **1989**, *569*, 7-15.

[17] E. Mayer, *Angew. Chem. Int. Ed. Engl.* **1971**, *10*, 416-417; *Angew. Chem.* **1971**, *83*, 440-440.

[18] a) F. Dornhaus, M. Bolte, H.-W. Lerner, M. Wagner, *Eur. J. Inorg. Chem.* **2006**, 5138-5147; b) H. C. Miller, E. L. Muetterties, US 2999864, **1961**.

[19] a) R. E. Hester, E. Mayer, *Spectrochim. Acta Mol. Biomol. Spectrosc.* **1967**, *23*, 2218-2220; b) M. R. Anstey, M. T. Corbett, E. H. Majzoub, J. G. Cordaro, *Inorg. Chem.* **2010**, *49*, 8197-8199; c) E. Mayer, A. W. Laubengayer, *Monatsh. Chem.* **1970**, *101*, 1138-1144; d) F. Dornhaus, M. Bolte, H.-W. Lerner, M. Wagner, *Eur. J. Inorg. Chem.* **2006**, 1777-1785; e) K. X. Bhattacharyya, S. Dreyfuss, N. Saffon-Merceron, N. Mézailles, *Chem. Commun.* **2016**, *52*, 5179-5182.

[20] A. B. Burg, *Inorg. Chem.* **1978**, *17*, 593-599.

[21] L. D. Schwartz, P. C. Keller, *Inorg. Chem.* **1973**, *12*, 947-949.

[22] H.-G. von Schnering, M. Somer, M. Hartweg, K. Peters, *Angew. Chem. Int. Ed. Engl.* **1990**, *29*, 65-67; *Angew. Chem.* **1990**, *102*, 63-64.

[23] In contrast, reaction of **1a** with $KAsH_2$ requires prolonged reaction times and results in a mixture of unconsumed **1a**, **2** and the product **3**.

[24] Only traces of the used excess of **1b** can be identified in the ^{11}B NMR spectrum.

[25] Compound **4**$(thf)_2$ is highly disordered in the solid state. Four independent molecules can be found in the unit cell. The values of the highest occupied anion (81%) are used for the discussion.

See Supporting Information for further Information.

[26] Rotational disorder along the E-B-axis leads to the different conformations. Higher occupied conformations are shown here.

See Supporting Information for further Information.

[27] See Supporting Information for further Information

[28] K.-C. Schwan, A. Adolf, C. Thoms, M. Zabel, Al. Y. Timoshkin, M. Scheer, Dalton Trans. 2008, 5054-5058.

[29] $ClBH_2$-NMe_3 is a starting material for H_2P-BH_2-NMe_3 (see Ref. [7]). Reaction with H_2P-BH_2-NMe_3 generated without $ClBH_2$-NMe_3 does not yield **6**. However, the formation of **6** is reproducible also with different batches of H_2P-BH_2-NMe_3 generated from $ClBH_2$-NMe_3.

[30] H. A. Kalviri, F. Gärtner, G. Ye, I. Korobkova, R. T. Baker, *Chem. Sci.* **2015**, *6*, 618-624.

3.5 Supporting Information

3.5.1 Synthetic Procedures

All manipulations were performed under an atmosphere of dry argon using standard glovebox and Schlenk techniques. All solvents are degassed and purified by standard procedures. The compounds H_2E-BH_2-NMe_3 (E = P, As),[1] $ClBH_2$-NMe_3,[2] $NaPH_2$,[3] $KAsH_2$,[4] and NHC^{dipp}[5] were prepared according to literature procedures.

The NMR spectra were recorded on either an Avance 400 spectrometer (^{1}H: 400.13 MHz, ^{31}P: 161.976 MHz, ^{11}B: 128.378 MHz, ^{13}C{^{1}H}: 100.623 MHz) with δ [ppm] referenced to external $SiMe_4$ (^{1}H, ^{13}C), H_3PO_4 (^{31}P), $BF_3{\cdot}Et_2O$ (^{11}B).

IR spectra were recorded on a DIGILAB (FTS 800) FT-IR spectrometer. All mass spectra were recorded on a ThermoQuest Finnigan TSQ 7000 (ESI-MS) or a Finnigan MAT 95 (FDMS and EI-MS).

The C, H, N analyses were measured on an Elementar Vario EL III apparatus.

General remarks for C, H, N analyses: C, H, N analyses were carried out repeatedly. Different amounts of coordinating THF have been found in nearly all cases. Total removal of the THF was not always possible, however C, H, N analyses are in good agreement with the expected values considering a varying THF content (0.2 % tolerance).

Synthesis of $[Na(C_{12}H_{24}O_6)(thf)_2][H_2P$-$BH_2$-$PH_2]$ (**2**$(thf)_2$):

A solution of 53 mg (0.50 mmol) H_2P-BH_2-NMe_3 in 1 mL toluene is added to a suspension of 30 mg (0.53 mmol) $NaPH_2$ in 20 ml THF. After sonication of the mixture for 2.5 h, the solution is filtrated onto 132 mg (0.5 mmol) solid $C_{12}H_{24}O_6$ (18-crown-6). The solution is layered with 60 mL of *n*-hexane. **2**$(thf)_2$ crystallizes at 4 °C as colourless blocks. The crystals are separated and washed with cold *n*-hexane (0 °C, 3 × 5 mL).

Yield of $[Na(C_{12}H_{24}O_6)][H_2P$-$BH_2$-$PH_2]$ (**2**): 103 mg (56 %).

^{1}H NMR (THF-d_8, 25 °C): δ = 0.93 (d, $^1J_{H,P}$ = 172 Hz, 4H, PH_2), 1.09 (qt, $^1J_{H,B}$ = 99 Hz, 2H, BH_2), 3.64 (s, 24H, $C_{12}H_{24}O_6$).

^{31}P NMR (THF-d_8, 25 °C): δ = -175.0 (tm, $^1J_{H,P}$ = 172 Hz, br, PH_2).

^{31}P{^{1}H} NMR (THF-d_8, 25 °C): δ = -175.0 (q, $^1J_{B,P}$ = 26 Hz, PH_2).

^{11}B NMR (THF-d_8, 25 °C): δ = -34.7 (tt, $^1J_{B,P}$ = 26 Hz, $^1J_{B,H}$ = 99 Hz, BH_2).

^{11}B{^{1}H} NMR (THF-d_8, 25 °C): δ = -34.7 (t, $^1J_{B,P}$ = 26 Hz, BH_2).

^{13}C NMR (THF-d_8, 25 °C): δ = 70.6 (s, $C_{12}H_{24}O_6$).

IR (KBr): $\tilde{\nu}$ = 2900 (vs, CH), 2870 (s, CH), 2825 (m), 2796 (m), 2747 (w), 2747 (w), 2712 (w), 2690 (w), 2326 (s, br, BH), 2311 (s, br, BH), 2270 (s, PH), 2253 (s, PH), 2141 (w), 1979 (w), 1931 (w), 1887 (w), 1839 (vw), 1471 (m), 1455 (m), 1435 (w), 1410 (vw), 1352 (s), 1283 (m), 1250 (m), 1237 (m), 1109 (vs, CO), 1075 (m), 1058 (w), 966 (vs), 841 (m), 765 (w), 711 (w), 652 (w), 531 (w).

ESI-MS (THF) anion: *m/z* = 79 (100 %, $[H_2P\text{-}BH_2\text{-}PH_2]^-$).

ESI-MS (THF) cation: *m/z* = 287 (100 %, $[Na(C_{12}H_{24}O_6)]^+$), 653 (8% $([Na(C_{12}H_{24}O_6)]^+)_2[H_2P\text{-}BH_2\text{-}PH_2]^-$).

Elemental analysis (%) calculated for $C_{12}H_{30}BNaO_6P_2$ (**2**): C: 39.32, H: 8.26; found: C: 39.30, H: 8.40.

Synthesis of $[K(C_{12}O_6H_{24})][H_2As\text{-}BH_2\text{-}AsH_2]$ (**3**):

A solution of 298 mg (2.0 mmol) $H_2As\text{-}BH_2\text{-}NMe_3$ in 2 mL toluene is added to a suspension of 254 mg (2.2 mmol) $KAsH_2$ in 20 ml THF. After sonication of the mixture for 8 h, the solution is filtrated onto 530 mg (2.0 mmol) solid $C_{12}O_6H_{24}$ (18-crown-6). The solution is layered with 60 mL of toluene. **3** crystallizes at 3 °C as colourless blocks. The crystals are separated and washed with cold toluene (-30 °C, 2 x 5 mL).

Yield of $[K(C_{12}O_6H_{24})][H_2As\text{-}BH_2\text{-}AsH_2]$: 685 mg (73%).

^{1}H NMR (THF-d_8, 25 °C): δ = 0.15 (s, 4H, AsH_2), 1.48 (q, $^1J_{H,B}$ = 106 Hz, 2H, BH_2), 3.64 (s, $C_{12}O_6H_{24}$).

^{11}B NMR (THF-d_8, 25 °C): δ = -34.5 (t, $^1J_{B,H}$ =106 Hz, BH2).

^{11}B{^{1}H} NMR (THF-d_8, 25 °C): δ = -34.5 (s, BH_2).

^{13}C{^{1}H} NMR (THF-d_8, 25 °C): δ = 72.0 (s, $C_{12}O_6H_{24}$).

IR (KBr): $\tilde{\nu}$ = 2899 (m, CH), 2825 (vw), 2352 (m, BH), 2044 (m, AsH), 1632 (vw), 1471 (w), 1351 (m), 1284 (vw), 1251 (w), 1106 (vs, CO), 962 (s), 839 (w), 689 (vw), 590 (vw), 526 (vw).

ESI-MS (THF) anion: *m/z* = 166.6 (100%, $[H_2As\text{-}BH_2\text{-}AsH_2]^-$), 88.7 (20%, $[H_2As\text{-}BH]^-$), 76.7 (6%, $[H_2As]^-$).

Elemental analysis (%) calculated for $C_{12}H_{30}O_6As_2BK$ (**3**): C: 30.65, H: 6.43; found: C: 30.93, H: 6.23.

Synthesis of $[Na(C_{12}O_6H_{24})(thf)_2][H_2P\text{-}BH_2\text{-}AsH_2]$ (**4**$(thf)_2$):

A solution of 97 mg (0.65 mmol) $H_2As\text{-}BH_2\text{-}NMe_3$ in 0.65 mL toluene is added to a suspension of 33 mg (0.5 mmol) $NaPH_2$ in 15 mL THF. After sonication of the mixture for 1 h, the crude product is precipitated in cold *n*-hexane (-30 °C) and washed with cold *n*-hexane (-30 °C, 2 x 5 mL). The supernatant is decanted off and the residue is solved in 20 mL of a 1:1 mixture of THF/toluene and filtrated on 121 mg (0.45 mmol) $C_{12}O_6H_{24}$ (18-crown-6). The solution is layered with 60 mL of *n*-hexane. **4**$(thf)_2$ crystallizes at -30 °C as pale brown blocks. The crystals are separated and washed with cold *n*-hexane (-30 °C, 2 x 5 mL).

Yield of $[Na(C_{12}O_6H_{24})][H_2P\text{-}BH_2\text{-}AsH_2]$ (**4**): 156 mg (76%).

^{1}H NMR (THF-d_8, 25°C): δ = -0.04 (s, br, 2H, AsH_2), 1.12 (d, $^1J_{H,P}$ = 173 Hz, 2H, PH_2), 1.29 (q, $^1J_{H,B}$ = 102 Hz, 2H, BH_2), 3.64 (s, $C_{12}O_6H_{24}$).

^{31}P NMR (THF-d_8, 25°C): δ = -174.8 (tm, $^1J_{P,H}$ = 173 Hz, PH_2).

^{31}P{^{1}H} NMR (THF-d_8, 25°C): δ = -174.8 (q, $^1J_{P,B}$ = 27 Hz, PH_2).

^{11}B NMR (THF-d_8, 25°C): δ = -34.4 (td, $^1J_{B,P}$ = 27 Hz, $1J_{B,H}$ = 102 Hz, BH_2).

^{11}B{^{1}H} NMR (THF-d_8, 25°C): δ = -34.4 (d, $^1J_{B,P}$ = 27 Hz, BH_2).

^{13}C{^{1}H} NMR (THF-d_8, 25°C): δ = 69.7 (s, $C_{12}O_6H_{24}$).

IR (KBr): $\tilde{\nu}$ = 2900 (s, CH), 2825 (w, CH), 2796 (vw, CH), 2746 (vw, CH), 2712 (vw, CH), 2690 (vw, CH), 2343 (s, BH), 2324 (s, BH), 2248 (m, PH), 2052 (m, AsH), 1627 (vw), 1472 (m), 1454 (w), 1434 (vw), 1351 (s), 1283 (w), 1251 (m), 1107 (vs, CO), 1058 (w), 964 (s), 838 (m), 803 (vw), 744 (vw), 609 (vw), 527 (vw).

ESI-MS (THF) anion: *m*/*z* = 122.8 (100%, $[H_2P\text{-}BH_2\text{-}AsH_2]^-$), 168.8 (32%, $[H_2P\text{-}BH_2\text{-}AsH_2\text{-}BH_2\text{-}PH_2]^-$).

Elemental analysis (%) calculated for $C_{12}H_{30}O_6AsBNaP$ (**4**): C: 35.15, H: 7.37; found: C: 35.16, H: 7.22.

Synthesis of $[Na(C_{12}O_6H_{24})(thf)_2][H_2As\text{-}BH_2\text{-}PH_2\text{-}BH_2\text{-}AsH_2]$ (**5**$(thf)_2$):

A solution of 626 mg (4.2 mmol) $H_2As\text{-}BH_2\text{-}NMe_3$ in 4 mL toluene is added to a suspension of 110 mg (2.0 mmol) $NaPH_2$ in 20 ml THF. After sonication of the mixture for 7.5 h, the solution is filtrated onto 502 mg (1.9 mmol) solid $C_{12}O_6H_{24}$ (18-crown-6). The solution is layered with 60 mL of *n*-hexane. (**5**$(thf)_2$) crystallizes at -30 °C as colourless blocks. The crystals are separated and washed with cold *n*-hexane (-30 °C, 2 x 5 mL).

Yield of $[Na(C_{12}O_6H_{24})(thf)_{0.45}][H_2As\text{-}BH_2\text{-}PH_2\text{-}BH_2\text{-}AsH_2]$ (**5**$(thf)_{0.45}$): 844 mg (83%).

^{1}H NMR (THF-d_8, 25 °C): δ = -0.02 (m, 4H, AsH_2), 1.13 (q, $^1J_{H,B}$ = 105 Hz, 4H, BH_2), 3.60 (dm, $^1J_{H,P}$ = 307 Hz, 2H, PH_2), 3.62 (s, $C_{12}O_6H_{24}$).

^{31}P NMR (THF-d_8, 25 °C): δ = -56.0 (tm, $^1J_{P,H}$ = 307 Hz, PH_2).

^{31}P{^{1}H} NMR (THF-d_8, 25 °C): δ = -56.0 (h, $^1J_{P,B}$ = 58 Hz, PH_2).

^{11}B NMR (THFd_8, 25°C): δ = -37.4 (td, $^1J_{B,H}$ =105 Hz, $^1J_{B,P}$ = 58 Hz, BH_2).

^{11}B{^{1}H} NMR (THF-d_8, 25°C): δ = -37.4 (d, $^1J_{B,P}$ = 58 Hz, BH_2).

^{13}C{^{1}H} NMR (THF-d_8, 25 °C): δ = 70.6 (s, $C_{12}O_6H_{24}$).

IR (KBr): = 2946 (m), 2901 (s, CH), 2862 (s), 2828 (s), 2797 (m), 2748 (w), 2714 (w), 2691 (vw), 2380 (s, BH), 2355 (s, BH), 2331 (s, BH), 2220 (w, PH), 2087 (s, AsH), 2052 (s, AsH), 1981 (w), 1930 (vw), 1795 (vw), 1617 (vw), 1472 (s), 1452 (m), 1435 (w), 1352 (vs), 1284 (m), 1248 (s), 1236 (m), 1109 (vs, CO), 965 (vs), 908 (s), 837 (s), 810 (m), 762 (w), 659 (w), 618 (vw), 570 (vw), 531 (w), 489 (vw).

ESI-MS (THF) anion: *m/z* = 212.7 (100%, $[H_2As\text{-}BH_2\text{-}PH_2\text{-}BH_2\text{-}AsH_2]^-$), 122.8 (40%, $[H_2As\text{-}BH\text{-}PH_2]^-$).

Elemental analysis (%) calculated for $C_{12}H_{34}As_2B_2NaO_6P(thf)_{0.45}$ (**5**$(thf)_{0.45}$): C: 31.14, H: 7.12; found: C: 31.48, H: 6.81.

Reaction of NHC^{dipp} with $H_2P\text{-}BH_2\text{-}NMe_3$ in the presence of $ClBH_2\text{-}NMe_3$:

To a solution of 400 mg NHC^{dipp} (1.03 mmol) in 20 ml toluene, a solution of 105 mg (1 mmol) $H_2P\text{-}BH_2\text{-}NMe_3$ in 10 mL toluene is added drop wise at room temperature. After the mixture was stirred for 30 min, it is refluxed for further 3 h. After cooling to room temperature the solution is layered with *n*-pentane. Colourless needles of $[NHC^{dipp}\text{-}BH_2\text{-}PH_2\text{-}BH_2\text{-}NHC^{dipp}]^+[B_5P_5H_{19}]^-$ (**6)** can be obtained by storing the solution for 4 months.

Yield of **6**: 30 mg (20%);

^{31}P NMR (CD_3CN, 25 °C): δ = -125.0 (t, br, cation).

^{31}P{^{1}H} NMR (CD_3CN, 25 °C): δ = -125.0 (s, br, cation).

In the $^{11}B\{^1H\}$ and $^{31}P\{^1H\}$ NMR spectra many broad and overlapping signals are observed. An accurate assignment of the signals is not possible due to the broadness of the signals and the very complex spin system leading to sophisticated coupling pattern.

ESI-MS (CH_3CN) cation: *m/z* = 835.6 (100%, $[NHC^{dipp}\text{-}BH_2\text{-}PH_2\text{-}BH_2\text{-}NHC^{dipp}]^+$).

ESI-MS (CH_3CN) anion: *m/z* = 227.9 (100%, $[B_5P_5H_{19}]^-$).

3.5.2 X-ray Diffraction Analysis

The X-ray diffraction experiments were performed on either a SuperNova diffractometer with Atlas CCD detector (**2**$(thf)_2$, **6**) or a GV50 diffractometer with TitanS2 detector (**3, 4**$(thf)_2$, **5**$(thf)_2$) from Rigaku Oxford Diffraction (formerly Agilent Technologies) applying Cu-*Kα* radiation (λ = 1.54178 Å) or Cu-*Kβ* radiation (λ = 1.39222 Å) in the case of **4**(thf)2. The measurements were performed at 123 K. Crystallographic data together with the details of the experiments are given in the Table S 3.1 - Table S 3.3 (see below).

Absorption corrections were applied semi-empirically from equivalent reflections or analytically (SCALE3/ABSPACK algorithm implemented in CrysAlisPro software by Rigaku Oxford Diffraction).[6]

All structures were solved using SIR97[7],SHELXT[8] and OLEX.[9c] Least square refinements against *F*2 in anisotropic approximation were done using SHELXL.[8] The hydrogen positions of the methyl groups were located geometrically and refined riding on the carbon atoms. Hydrogen atoms belonging to BH_2, PH_2 and AsH_2 groups were located from the difference Fourier map and refined without constraints (**3**, **6**) or with restrained E-H distances (**2**$(thf)_2$, **4**$(thf)_2$, **5**$(thf)_2$). **4**$(thf)_2$ was processed with Cu-*Kβ* radiation (λ = 1.39222 Å) for reason of more available data and better resolution to allow the refinement of the very minor disordered structure, which further required positional and displacement parameter restraints.

Figures were created with OLEX.[9]

CCDC-1501380 (**2**), CCDC-1501381 (**3**), CCDC-1501382 (**4**), CCDC-1501383 (**5**), and CCDC-1501384 (**6**) contain the supplementary crystallographic data for this paper. These data can be obtained free of charge at www.ccdc.cam.ac.uk/conts/retrieving.html (or from the Cambridge Crystallographic Data Centre, 12 Union Road, Cambridge CB2 1EZ, UK; Fax: + 44-1223-336-033; e-mail: deposit@ccdc.cam.ac.uk).

3.5.3. Solid State Structures

$[Na(C_{12}H_{24}O_6)(thf)_2][H_2P\text{-}BH_2\text{-}PH_2]$ $(2(thf)_2)$:

2$(thf)_2$ crystallizes from a THF solution layered by the 3-4-fold amount of *n*-hexane at 4 °C as colourless blocks in the monoclinic space group *P*2*/c*. Figure S 3.1 shows the structure of **2**$(thf)_2$ in the solid state. Rotational disorder of H atoms on the P atoms results in a mixture of different conformers.

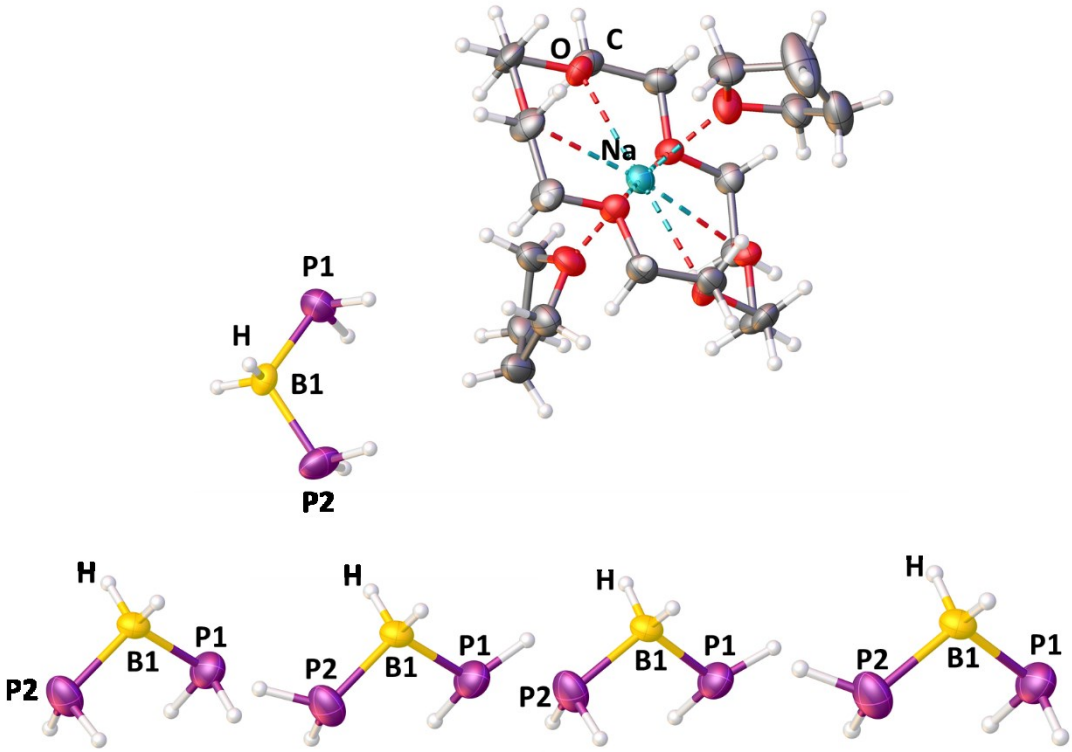

Figure S 3.1. Top: Molecular structure of **2**$(thf)_2$ in the solid state. Selected bond lengths [Å] and angles [°]: P1-B: 1.960(3), P2-B: 1.963(3), ∠(P1-B-P2): 110.4(1). Bottom: different possible conformers of the cationic part of **2**$(thf)_2$.

$[K(C_{12}H_{24}O_6)][H_2As\text{-}BH_2\text{-}AsH_2]$ (3):

3 crystallizes from a THF solution layered by the 3-4-fold amount of *n*-hexane at 3 °C as colourless blocks in the triclinic space group $P\overline{1}$. Figure S 3.2 shows the structure of **3** in the solid state. Disorder of AsH_2 atoms results in a mixture of different conformers. Direct contact of anion and cation leads to a 1D polymeric structure in the solid state.

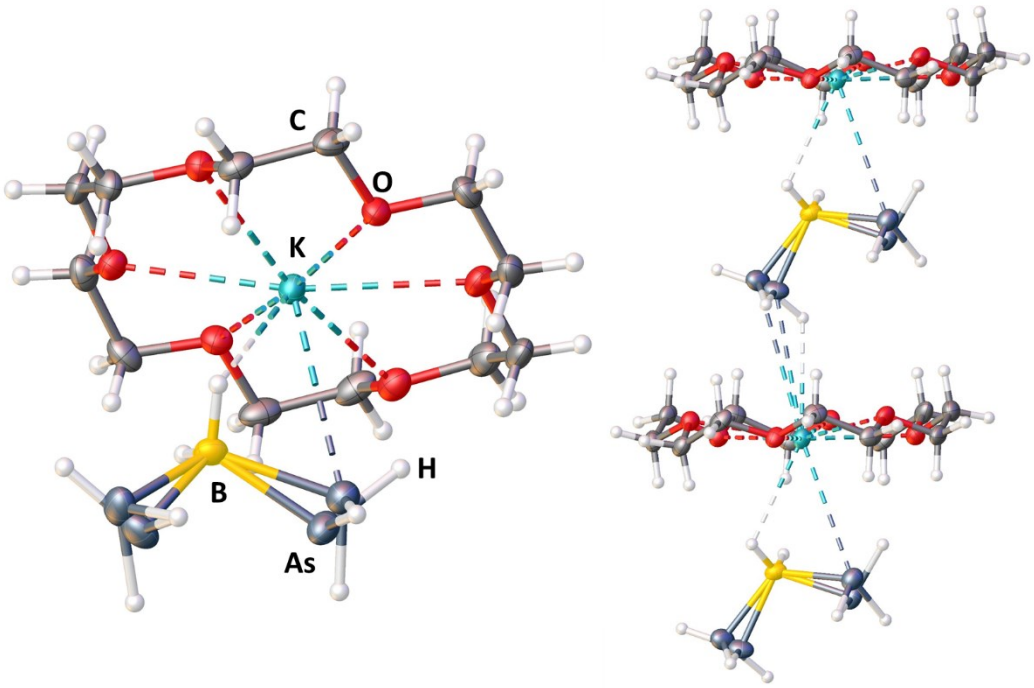

Figure S 3.2. Molecular structure of **3** in the solid state. Selected bond lengths [Å] and angles [°]: As-B: 2.062(2) – 2.126(2), ∠(A-B-As): 109.47(2) – 110.99(2).

$[Na(C_{12}H_{24}O_6)(thf)_2][H_2P\text{-}BH_2\text{-}AsH_2]$ (4)$(thf)_2$):

4$(thf)_2$ crystallizes from a THF/*n*-hexane mixture at -28 °C as brown blocks in the triclinic space group $P\overline{1}$. Figure S 3.3 shows the structure of **4**$(thf)_2$ in the solid state.

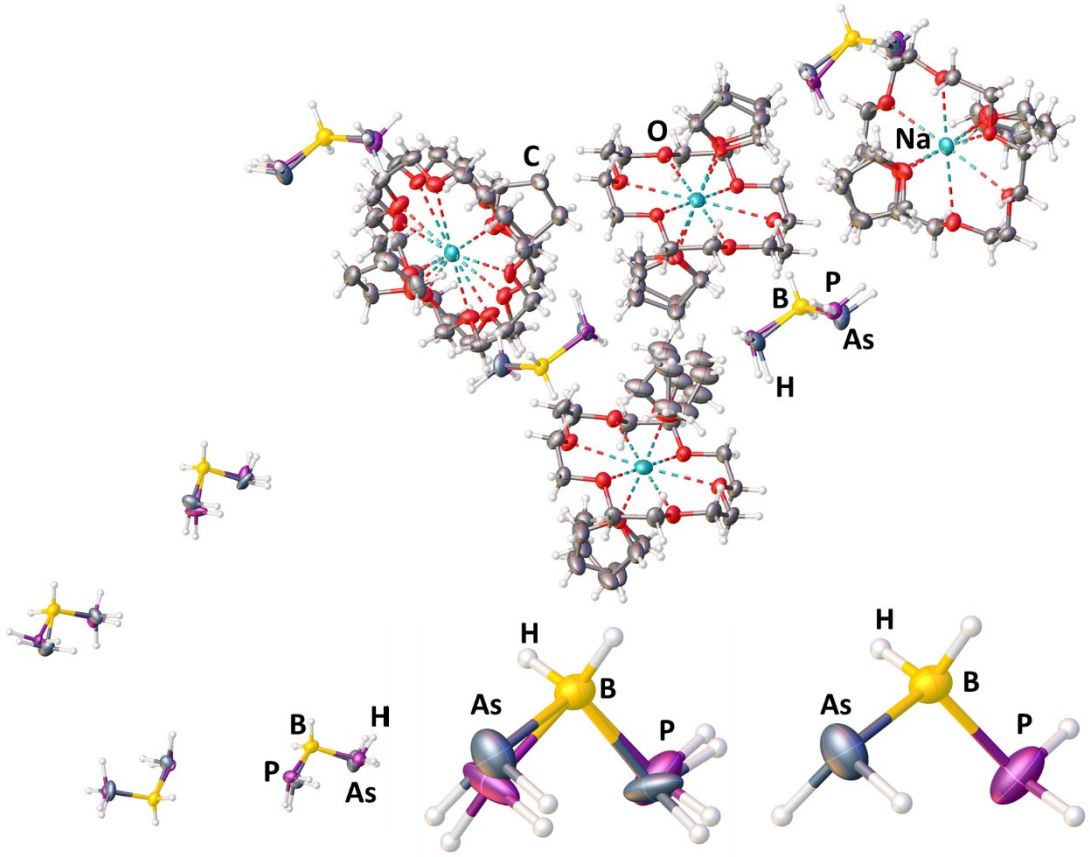

Figure S 3.3. Molecular structure of **4**$(thf)_2$ in the solid state. Selected bond lengths [Å] and angles [°]: P-B: 1.975(4), As-B: 2.050(2), ∠(P-B-As): 112.4(2). Top: highly disordered solid state structure of **4**$(thf)_2$; bottom, left: 4 independent anions middle: each position of the anions show superimposed anions with inverted P/As positions, right: highest occupied anion (81.2 %) used for discussion of values and conformation.

$[Na(C_{12}H_{24}O_6)(thf)_2][H_2As\text{-}BH_2\text{-}H_2P\text{-}BH_2\text{-}AsH_2]$ (5)$(thf)_2$):

5$(thf)_2$ crystallizes from a THF/*n*-hexane mixture at -28 °C as colourless plates in the monoclinic space group C*2/c*. Figure S 3.4 shows the structure of **5**$(thf)_2$ in the solid state.

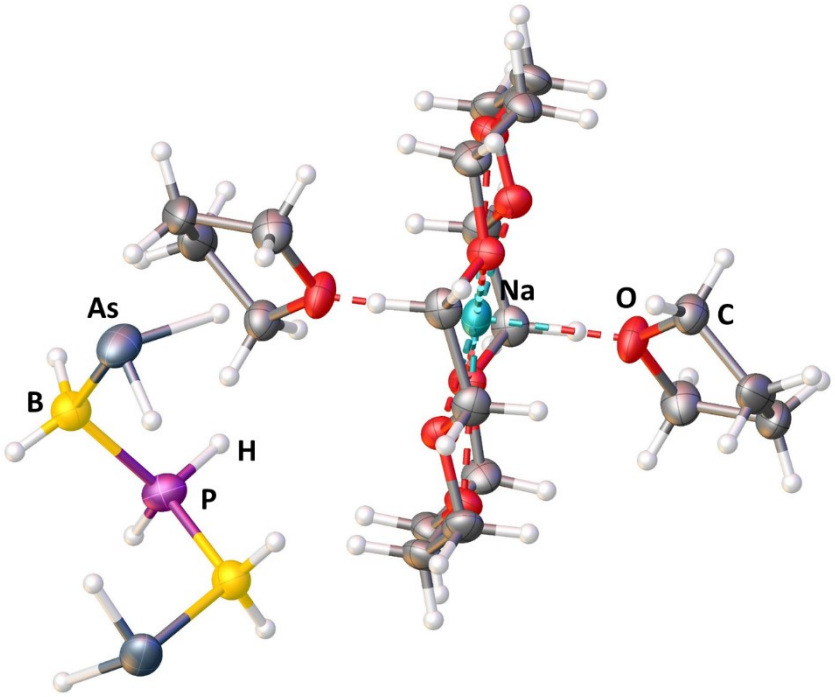

Figure S 3.4. Molecular structure of **5**$(thf)_2$ in the solid state. Selected bond lengths [Å] and angles [°]: As-B: 2.081(3), P-B: 1.947(3), ∠(As-B-P): 110.2(2), ∠(B-P-B): 122.9(2).

$[NHC^{dipp}\text{-}BH_2\text{-}PH_2\text{-}BH_2\text{-}NHC^{dipp}][B_5P_5H_{19}]$ (6):

6 crystallizes from a toluene solution layered *n*-hexane at room temperature as colourless blocks in the triclinic space group $P\overline{1}$. Figure S 3.5 and Figure S 3.6 show the structure of **6** in the solid state.

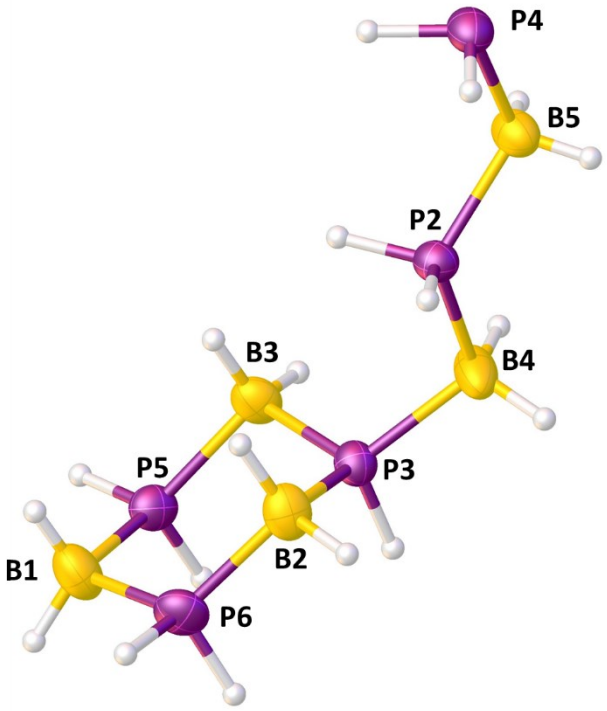

Figure S 3.5. Molecular structure of the anion of **6** in the solid state. Selected bond lengths [Å] and angles[°]: P2-B4: 1.939(3), P2-B5: 1.928(3), P3-B4: 1.948(3), P3-B3: 1.952(3), P3-B2: 1.941(3), P4-B5: 1.964(3), P5-B1: 1.941(3), P5-B3: 1.945(2), P6-B1: 1.930(3), P6-B2: 1.930(3), ∠(B4-P2-B5): 119.05(13), ∠(B2-P3-B3): 112.18(12), ∠(B2-P3-B4) 114.49(13), ∠(B3-P3-B4): 111.25(12), ∠(B1-P5-B3): 117.74(12), ∠(B1-P6-B2): 118.64(13), ∠(P5-B1-P6): 106.96(16), ∠(P3-B2-P69: 107.75(12), ∠(P3-B3-P5): 106.66(11), ∠(P2-B4-P3): 108.94(15), ∠(P2-B5-P4): 114.65(16).

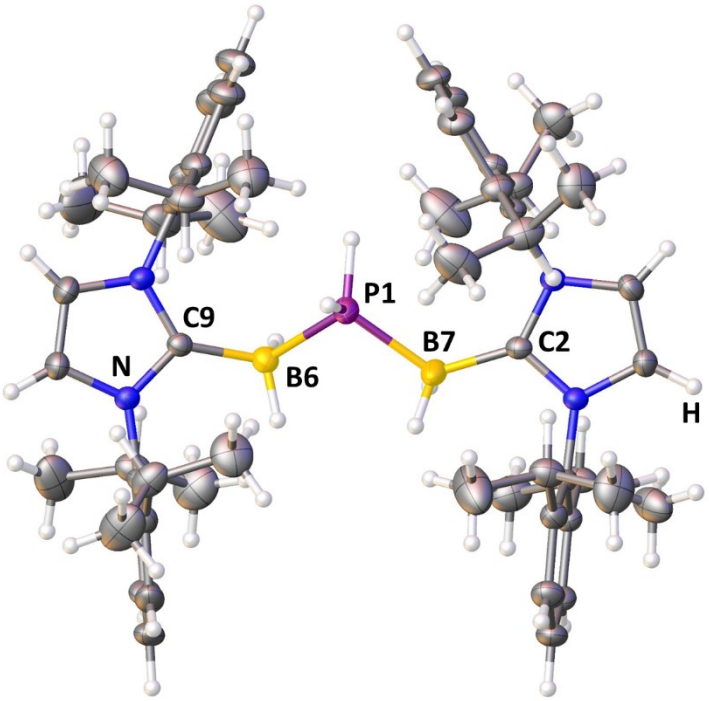

Figure S 3.6. Molecular structure of the cation of **6** in the solid state. Selected bond lengths [Å] and angles [°]: P1-B6: 1.948(2), P1-B7: 1.929(2), C2-B7: 1.589(3), C9-B6: 1.592(3), ∠(B6-P1-B7): 104.03(10), ∠(P1-B6-C9): 118.41(14), ∠(P1-B7-C2): 124.65(15).

3.5.4 Crystallographic Information

Table S 3.1. Crystallographic data for compounds **2**$(thf)_2$ and **3**.

	2$(thf)_2$	**3**
Emipirical formula	$C_{20}H_{46}BNaO_8P_2$	$C_{12}H_{30}As_2BKO_6$
Formula weight *M*	510.31 g/mol	470.11 g/mol
Crystal	colourless block	colourless block
Crystal size [mm³]	0.24 x 0.12 x 0.11	0.53 x 0.33 x 0.22
Temperature *T*	123(1) K	123(1) K
Cristal system	monoclinic	triclinic
Space group	*P2/c*	$P\bar{1}$
Unit cell dimensions	*a* = 11.0550(3) Å	*a* = 8.73491(20) Å
	b = 13.4206(3) Å	*b* = 9.3238(2) Å
	c = 19.7417(5) Å	*c* = 12.9306(3) Å
	α = 90°	*α* = 82.2216(19)°
	β = 102.592(2)°	*β* = 89.2853(18)°
	γ = 90°	*γ* = 80.7236(19)°
Volume *V*	2858.52(13) Å^3	1029.72(4) Å^3
Formula units *Z*	4	2
Absorption coefficient $\mu_{Cu\text{-}K\alpha}$	1.847 mm^{-1}	6.010 mm^{-1}
Density (calculated) ρ_{calc}	1.186 g/cm^3	1.516 g/cm^3
F(000)	1104	480
Theta range θ_{min} / θ_{max}	4.01 / 67.08°	3.45 / 73.80°
Absorption correction	gaussian	Gaussian
Index ranges	-12 < *h* < 12	-10 < *h* < 10
	-15 < *k* < 16	-11 < *k* < 11
	-23 < *l* < 23	-16 < *l* < 16
Reflections collected	31100	19920
Independent reflections [$I > 2\sigma(I)$]	3927 (R_{int} = 0.0554)	4077 (R_{int} = 0.0375)
Completeness to full θ	0.986	1.000
Transmission T_{min} / T_{max}	0.740 / 0.852	0.161 / 0.414
Data / restraints / parameters	5036 / 15 / 320	4149 / 0 / 344
Goodness-of-fit on F^2 *S*	1.037	1.106
Final *R*-values [$I > 2\sigma(I)$]	R_1 = 0.04858	R_1 = 0.0288
	wR_2 = 0.1085	wR_2 = 0.0765
Final *R*-values (all data)	R_1 = 0.0630	R_1 = 0.0292
	wR_2 = 0.1118	wR_2 = 0.0769
Largest difference hole	-0.36	-0.48
and peak $\Delta\rho$	0.42 eÅ^{-3}	0.39 eÅ^{-3}

Table S 3.2. Crystallographic data for compounds **4**$(thf)_2$ and **5**$(thf)_2$.

	4$(thf)_2$	**5**$(thf)_2$
Emipirical formula	$C_{20}H_{24}AsBNaO_8P$	$C_{20}H_{50}As_2B_2NaO_8P$
Formula weight *M*	554.26 g/mol	6.44.02 g/mol
Crystal	brown block	colourless block
Crystal size [mm³]	0.22 x 0.15 x 0.12	0.26 x 0.24 x 0.14
Temperature *T*	123(1) K	123(1)K
Cristal system	tricilinc	monoclinic
Space group	$P\bar{1}$	*C2/c*
Unit cell dimensions	*a* = 12.84130(19) Å	*a* = 17.5090(7) Å
	b = 21.2345(3) Å	*b* = 10.5819(3) Å
	c = 23.0230(3) Å	*c* = 18.5776(11) Å
	α = 70.6062(14)°	*α* = 90°
	β = 78.7402(13)°	*β* = 113.297(6)°
	γ = 76.7539(13)°	*γ* = 90°
Volume *V*	5715.36(16) Å^3	3161.4(3) Å^3
Formula units *Z*	8	4
Absorption coefficient $\mu_{Cu\text{-}K\alpha}$	1.288 mm^{-1}	3.536 mm^{-1}
Density (calculated) ρ_{calc}	1.948 g/cm^3	1.353 g/cm^3
F(000)	2352	1244
Theta range θ_{min} / θ_{max} / θ_{full}	3.87 / 74.27°	5.00 / 73.82°
Absorption correction	multi-scan	gaussian
Index ranges	-17 < *h* < 15	-21 < *h* < 15
	-29 < *k* < 26	-8 < *k* < 12
	-31 < *l* < 29	-22 < *l* < 23
Reflections collected	70208	4909
Independent reflections [$I > 2\sigma(I)$]	24111 (R_{int} = 0.0455)	2694 (R_{int} = 0.0128)
Completeness to full θ	0.994	0.983
Transmission T_{min} / T_{max}	0.787 / 1.000	0.532 / 0.698
Data / restraints / parameters	30676 / 1286 / 1677	3023 / 5 / 176
Goodness-of-fit on F^2 *S*	1.025	1.044
Final *R*-values [$I > 2\sigma(I)$]	R_1 = 0.0568	R_1 = 0.0347
	wR_2 = 0.1539	wR_2 = 0.0959
Final *R*-values (all data)	R_1 = 0.0709	R_1 = 0.0384
	wR_2 = 0.1684	wR_2 = 0.0990
Largest difference hole	-0.80	-0.89
and peak $\Delta\rho$	1.02 eÅ^{-3}	0.58 eÅ^{-3}

Table S 3.3. Crystallographic data for compound **6**.

	6
Emipirical formula	$C_{54}H_{97}B_7N_4P_6$
Formula weight *M*	1063.84 g/mol
Crystal	colourless block
Crystal size [mm³]	0.23 x 0.20 x 0.18
Temperature *T*	123(1) K
Cristal system	tricilinc
Space group	$P\bar{1}$
Unit cell dimensions	*a* = 10.7534(4) Å *b* = 16.4085(4) Å *c* = 19.562(5) Å *α* = 81.297(2)° *β* = 75.959(2)° *γ* = 89.987(2)°
Volume *V*	3307.68(15) Å^3
Formula units *Z*	2
Absorption coefficient $\mu_{Cu\text{-}K\alpha}$	1.764 mm^{-1}
Density (calculated) ρ_{calc}	1.068 g/cm^3
F(000)	1148
Theta range θ_{min} / θ_{max} / θ_{full}	3.32 / 70.78°
Absorption correction	analytical
Index ranges	-12 < *h* < 13 -19 < *k* < 16 -23 < *l* < 23
Reflections collected	24139
Independent reflections [$I > 2\sigma(I)$]	9745 (R_{int} = 0.0255)
Completeness to full θ	0987
Transmission T_{min} / T_{max}	0.751 / 0.930
Data / restraints / parameters	12250 / 0 / 756
Goodness-of-fit on F^2 *S*	1.068
Final *R*-values [$I > 2\sigma(I)$]	R_1 = 0.0461 wR_2 = 0.1310
Final *R*-values (all data)	R_1 = 0.0572 wR_2 = 0.1364
Largest difference hole and peak $\Delta\rho$	-0.456 0.878 eÅ^{-3}

3.5.5 NMR Spectroscopy

$[Na(C_{12}H_{24}O_6)(thf)_2][H_2P\text{-}BH_2\text{-}PH_2]$ $(2(thf)_2)$:

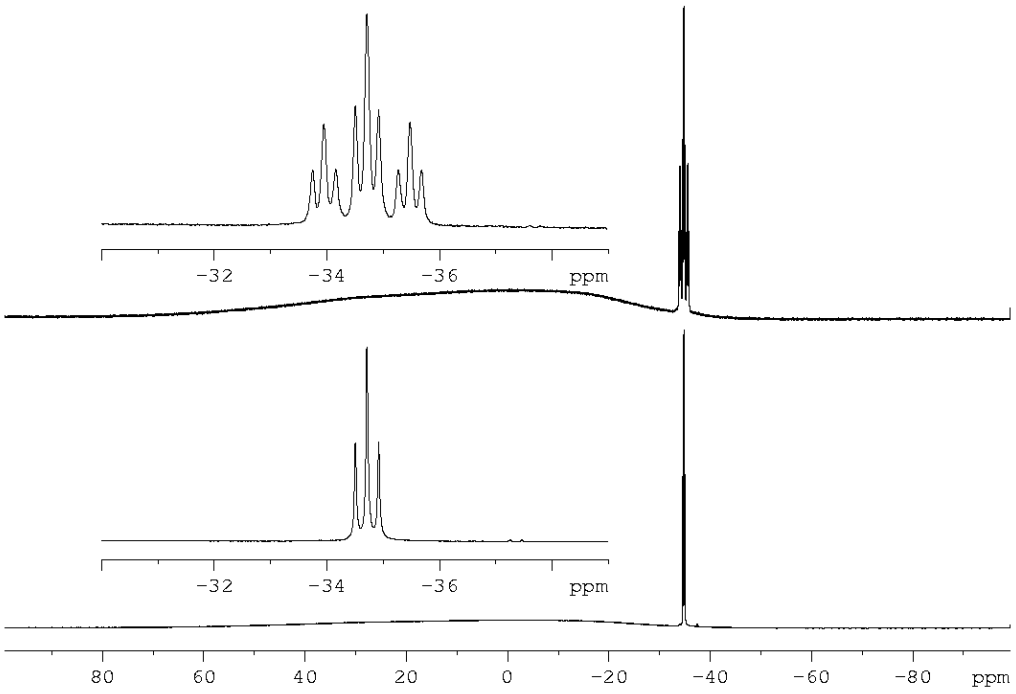

Figure S 3.7. $^{11}B\{^1H\}$ (bottom) and ^{11}B NMR spectrum (top) of **2** in THF-d_8.

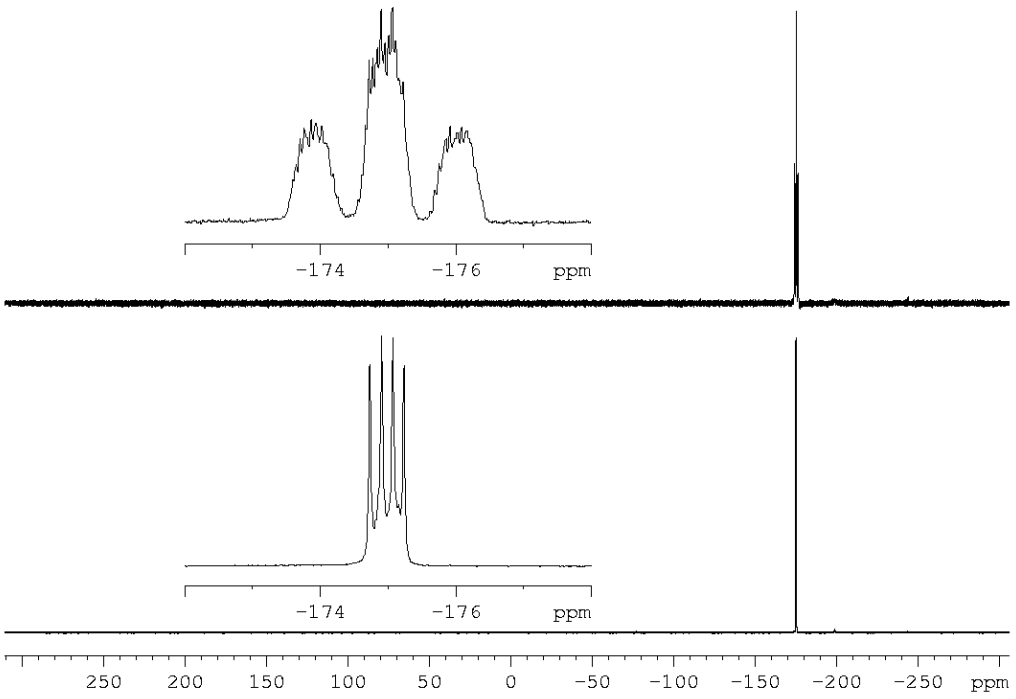

Figure S 3.8. $^{31}P\{^1H\}$ (bottom) and ^{31}P NMR spectrum (top) of **2** in THF-d_8.

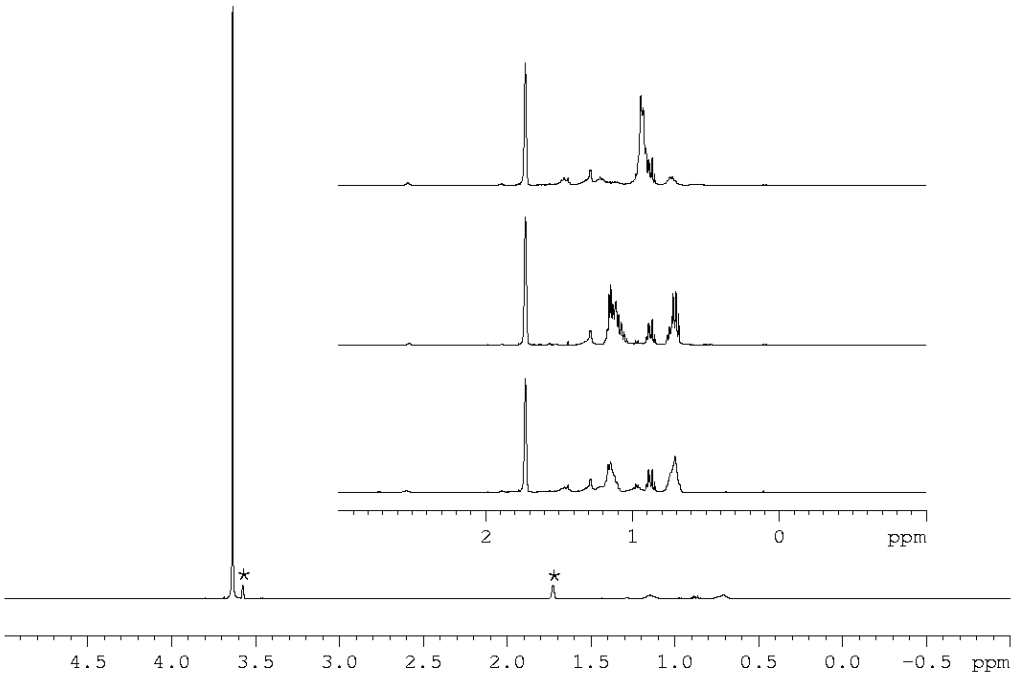

Figure S 3.9. ^{1}H NMR spectrum of **2** in THF-d_8. * = solvent (THF-d_8).
Magnified part shows ^{1}H, $^{1}H\{^{11}B\}$, $^{1}H\{^{31}P\}$ NMR (from bottom to top) of the anion.

$[K(C_{12}H_{24}O_6)][H_2As\text{-}BH_2\text{-}AsH_2]$ (3):

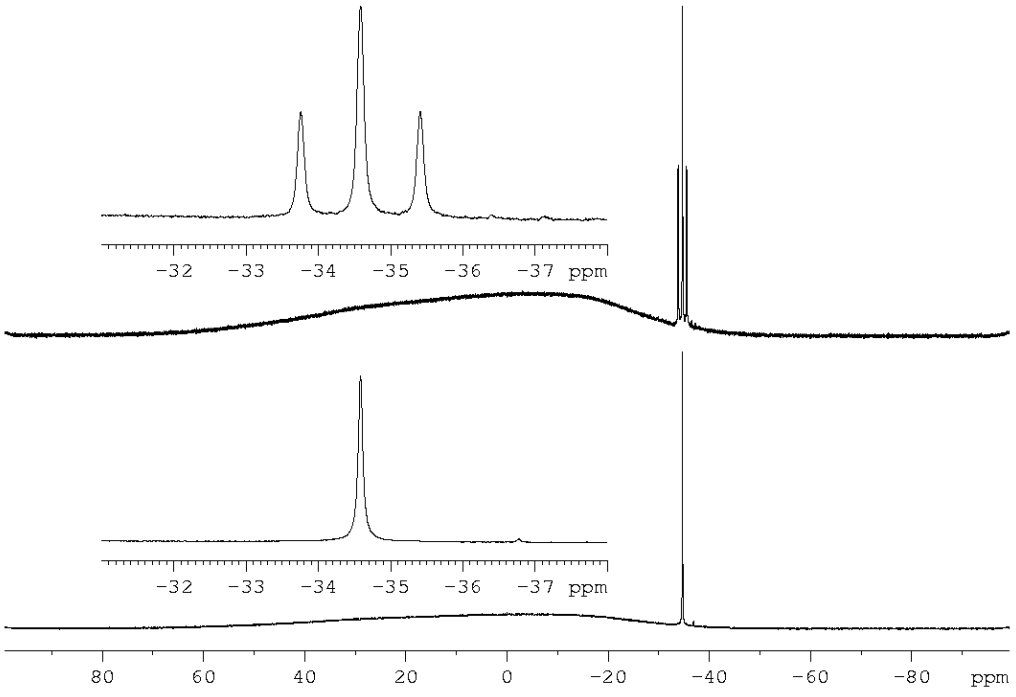

Figure S 3.10. $^{11}B\{^{1}H\}$ (bottom) and ^{11}B NMR spectrum (top) of **3** in THF-d_8.

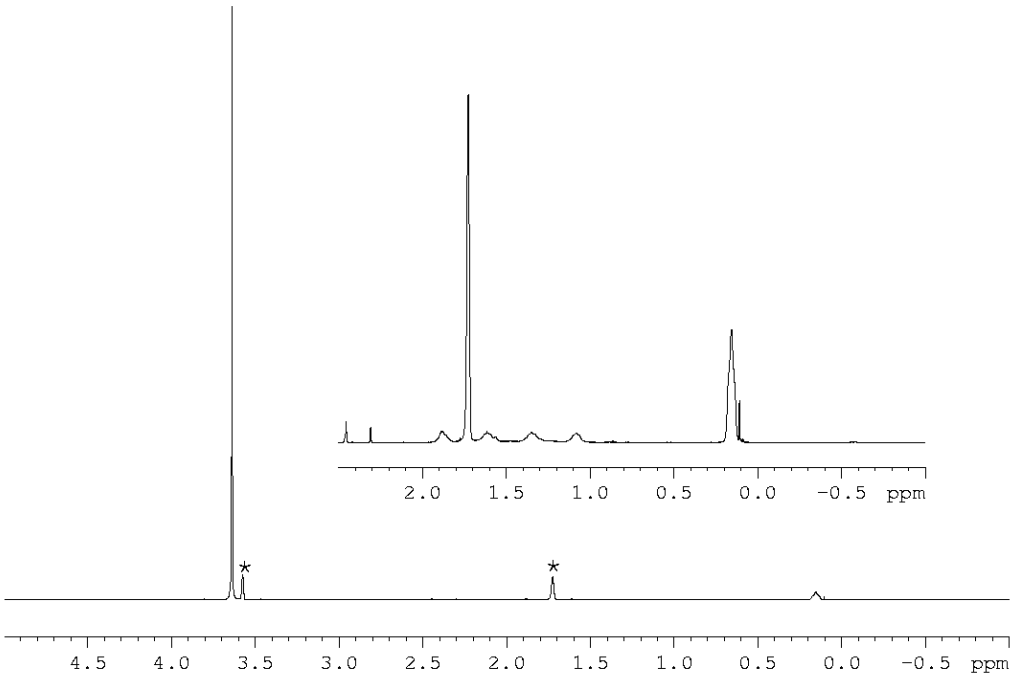

Figure S 3.11. ^{1}H NMR spectrum of **3** in THF-d_8. * = solvent (THF-d_8).

$[Na(C_{12}H_{24}O_6)(thf)_2][H_2P\text{-}BH_2\text{-}AsH_2]$ $(4(thf)_2)$:

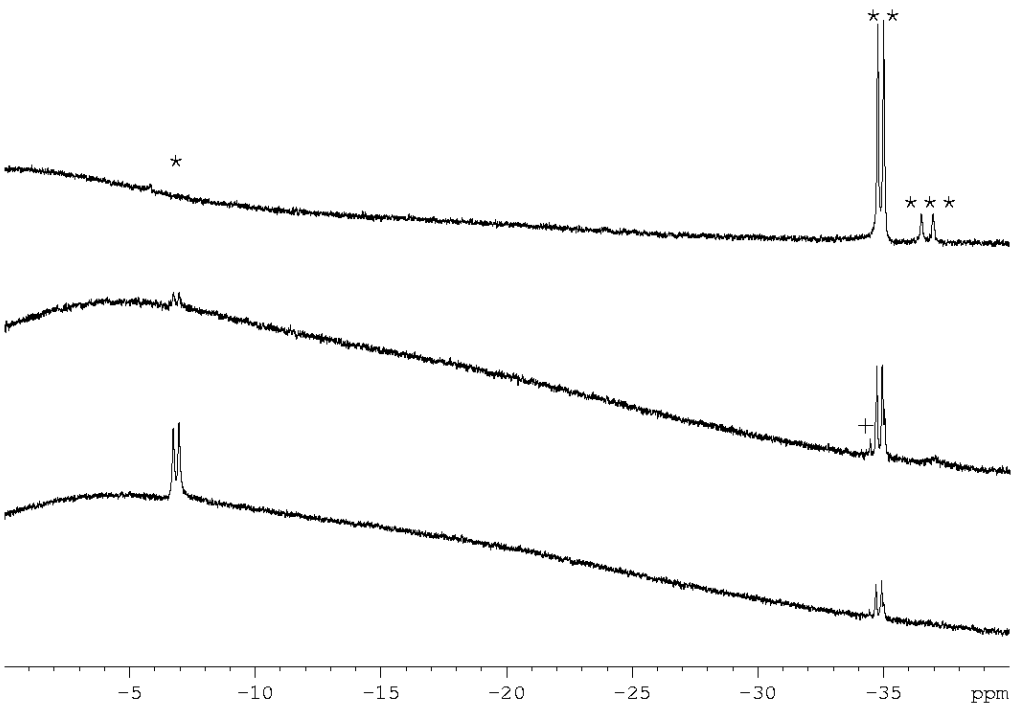

Figure S 3.12. $^{11}B\{^{1}H\}$ of the reactions:
$H_2As\text{-}BH_2\text{-}NMe_3$ (exc.) + $NaPH_2$ (top) after 1h sonication, $H_2P\text{-}BH_2\text{-}NMe_3$ + $KAsH_2$ after 30h sonication (middle), $H_2P\text{-}BH_2\text{-}NMe_3$ + $KAsH_2$ after 6h sonication (bottom); * = $H_2P\text{-}BH_2\text{-}NMe_3$; ** = **4**; *** = **5**; + = **2**.

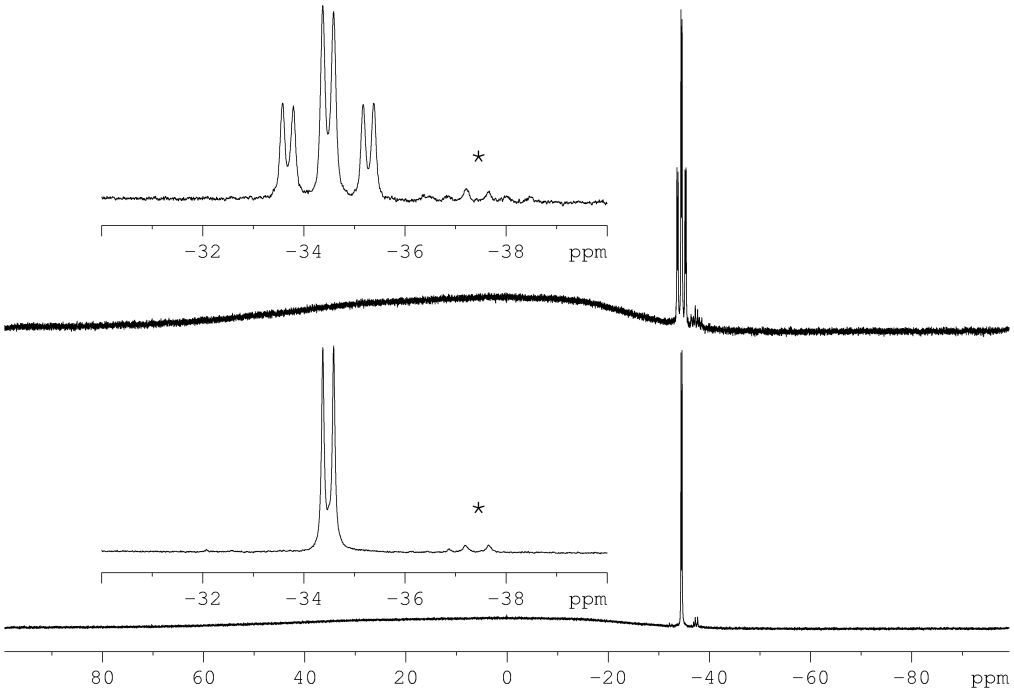

Figure S 3.13. $^{11}B\{^{1}H\}$ (bottom) and ^{11}B NMR spectrum (top) of **4** in THF-d_8. * = **5**.

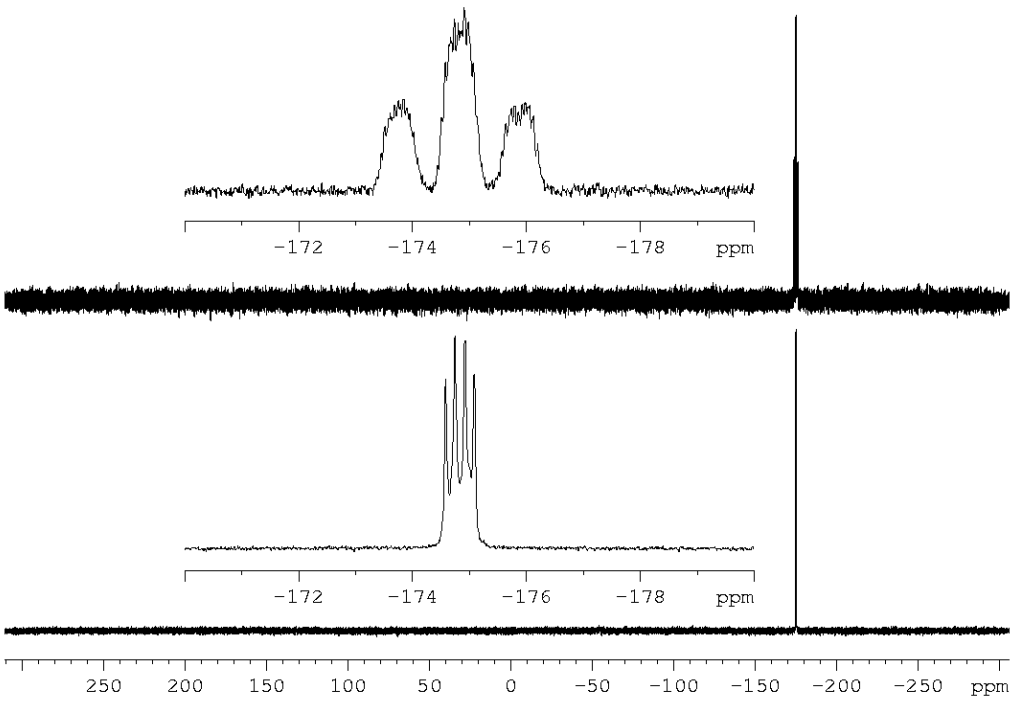

Figure S 3.14. $^{31}P\{^{1}H\}$ (bottom) and ^{31}P NMR spectrum (top) of **4** in THF-d_8.

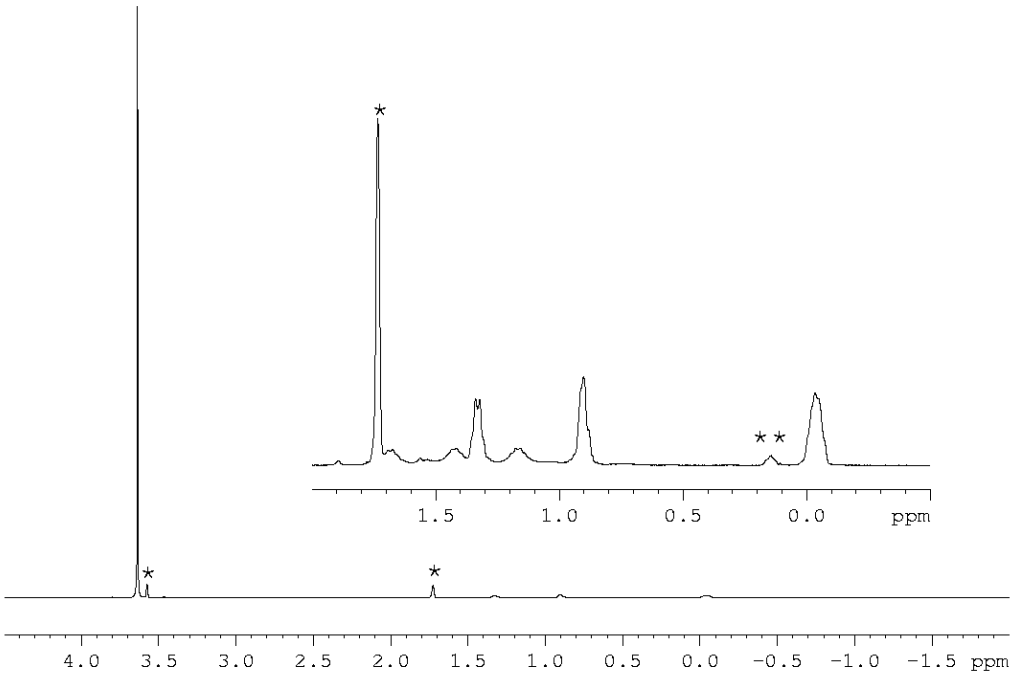

Figure S 3.15. ^{1}H NMR spectrum of **4** in THF-d_8. * = solvent (THF-d_8). ** = silicon grease.

$[Na(C_{12}H_{24}O_6)(thf)_2][H_2As\text{-}BH_2\text{-}PH_2\text{-}BH_2\text{-}AsH_2]$ $(5(thf)_2)$:

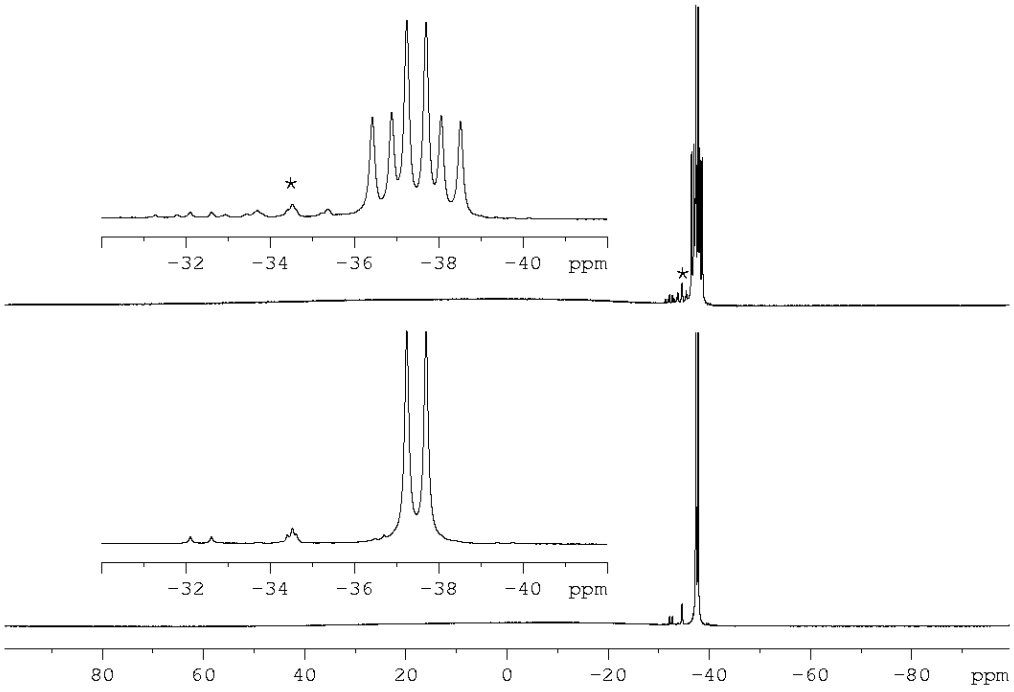

Figure S 3.16. ^{11}B{^{1}H} (bottom) and ^{11}B NMR spectrum (top) of **5** in THF-d_8. * = **2**.

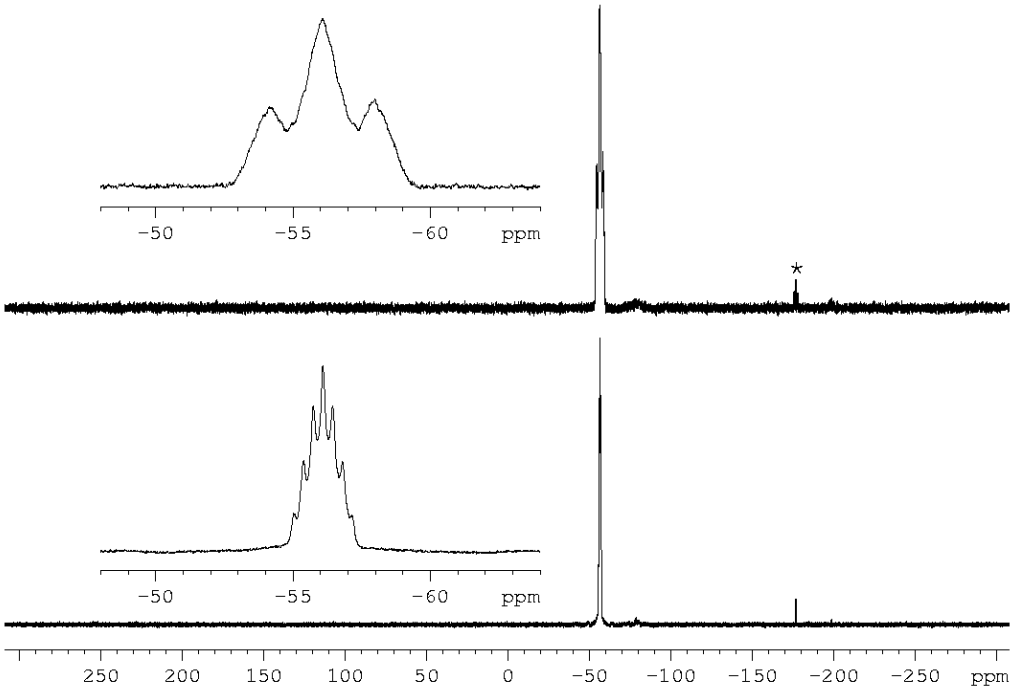

Figure S 3.17. $^{31}P\{^{1}H\}$ (bottom) and ^{31}P NMR spectrum (top) of **5** in THF-d_8. * = **2**.

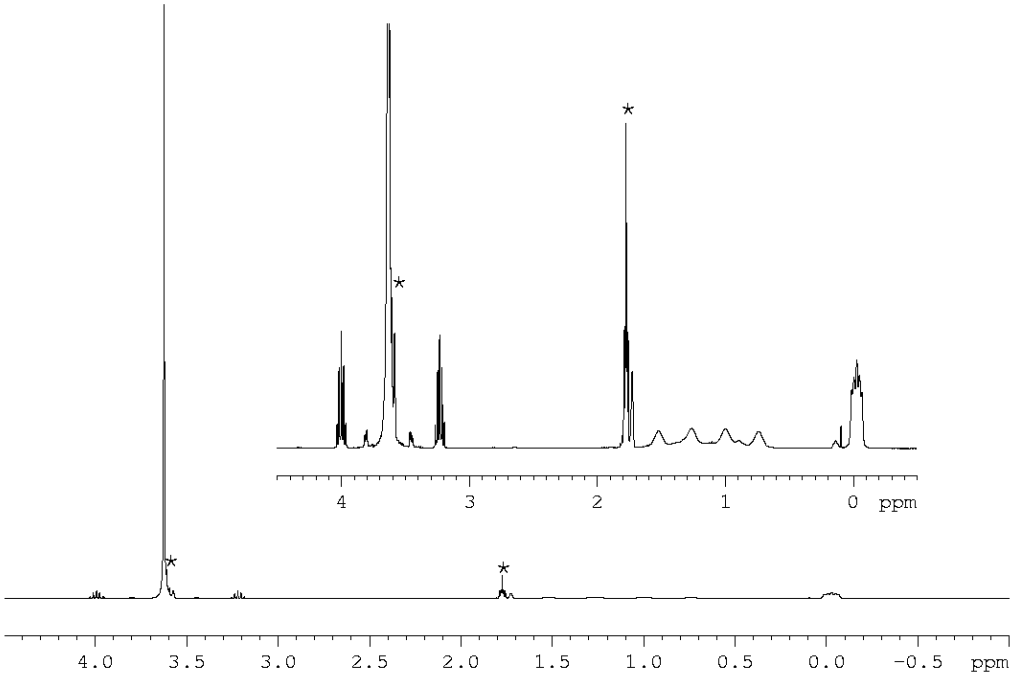

Figure S 3.18. ^{1}H NMR spectrum of **5** in THF-d_8. * = solvent (THF-d_8).

3.5.6 Computational Details

All calculations have been performed with the TURBOMOLE program package[10] at the B3LYP[11]/def2-TZVP[12] level of theory. The solvent effects were incorporated via the Conductor-like Screening Model (COSMO)[13] using the dielectric constant of THF (ε = 7.250). The natural population analysis[14] was performed as implemented in TURBOMOLE. Computations for the reactions leading to **6** have been performed at B3LYP/def2-TZVP level of theory using Gaussian[15] program package.

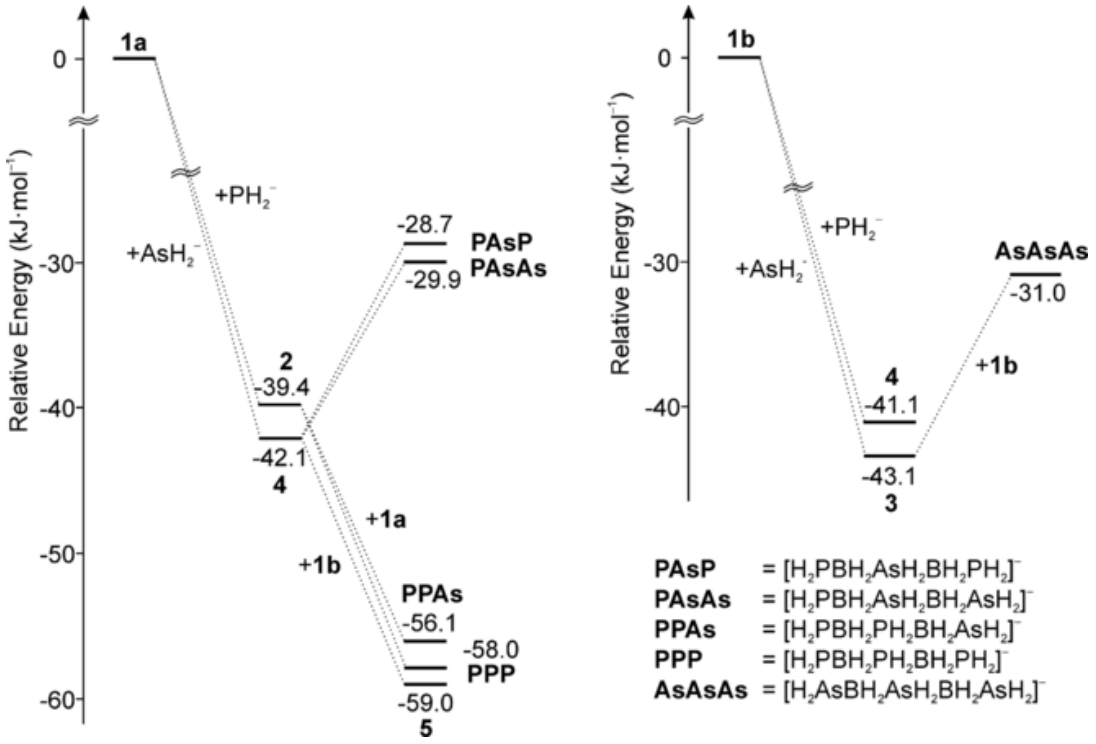

Figure S 3.19. Energy profile of the reaction of **1a**,**b** with P and As centered nucleophiles. Relative energies calculated at the B3LYP/def2-TZVP level (ε = 7.250).

Table S 3.4. Cartesian coordinates of the optimized geometry of $H_2P\text{-}BH_2\text{-}NMe_3$ at the B3LYP/def2-TZVP level of theory.

Atom	x	y	z
P	0.8598344	1.7155207	-1.9878152
B	0.0158590	0.0284541	-1.4117586
N	-0.1400305	-0.2796776	0.1934342
H	0.6817659	-0.8778866	-1.8564589
H	-1.1077114	0.0162975	-1.8587754
C	1.1849909	-0.3413286	0.8714353
H	1.0493517	-0.6070863	1.9206258
H	1.7994654	-1.0907734	0.3777127
H	1.6698004	0.6282282	0.7990155
C	-0.8044869	-1.6084432	0.3366845
H	-1.7770703	-1.5712619	-0.1477669
H	-0.1898681	-2.3646193	-0.1454302
H	-0.9256850	-1.8479085	1.3941445
C	-0.9855238	0.7438430	0.8691413
H	-1.9529993	0.7851444	0.3739725
H	-1.1181867	0.4768298	1.9183712
H	-0.5008776	1.7135249	0.7965648
H	2.0530779	1.7746596	-1.2197323
H	0.1882942	2.7064834	-1.2233648

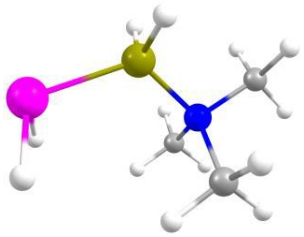

Energies [a.u.]:

Total energy = -543.0054072929

Totoal energy + OC corr. = -543.0067895353

Table S 3.5. Cartesian coordinates of the optimized geometry of $[H_2P\text{-}BH_2\text{-}PH_2]^-$ at the B3LYP/def2-TZVP level of theory.

Atom	x	y	z
P	-1.3531610	0.0547375	-1.0511612
B	-0.0404165	-0.9332243	0.0652330
H	-0.5060569	0.9208982	-1.7988087
H	-1.7693366	1.0888114	-0.1654181
P	1.3594869	0.0836579	1.0408251
H	0.5333975	-1.7185655	-0.6680595
H	-0.6752183	-1.5564899	0.8972437
H	0.5948442	1.1141733	1.6574222
H	1.8564606	0.9460013	0.0227235

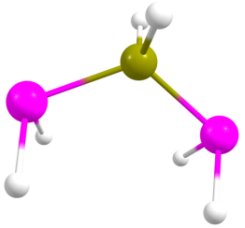

Energies [a.u.]:

Total energy = -711.1959121414

Totoal energy + OC corr. = -711.2050218092

Table S 3.6. Cartesian coordinates of the optimized geometry of $[H_2P\text{-}BH_2\text{-}PH_2\text{-}BH_2\text{-}PH_2]^-$ at the B3LYP/def2-TZVP level of theory.

Atom	x	y	z
P	-0.4582114	1.6715006	-2.8308811
P	0.0655525	0.0804400	0.0245575
P	0.8644123	-1.1798490	2.9796824
B	-0.8622876	0.1009451	-1.6942667
B	-0.1815110	-1.3704415	1.3089482
H	-0.6153482	2.7431549	-1.9083593
H	0.9628309	1.7116792	-2.7730233
H	-2.0499227	0.0896308	-1.4549133
H	-0.5317801	-0.9031136	-2.2862612
H	-0.1761902	1.3065739	0.6796908
H	0.1552084	-2.3936576	0.7544332
H	-1.3600713	-1.3985906	1.5884731
H	0.5821563	0.1659216	3.3451745
H	1.4476301	0.2418979	-0.2093735
H	2.1575322	-0.8660917	2.4761187

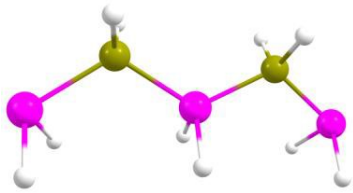

Energies [a.u.]:

Total energy = -1079.7878093563

Totoal energy + OC corr. = -1079.7960484021

Table S 3.7. Cartesian coordinates of the optimized geometry of $H_2As\text{-}BH_2\text{-}NMe_3$ at the B3LYP/def2-TZVP level of theory.

Atom	x	y	z
As	2.8689301	1.6581475	-5.3062478
B	1.9741318	-0.1266893	-4.6634616
N	1.8270776	-0.4181914	-3.0619224
H	2.6451149	-1.0260778	-5.1097831
H	0.8527438	-0.1286195	-5.1112397
C	3.1542262	-0.4761172	-2.3864744
H	3.0200696	-0.7358498	-1.3356840
H	3.7669076	-1.2288039	-2.8773892
H	3.6389620	0.4926979	-2.4670197
C	1.1631534	-1.7473122	-2.9065209
H	0.1888320	-1.7138016	-3.3875941
H	1.7767174	-2.5066018	-3.3849257
H	1.0461310	-1.9782658	-1.8467588
C	0.9824986	0.6085369	-2.3886363
H	0.0130425	0.6448973	-2.8801939
H	0.8550021	0.3468259	-1.3375278
H	1.4653219	1.5782835	-2.4703199
H	4.1281936	1.7047832	-4.4399848
H	2.1509136	2.6956193	-4.4422091

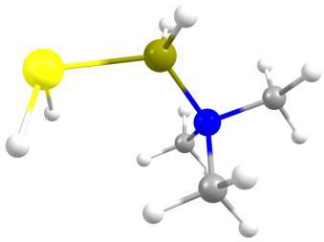

Energies [a.u.]:

Total energy = -2437.4660514505

Totoal energy + OC corr. = -2437.4666225610

Table S 3.8. Cartesian coordinates of the optimized geometry of $[H_2P\text{-}BH_2\text{-}AsH_2]^-$ at the B3LYP/def2-TZVP level of theory.

Atom	x	y	z
As	-0.5065333	1.5232688	-1.0821361
B	-0.7137413	0.0473711	0.4107771
H	-1.5756287	-0.7106836	0.0157003
H	-1.0778722	0.6383312	1.4085826
H	0.6126548	-1.9653352	1.5814004
H	0.2319877	0.7123944	-2.1548058
H	0.7957477	2.1921117	-0.6245849
P	1.0162025	-0.8320963	0.8114507
H	1.2171829	-1.6053621	-0.3663842

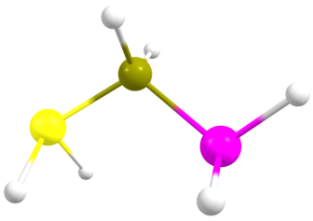

Energies [a.u.]:

Total energy = -2605.6578666880

Totoal energy + OC corr. = -2605.6655076554

Table S 3.9. Cartesian coordinates of the optimized geometry of $[H_2As\text{-}BH_2\text{-}AsH_2]^-$ at the B3LYP/def2-TZVP level of theory.

Atom	x	y	z
As	-0.5522444	1.5408292	-1.0980684
B	-0.7401190	0.0768613	0.4037264
H	-1.5774437	-0.7105815	0.0219210
H	-1.1012051	0.6621361	1.4039667
H	0.6491147	-2.0406623	1.6598231
H	0.2008856	0.7375150	-2.1657960
H	0.7371001	2.2360666	-0.6428434
As	1.1105208	-0.8228424	0.8390998
H	1.2733909	-1.6793219	-0.4218292

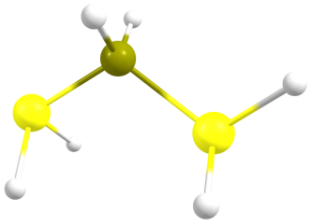

Energies [a.u.]:

Total energy = -4500.1193812501

Totoal energy + OC corr. = -4500.1257410262

Table S 3.10. Cartesian coordinates of the optimized geometry of $[H_2As\text{-}BH_2\text{-}PH_2\text{-}BH_2\text{-}PH_2]^-$ at the B3LYP/def2-TZVP level of theory.

Atom	x	y	z
As	-1.5937330	1.0473730	-2.1654197
B	-1.6742319	-0.0823280	-0.3947643
H	-2.5399469	-0.9158254	-0.5369312
H	-1.9207250	0.6735251	0.5145116
H	-0.2322608	-1.9517037	1.0196587
H	-0.9543642	0.0161430	-3.1013153
H	-0.2629165	1.7731279	-1.9647763
P	1.5449021	0.9519553	2.1394908
P	-0.0015767	-1.0012073	-0.0011826
B	1.6583027	-0.0704163	0.4472138
H	2.5248562	-0.9092627	0.5666742
H	1.9129228	0.6981200	-0.4508520
H	0.2457099	-1.9025680	-1.0608453
H	0.9593748	-0.0018009	3.0188855
H	0.3336864	1.6748679	1.9696523

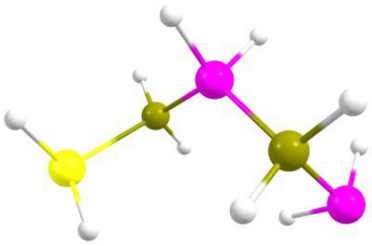

Energies [a.u.]:

Total energy = -2974.2480191401

Totoal energy + OC corr. = -2974.2551705557

Table S 3.11. Cartesian coordinates of the optimized geometry of $[H_2P\text{-}BH_2\text{-}AsH_2\text{-}BH_2\text{-}PH_2]^-$ at the B3LYP/def2-TZVP level of theory.

Atom	x	y	z
P	-1.6615388	1.0374382	-2.1277185
B	-1.7844162	-0.0080216	-0.4567341
H	-2.6501814	-0.8433400	-0.5731406
H	-2.0006341	0.7411946	0.4655571
H	-0.2887381	-2.0252445	1.0965986
H	-1.1107898	0.0866298	-3.0310399
H	-0.4323184	1.7299265	-1.9587139
P	1.6951760	0.9545034	2.1395519
As	-0.0173842	-1.0161958	-0.0065382
B	1.7827147	-0.0740577	0.4559176
H	2.6196731	-0.9395418	0.5620964
H	2.0243145	0.6786090	-0.4572111
H	0.2197451	-2.0198683	-1.1223676
H	1.1161612	0.0104842	3.0322366
H	0.4882164	1.6874840	1.9815056

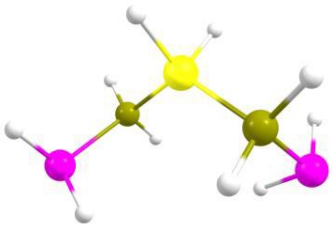

Energies [a.u.]:

Total energy = -2974.2363366082

Totoal energy + OC corr. = -2974.2443719177

Table S 3.12. Cartesian coordinates of the optimized geometry of $[H_2As\text{-}BH_2\text{-}AsH_2\text{-}BH_2\text{-}PH_2]^-$ at the B3LYP/def2-TZVP level of theory.

Atom	x	y	z
P	-1.6436424	1.0080491	-2.1609215
B	-1.7762361	-0.0138297	-0.4763221
H	-2.6394886	-0.8526041	-0.5868757
H	-1.9986508	0.7473743	0.4340146
H	-0.2821726	-2.0027217	1.1197018
H	-1.0867800	0.0452978	-3.0477199
H	-0.4160561	1.7037434	-1.9937892
As	1.7216208	1.0249626	2.2017608
As	-0.0125459	-1.0176632	-0.0046765
B	1.7896114	-0.0814541	0.4213173
H	2.6299579	-0.9399746	0.5393032
H	2.0233198	0.6753242	-0.4883249
H	0.2149321	-2.0457362	-1.1009743
H	1.0818838	-0.0117696	3.1305000
H	0.3942468	1.7610016	2.0130063

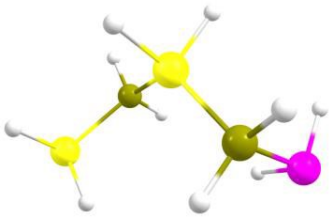

Energies [a.u.]:

Total energy = -4868.6976688547

Totoal energy + OC corr. = -4868.7046299587

Table S 3.13. Cartesian coordinates of the optimized geometry of $[H_2As\text{-}BH_2\text{-}PH_2\text{-}BH_2\text{-}AsH_2]^-$ at the B3LYP/def2-TZVP level of theory.

Atom	x	y	z
As	-1.5846785	1.0121875	-2.2025493
B	-1.6680616	-0.0799991	-0.4087860
H	-2.5350989	-0.9148797	-0.5346245
H	-1.9123630	0.6941282	0.4848739
H	-0.2306033	-1.9270026	1.0420552
H	-0.9344745	-0.0341700	-3.1141135
H	-0.2591286	1.7500497	-2.0106842
As	1.5846647	1.0122580	2.2024435
P	-0.0000168	-1.0001143	0.0000189
B	1.6680488	-0.0799946	0.4087207
H	2.5350896	-0.9148681	0.5345860
H	1.9123267	0.6940894	-0.4849830
H	0.2305082	-1.9272005	-1.0418664
H	0.9348872	-0.0342655	3.1141236
H	0.2589002	1.7497818	2.0107850

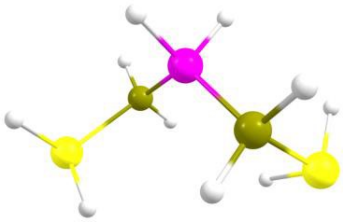

Energies [a.u.]:

Total energy = -4868.7096139978

Totoal energy + OC corr. = -4868.7156455547

Table S 3.14. Cartesian coordinates of the optimized geometry of $[H_2As\text{-}BH_2\text{-}AsH_2\text{-}BH_2\text{-}AsH_2]^-$ at the B3LYP/def2-TZVP level of theory.

Atom	x	y	z
As	-1.7052797	1.0310653	-2.2230143
B	-1.7857083	-0.0505324	-0.4280993
H	-2.6402982	-0.8967930	-0.5327133
H	-2.0032180	0.7213383	0.4723950
H	-0.2350468	-2.0236336	1.1131354
H	-1.0795706	-0.0253746	-3.1390004
H	-0.3686219	1.7527889	-2.0451015
As	1.7051254	1.0307792	2.2231449
As	0.0000774	-1.0165172	-0.0001554
B	1.7858713	-0.0508197	0.4282264
H	2.6403027	-0.8972102	0.5331046
H	2.0037550	0.7210617	-0.4721662
H	0.2349673	-2.0234558	-1.1136388
H	1.0789573	-0.0255092	3.1389951
H	0.3686870	1.7528121	2.0448878

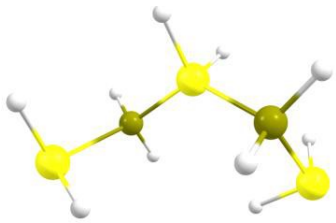

Energies [a.u.]:

Total energy = -6763.1590226114

Totoal energy + OC corr. = -6763.1649054982

Table S 3.15. Cartesian coordinates of the optimized geometry of $[PH_2]^-$ at the B3LYP/def2-TZVP level of theory.

Atom	x	y	z
P	-0.1919930	0.6301842	0.0000000
H	1.0838485	-0.0141223	0.0000000
H	-0.8918555	-0.6160619	0.0000000

Energies [a.u.]:

Total energy = -342.5923938047

Totoal energy + OC corr. = -342.6060724616

Table S 3.16. Cartesian coordinates of the optimized geometry of $[AsH_2]^-$ at the B3LYP/def2-TZVP level of theory.

Atom	x	y	z
As	-0.2099417	0.6891014	0.0000000
H	1.1552451	-0.0245626	0.0000000
H	-0.9453034	-0.6645388	0.0000000

Energies [a.u.]:

Total energy = -2237.0581667815

Totoal energy + OC corr. = -2237.0655375638

Table S 3.17. Total Energies E^o_0, sum of electronic and thermal enthalpies H^o_{298} (Hartree) and standard entropies S^o_{298} (cal·mol^{-1}K^{-1}) for studied compounds. B3LYP/def2-TZVP level of theory.

Compound	E^o_0	H^o_{298}	S^o_{298}
PH_3	-343.1764512	-343.14869	50.196
NMe_3	-174.5440626	-174.417928	78.558
NHC^{dipp}	-1160.441004	-1159.841643	193.535
$[NHC^{dipp}H]Cl$	-1621.31482	-1620.700233	206.003
$H_2P\text{-}BH_2\text{-}NMe_3$ (**1**)	-543.2080302	-543.034204	108.485
$ClBH_2\text{-}NMe_3$	-660.8998472	-660.743217	85.322
$[NHC^{dipp}\text{-}BH_2\text{-}PH_2\text{-}BH_2\text{-}NHC^{dipp}]^+$ $[P_5B_5H_{19}]^-$ (**6**)	-4558.429538		

Table S 3.18. Optimized geometries of studied compounds, xyz coordinates in angstroms. B3LYP/def2-TZVP level of theory.

PH_3

Atom	x	y	z
P	0.	0.	0.8305114632
H	1.1913667072	0.	1.5998279015
H	-0.5956833536	1.0317538337	1.5998279015
H	-0.5956833536	-1.0317538337	1.5998279015

NMe_3

Atom	x	y	z
N	1.5949047982	-1.35055436	2.6588865249
C	2.7609262991	-1.5495877419	3.4988622542
C	1.7495033904	-1.9814513274	1.3616402316
C	0.3740114959	-1.7693787907	3.3212952312
H	2.6408595055	-1.5941036105	0.8643038217
H	0.8854070682	-1.7557485639	0.7337124563
H	1.8460526346	-3.0814411752	1.425351961
H	3.6502162067	-1.1631222671	2.9971597732
H	2.9419395849	-2.6135126128	3.7410536367
H	2.6386130294	-1.0071538802	4.4383847138
H	0.2565743877	-1.2264959239	4.2611804376
H	0.3556932562	-2.8516584369	3.5486579716
H	-0.4872748724	-1.5441092642	2.6893641316

NHC^{dipp}

Atom	x	y	z
C	0.3168121989	2.1973201627	1.0910635023
N	1.1332241925	2.0501967135	2.2084466914
C	0.8611717166	0.9029727387	2.9064612606
N	-0.1526435616	0.3519578231	2.1753997316
C	-0.4976163198	1.123689991	1.0683597427
H	0.3874083824	3.0378175035	0.4242564181
H	-1.2751096114	0.8444847091	0.3794302812
C	2.1458279403	3.018163564	2.5649724516
C	-0.8039978644	-0.8908433904	2.5009610438
C	4.0526166243	4.9722128729	3.1188349455
C	1.8028157012	4.0996143459	3.4024176933
C	3.4474900678	2.8808112998	2.04026512
C	4.3769764186	3.8825263422	2.3316999397
C	2.7808159843	5.0653776341	3.653672293
C	0.4781132639	4.2911638654	4.1430398562
C	3.9840310045	1.6930670579	1.2393678776
H	5.3792453354	3.7925161761	1.9310272757
H	2.5296241877	5.9042575672	4.2911411428
H	4.7902508624	5.7379957004	3.3242669111
C	-2.0919005066	-3.2757828348	3.0798910495

C	-0.2984955443	-2.0872829523	1.9662015258
C	-1.9404973684	-0.8704604217	3.3261406454
C	-2.5698123669	-2.084422264	3.6008285378
C	-0.9661100504	-3.2728625461	2.272609845
C	0.936208111	-2.1347254431	1.0799946149
C	-2.4988397759	0.4108525223	3.9249707474
H	-3.4467839304	-2.0961233474	4.2354751169
H	-0.5957857653	-4.2088851915	1.8742207763
H	-2.5950013295	-4.2077817863	3.3063606389
H	0.5609206453	5.2883607353	4.5841057669
C	0.3437754105	3.3110326099	5.3205378322
C	-0.7928625402	4.3340190086	3.2844530648
H	1.1910182773	3.4092994315	6.0019337319
H	0.3130317279	2.2755182924	4.9813091797
H	-0.5683155345	3.525047402	5.8836250615
H	-0.674215933	5.0046290192	2.4306944049
H	-1.6205293197	4.7121166678	3.8892765868
H	-1.0821010667	3.356261423	2.9065047471
H	4.9808615949	2.0129175217	0.9234212808
C	3.242454342	1.3436054608	-0.0576779897
C	4.1926091083	0.4588143655	2.1328559226
H	4.8518751138	0.6963833953	2.9699380605
H	4.6558801788	-0.3463971695	1.5568405145
H	3.2513180357	0.0980706622	2.5477610339
H	3.0669025331	2.2322342675	-0.6677755715
H	2.2835751779	0.8620920347	0.1189836118
H	3.8543412234	0.6549069064	-0.6451219241
H	-1.845058936	1.2295374783	3.6305314461
C	-2.4969916784	0.3661092279	5.4603548165
C	-3.9020990648	0.724688488	3.3831563765
H	-3.9006409587	0.8006085605	2.2941548881
H	-4.2623612655	1.6733744976	3.7873021132
H	-4.6203508041	-0.0496938177	3.6613497713
H	-1.4952710033	0.1725827409	5.8455904515
H	-3.1618189353	-0.4123234883	5.84109141
H	-2.8387951999	1.3207615142	5.8662161856
C	2.0446016893	-2.9994857755	1.6989153374
H	1.3296481024	-1.1231121935	1.0011748696
C	0.5951642462	-2.6080552657	-0.341568053
H	0.2122799121	-3.6309650753	-0.3411327259
H	1.4858576739	-2.5864029361	-0.9734890679
H	-0.1613951904	-1.970398409	-0.802764082
H	1.7406458636	-4.0453460192	1.7807709131
H	2.3071443149	-2.6452366805	2.6963531825
H	2.9424645674	-2.9635011687	1.0780599226

[NHC^{dipp}H]Cl

Atom	x	y	z
C	-0.1907547326	2.0060937734	0.8961081732
N	0.7060979974	2.1890952889	1.9366857115
N	-0.1768393222	0.2294647207	2.1941737186

C	-0.7425601382	0.7820991002	1.0565200036
H	-0.3498992704	2.7583044618	0.1461782806
H	-1.477231956	0.2554839749	0.4754904544
C	1.5104062744	3.3875494417	2.124755501
C	-0.5040860169	-1.0880984012	2.7155434869
C	2.9659295712	5.7345624859	2.3367064532
C	0.9782586739	4.4488560707	2.8823946985
C	2.7746638846	3.4588968064	1.5082065399
C	3.4757253843	4.6606196368	1.6308976393
C	1.7375954874	5.6184649093	2.9605078509
C	-0.3060702248	4.436773711	3.7131626131
C	3.5160856132	2.330466298	0.7893453563
H	4.4493538879	4.7410899465	1.1643208437
H	1.3493459825	6.4494367274	3.5357215409
H	3.5306970727	6.655182917	2.4117872037
C	-1.2154320351	-3.5990929356	3.5945381325
C	0.2329974345	-2.1901523182	2.2597338765
C	-1.5597001589	-1.202239018	3.6310915251
C	-1.9009839602	-2.4864291956	4.0524453082
C	-0.1549603685	-3.4486215011	2.7167917868
C	1.4538109883	-2.0656533376	1.3636542948
C	-2.2846898415	-0.0054533757	4.2234920356
H	-2.7062932388	-2.6126579555	4.7637052333
H	0.3948730696	-4.3216373375	2.391409586
H	-1.4955517765	-4.5864611301	3.9396446749
H	-0.4425334092	5.4830979583	3.9982890357
C	-0.1156991462	3.659087417	5.0268243257
C	-1.603218683	4.0473116388	2.992178959
H	0.7310539693	4.0503973617	5.591470249
H	0.076931641	2.5977297852	4.8740735193
H	-1.0099045589	3.7554484682	5.646970281
H	-1.7054549304	4.5673963661	2.0372387434
H	-2.4539208597	4.3319827828	3.6146353695
H	-1.686444763	2.9781881947	2.8085312536
H	4.3655974746	2.8334414664	0.3202407604
C	2.7811803752	1.6311686576	-0.3617368225
C	4.1151309319	1.3275623129	1.7903809808
H	4.7509834203	1.8350897219	2.516360648
H	4.7262800983	0.5943600883	1.2589857651
H	3.360763067	0.7880703207	2.3620423991
H	2.3171903115	2.3506106046	-1.0399459701
H	2.0134890296	0.9392378597	-0.0217964042
H	3.501518804	1.0500759689	-0.9410705678
H	-1.9234916544	0.8942456395	3.7255060129
C	-1.942872821	0.1378978096	5.7169391375
C	-3.8016580216	-0.0659604464	3.9937399408
H	-4.0455989896	-0.1457196661	2.9321707916
H	-4.2769811888	0.8364948586	4.3836757031
H	-4.2518534279	-0.9197461763	4.5033869568
H	-0.8632922179	0.1824134175	5.8732286116
H	-2.332023261	-0.707659988	6.2884987491

H	-2.3937727518	1.047472995	6.1203215068
C	2.7270044529	-2.4355678063	2.1446240981
H	1.5541784159	-1.0222146849	1.0652009955
C	1.3216629114	-2.8892995424	0.0745524395
H	1.2627647758	-3.9587231379	0.2848619588
H	2.1920537744	-2.7284372749	-0.5649400098
H	0.4296298518	-2.611903736	-0.49124434
H	2.7194664203	-3.491425068	2.4242574929
H	2.8160529631	-1.8451948102	3.0586438491
H	3.6110029671	-2.2616240811	1.5268498657
C	0.699393359	1.0963271595	2.715145928
H	1.2999203425	0.8899959713	3.6488373575
Cl	2.1545466068	0.2002788311	5.2628946359

H_2P-BH_2-NMe_3 (1)

Atom	x	y	z
H	0.2083594281	0.350599684	0.1140560667
P	0.1168094065	1.1526399922	1.2853420265
H	-1.0560859617	0.500265053	1.7568123395
B	1.5247985814	0.40277021	2.4374027369
H	2.5981121773	0.6952998283	1.9687274425
N	1.5942874705	-1.2485555526	2.6413351099
H	1.3785388932	0.8396539357	3.5531862724
C	2.7384724021	-1.5338008212	3.5480129446
C	1.824620337	-1.9425042252	1.3485517778
C	0.3500738104	-1.767970353	3.2642695903
H	2.7332896984	-1.5507790819	0.8976793875
H	0.9871529263	-1.7449831082	0.6853500341
H	1.9243412077	-3.017678194	1.511917794
H	3.6493149335	-1.1504631581	3.095508635
H	2.8281090405	-2.609595191	3.7150187262
H	2.5735131782	-1.023126487	4.4931807656
H	0.1868542994	-1.2493716848	4.2059857477
H	0.4388842053	-2.8418529094	3.4418104004
H	-0.4879701972	-1.5703809875	2.6018169562

ClBH_2-NMe_3

Atom	x	y	z
B	1.5467133738	0.4053009722	2.4169312337
H	2.583553425	0.6865449347	1.881271928
N	1.5942069489	-1.2292359833	2.6400915723
H	1.3912184677	0.874394683	3.5109325019
C	2.7566606873	-1.5102756958	3.5229916625
C	1.7805936615	-1.9396942004	1.3462213469
C	0.3517527805	-1.7145834644	3.2991336857
H	2.6985559282	-1.5859784286	0.8829887194
H	0.9427683324	-1.706838025	0.6953205761
H	1.8393774777	-3.016031997	1.5177000267
H	3.6615726823	-1.1478137605	3.0415717584

H	2.83616376	-2.5834290128	3.7048613585
H	2.6205435418	-0.9838019107	4.464430441
H	0.2358965055	-1.1979918568	4.2489044326
H	0.4146952498	-2.7915764476	3.4649283983
H	-0.4965307991	-1.4800796147	2.6625270514
Cl	0.0935950074	0.8252417974	1.3053564478

$[NHC^{dipp}\text{-}BH_2\text{-}PH_2\text{-}BH_2\text{-}NHC^{dipp}]^+$ $[P_5B_5H_{19}]^-$ (6)

Atom	x	y	z
C	0.178133000	4.448101000	1.620246000
N	0.043406000	3.077166000	1.554986000
N	-1.391196000	3.920157000	0.172236000
C	-0.716774000	4.977234000	0.758449000
H	0.898176000	4.918224000	2.263707000
H	-0.931760000	5.997863000	0.501233000
C	0.830229000	2.130754000	2.329548000
C	-2.441633000	4.135112000	-0.810730000
C	2.151179000	0.098949000	3.669852000
C	0.365633000	1.744390000	3.604436000
C	2.023333000	1.619835000	1.781054000
C	2.650103000	0.580001000	2.474513000
C	1.043141000	0.701087000	4.239033000
C	-0.685570000	2.440796000	4.480734000
C	2.822118000	2.159554000	0.590140000
H	3.554651000	0.153308000	2.059817000
H	0.693381000	0.370521000	5.209720000
H	2.645458000	-0.722709000	4.172241000
C	-4.419100000	4.715844000	-2.654782000
C	-2.103887000	4.175761000	-2.174100000
C	-3.746224000	4.387120000	-0.351627000
C	-4.722715000	4.674987000	-1.304402000
C	-3.124991000	4.467891000	-3.078801000
C	-0.696232000	3.949933000	-2.699606000
C	-4.125852000	4.399296000	1.120883000
H	-5.735325000	4.876653000	-0.980629000
H	-2.894829000	4.505039000	-4.135033000
H	-5.192035000	4.945141000	-3.377785000
H	-1.009909000	1.665423000	5.179942000
C	-1.964576000	3.005028000	3.858560000
C	0.001996000	3.529630000	5.328753000
H	-2.469831000	2.284455000	3.218711000
H	-1.780881000	3.913914000	3.288313000
H	-2.656670000	3.268891000	4.661331000
H	0.861380000	3.129727000	5.867047000
H	-0.698730000	3.941102000	6.058991000
H	0.353916000	4.354414000	4.705238000
H	3.426455000	1.311691000	0.263467000
C	3.807752000	3.231612000	1.096450000
C	2.092973000	2.660353000	-0.655043000
H	1.352302000	1.947086000	-1.008755000

H	2.821708000	2.787532000	-1.455984000
H	1.622442000	3.631057000	-0.496398000
H	4.427605000	2.855101000	1.909960000
H	3.278948000	4.120862000	1.450697000
H	4.470034000	3.538155000	0.285020000
H	-3.278019000	4.026626000	1.690245000
C	-5.313144000	3.475228000	1.428325000
C	-4.411731000	5.829093000	1.610501000
H	-3.558766000	6.489236000	1.444505000
H	-4.634246000	5.828033000	2.679668000
H	-5.269548000	6.260504000	1.090440000
H	-5.125906000	2.456140000	1.087994000
H	-6.231090000	3.822730000	0.950742000
H	-5.495648000	3.445211000	2.504492000
C	-0.646586000	2.878401000	-3.798390000
H	-0.081468000	3.589710000	-1.879769000
C	-0.074302000	5.267517000	-3.193069000
H	-0.639873000	5.681607000	-4.030669000
H	0.947773000	5.093399000	-3.532692000
H	-0.047320000	6.022306000	-2.404090000
H	-1.171109000	3.199956000	-4.700664000
H	-1.095770000	1.945500000	-3.456576000
H	0.387573000	2.671274000	-4.078676000
C	-0.918768000	2.738880000	0.653142000
B	-1.273414000	1.278583000	0.091339000
H	-1.918057000	1.378825000	-0.916106000
P	-2.284896000	0.039449000	1.231990000
H	-0.249313000	0.680115000	-0.096456000
B	-2.061472000	-1.918500000	1.141086000
H	-3.643084000	0.414201000	1.303911000
H	-1.947480000	0.229336000	2.580683000
H	-0.882095000	-2.038516000	1.311282000
C	-2.541390000	-2.795577000	-0.106946000
H	-2.683098000	-2.267465000	2.113567000
N	-3.813930000	-2.994660000	-0.543825000
C	-3.830520000	-3.942671000	-1.552341000
C	-2.554929000	-4.339750000	-1.738151000
N	-1.771245000	-3.640436000	-0.842783000
C	-5.016827000	-2.374031000	-0.027070000
H	-4.741836000	-4.245369000	-2.033164000
H	-2.133605000	-5.060548000	-2.412919000
C	-0.325067000	-3.804506000	-0.754706000
C	-7.339896000	-1.227945000	0.934027000
C	-5.602179000	-1.321456000	-0.752603000
C	-5.593690000	-2.894481000	1.145114000
C	-6.759959000	-2.288700000	1.610264000
C	-6.771524000	-0.759741000	-0.238537000
C	-5.060101000	-0.828703000	-2.086796000
C	-5.050849000	-4.119062000	1.866932000
H	-7.227420000	-2.661926000	2.511349000
H	-7.246591000	0.053374000	-0.770654000

H	-8.246458000	-0.774372000	1.314920000
C	2.429940000	-3.988228000	-0.510008000
C	0.488080000	-3.071439000	-1.641247000
C	0.212765000	-4.705532000	0.188297000
C	1.604762000	-4.764482000	0.283152000
C	1.871658000	-3.171072000	-1.473416000
C	0.061626000	-2.244961000	-2.858682000
C	-0.531488000	-5.662232000	1.130053000
H	2.044325000	-5.441685000	1.005633000
H	2.517064000	-2.585217000	-2.114189000
H	3.505235000	-4.023696000	-0.396714000
C	-4.947533000	0.698718000	-2.166231000
C	-5.919048000	-1.360362000	-3.248388000
H	-4.055266000	-1.227476000	-2.214304000
H	-4.329059000	1.101464000	-1.365130000
H	-5.924126000	1.183706000	-2.118971000
H	-4.487147000	0.986705000	-3.112391000
H	-6.936065000	-0.965706000	-3.195087000
H	-5.987389000	-2.449363000	-3.241059000
H	-5.490078000	-1.057095000	-4.205342000
C	-4.972971000	-3.935559000	3.388217000
H	-4.035418000	-4.296197000	1.518687000
C	-5.884960000	-5.362854000	1.512328000
H	-6.918078000	-5.250277000	1.847984000
H	-5.468564000	-6.249031000	1.995376000
H	-5.902592000	-5.543627000	0.436155000
H	-4.401101000	-3.045647000	3.651800000
H	-4.480467000	-4.798466000	3.839869000
H	-5.962671000	-3.853439000	3.841330000
C	-1.191361000	-1.372915000	-2.768339000
C	0.010156000	-3.137730000	-4.113075000
H	0.892203000	-1.553885000	-3.012905000
C	-0.905102000	-5.026366000	2.477304000
H	0.224000000	-6.417692000	1.360264000
C	-1.707729000	-6.448676000	0.539501000
H	-1.199809000	-0.766545000	-1.865121000
H	-2.111546000	-1.954585000	-2.823044000
H	-1.198547000	-0.688000000	-3.618580000
H	-0.813523000	-3.854986000	-4.067410000
H	0.938080000	-3.695734000	-4.239510000
H	-0.134971000	-2.521721000	-5.003044000
H	-1.960037000	-7.271761000	1.211770000
H	-1.454954000	-6.882645000	-0.429764000
H	-2.607220000	-5.847455000	0.419279000
H	-0.040392000	-4.543445000	2.934115000
H	-1.264135000	-5.797759000	3.163564000
H	-1.682595000	-4.271823000	2.376725000
H	8.702472000	1.135427000	3.320279000
P	8.709639000	0.086712000	2.379042000
P	7.149747000	-1.339620000	-0.008044000
P	10.336021000	-1.203245000	0.021769000

B	8.762325000	-1.270136000	-1.121676000
B	10.410180000	0.151326000	1.424811000
B	7.051969000	0.071818000	1.353425000
H	7.223665000	-2.553251000	0.717339000
H	10.585213000	-2.470590000	0.589792000
H	8.754190000	-0.219976000	-1.714919000
H	11.334771000	-0.033383000	2.169990000
H	6.997867000	1.138864000	0.792756000
H	8.723782000	-1.001158000	3.277565000
B	5.486682000	-1.521150000	-1.035161000
H	11.506730000	-1.083374000	-0.752037000
H	8.830835000	-2.227325000	-1.847658000
H	10.438951000	1.217099000	0.863740000
H	6.126510000	-0.117299000	2.103668000
B	3.569423000	-0.016810000	-3.336575000
P	3.397041000	1.511315000	-4.580252000
P	5.271077000	-0.132901000	-2.385922000
H	3.445223000	-1.047481000	-3.958182000
H	4.564504000	1.367650000	-5.378997000
H	6.336998000	-0.193566000	-3.303632000
H	4.553023000	-1.423148000	-0.275675000
H	2.718866000	0.078808000	-2.480329000
H	5.561906000	1.124116000	-1.815807000
H	5.498546000	-2.577011000	-1.619847000
H	3.961398000	2.566031000	-3.805839000

3.5.7 References

[1] C. Marquardt, A. Adolf, A. Stauber, M. Bodensteiner, A. V. Virovets, A. Y. Timoshkin, M. Scheer, *Chem. Eur. J.* **2013**, *19*, 11887-11891.

[2] G. E. Ryschkewitsch, J. W. Wiggins, *Inorg. Synth.* **1970**, *12*,116.

[3] H. Jacobs, K. M. Hassiepen, *ZAAC*, **1985**, *531*, 108-118.

[4] W.C. Johnson, A. Pechukas, *J. Am. Chem. Soc.* **1937**, *59*, 2068-71.

[5] L. Hintermann, *Beilstein J. Org. Chem*. **2007**, *3*, No.22.

[6] Agilent Technologies **2006**-**2011**, CrysAlisPro Software system, different versions, Agilent Technologies UK Ltd, Oxford, UK.

[7] A. Altomare, M. C.Burla, M. Camalli, G. L. Cascarano, C. Giacovazzo, A. Guagliardi, A.G. G. Moliterni, G. Polidori, R. Spagna, *J. Appl. Cryst.* **1999**, *32*, 115-119.

[8] G. M. Sheldrick, *Acta Cryst.* **2008**, *A64*, 112-122.

[9] a) E. Keller, **1997**, SCHAKAL99, Freiburg. b) K. Brandenburg, H. Putz, **2005**, DIAMOND 3, Crystal Impact GbR, Postfach 1251, D-53002 Bonn. c) O.V. Dolomanov, L.J. Bourhis, R.J. Gildea, J.A.K. Howard, H.Puschmann, OLEX2: A complete structure solution, refinement and analysis program, *J. Appl. Cryst*. **2009**. *42*, 339-341.

[10] a) R. Ahlrichs, M. Bär, M. Häser, H. Horn, C. Kölmel, *Chem. Phys. Lett.* **1989**, *162*, 165-169; b) O. Treutler, R. Ahlrichs, *J. Chem. Phys.* **1995**, *102*, 346-354.

[11] a) P. A. M. Dirac, *Proc. Royal Soc. A,* **1929**, *123*, 714; b) J. C. Slater, *Phys. Rev.* **1951**, *81*, 385; c) S. H. Vosko, L. Wilk, M. Nusair, *Can. J. Phys.* **1980**, *58*, 1200; d) A. D. Becke, *Phys. Rev. A,* **1988**, *38*, 3098; e) C. Lee, W. Yang, R. G. Parr, *Phys. Rev. B,* **1988**, *37*, 785; f) A. D. Becke, *J. Chem. Phys.* **1993**, *98*, 5648.

[12] a) A. Schäfer, C. Huber, R. Ahlrichs, *J. Chem. Phys.* **1994**, *100*, 5829; b) K. Eichkorn, F. Weigend, O. Treutler, R. Ahlrichs, *Theor. Chem. Acc.* **1997**, *97*, 119.

[13] A. Klamt, G. Schüürmann, *J. Chem. Soc. Perkin Trans. 2*, **1993**, 799-805; A. Schäfer, A. Klamt, D. Sattel, J. C. W. Lohrenz, F. Eckert, *Phys. Chem. Chem. Phys.* **2000**, *2*, 2187-2193.

[14] A. Reed, R. B. Weinstock, F. Winhold, *J. Chem. Phys.* **1985**, *83*, 735-746.

[15] M. J. Frisch, G. W. Trucks, H. B. Schlegel, G. E. Scuseria, M. A. Robb, J. R. Cheeseman, J. A. Montgomery, Jr., T. Vreven, K. N. Kudin, J. C. Burant, J. M. Millam, S. S. Iyengar, J. Tomasi, V. Barone, B. Mennucci, M. Cossi, G. Scalmani, N. Rega, G. A. Petersson, H. Nakatsuji, M. Hada, M. Ehara, K. Toyota, R. Fukuda, J. Hasegawa, M. Ishida, T. Nakajima, Y. Honda, O. Kitao, H. Nakai, M. Klene, X. Li, J. E. Knox, H. P. Hratchian, J. B. Cross, V. Bakken, C. Adamo, J. Jaramillo, R. Gomperts, R. E. Stratmann, O. Yazyev, A. J. Austin, R. Cammi, C. Pomelli, J. W. Ochterski, P. Y. Ayala, K. Morokuma, G. A. Voth, P. Salvador, J. J. Dannenberg, V. G. Zakrzewski, S. Dapprich, A. D. Daniels, M. C. Strain, O. Farkas, D. K. Malick, A. D. Rabuck, K. Raghavachari, J. B. Foresman, J. V. Ortiz, Q. Cui, A. G. Baboul, S. Clifford, J. Cioslowski, B. B. Stefanov, G. Liu, A. Liashenko, P. Piskorz, I. Komaromi, R. L. Martin, D. J. Fox, T. Keith, M. A. Al-Laham, C. Y. Peng, A. Nanayakkara, M. Challacombe, P. M. W. Gill, B. Johnson, W. Chen, M. W. Wong, C. Gonzalez, and J. A. Pople, Gaussian03, revision B.05. Gaussian, Inc., Wallingford CT, **2004**.

Preface

The following chapter has been compiled for future publication.

Authors

Tobias Kahoun, Michael Bodensteiner, Alexey Y. Timoshkin, Manfred Scheer.

Author contributions

The synthesis and characterization of compounds **3c**, **4d**, **5**, **6**, **7**, **8**, **9**, **10**, **11**, **12**, **13** were performed by Tobias Kahoun.

X-ray structural analyses of **3c**, **3c**$(thf)_2$, **4d**$(thf)_2$, **5**$(thf)_2$, **6**$(thf)_4$, **7**$(thf)_2$, **8**$(thf)_2$, **9**$(thf)_2$, **10** were performed by Tobias Kahoun and Dr. Michael Bodensteiner.

DFT-calculations were performed by Prof. Dr. Alexey Y. Timoshkin (St. Petersburg State Univeristy).

The manuscript (including supporting information, figures, schemes and graphical abstract) was written by Tobias Kahoun.

4 Coordination Chemistry of Anionic Pnictogenylborane Derivatives

Tobias Kahoun, Michael Bodensteiner, Alexey Y. Timoshkin, Manfred Scheer.

Abstract:

We report on the synthesis and structural characterization of organosubstituted anionic pnictogenylborane derivatives as well as their coordination behavior towards trasition metal fragments and ions. Coordination of anionic pnictogenylborane derivatives of the type $[M(C_{12}H_{24}O_6)][R^1HE\text{-}BH_2\text{-}R^1EH]$ (**1a**: E = P, R^1 = H, M = Na; **2b**: E = As, R^1 = H, M = K; **3c**: E = P, R^1 = ^{t}Bu, M = Na; **4d**: E = As, R^1 = ^{t}Bu, M = Na) and $[Na(C_{12}H_{24}O_6)][H_2As\text{-}BH_2\text{-}PH_2\text{-}BH_2\text{-}AsH_2]$ (**2a**) towards $W(CO)_4$ fragments results in the formation of mononuclear cyclic compounds revealing a four membered ring (**5**: [(**1a**)$W(CO)_4$]; **8**: [(**3c**)$W(CO)_4$]; **9**: [(**4d**)$W(CO)_4$]), a six membered ring (**7**: [(**2a**)$W(CO)_4$]) as well as a dinuclear compound revealing an eight membered ring (**6**: ([(**2b**)$W(CO)_4$])$_2$). Reactions of the *tert*-butyl substituted pnictogenylboranes ^{t}BuEH-BH_2-NMe_3 (**3**: E = P; **4**: E = As) with corresponding pnictogen based substituted nucleophiles of the type $[^t BuEH]^-$ (**c**: E = P, **d**: E = As) lead to the formation of the symmetrical compounds $[Na(C_{12}H_{24}O_6)][^t BuEH\text{-}BH_2\text{-}^t BuEH]$ (**3c**: E = P, **4d**: E = As). The solid state structure of all compounds has been determind by X-ray structural analysis. Additionally, they were characterized by multinuclear NMR spectroscopy, mass spectrometry and IR spectroscopy. DFT calculations allow a deeper insight into thermodynamic parameters of the reactions.

Reaction of the three membered anionic compound $Na[H_2P\text{-}BH_2\text{-}PH_2]$ (**1a**) with $[Cu(MeCN)_4][BF_4]$ leads to the coordination product $[Cu_2Na_2(H_2P\text{-}BH_2\text{-}PH_2)_4]$ (**10**) which represents a 3-dimensional scaffold with an adamantane-like repeating unit of Cu ions.

4.1 Introduction

Beside the metal center ligands are an inevitable part of coordination chemistry. While in mononuclear complexes the variation of the metal center is limited by the stability of the oxidation state, the diversity of ligands is almost endless. Despite the steadily increasing amount of ligands with different shapes and properties many of them reveal group 15 and 16 elements as coordination sites. Especially compounds with multiple terminal functional groups, like amines or carboxylates, are widely used as units for linking metal fragments, aiming to build up three dimensional scaffolds. Such metal organic frameworks (MOFs) are representing porous materials. Depending on the branching, the flexibility and the length of the linker individual void sizes are adjustable.[1] Similar to the influence of the linkers in MOFs, the ligands in complexes have a crucial influences on their properties. Cutting down on only pnictogen containing derivatives, with greater focus on nitrogen, a variety of organic ligands is accessible.[2] Switching from nitrogen containing ligands to its heavier congener phosphorus, the range of widely used ligands shrinks to phosphines (**I**; Me[3], Et[4], ^{i}Pr[5], ^{t}Bu[6], Ph[7], Cy[8], Me/^{i}Pr[9]) or bis(phosphines) with phenyl substituents in most cases (**II**; n = 1[10], 2[11], 3[12], 4[13]).

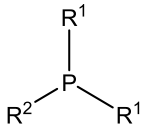

$R^1 = R^2$ = Me, Et, ^{i}Pr, ^{t}Bu, Ph, Cy
R^1 = Me, R^2 = ^{i}Pr

I

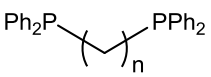

n = 1, 2, 3, 4

II

For the arsenic case the AsR_3 ligands can be summed up for the most part by $AsPh_3$[14] while diarsinoalkanes are mainly covered by derivatives with a methylene[15] or ethyl[16] backbone. In comparison to the pnictogen containing compounds bearing an organic backbone, the coordination chemistry of all inorganic ligands is mainly dominated by polypnictogen ligands of phosphorus and arsenic as building units for complexes.[17] Due to the lack of linear inorganic ligands and linkers corresponding complexes and coordination products are barely studied. Our research group was recently able to synthesize the first inorganic, hydrogen substituted, anionic compounds with two terminal phosphine and arsine groups, respectively (**III**, a).[18] Here in we report on the synthesis of the *tert*-butyl substituted derivatives (**III**, b). Compared to their parent analogs (**III**, a) these compounds bear sterically more demanding but electron donating substitutents, with the aim to increase the electron density on the pnictogen atoms.

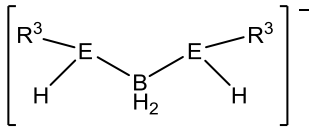

a) E = P, As; R^3 = H
b) E = P, As; R^3 = ^{t}Bu

III

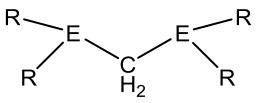

E = P, As
R = org. subst.

IV

Due to their similarity towards bis(phosphines) (**IV**) their chelating coordination behavior towards a $W(CO)_4$ fragment is investigated here. Further, it is investigated whether these compounds are suitable for linking "naked" metal atoms to obtain inorganic MOF-analogs.

4.2 Results and Discussion

Sonication of pnictogen nucleophiles of the type MEH_2 (**a**: E = P, M = Na; **b**: E = As, M = K) with an equimolar amount of H_2E-BH_2-NMe_3 (**1**: E = P; **2**: E = As) leads to the substitution of the Lewis base NMe_3 and the formation of $[M(C_{12}H_{24}O_6)][H_2E\text{-}BH_2\text{-}EH_2]$ (**1a**: E = P, M = Na; **2b**: E = As, M = K) after addition of equivalent amounts of 18-crown-6 (Scheme 4.1). Changing the stoichiometry to two equivalents of H_2As-BH_2-NMe_3 (**2**) with one equivalent $NaPH_2$ (**a**) leads to the five membered chain $[Na(C_{12}H_{24}O_6)][H_2As\text{-}BH_2\text{-}PH_2\text{-}BH_2\text{-}AsH_2]$ (**2a**) in the presence of one equivalent of 18-crown-6 (Scheme 4.1).[18]

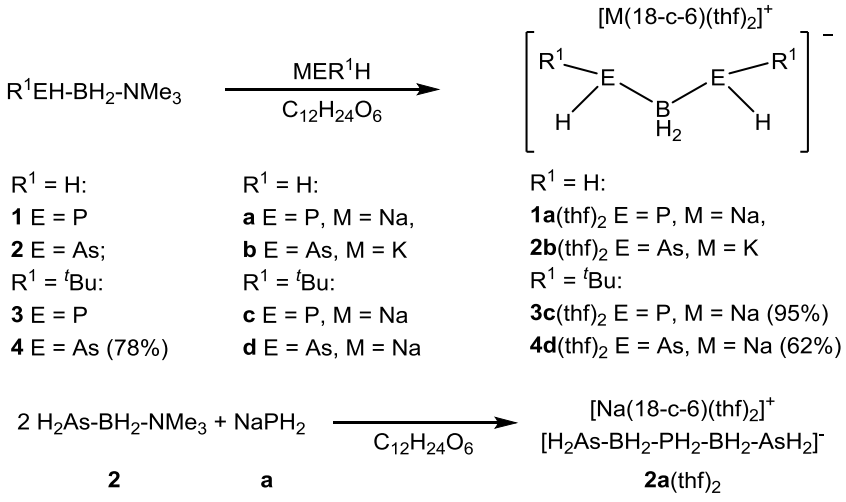

Scheme 4.1. Substitution of NMe_3 in Lewis base stabilized pnictogenylboranes of the type R^1EH-BH_2-NMe_3 [E = P, As; R1 = H, ^{t}Bu) by pnictogen based nucleophiles. Isolated yields are given in parentheses. 18-c-6 = 18-crown-6 ($C_{12}H_{24}O_6$).

According to the previously described reactions, $[Na(C_{12}H_{24}O_6)][^tBuEH\text{-}BH_2\text{-}^tBuEH]$ (**3c**: E = P; **4d**: E = As) is accessible by reaction of *tert*-butyl substituted pnictogenylboranes $^tBuEH\text{-}BH_2\text{-}NMe_3$ (**3**: E = P; **4**: E = As) with Na^tBuEH (**c**: E = P; **d**: E = As) at room temperature and subsequent addition of 18-crown-6 (Scheme 4.1).[19] Due to the extreme sensitivity towards moisture, which results in the protonation of the nucleophile, an excess of $NaNH_2$ is used for the *in situ* synthesis of Na^tBuEH (E = P, As).

Reactions of **1a**, **2b**, **2a**, **3c** and **4d** with equivalent amounts of $[W(CO)_4(nbd)]$ (nbd = bicyclo[2.2.1]hepta-2,5-diene) lead to formation of the corresponding coordination products **5**-**9** in good to excellent yields (Scheme 4.2).

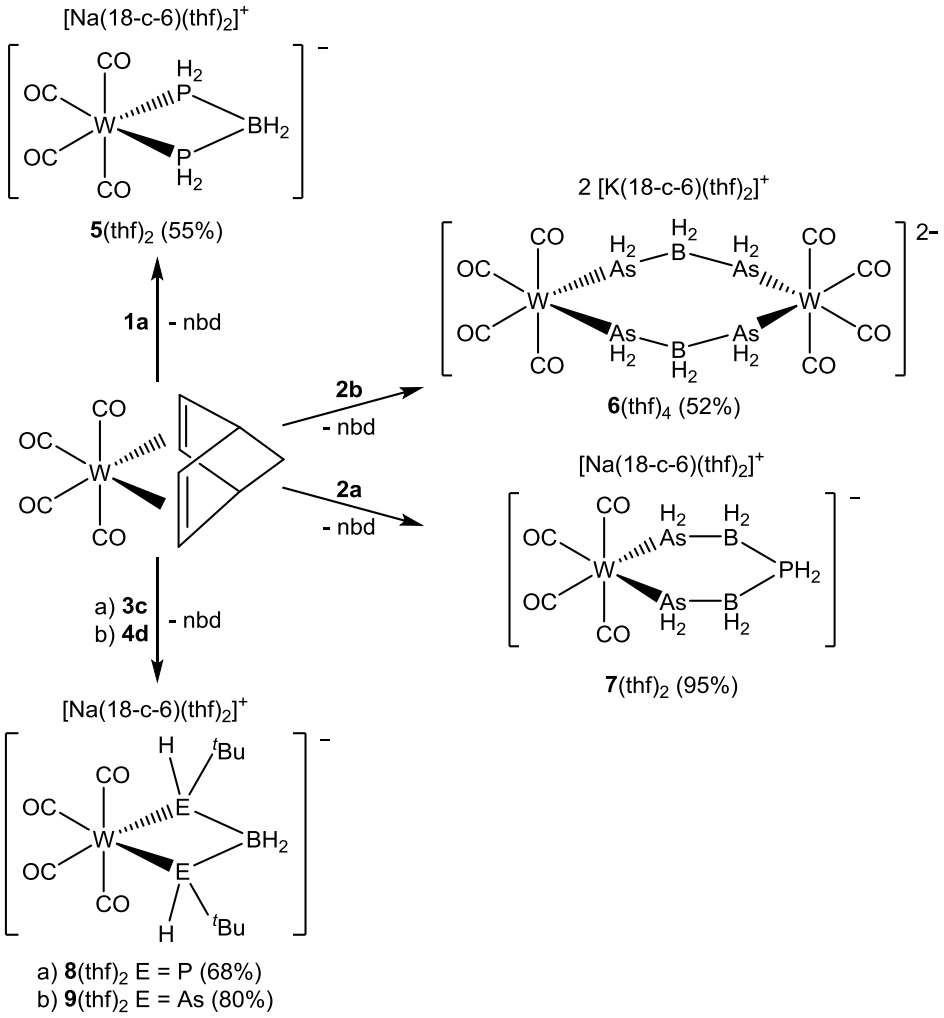

Scheme 4.2. Reaction of **1a**, **2b**, **2a**, **3c** and **4d** with $[W(CO)_4(nbd)]$ (nbd = bicyclo[2.2.1]hepta-2,5-diene). Isolated yields are given in parentheses. 18-c-6 = 18-crown-6 ($C_{12}H_{24}O_6$).

According to heteronuclear NMR spectroscopy of the crude reaction solutions, compounds **5**-**9** are accessible without the formation of side products. The ^{31}P NMR spectra of the isolated compounds **5**, **7** and **8** show a high-field shift in comparison to the corresponding starting material **1a**, **2a** and **3c**

(Table 4.1). Due to the chirality of **8** as well as **3c**, for both compounds two signals appear for the phosphorus atoms within the ^{31}P NMR spectra indicating the existence of two enantiomers. Contrary to the ^{31}P NMR spectra the shift in the ^{11}B NMR spectra of compounds **5**, **6**, **8** and **9** is directed slightly to the low-field in comparison to the starting material. An exception can be observed for compound **7**, there the ^{11}B NMR shift is identical to the uncoordinated compound **2a** (Table 4.1). Within the ^{11}B NMR spectra of the dinuclear compound **6** only a broad signal can be observed, allowing no clear indication for the formation of a mononuclear derivative.

Table 4.1. NMR parameter of starting material (**1a**, **2b**, **2a**, **3c**, **4d**)[18] and isolated coordination products (**5**, **6**, **7**, **8**, **9**).

Cmpnd.	^{31}P δ [ppm]	^{11}B δ [ppm]	$^{1}J_{B,P}$ [Hz]	$^{1}J_{P,H}$ [Hz]	$^{1}J_{B,H}$ [Hz]
1a	-175.0	-34.7	26	172	99
5	-201.0	-18.8	55		96
2b	-	-34.5	-	-	106
6		-31.1			
2a	-56.0	-37.4	58	307	105
7	-102.2	-37.4	66	328	108
3c	-44.3	-32.3	30	166	96
8	-64.6 / -70.3	-20.6		279 / 279	97
4d	-	-31.4	-	-	104
9		-11.1			103

In the ESI-MS (anion) spectra the molecular ion peak of each compounds anion can be detected. For compound **6** only a signal of the dianionic species $([W(CO)_4[H_2As\text{-}BH_2\text{-}AsH_2])_2$ can be observed.

The solid state structure of all products was also investigated by single crystal X-ray diffraction. Crystals suitable for X-ray diffraction can be obtained by layering THF solutions with *n*-hexane and storing at -28 °C. The X-ray structures of compounds **5**$(thf)_2$, **7**$(thf)_2$, **8**$(thf)_2$ and **9**$(thf)_2$ reveal mononuclear coordination complexes bearing a four membered (**5**$(thf)_2$, **8**$(thf)_2$, **9**$(thf)_2$) and a six membered heterocycle (**7**$(thf)_2$), respectively (Figure 4.1). Only for compound **6**$(thf)_4$ a dinuclear species can be observed leading to a doubly negatively charged, eight-membered ring (Figure 4.1). While in the solid state structure of compounds **5**$(thf)_2$, **7**$(thf)_2$, **8**$(thf)_2$ and **9**$(thf)_2$ the anionic pnictogen boron chain seves as chelating ligand in compound **6**$(thf)_4$ two tungsten fragments are linked by $[H_2As\text{-}BH_2\text{-}AsH_2]^-$ units (Figure 4.1). Compounds **8**$(thf)_2$ and **9**$(thf)_2$ crystalize in the non-centrosymmetric space group *P*1. According to disorder observed in the solid state structure two enantiomers *S*,*R* and *R*,*S* can be identified.[20] For **8** as well as for **9** an enantiomeric ratio of 50:50 can be determind. In Figure 4.1 only the *S*,*R* isomer of both compounds is shown. Additionally each unit cell of the solid state structure of compounds **8** and **9** includes two ion pairs.[20]

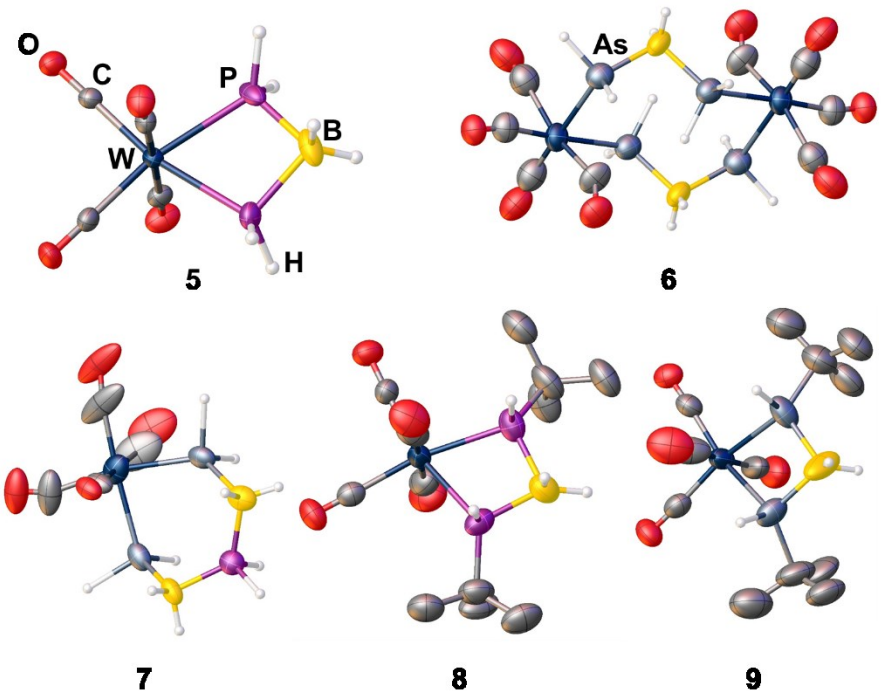

Figure 4.1. Molecular structures of the anions of **5**-**9** in the solid state. Hydrogen atoms bonded to carbon and counter ions are omitted for clarity. Thermal ellipsoids are drawn with 50% probability. Selected bond length [Å] and angles [°][20]: 5: P-B 1.957(4) – 1.982(5), P-W 2.5506(7) – 2.5531(7), P-B-P 93.0(1), P-W-P 68.08(3), W-P-B-P 12.142; **6**: As-B 2.06(1) – 2.10(2), As-W 2.594(2) – 2.666(3), As-B-As 105.013 – 105.161, As-W-As 88.52(5) – 89.08(6); **7**: As-B 2.09(3) – 2.17(4), P-B 1.95(3) – 1.99(3), As-W 2.622(3) – 2.627(4), As-B-P 103(2) – 107(2), B-P-B 64.964, As-W-As 85.06(9), **8**: P-B 1.90(1) – 1.91(1), P-C 1.81(3) – 1.85(3), P-W 2.550(5) – 2.574(5), P-B-P 92.2(8) – 92.6(8), B-P-C 117(1) – 119(2), P-W-P 65.1(1), W-P-B-P 11.884 – 15.101; **9**: As-B 2.05(2) – 2.07(2), As-C 1.93(5) – 2.00(5), As-W 2.672(3) – 2.685(3), As-B-As 91(1), B-As-C 114(2) – 118(2), As-W-As 66.3(1) – 66.5(1), W-As-B-As 9.185 – 14.812.

Comparing the structural data of the free anionic chain like compounds with their coordinated analogs the bond length between the BH_2 groups and terminal phosphine (**5**) and arsine (**6**, **7**) groups, respectively, are quite similar (Table 4.2). In compound **7** the distance between the secondary phosphine group and the neighbored BH_2 groups is comparable to the starting material (Table 4.2). Contrary to compounds **5**, **6** and **7** the pnictogen boron bond of the *tert*-butyl substituted derivatives (**8**, **9**) is slightly shortened in comparison to **3c** and **4d** (Table 4.2). Focusing on the angles between the pnictogen atoms bridged by BH_2 groups a clear decrease of the values can be observed. For compounds **5**, **8** and **9**, the four membered ring motive form an E-B-E angle of around 90° while compounds **6** and **7** allow wider angles due to the larger ring size. The B-E-C angles of the *tert*-butyl substituents in compounds **8** and **9** are increased by approximate 10° comparing to the starting material **3c** and **4d** (Table 4.2). Concerning the B-P-B angle of compound **7** an increase from 122.9(2)° to 125(1)° can be observed.

Table 4.2. Comparison of selected bond length and angles of the starting materials **1a**[18], **2b**[18], **2a**[18], **3c**, **4d** and compounds **5**, **6**, **7**, **8**, **9**.

Cmpnd	E-B [Å]	E'-B [Å]	E-C [Å]	E-B-E' [°]	B-E-C [°]
E = P					
1a	1.960(3) – 1.963(3)	-	-	110.4(1)	-
5	1.957(4) – 1.982(5)			93.0(1)	
E = As					
2b	2.062(2) – 2.069(2)	-	-	109.47(2) – 110.99(2)	-
6	2.06(1) – 2.10(2)			105.012 – 105.161	
E = As, E' = P					
2a	2.081(3)	1.947(3)	-	110.2(2)	-
7	2.09(3) – 2.17(4)	1.95(3) – 1.99(3)		103(2) – 107(2)	
E = P					
3c	1.943(4) – 1.973(9)	-	1.85(1) – 1.867(6)	106.8(3) – 109.7(4)	108.1(2) – 108.8(2)
8	1.90(1) – 1.91(1)		1.81(3) – 1.85(3)	92.2(8) – 92.6(8)	117(1) – 119(2)
E = As					
4d	2.066(4) – 2.100(4)	-	1.980(4) – 2.041(3)	100.9(2) – 104.6(2)	103.6(1) – 105.0(2)
9	2.05(2) – 2.07(2)		1.93(5) – 2.00(5)	91(1)	114(2) – 118(2)

To rationalize the different reactivity of **1a** and **2b** towards $[W(CO)_4(nbd)]$ DFT calculations were performed. The reaction energies in the gas phase reveal that the formation of the dimer is favored by -27.4 kJ·mol^{-1} for **1a** and only -6.4 kJ·mol^{-1} for **2b**. These results suggest, that also in the reaction of **1a** with $[W(CO)_4(nbd)]$ a dimeric complex should be expected. In the case of phosphorus the dimer would be the expected product. Instead, experimentally the monomeric complex **5** is formed. A closer look to the thermodynamic parameters shows, that the formation of **5** is entropically favored (**5**: ΔS^0_{298} = 13.3 J·mol^{-1}K^{-1}; (**5**)$_2$: ΔS^0_{298} = -146.2 J·mol^{-1}K^{-1}) which probably determines the outcome of the reaction. Similarly, the entropy term for the arsenic derivative favors the building of the monomeric complex $[(CO)_4W(H_2As\text{-}BH_2\text{-}AsH_2)]^-$ (**6**$_{0.5}$) (**6**$_{0.5}$: 9.0 J·mol^{-1}K^{-1}; **6**: ΔS^0_{298} = -157.2 J·mol^{-1}K^{-1}). Very probably, the formation of **5** is kinetically controlled, while **6** represents the thermodynamic product of the reaction, which can be explained by the weaker As-W bonds.

As shown by compound **6** the anionic chain like compounds can not only serve as chelating ligands but also as a linker between transition metal fragments. Therefore, two equivalents of **1a** are reacted with one equivalent of $[Cu(CH_3CN)_4][BF_4]$. By substitution of the acetonitrile ligands a three dimensional MOF-like scaffold is formed (Scheme 4.3).

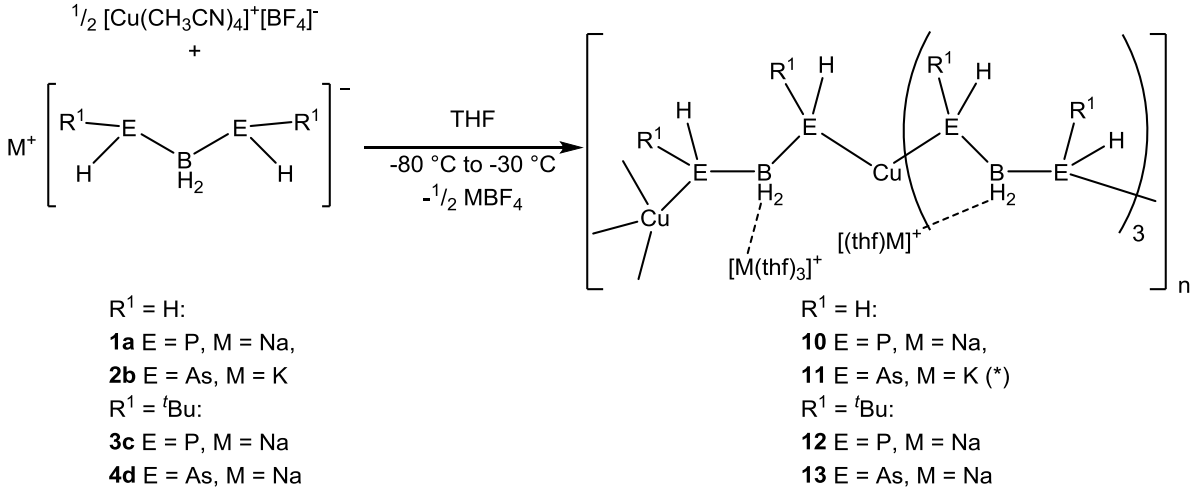

R^1 = H:
1a E = P, M = Na,
2b E = As, M = K
R^1 = *t*Bu:
3c E = P, M = Na
4d E = As, M = Na

R^1 = H:
10 E = P, M = Na,
11 E = As, M = K (*)
R^1 = *t*Bu:
12 E = P, M = Na
13 E = As, M = Na

Scheme 4.3. Reaction of $[R^1R^2E\text{-}BH_2\text{-}ER^1R^2]^-$ (E = P, As; $R^1 = R^2$ = H; R^1 = H, R^2 = ^{t}Bu) units with $[Cu(CH_3CN)_4][BF_4]$. (*) The formation of compound **11** cannot be observed at any time, decomposition of the starting material occurs instead.

According to the ^{31}P NMR spectrum of the reaction mixture the conversion of **1a** with $[Cu(CH_3CN)_4][BF_4]$ is quantitative. A shift of the resonance signal attributed to the PH_2 groups from -175.0 ppm to -167.4 ppm can be observed for the resulting product **10**. This low field shift can be explained by the coordination of the lone pair, located at the terminal phosphine atom, towards the copper(I) ion resulting in a decreased electron density on the phosphorus atom. In the ^{11}B NMR spectra a shift to higher field from -34.7 ppm to -35.4 ppm occurs.[18] In the ESI-MS (anion mode) spectrum among the peak of other molecular ion fragments a peak for $[Cu_2(H_2P\text{-}BH_2\text{-}PH_2)_3]^-$ can be detected.[21] This fragment clearly indicates the linking character of the used $[H_2P\text{-}BH_2\text{-}PH_2]^-$ between the copper ions. Crystals suitable for X-ray diffraction can be obtained by layering a THF solution with *n*-hexane and storing at -28 °C. The unit cell for the product **10** shows a molecular composition of $[Cu_2Na_2(thf)_4[H_2P\text{-}BH_2\text{-}PH_2]_4]$ (Scheme 4.3). Both copper ions are linked by $[H_2P\text{-}BH_2\text{-}PH_2]^-$ units and tetrahedrally coordinated by PH_2 groups (Figure 4.2). One $[Na(thf)]^+$ fragment (Na2) is coordinated by three neighbored BH_2 groups via the hydridic hydrogen atoms, while a second Na^+ ion (Na1) is coordinated by only one BH_2 group of the $[H_2P\text{-}BH_2\text{-}PH_2]^-$ unit and three THF molecules (Figure 4.2). The distances between the hydrogen atoms of the borane groups and the sodium ions is between 2.2(2) Å and 2.5(2) Å which is considerably longer than the sum of the covalent radii of Na and H (1.87 Å)[22] but below the sum of the van der Waals (vdW) radii (3.37 Å)[23]. The distance between the copper (Cu2) and the sodium atom (Na2) is found to be 3.375(2) Å. This value also exceeds the sum of the covalent radii of Cu and Na (2.67 Å)[23] but is below the sum of the van der Waals radii (3.7 Å) of both atoms.[24]

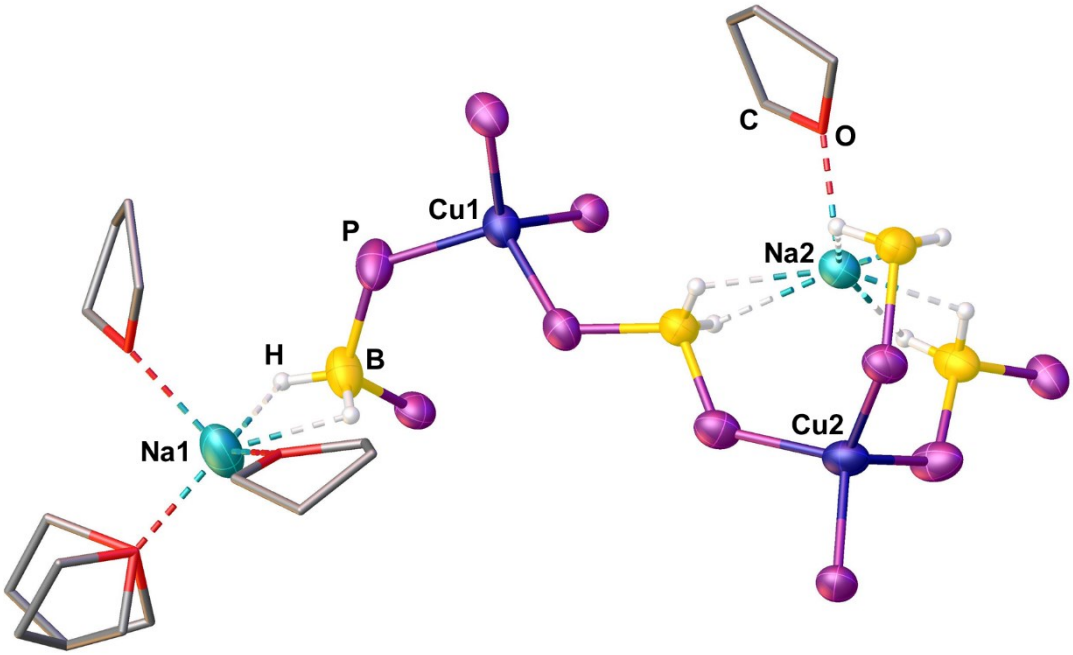

Figure 4.2. Environment of the copper atoms in compound **10**. Hydrogen atoms bonded to carbon and phosphorus are omitted for clarity. Thermal ellipsoids are drawn with 50% probability, THF-molecules are drawn as tubes. Selected bond length [Å] and angles [°]: P-B 1.938(8) – 1.967(8), P-Cu 2.288(2) – 2.300(2), Cu2-Na 3.375(2), H-Na 2.2(2) – 2.5(2), P-B-P 113.3(4) – 113.9(4), P-Cu-P 102.84(6) – 118.22(7).

The P-B bond lengths in compound **10** are almost unchanged comparing to the starting material (**10**: 1.938(8) – 1.967(8) Å, **1a**: 1.960(3) – 1.963(3) Å). However, the value of the P-B-P-angle are slightly wider (**10**: 113.3(4) – 113.9(4) Å, **1a**: 110.4(1) Å).

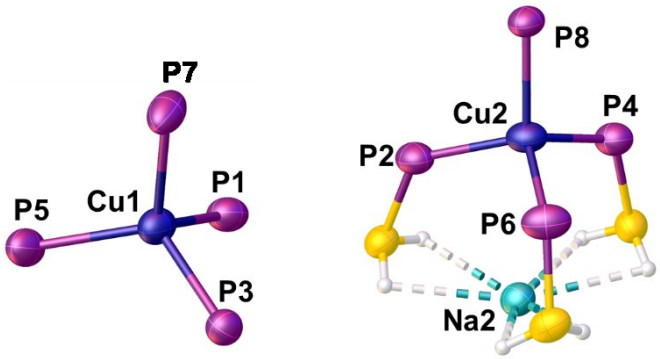

Figure 4.3. Tetrahedral coordination of the phosphorus atoms towards copper ions. Hydrogen atoms bonded to phosphorus are omitted for clarity. Thermal ellipsoids are drawn with 50% probability.

While the phosphine groups coordinating to Cu2 are arranged in a way close to the tetrahedral angle of 109.47° the deviations in case of Cu1 are more significant (Figure 4.3, Table 4.3). Coordination of the sodium ion near Cu2 leads to a more rigid environment resulting in more uniform angle values.

Table 4.3. Bond length [Å] and angles [°] of phosphorus atoms bonded to copper ions.

	X = 1	X = 2
P-Cu(X) [Å]	2.288(2) – 2.298(2)	2.290(2) – 2.300(2)
P-Cu(X)-P [°]	102.84(6)	105.80(7)
	106.60(7)	107.121
	107.57	107.333
	109.73(7)	111.679
	111.74(8)	112.266
	118.22(7)	112.595

The bond lengths between the copper atoms and the coordinating PH_2 groups is overall very similar. With a value around 2.288(2) to 2.300(2) it is in between the range of a covalent bond (2.23 Å)[22] and the sum of the van der Waals radii (3.23 Å)[23,24] confirming a coordinative interaction.

Stacking multiple elemental cells reveal a solid state structure of **10** where the Cu-atoms linked by $[H_2P\text{-}BH_2\text{-}PH_2]^-$ units arrange in a three dimensional scaffold with an adamantane-like repeating unit comparable to a cubic diamond crystal structure (Figure 4.4).

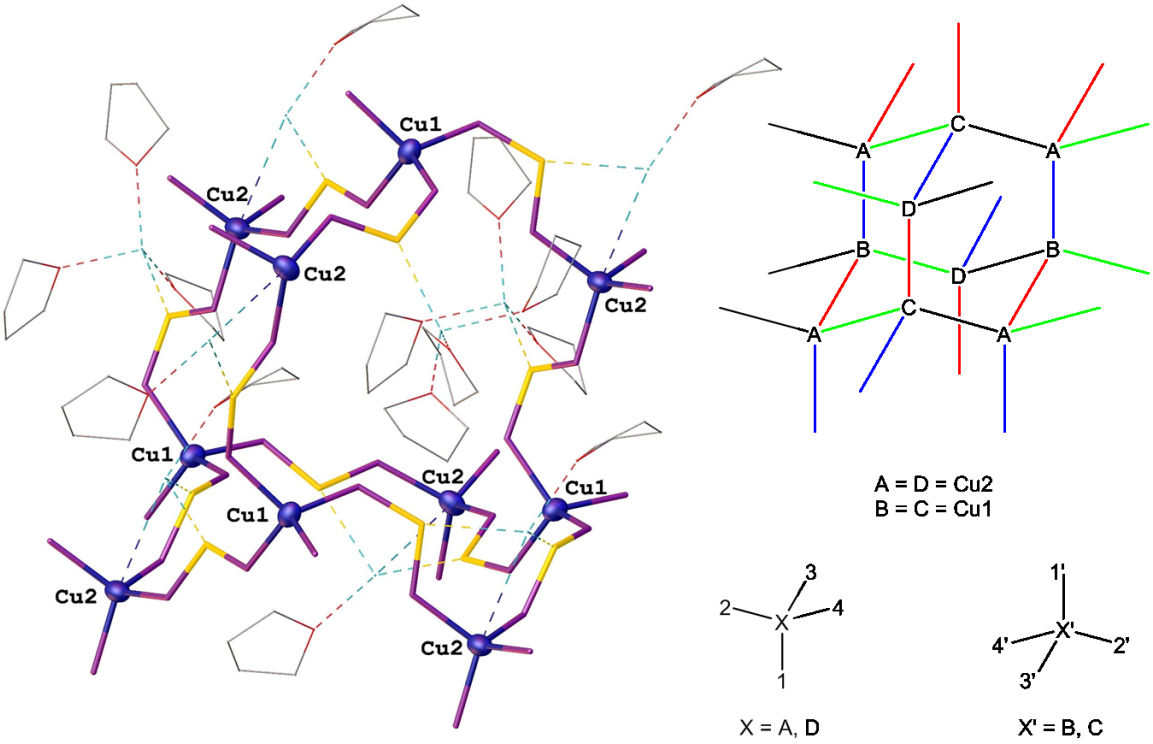

Figure 4.4. Expanded molecular structure of **10**; Hydrogen atoms are omitted for clarity. Left*:* grown molecular structure of **10** in solid state, thermal ellipsoids are drawn with 50% probability, C-, O- and Na-atoms are drawn as wireframe, P- and B-atoms are drawn as tubes*;* right top: model of the adamantane-like repeating unit with given bond length [Å]: 7.521 (green), 6.848 (red), 6.675 (blue), 6.582 (black); right bottom: corresponding tetrahedral coordination centers with given values in Table 4.4.

While in the diamond structure the scaffold is based on tetrahedrally linked carbon atoms with identical angles of 109°28’ (109.47°) and distances of 0.154 nm the determined scaffold of compound

10 is highly distorted.[25] Beside four unequal distances between the copper atoms (Figure 4.4) also the angles differ significantly (Table 4.4) in comparison to values found within the diamond structure.

Table 4.4. Angles between Cu-atoms of the adamantane-like unit (shown in Figure 4.4 bottom right).

∠	∠(Cu1-Cu2-Cu1) (X = A, D) [°]		∠(Cu2-Cu1-Cu2) (X = B, C) [°]	
	X = A	X = D	X = B	X = C
1-X-2	118.805	106.303	128.413	97.555
1-X-3	92.629	92.629	92.629	92.629
1-X-4	104.078	130.147	113.901	118.418
2-X-3	130.147	104.078	118.418	113.901
2-X-4	102.284	102.284	102.284	102.284
3-X-4	106.303	118.805	97.555	128.413

The sodium atoms with coordinated THF-molecules are located inside of the voids of the scaffold but are not directly involved as building units of the scaffold structure.

Expecting similar results according to the reaction of **1a** with $[Cu(CH_3CN)_4][BF_4]$, analog reactions are carried out with compounds **3c** and **4d**. Crystallization or even isolation of the products was not possible due to great solubility even in *n*-hexane. Additionally at temperatures over -15 °C as well as by completely removing the solvent under reduced pressure, decomposition can be observed. Therefore, investigations of these reactions are restricted to multinuclear NMR spectroscopy and mass spectrometry. According to the ^{31}P NMR spectrum of the reaction mixture the conversion of **3c** with $[Cu(CH_3CN)_4][BF_4]$ is quantitative (Scheme 4.3). For the resulting product **12** two signals can be observed which are low field shifted from -44.3 ppm (**3c**) to -38.9 ppm and -28.2 ppm, respectively. The number of signals is probably caused by the two enantiomers, similar to the ^{31}P NMR spectra of compound **3c** and **8**. In the ^{11}B NMR spectra the broadened signal of the product is slightly high field shifted from -32.3 ppm (**3c**) to -34.9 ppm. In the ESI-MS (anion mode) spectrum a peak for a $[Cu_2(^t\text{BuPH-BH}_2\text{-}^t\text{BuPH})_3]^-$ fragment can be detected. The low field shift within the ^{31}P NMR spectrum clearly indicates a coordination of the phosphorus atoms towards the copper ion. This assumption is supported by the molecular ion peak occurring in the ESI-MS spectrum, additionally proving that the used $[^t\text{BuPH-BH}_2\text{-}^t\text{BuPH}]^-$ serves as a linker between Cu(I) ions.

For a quantitative reaction of **4d** with $[Cu(CH_3CN)_4][BF_4]$ an excess of the copper salt is necessary. Comparable to compound **12**, in the ^{11}B NMR spectrum of the crude reaction mixture the signal of the expected coordination product **13** is broadened and slightly high field shifted from -31.4 ppm to -32.2 ppm in comparison to the starting material **4d**. Analog to compounds **10** and **12** in the ESI-MS spectrum a peak for a $[Cu_2(^t\text{BuAsH-BH}_2\text{-}^t\text{BuAsH})_3]^-$ fragment can be observed. However the signal of this fragment is decaying extremely fast what indicates a great sensitivity and instability of the assumed coordination compound **13**. Storing the pale orange reaction solution at room temperature for a few hours leads to a subsequent darkening and precipitation of black solid.

Adding **2b** to a solution of $[Cu(CH_3CN)_4][BF_4]$ even at -80 °C immediately turns the reaction solution black and no clear indication for product formation can be observed. In the ESI-MS spectrum molecular ion peaks of $[(H_2As\text{-}BH_2)_nAsH_2]^-$ fragments (n = 2, 3, 4) and a decaying signal of a $[CuAs_6B_4H_{20}]^-$ fragment can be detected.

4.3 Conclusion

An easy synthetic approach for *tert*-butyl substituted anionic pnictogenylborane derivatives is presented here. Reacting Na^{t}BuEH with ^{t}BuEH-BH_2-NMe_3 leads to formation of the corresponding product $[Na)C_{12}H_{24}O_6)][^t$BuEH-BH_2-^{t}BuEH] (**3c**: E = P; **4d**: E = As). Reactions of the obtained organosubstituted anionic chain like compounds (**3c**, **4d**) as well as their hydrogen substituted derivatives (**1a**, **2b**, **2a**) with $[W(CO)_4(nbd)]$ lead to the corresponding coordination products **5**-**9** revealing cyclic motifs. The formation of mononuclear complexes (**5**, **7**, **8**, **9**) can be observed. Further the dinuclear species **6** is accessible revealing an eight membered heterocycle. Here the $[H_2As\text{-}BH_2\text{-}AsH_2]^-$ units serve as linkers between the transition metal fragments. Reaction of **1a** with Cu(I) ions leads to a MOF-like three dimensional scaffold including a distorted adamantan like repeating unit. Investigations by multinuclear NMR spectroscopy and mass spectrometry indicate similar reactivity for compounds **3c** and **4d** with Cu(I) ions while for **2b** no product formation can be observed. The here presented results prove anionic pnictogenylborane derivatives as suitable reactants for coordination chemistry. In Addition to their role as chelating ligands these compounds prove to be viable candidates for linking transition metal fragments to build up more sophisticated three dimensional structures. The synthesis of other substituted derivatives as well as the investigation of the coordination behavior towards other transition metal ions and fragments is part of current investigations.

4.4 References

[1] H. Furukawa, K. E. Cordova, M. O'Keeffe, O. M. Yaghi, *Science* **2013**, *341*, 1230444.

[2] a) S. Rautiainen, D. Di Francesco, S. N. Katea, G. Westin, D. N. Tungasmita, J. S. M. Samec, *Chem. Sus. Chem*, **2018**, *11*, 1-6; b) M.-L. Chen, X.-F. Xu, Z.-X. Cao, Q.-M. Wang, *Inorg. Chem.*, **2008**, *47*, 1877-1879; c) R. J. Schwamm, M. D. Anker, M. Lein, M. P. Coles, *Angew. Chem. Int. Ed.* **2019**, *58*, 1489-1493; d) H. I. Buvailo, O. V. Desiatkina, , V. G. Makhankova, V. N. Kokozay, K. V. Domasevitch, I. V. Omelchenko, V. V. Dyakonenko, *J. Solid State Chem.* **2019**, *270*, 563-568; e) X. Jiang, M. L. Naitana, N. Desbois, V. Quesneau, S. Brandès, Y. Rousselin, W. Shan, W. R. Osterloh, V. Blondeau-Patissier, C. P. Gros, K. M. Kadish, *Inorg. Chem.* **2018**, *57*, 1226-1241; f) S. Abdolmaleki, N. Yarmohammadi, H. Adibi, M. Ghadermazi, M. Ashengroph, H. A. Rudbari, G. Bruno, *Polyhedron* **2019**, *159*, 239-250; g) S. Nayak, A. C. Dash, G. K. Lahiri, *Transit. Metal. Chem.* **2008**, *33*, 39-53; h) G. Ali, P. E. VanNatta, D. A. Ramirez, K. M. Light, M. T. Kieber-Emmons, *J. Am. Chem. Soc.* **2017**, *139*, 18448-18451.

[3] a) X. Qi, T. Zheng, J. Zhou, Y. Dong, X. Zuo, X. Li, H. Sun, O. Fuhr, D. Fenske, *Organometallics* **2019**, *38*, 268-277; b) W.-F. Liaw, D.-S. Ou, Y.-C. Horng, C.-H. Lai, G.-H. Lee, S.-M. Peng, *Inorg. Chem.* **1994**, *33*, 2495-2496; c) A. M. Baranger, R. G. Bergman, *J. Am. Chem. Soc.* **1994**, *116*, 3822-3835.

[4] a) K. W. Muir, R. Walker, J. Chatt, R. L. Richards, G. H. D. Royston, *J. Organomet. Chem.* **1973**, *56*, C30-C32; b) L.-B. Han, F. Mirzaei, S. Shimada, *Heteroatom Chem.* **2018**, *29*, e21463; c) F. R. Kreissl, N. Ullrich, J. Ostermeier, W. Schuett, *J. Organomet. Chem.* **1993**, *459*, C6-C8.

[5] a) M. R. Elsby, J. Liu, S. Zhu, L. Hu, G. Huang, S. A. Johnson, *Organometallics* **2019**, *38*, 436-450; b) J. C. Babon, M A. Esteruelas, I. Fernandez, A. M. Lopez, E. Onate, *Organometallics* **2018**, *37*, 2014-2017; c) M. A. Esteruelas, I. Fernandez, A. Herrera, M. Martin-Ortiz, R. Martinez-Alvarez, M. Olivan, E. Onate, M. A. Sierra, M. Valencia, *Organometallics* **2010**, *29*, 976-986.

[6] a) Q. Jiang, D. M. Peacock, J. F. Hartwig, T. R. Cundari, *Tetrahedron* **2019**, *75*, 137-143; b) Y. Tan, F. Barrios-Landeros, J. F. Hartwig, *J. Am. Chem. Soc.* **2012**, *134*, 3683-3686; c) A. Lorenz, D. Fenske, *Z. Anorg. Allg. Chem.* **2001**, *627*, 2232-2248.

[7] a) J. A. Osborn, G. Wilkinson, *Inorg. Syn.* **1967**, *10*, 67-71; b) S. Zubair, F. Asghar, A. Badshah, B. Lal, R. A. Hussain, S. Tabassum, M. N. Tahir, *J. Organomet. Chem.* **2019**, *879*, 60-68; c) R. Ramachandran, R. J. Puddephatt, *Inorg. Chem.* **1993**, *32*, 2256-2260.

[8] a) T. Chen, L.-B. Han, *Heteroatom Chem.* **2018**, *29*, e21460; b) T. Kawashima, M. Ohashi, S. Ogoshi, *J. Am. Chem. Soc.* **2018**, *140*, 17423-17427; c) M. A. Esteruelas, F. J. Lahoz, M. Olivan, E. Onate, L. A. Oro, *Organometallics* **1995**, *14*, 3486-96.

[9] P. W. Smith, S. R. Ellis, R. C. Handford, T. Don Tilley, *Organometallics* **2019**, *38*, 336–342.

[10] a) A. M. Bradford, E. Kristof, M. Rashidi, D.-S. Yang, N. C. Payne, R. J. Puddephatt, *Inorg. Chem.* **1994**, *33*, 2355-2363; b) W. Liang, K. Nakajima, K. Sakata, Y. Nishibayashi, *Angew. Chem. Int. Edit.* **2019**, *58*, 1168-1173; c) Q.-H. Jin, L.-L. Song, K.-Y. Hu, L.-L. Zhou, Y.-Y. Zhang, R. Wang, *Inorg. Chem. Commun.* **2010**, *13*, 62-65.

[11] a) J. Bailey, M. J. Church, M. J. Mays, *J. Coord. Chem.* **1973**, *3*, 63-65; b) H. Seino, Y. Ishii, M. Hidai, *Organometallics* **1994**, *13*, 364-369; c) S. Donovan-Mtunzi, R. L. Richards, J. Mason, *J. Chem. Soc. Dalton Trans.* **1984**, *0*, 469-474.

[12] a) M. O. Sanchez-Guadarrama, D. Martinez-Velazquez, N. Zuniga-Villarreal, *Inorg. Chim. Acta* **2019**, *487*, 247-256; b) S. H. Chong, D. J. Young, T. S. A. Hor, *Chem. Asian J.* **2007**, *2*, 1356-1362; c) A. B. Chaplin, P. J. Dyson, *Eur. J. Inorg. Chem.* **2007**, *31*, 4973-4979.

[13] a) T. H. O. Leite, G. Grawe, J. Honorato, B. N. Cunha, O. R. Nascimento, P. S. de Vargas, C. Donatoni, K. T. Oliveira, J. M. S. Lopes, N. M. Barbosa Neto, W. C. Moreira, L. R. Dinelli, A. A. Batista, *Inorg. Chem.* **2019**, *58*, 1030-1039; b) T. Niksch, H. Goerls, M. Friedrich, R. Oilunkaniemi, R. Laitinen, W. Weigand, *Eur. J. Inorg. Chem.* **2010**, *1*, 74-94; c) R. Hourihane, G. Gray, T. Spalding, T. Deeney, *J. Organomet. Chem.* **2002**, *642*, 40-47.

[14] a) R. N. Pandey, S. S. Kumar, K. Shahi, *Int. J. Chem. Sci.* **2014**, *12*, 672-678; b) M. El-khateeb, *J. Mol. Struct.* **2016**, *1123*, 300-304; c) J. A. Clark, M. Kilner, *J. Organomet. Chem.* **1988**, *347*, 107-13.

[15] a) S. S. Sirat, O. B. Shawkataly, I. A. Razak, *Polyhedron* **2018**, *155*, 493-499; b) O. Bin Shawkataly, I. A. Khan, S. Syaida Sirat, H.-K. Fun, M. Mustaqim Rosli, *Z. Anorg. Allg. Chem.* **2014**, *640*, 1397-1402; c) O. Bin Shawkataly, I. A. Khan, C. S. Yeap, H.-K. Fun, *Acta Crystallogr., Section E: Structure Reports Online* **2010**, *66*, m227-m228, Sm227/1-Sm227/16; d)T. Thomas, D. Pugh, I. P. Parkin, C. J. Carmalt, *Dalton T.* **2010**, *39*, 5325-5331.

[16] a) W. Levason, F. M. Monzittu, G. Reid, W. Zhang, *Chem. Commun.* **2018**, *54*, 11681-11684; b) J.-Y. Tsai, C. Xia, M. A. Esteruelas, E. O. Rodriguez, T. Bolano, A. U. Palacios, *U.S. Pat. Appl. Publ.* **2015**, US 20150129840 A1 20150514; c) S. Aime, R. Gobetto, G. Minghetti, A. L. Bandini, G. Banditelli, *J. Clust. Sci.* **1994**, *5*, 523-33.

[17] a) I. Haiduc, I. Silaghi-Dumitrescu, *Coordin. Chem. Rev.* **1986**, *74*, 127-270; b) M. Scheer, *Dalton Trans.* **2008**, 4372–4386; c) P.-H. Zhao, M.-Y. Hu, J.-R. Li, Z.-Y. Ma, Y.-Z. Wang, J. He, Y.-L. Li, X.-F. Liu, *Organometallics* **2019**, *38*, 385–394.

[18] C. Marquardt, T. Kahoun, A. Stauber, G. Balázs, M. Bodensteiner , A. Y. Timoshkin, M. Scheer, *Angew. Chem. Int. Ed.* **2016,** *55*, 14828-14832; *Angew. Chem.* **2016**, *128*, 15048-15052.

[19] Using a teflon coated stirring bar in combination with Na^{t}BuEH (E = P, As) reproducibly turns the reaction solution green and the teflon coat becomes black. So glas coated stirring bars were used.

[20] See Supporting Information for further information; Subchapter 4.5.3: **5**(thf)$_2$ - **9**(thf)$_2$.

[21] See Supporting Information for further information; Subchapter 4.5.3: **10**(thf)$_4$.

[22] P. Pyykkö, M. Atsumi, *Chem. Eur. J.* **2009**, *15*, 12770-12779.

[23] M. Mantina, A. C. Chamberlin, R. Valero, C. J. Cramer, D. G. Truhlar, *J. Phys. Chem. A* **2009**, *113*, 5806–5812.

[24] A. Bondi, *J. Phys. Chem.* **1964**, *68*, 441-451.

[25] W. Kleber, H.-J. Bautsch, J. Bohm: *Einführung in die Kristallographie,* Oldenbourg Verlag, **2002**, 157.

4.5 Experimental Section

4.5.1 Synthetic Procedures

All manipulations were performed under an atmosphere of dry argon/ nitrogen using standard glove-box and Schlenk techniques. All solvents were degassed and purified by standard procedures. The compounds $[M(C_{12}H_{24}O_6)][H_2E\text{-}BH_2\text{-}EH_2]$ (E = P, M = Na; E = As, M = K)[1], $[Na(C_{12}H_{24}O_6)][H_2As\text{-}BH_2\text{-}PH_2\text{-}BH_2\text{-}AsH_2]$[1], $[W(CO)_4(nbd)]$ (nbd = C_7H_8)[2], ^{t}BuPH$_2$[3], ^{t}BuAsH$_2$[4], were prepared according to literature procedures. Other chemicals were obtained from TCI Chemicals ($[Cu(C_2H_3N)_4][BF_4]$). Na^{t}BuPH was firstly synthesised in 2015 without further characterisation.[5]

The NMR spectra were recorded on either an Avance 400 spectrometer (**3c**, **4d**, **5**, **6**, **7**, **8**, **9**, **10**, **12**, **13**) (^{1}H: 400.13 MHz, ^{31}P: 161.976 MHz, ^{11}B: 128.378 MHz, ^{13}C{^{1}H}: 100.623 MHz) with δ [ppm] referenced to external $SiMe_4$ (^{1}H, ^{13}C), H_3PO_4 (^{31}P), $BF_3{\cdot}Et_2O$ (^{11}B) or an **Avance III HD 600** spectrometer (**3c**, **4d**, **8**, **9**) (^{1}H: 600.13 MHz).

IR spectra were recorded on a Thermo Scientific (NICOLET iS 5, iD1 Transmission) FT-IR spectrometer (**3c**, **4d**, **5**, **6**, **7**, **8**, **9**) with $\tilde{\nu}$ [cm^{-1}]. Mass spectra were recorded either on a Waters/Micromass LCT-TOF classic (**3c**, **4d**, **5**, **6**, **7**, **8**, **9**, **10**, **12**, Mass Spectrometer in Working group, ESI-MS) or an Agilent Q-TOF 6540 UHD (**13**, Mass Spectrometer Department of University of Regensburg).

The C, H, N analyses were measured on an Elementar Vario EL III apparatus (**3c**, **4d**, **5**, **6**, **7**, **8**, **9**).

General remarks for C, H, N analyses:

C, H, N analyses were carried out repeatedly. Different amounts of coordinating THF have been found in nearly all cases. Total removal of the THF was not always possible, however C, H, N analyses are in good agreement with the expected values considering a varying THF-content (0.5 % tolerance).

Synthesis of Na^{t}BuPH: 1.2 mL (900 mg, 10.00 mmol) ^{t}BuPH$_2$ is added to a suspension of 390 mg (10.00 mmol) $NaNH_2$ in 10 mL THF at -50°C. The solution is stirred for 5 h at room temperature, until all $NaNH_2$ is consumed. A clear yellow solution is obtained which is degassed three times to remove NH_3. The solution is used as a 1 M stock solution of Na^{t}BuPH in THF.

Yield of Na^{t}BuPH: (100%, according to ^{31}P NMR).

^{31}P NMR (C_6D_6, 25 °C): δ = -81.4 (dm, $^1J_{P,H}$ = 157 Hz, ^{t}BuPH).

$^{31}P\{^{1}H\}$ NMR (C_6D_6, 25 °C): δ = -81.4 (s, ^{t}BuPH).

Synthesis of Na^{t}BuAsH: 268 mg (2.00 mmol) ^{t}BuAsH$_2$ in 2 ml toluene is added to a suspension of 78 mg (2.00 mmol) $NaNH_2$ in 5 mL THF and a glas stirring bar. The solution is stirred for 16 h at room temperature, until all $NaNH_2$ is consumed. A clear yellow solution is obtained which is degassed three times to remove NH_3. The conversion is assumed to be quantitative.

Synthesis of ^{t}BuAsH-BH$_2$-NMe$_3$ (**4**): A solution of 400 mg (2.00 mmol) IBH$_2$-NMe$_3$ in 5 ml THF is added to a solution of 312 mg (2.00 mmol) Na^{t}BuAsH in 5 ml THF and a glas stirring bar at -80 °C. The reaction mixture is stirred for 16 h and allowed to reach room temperature. All volatiles are removed *in vacuo* at -35 °C. The residue is dissolved in 4 ml *n*-hexane, filtrated over diatomaceous earth and dried *in vacuo*.

Yield of ^{t}BuAsH-BH$_2$-NMe$_3$: 321 mg (78%).

The NMR sample is taken from the crude product before filtration.

^{1}H NMR (C_6D_6, 25 °C): δ = 1.64 (s, 9H, C(CH$_3$)$_3$), 1.91 (s, 9H, N(CH$_3$)$_3$), 2.11 (s, 1H, AsH), 3.01 (q, br, $^{1}J_{H,B}$ = 108 Hz, 2H, BH$_2$).

^{11}B NMR (C_6D_6, 25 °C): δ = -5.2 (t, $^{1}J_{H,B}$ = 108 Hz, BH$_2$).

$^{11}B\{^{1}H\}$ NMR (C_6D_6, 25 °C): δ = -5.2 (s, BH$_2$).

Synthesis of [Na($C_{12}H_{24}O_6$)(thf)$_2$][^{t}BuPH-BH$_2$-^{t}BuPH] (**3c**(thf)$_2$):

A solution of 322 mg (2.00 mmol) ^{t}BuPH-BH$_2$-NMe$_3$ in 4 ml THF is added to a solution of 224 mg (2.00 mmol) Na^{t}BuPH and 80 mg (2.00 mmol) $NaNH_2$ in 8 ml THF at -80 °C while using a glass coated stirring bar. The solution is allowed to reach room temperature and stirred for 4 d. Subsequently 528 mg (2.00 mmol) solid $C_{12}H_{24}O_6$ (18-crown-6) are added to the solution. All volatiles are removed *in vacuo* and the residue is dissolved in 6 ml toluene. After filtration the solvent is removed *in vacuo* and the remaining pale yellow solid is dissolved in THF. **3c**(thf)$_2$ crystallizes at -28 °C as pale yellow needles. The supernatant is decanted, the crystals are washed two times with 5 ml diethyl ether at -30 °C and dried *in vacuo*. A second fraction can be obtained by storing the concentrated supernatant at -28 °C again to rise the yield. **3c** crystallizes from a toluene solution layered with 3-4-fold amount of pentane at -28 °C.

Yield of [Na($C_{12}H_{24}O_6$)(thf)$_{0.6}$][^{t}BuPH-BH$_2$-^{t}BuPH] (**3c**(thf)$_{0.6}$): 995 mg (95%).

^{1}H NMR (toluene-d_8, 25 °C): δ = 1.56 (m, br, 1H, B<u>H</u>^{a}H^{b}), 1.61 (m, 18H, ^{t}Bu), 1.94 (m, br, 1H, BH^{a}<u>H</u>^{b}), 2.36 (dm, $^{1}J_{H,P}$ = 202 Hz, ^{t}BuP<u>H</u>), 2.48 (dm, $^{1}J_{H,P}$ = 202 Hz, ^{t}BuP<u>H</u>), 3.32 (s, 24H, $C_{12}H_{24}O_6$).

^{11}B NMR (toluene-d_8, 25 °C): δ = -32.0 (tq, $^{1}J_{B,H}$ = 96 Hz, $^{1}J_{B,P}$ = 34 Hz, BH_2).

^{11}B{^{1}H} NMR (toluene-d_8, 25 °C): δ = -32.0 (q, $^{1}J_{B,P}$ = 34 Hz, BH_2).

^{31}P NMR (toluene-d_8, 25 °C): δ = -48.4 (m, br, ^{t}BuPH).

^{31}P{^{1}H} NMR (toluene-d_8, 25 °C): δ = -48.4 (m, ^{t}BuPH).

^{13}C{^{1}H} NMR (toluene-d_8, 25 °C): δ = 27.2 (m, <u>C</u>$(CH_3)_3$), 33.8 (m, CH_3), 69.5 (s, $C_{12}H_{24}O_6$).

^{11}B NMR (thf-d_8, 25 °C): δ = -32.3 (tt, $^{1}J_{B,H}$ = 96 Hz, $^{1}J_{B,P}$ = 30 Hz, BH_2).

^{11}B{^{1}H} NMR (thf-d_8, 25 °C): δ = -32.3 (t, $^{1}J_{B,P}$ = 30 Hz, BH_2).

^{31}P NMR (thf-d_8, 25 °C): δ = -44.3 (d, br, $^{1}J_{P,H}$ = 166 Hz, ^{t}BuPH).

^{31}P{^{1}H} NMR (thf-d_8, 25 °C): δ = -44.3 (m, ^{t}BuPH).

IR (KBr): $\tilde{\nu}$ = 2910 (s, CH), 2884 (s, CH), 2850 (s, CH), 2755 (vw), 2689 (vw), 2319 (w, BH), 2237 (w, PH), 1471 (w), 1456 (w), 1352 (m), 1285 (vw), 1249 (w), 1185 (vw), 1110 (vs), 1023 (vw), 962 (m), 909 (vw), 839 (w), 814 (w).

ESI-MS (THF) anion: *m/z* = 191.1 (100%, [^{t}BuPH-BH_2-^{t}BuPH]$^{-}$), 293.2 (100 %, [^{t}BuPH-BH_2-^{t}BuPH-BH_s-^{t}BuPH]$^{-}$).

Elemental analysis (%) calculated for $C_{20}H_{46}As_2BNaO_6(thf)_{0.6}$ (**3c**$(thf)_{0.6}$): C: 51.58, H: 9.81; found: C: 51.92, H: 9.42.

<u>Synthesis of [Na($C_{12}H_{24}O_6$)$(thf)_2$][^{t}BuAsH-BH_2-^{t}BuAsH] (**4d**$(thf)_2$):</u>

A solution of 243 mg (1.56 mmol) Na^{t}BuAsH in 5 ml THF is added to a solution of 320 mg (1.56 mmol) ^{t}BuAsH-BH_2-NMe_3 in 4 ml THF at -80 °C. The solution is stirred for 16 h while allowed to reach room temperature. The yellow solution is filtrated on 400 mg (1.51 mmol) solid $C_{12}H_{24}O_6$ (18-crown-6) and concentrated *in vacuo*. **4d**$(thf)_2$ crystallizes at -28 °C as yellow needles. The supernatant is decanted, the crystals are washed two times with 5 ml diethyl ether at -30 °C and dried *in vacuo*. A second fraction can be obtained by storing the concentrated supernatant at -28 °C again to rise the yield.

<u>Yield of [Na($C_{12}H_{24}O_6$)][^{t}BuAsH-BH_2-^{t}BuAsH] (**4d**):</u> 530 mg (62 %).

^{1}H NMR (toluene-d_8, 25 °C): δ = 1.69 (m, 2H, ^{t}BuAs<u>H</u>), 1.73 (d, $^{4}J_{H,H}$ = 2 Hz, 18H, ^{t}Bu), 1.95 – 2.72 (m, BH_2), 3.29 (s, 24H, $C_{12}H_{24}O_6$).

^{11}B NMR (toluene-d_8, 25 °C): δ = -30.0 (t, $^1J_{B,H}$ = 104 Hz, BH_2).

^{11}B{^{1}H} NMR (toluene-d_8, 25 °C): δ = -30.0 (s, BH_2).

^{13}C{^{1}H} NMR (toluene-d_8, 25 °C): δ = 26.3 (d, $^1J_{C,As}$ = 15 Hz, $\underline{C}(CH_3)_3$), 34.4 (d, $^2J_{C,As}$ = 2 Hz, CH_3), 69.0 (s, $C_{12}H_{24}O_6$).

^{11}B NMR (thf-d_8, 25 °C): δ = -31.4 (t, $^1J_{B,H}$ = 104 Hz, BH_2).

^{11}B{^{1}H} NMR (thf-d_8, 25 °C): δ = -31.4 (s, BH_2).

IR (KBr): $\tilde{\nu}$ = 2899 (s, CH), 2875 (s, CH), 2844 (s, CH), 2746 (vw), 2689 (vw), 2388 (w, BH), 2348 (w, BH), 2323 (w, BH), 2226 (vw), 2012 (w, AsH), 1470 (m), 1455 (m), 1352 (s), 1285 (w), 1249 (m), 1109 (vs), 1020 (vw), 962 (m), 919 (w), 837 (w), 767 (vw), 738 (vw), 707 (vw), 684 (vw), 593 (vw), 530 (vw).

ESI-MS (THF) anion: *m/z* = 279.0 (100%, [^{t}BuAsH-BH_2-^{t}BuAsH]$^-$), 425.0 (40 %, [^{t}BuAsH-BH_2-^{t}BuAsH-BH_s-^{t}BuAsH]$^-$).

Elemental analysis (%) calculated for $C_{20}H_{46}As_2BNaO_6$ (**4d**): C: 42.42, H: 8.19; found: C: 42.41, H: 7.74.

Synthesis of $[Na(C_{12}H_{24}O_6)(thf)_2][(CO)_4W(H_2P\text{-}BH_2\text{-}PH_2)]$ (**5**$(thf)_2$):

A solution of 64 mg (0.17 mmol) $W(CO)_4(C_7H_8)$ in 8 ml THF is added drop wise to a solution of 34 mg (0.33 mmol) $Na[H_2P\text{-}BH_2\text{-}PH_2]$ in 2 ml THF. The solution is stirred for 16 h at room temperature. After filtration on 87 mg (0.33 mmol) solid $C_{12}H_{24}O_6$ (18-crown-6) the yellow solution is layered with 30 ml of *n*-hexane. **5**$(thf)_2$ crystallizes at -28 °C as clear yellow blocks. The solvent is decanted, the crystals are separated, washed with cold *n*-hexane (0 °C, 3 x 5 ml) and dried *in vacuo*.

Yield of $[Na(C_{12}H_{24}O_6)(thf)]^+[(CO)_4W(H_2P\text{-}BH_2\text{-}PH_2)]^-$ (**5**$(thf)_2$): 68 mg (55%).

^{1}H NMR (THF-d_8, 25 °C): δ = 2.25 (m, 4H, PH_2), 3.47 (m, 2H, BH_2), 3.62 (s, 24H, $C_{12}H_{24}O_6$).

^{11}B NMR (THF-d_8, 25 °C): δ = -18.8 (tt, $^1J_{B,H}$ = 96 Hz, $^1J_{B,P}$ = 55 Hz, BH_2).

^{11}B{^{1}H} NMR (THF-d_8, 25 °C): δ = -18.8 (t, $^1J_{B,P}$ = 55 Hz, BH_2).

^{31}P NMR (toluene-d_8, 25 °C): δ = -201.0 (m, br, PH_2).

^{31}P{^{1}H} NMR (THF-d_8, 25 °C): δ = -201.0 (m, PH_2).

^{13}C{^{1}H} NMR (THF-d_8, 25 °C): δ = 70.6 (s, $C_{12}H_{24}O_6$), 207.4 (t, $^2J_{C,P}$ = 7 Hz, $C^a{\equiv}O$), 214.5 (t, $^2J_{C,P}$ = 6 Hz, $C^b{\equiv}O$).

IR (KBr): $\tilde{\nu}$ = 2902 (m), 2831 (w), 2426 (w, BH), 2375 (w, BH), 2310 (m, PH), 2252 (w, PH), 1996 (m), 1873 (vs, CO), 1820 (vs, CO), 1631 (vw), 1471 (w), 1453 (w), 1352 (m), 1284 (w), 1249 (w), 1108 (s, CO), 1077 (m), 962 (m), 835 (w), 764 (w), 605 (w), 581 (w).

ESI-MS (THF): anion: *m/z* = 374.8 (100%, $[(CO)_4W(H_2P\text{-}BH_2\text{-}PH_2]^-$).

Elemental analysis (%) calculated for $C_{16}H_{30}BNaO_{10}P_2W$(thf) (**5**(thf)): C: 32.69, H: 5.21; found: C: 32.82, H: 5.21.

Synthesis of $([K(C_{12}H_{24}O_6)(thf)_2][(CO)_4W(H_2As\text{-}BH_2\text{-}AsH_2)])_2$ (**6**$(thf)_4$):

A solution of 160 mg (0.41 mmol) $W(CO)_4(C_7H_8)$ in 3 ml THF is added to a solution of 141 mg (0.30 mmol) $[K(C_{12}H_{24}O_6)][H_2As\text{-}BH_2\text{-}AsH_2]$ in 3 ml THF at -80 °C. The solution is allowed to reach room temperature and stirred for 16 h. The yellow solution is layered with 24 ml of *n*-hexane. **6**$(thf)_4$ crystallizes at -28 °C as clear yellow blocks. The solvent is decanted, crystals are separated, washed with cold *n*-hexane (0 °C, 2 × 5 mL) and dried *in vacuo*.

Yield of $([K(C_{12}H_{24}O_6)(thf)_{0.5}][(CO)_4W(H_2As\text{-}BH_2\text{-}AsH_2)])_2$ (**6**(thf)): 124 mg (52%).

^{1}H NMR (THF-d_8, 25 °C): δ = 1.52 (m, 4H, AsH_2), 2.27 (m, 2H, BH_2), 3.64 (s, 24H, $C_{12}H_{24}O_6$).

^{11}B NMR (THF-d_8, 25 °C): δ = -31.1 (s, br, BH_2).

^{11}B{^{1}H} NMR (THF-d_8, 25 °C): δ = -31.1 (s, br, BH_2).

^{13}C{^{1}H} NMR (THF-d_8, 25 °C): δ = 71.0 (s, $C_{12}H_{24}O_6$), 206.9 (s, $C^a{\equiv}O$), 211.5 (s, $C^b{\equiv}O$).

IR (KBr): $\tilde{\nu}$ = 2906 (m), 2834 (w), 2432 (w, BH), 2387 (w, BH), 2339 (w, BH), 2092 (m, AsH), 2059 (w, AsH), 1990 (s), 1858 (vs, CO), 1815 (vs, CO), 1633 (vw), 1470 (w), 1453 (w), 1351 (m), 1284 (w), 1249 (w), 1108 (s, CO), 962 (m), 837 (w), 713 (vw), 660 (w, br), 604 (w), 580 (m).

ESI-MS (THF): anion: *m/z* = 462.9 (*z* = 2, 30%, $[((CO)_4W(H_2As\text{-}BH_2\text{-}AsH_2)_2]^{2-}$).

Elemental analysis (%) calculated for $C_{32}H_{60}As_4B_2K_2O_{20}W_2$(thf) (**6**(thf)): C: 26.93, H: 4.27; found: C: 27.21, H: 4.19.

Synthesis of $[Na(C_{12}H_{24}O_6)(thf)_2][(CO)_4W(H_2As\text{-}BH_2\text{-}PH_2\text{-}BH_2\text{-}AsH_2)]$ (**7**$(thf)_2$):

A solution of 117 mg (0.30 mmol) $W(CO)_4(C_7H_8)$ in 3 ml THF is added drop wise to a solution of 150 mg (0.30 mmol) $[Na(C_{12}H_{24}O_6)][H_2As\text{-}BH_2\text{-}PH_2\text{-}BH_2\text{-}AsH_2]$ in 4 ml THF at -80 °C. The solution is allowed to reach room temperature and stirred for 16 h. After filtration the yellow solution is layered with 30 ml

of *n*-hexane. **7**$(thf)_2$ crystallizes at -28 °C as clear yellow blocks. The solvent is decanted, the crystals are separated, washed with cold *n*-hexane (0 °C, 2 x 6 ml) and dried *in vacuo*.

Yield of $[Na(C_{12}H_{24}O_6)(thf)_{0.16}][(CO)_4W(H_2As\text{-}BH_2\text{-}PH_2\text{-}BH_2\text{-}AsH_2)]$ (**7**$(thf)_{0.16}$): 231 mg (95%).

^{1}H NMR (THF-d_8, 25 °C): δ = 1.30 (dm, 4H, AsH_2), 1.69 (q, br, $^1J_{H,B}$ = 108 Hz, 4H, BH_2), 3.63 (s, 24H, $C_{12}H_{24}O_6$), 3.70 (dm, $^1J_{H,P}$ = 328 Hz, 2H, PH_2).

^{11}B NMR (THF-d_8, 25 °C): δ = -37.4 (td, $^1J_{B,H}$ = 108 Hz, $^1J_{B,P}$ = 66 Hz, BH_2).

^{11}B{^{1}H} NMR (THF-d_8, 25 °C): δ = -37.4 (d, $^1J_{B,P}$ = 66 Hz, BH_2).

^{31}P NMR (toluene-d_8, 25 °C): δ = -102.2 (t, br, $^1J_{P,H}$ = 328 Hz, PH_2).

^{31}P{^{1}H} NMR (THF-d_8, 25 °C): δ = -102.2 (m, PH_2).

^{13}C{^{1}H} NMR (THF-d_8, 25 °C): δ = 70.6 (s, $C_{12}H_{24}O_6$), 205.9 (s, $C^a{\equiv}O$), 210.3 (s, $C^b{\equiv}O$).

IR (KBr): $\tilde{\nu}$ = 2912 (m), 2418 (w, BH), 2377 (m, PH), 2341 (w, PH), 2138 (w, AsH), 2111 (m, AsH), 1998 (s), 1878 (vs, CO), 1859 (vs, CO), 1804 (vs, CO), 1634 (vw), 1470 (w), 1451 (w), 1351 (w), 1298 (vw), 1284 (vw), 1249 (w), 1107 (s, CO), 961 (s), 891 (w), 834 (w), 761 (vw), 710 (w), 668 (vw), 607 (w), 578 (w).

ESI-MS (THF): anion: *m/z* = 508.8 (100%, $[(CO)_4W(H_2As\text{-}BH_2\text{-}PH_2\text{-}BH_2\text{-}AsH_2]^-$).

Elemental analysis (%) calculated for $C_{16}H_{34}As_2B_2NaO_{10}PW(thf)_{0.16}$ (**7**$(thf)_{0.16}$): C: 24.72, H: 4.40; found: C: 24.75, H: 4.40.

Synthesis of $[Na(C_{12}H_{24}O_6)(thf)_2][(CO)_4W(^t BuPH\text{-}BH_2\text{-}^t BuPH)]$ (**8**$(thf)_2$):

A solution of 39 mg (0.10 mmol) $W(CO)_4(C_7H_8)$ in 1 ml THF is added drop wise to a solution of 48 mg (0.10 mmol) $[Na(C_{12}H_{24}O_6)][^t BuPH\text{-}BH_2\text{-}^t BuPH]$ in 3 ml THF at -80 °C. The solution is allowed to reach room temperature and stirred for 16 h. After filtration the yellow solution is layered with 15 ml of *n*-hexane. **8**$(thf)_2$ crystallizes at -28 °C as clear yellow blocks. The solvent is decanted, the crystals are separated, washed with cold *n*-hexane (0 °C, 2 x 5 ml) and dried *in vacuo*.

Yield of $[Na(C_{12}H_{24}O_6)(thf)_{1.5}][(CO)_4W(^t BuPH\text{-}BH_2\text{-}^t BuPH)]$ (**8**$(thf)_{1.5}$): 60 mg (68%).

^{1}H NMR (THF-d_8, 25 °C): δ = 1.11 (m, 18H, ^{t}Bu), 2.97 (m, br, 1H, BH^aH^b), 3.06 (dm, $^1J_{H,P}$ = 283 Hz, 1H, $^t BuPH^a$), 3.14 (dm, $^1J_{H,P}$ = 300 Hz, 1H, $^t BuPH^b$), 3.15 (m, br, 1H, BH^aH^b), 3.63 (s, 24H, $C_{12}H_{24}O_6$).

^{11}B NMR (THF-d_8, 25 °C): δ = -20.6 (m, br, BH^aH^b).

^{11}B{^{1}H} NMR (THF-d_8, 25 °C): δ = -20.6 (m, br, BH^aH^b).

^{31}P NMR (toluene-d_8, 25 °C): δ = -64.6 (d, br, $^{1}J_{H,P}$ = 279 Hz, ^{t}BuPH^{b}), -70.3 (m, br, $^{1}J_{H,P}$ = 279 Hz, ^{t}BuPH^{a}).

^{31}P{^{1}H} NMR (THF-d_8, 25 °C): δ = -64.6 (m, ^{t}BuPH^{b}), -70.3 (m, br, ^{t}BuPH^{a}).

^{13}C{^{1}H} NMR (THF-d_8, 25 °C): δ = 27.2 (t, $^{1}J_{C,P}$ = 16 Hz, $\underline{C}^{b}(CH_3)_3$), 27.9 (t, $^{1}J_{C,P}$ = 19 Hz, $\underline{C}^{a}(CH_3)_3$), 30.0 (t, $^{2}J_{C,P}$ = 2 Hz, C($\underline{C}^{b}H_3)_3$), 30.2 (t, $^{2}J_{C,P}$ = 2 Hz, C($\underline{C}^{a}H_3)_3$), 70.6 (s, $C_{12}H_{24}O_6$), 206.7 (m, C^{c}≡O), 209.7 (m, C^{d}≡O), 211.5 (m, C^{e}≡O), 216.4 (m, C^{f}≡O).

IR (KBr): $\tilde{\nu}$ = 2958 (w), 2939 (w), 2916 (w), 2891 (w), 2856 (w), 2389 (vw, BH), 2340 (vw, PH), 2278 (vw, PH), 1987 (m), 1869 (vs, CO), 1799 (s, CO), 1635 (w), 1471 (w), 1456 (w), 1352 (w), 1250 (w), 1108 (s, CO), 1023 (w), 962 (w), 872 (vw), 838 (w), 819 (w), 738 (vw), 605 (w), 582 (w).

ESI-MS (THF): anion: *m/z* = 487.2 (100%, [$(CO)_4W(^{t}$BuPH-BH_2-^{t}BuPH]$^{-}$).

Elemental analysis (%) calculated for $C_{24}H_{46}BNaO_{10}P_2W(thf)_{1.5}$ (**8**$(thf)_{1.5}$): C: 40.80, H: 6.62; found: C: 41.14, H: 6.63.

Synthesis of [Na($C_{12}H_{24}O_6$)$(thf)_2$][$(CO)_4W(^{t}$BuAsH-BH_2-^{t}BuAsH)] (**9**$(thf)_2$):

A solution of 39 mg (0.10 mmol) $W(CO)_4(C_7H_8)$ in 2 ml THF is added drop wise to a solution of 57 mg (0.10 mmol) [Na($C_{12}H_{24}O_6$)][^{t}BuAsH-BH_2-^{t}BuAsH] in 3 ml THF at -70 °C. The solution is allowed to reach room temperature and stirred for 16 h. After filtration the yellow solution is layered with 20 ml of *n*-hexane. **9**$(thf)_2$ crystallizes at -28 °C as clear yellow blocks. The solvent is decanted, the crystals are separated, washed with cold *n*-hexane (0 °C, 2 x 5 ml) and dried *in vacuo*.

Yield of [Na($C_{12}H_{24}O_6$)$(thf)_2$][$(CO)_4W(^{t}$BuAsH-BH_2-^{t}BuAsH)] (**9**$(thf)_2$): 81 mg (80%).

^{1}H NMR (THF-d_8, 25 °C): δ = 1.19 (s, 18H, ^{t}Bu), 1.75 (m, 1H, ^{t}BuAs$\underline{H}^{a}$), 1.90 (m, 1H, ^{t}BuAsH^{b}), 3.35 + 4.25 (m, 1H, B$\underline{H}^{c}$H^{d}), 3.63 (s, 24H, $C_{12}H_{24}O_6$), 3.81 (m, 1H, BH$^{c}\underline{H}^{d}$).

^{11}B NMR (THF-d_8, 25 °C): δ = -10.8 (t, $^{1}J_{B,H}$ = 97 Hz, B$\underline{H}^{a}$H^{b}), -11.4 (t, $^{1}J_{B,H}$ = 97 Hz, BH$^{a}\underline{H}^{b}$).

^{11}B{^{1}H} NMR (THF-d_8, 25 °C): δ = -10.8 (s, B$\underline{H}^{a}$H^{b}), 11.4 (s, BH$^{a}\underline{H}^{b}$).

^{13}C{^{1}H} NMR (THF-d_8, 25 °C): δ = 28.4 (s, $\underline{C}^{b}(CH_3)_3$), 29.4 (s, $\underline{C}^{a}(CH_3)_3$), 30.9 (s, C($\underline{C}^{b}H_3)_3$), 31.1 (s, C($\underline{C}^{a}H_3)_3$), 70.6 (s, $C_{12}H_{24}O_6$), 208.3 (s, C^{c}≡O), 210.5 (s, C^{d}≡O), 212.1 (s, C^{e}≡O), 215.3 (m, C^{f}≡O).

IR (KBr): $\tilde{\nu}$ = 2958 (m), 2913 (m), 2885 (m), 2856 (m), 2420 (w, BH), 2365 (w, BH), 2340 (w, BH), 2073 (w, AsH), 1986 (s), 1870 (vs, CO), 1797 (vs, CO), 1470 (m), 1455 (m), 1352 (m), 1299 (vw), 1285 (vw), 1250 (w), 1108 (s, CO), 1019 (vw), 962 (m), 906 (vw), 836 (w), 748 (vw), 643 (vw), 607 (m), 580 (m).

ESI-MS (THF): anion: *m/z* = 574.9 (100%, $[(CO)_4W(^tBuAsH\text{-}BH_2\text{-}^tBuAsH]^-$).

Elemental analysis (%) calculated for $C_{24}H_{46}As_2BNaO_{10}W(thf)_2$ (**9**$(thf)_2$): C: 38.16, H: 6.21; found: C: 38.33, H: 6.12.

Synthesis of $[Cu_2Na_2(thf)_4(H_2P\text{-}BH_2\text{-}PH_2)_4]$ (**10**):

A solution of 51 mg (0.50 mmol) $Na[H_2P\text{-}BH_2\text{-}PH_2]$ in 3 ml THF is added to a solution of 80 mg (0.25 mmol) $[Cu(CH_3CN)_4][BF_4]$ in 6 ml THF at -80 °C. The solution is allowed to reach -30 °C and stirred for 2 h. The dark solution is filtrated over diatomaceous earth and the obtained clear solution is layered with 35 ml of *n*-hexane. **10**$(thf)_4$ crystallizes at -28 °C as clear colourless blocks. Isolation of the desired product was not possible because of thermolabile properties and decomposition of the crystalline product.

^{11}B NMR (THF + C_6D_6-capillary, 25 °C): δ = -35.4 (m, br, BH_2).

^{11}B{^{1}H} NMR (THF + C_6D_6-capillary, 25 °C): δ = -35.4 (m, br, BH_2).

^{31}P NMR (THF + C_6D_6-capillary, 25 °C): δ = -167.4 (m, br, PH_2).

^{31}P{^{1}H} NMR (THF + C_6D_6-capillary, 25 °C): δ = -167.4 (m, PH_2).

ESI-MS (THF): anion: *m/z* = 362.8 (100%, $[Cu_2(H_2P\text{-}BH_2\text{-}PH_2)_3]^-$), 316.8 (90%, $[Cu_2(PH_2)(H_2P\text{-}BH_2\text{-}PH_2)_2]^-$), 270.8 (30%, $[Cu_2(PH_2)_2(H_2P\text{-}BH_2\text{-}PH_2)]^-$), 224.8 (45%, $[Cu_2(PH_2)_3]^-$).

Synthesis of $[Cu_2Na_2(^tBuPH\text{-}BH_2\text{-}^tBuPH)_4]$ (**12**):

A solution of 95 mg (0.19 mmol) $[Na(C_{12}H_{24}O_6)][^tBuPH\text{-}BH_2\text{-}^tBuPH]$ in 1.5 ml THF-d_8 is added to 32 mg (0.10 mmol) $[Cu(CH_3CN)_4][BF_4]$ at -80 °C. The solution is allowed to reach -30 °C and used for analytical purpose. Isolation of the desired product was not possible because of thermolabile properties and decomposition after drying *in vacuo*. Crystallization was not successful because of great solubility in common organic solvents.

^{1}H NMR (THF-d_8, -23 °C): δ = 1.18 (m, br, 18H, $C(CH_3)_3$), 1.30 (m, br, 2H, BH_2), 2.85 (m, br, $^tBuPH^{a/b}$, 1H), 3.16 (m, br, $^tBuPH^{b/a}$, 1H).

^{11}B NMR (THF-d_8, -23 °C): δ = -34.9 (s, br, BH_2).

^{11}B{^{1}H} NMR (THF-d_8, -23 °C): δ = -34.9 (s, br, BH_2).

^{31}P NMR (THF-d_8, -23 °C): δ = -28.2 (d, br, $^1J_{P,H}$ = 208 Hz, $^tBuP^aH$), -38.9 (d, br , $^1J_{P,H}$ = 208 Hz, $^tBuP^bH$).

^{31}P{^{1}H} NMR (THF-d_8, -23 °C): δ = -28.2 (s, $^tBuP^aH$), -38.9 (s, $^tBuP^bH$).

^{13}C NMR (THF-d_8, -23 °C): δ = 29.1 (m, $\underline{C}(CH_3)_3$), 32.1 (m, br, $C(\underline{C}H_3)_3$).

ESI-MS (THF): anion: *m/z* = 699.1 (100%, $[Cu_2(^t$BuPH-BH_2-^{t}BuPH$)_3]^-$).

Synthesis of $[\underline{Cu_2Na_2}(^t$BuAsH-BH_2-^{t}BuAsH$)_4]$ (**13**):

A solution of 56 mg (0.10 mmol) $[Na(C_{12}H_{24}O_6)][^t$BuAsH-BH_2-^{t}BuAsH] in 1.5 ml THF-d_8 is added to 32 mg (0.10 mmol) $[Cu(CH_3CN)_4][BF_4]$ at -80 °C. The solution is allowed to reach -30 °C and used for analytical purpose. Isolation of the desired product was not possible because of thermolabile properties and decomposition after drying *in vacuo*. Crystallization was not successful because of great solubility in common organic solvents.

^{1}H NMR (THF-d_8, -30 °C): δ = 1.27 (m, br, $C(CH_3)_3$), 0.99-3.19 (m, br, BH_2) 2.26 (m, ^{t}BuAs$\underline{H}$).

^{11}B NMR (THF-d_8, -30 °C): δ = -32.2 (s, br, BH_2).

^{11}B{^{1}H} NMR (THF-d_8, -30 °C): δ = -32.2 (s, br, BH_2).

^{13}C NMR (THF-d_8, -30 °C): δ = 29.8 (m, $\underline{C}(CH_3)_3$), 32.7 (m, br, $C(\underline{C}H_3)_3$).

ESI-MS (THF): anion: *m/z* = 963.0 (40%, $[Cu_2(^t$BuAsH-BH_2-^{t}BuAsH$)_3]^-$).

4.5.2 X-ray Diffraction Analysis

The X-ray diffraction experiments were performed on a GV50 diffractometer with TitanS2 detector from Rigaku Oxford Diffraction (formerly Agilent Technologies) applying Cu-K_α radiation (λ = 1.54178 Å) (**3c**(thf)$_2$, **4d**(thf)$_2$, **5**(thf)$_2$, **6**(thf)$_4$, **7**(thf)$_2$, **8**(thf)$_2$, **9**(thf)$_2$, **10**) or Cu-K_β radiation (λ = 1.39222 Å) (**3c**). The measurements were performed at 123 K (**3c**, **4d**(thf)$_2$, **5**(thf)$_2$, **6**(thf)$_4$, **7**(thf)$_2$, **8**(thf)$_2$, **9**(thf)$_2$, **10**) or at 193 K (**3c**(thf)$_2$). Crystallographic data together with the details of the experiments are given in Table S 4.1 - Table S 4.5 (see below).

A Numerical absorption correction based on gaussian integration was performed over a multifaceted crystal model (**3c**, **4d**(thf)$_2$, **5**(thf)$_2$, **6**(thf)$_4$, **7**(thf)$_2$, **8**(thf)$_2$, **9**(thf)$_2$, **10**), a multi-scan absorption correction was performed (**3c**(thf)$_2$) or an empirical absorption correction using spherical harmonics as implemented in SCALE3/ ABSPACK (CrysAlisPro software by Rigaku Oxford Diffraction).[6]

All structures were solved using SIR97[7], SHELXT[8] and OLEX^2[9]. Least square refinements against F_2 in anisotropic approximation were done using SHELXL[10].

All non-hydrogen atoms were refined anisotropically. The hydrogen positions of the methyl groups were located geometrically and refined riding on the carbon atoms. Hydrogen atoms belonging to BH_2, PH_2 and AsH_2 groups were located from the difference Fourier map and refined without constraints (**6**(thf)$_4$**, 7**(thf)$_2$**, 9**(thf)$_2$) or with restrained X–H (X = B, P, As) distances (**3c**(thf)$_2$, **3c**, **4d**(thf)$_2$, **5**(thf)$_2$, **8**(thf)$_2$, **10**).

4.5.3 Solid State Structures

$[Na(C_{12}H_{24}O_6)(thf)_2][^tBuPH\text{-}BH_2\text{-}^tBuPH]$ (3c(thf)$_2$):

3c(thf)$_2$ crystallizes from a concentrated THF solution -28 °C as pale yellow needles in the monoclinic space group *C2/m*. Figure S 4.1 shows the molecular structure of **3c**(thf)$_2$ in solid state.

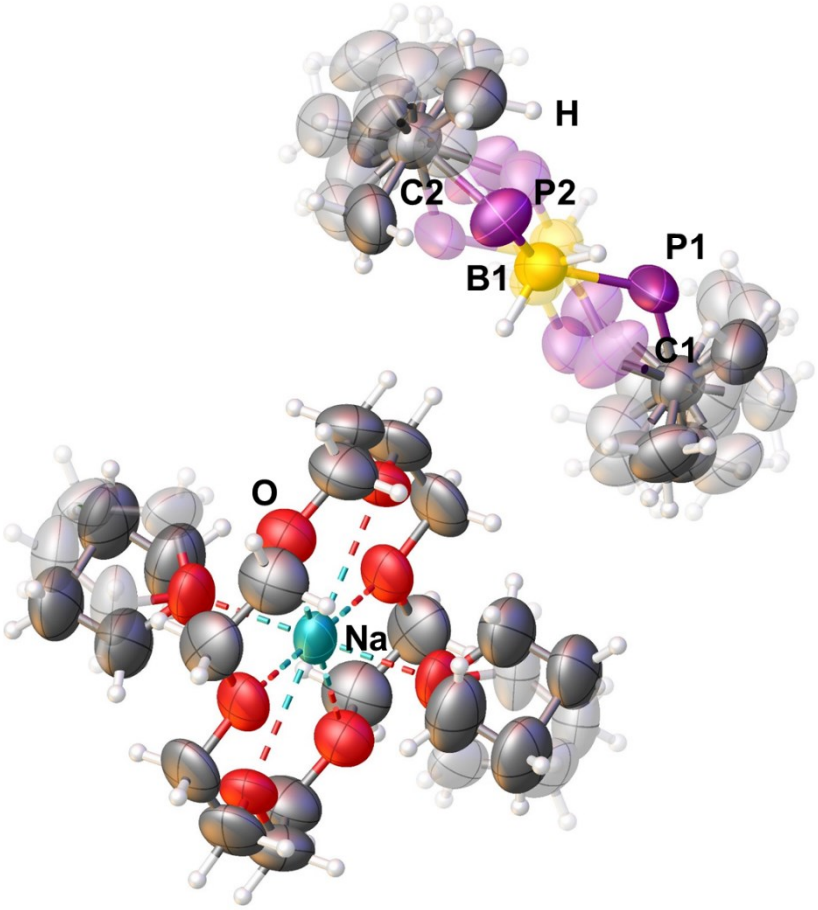

Figure S 4.1. Molecular structure of **3c**(thf)$_2$ in solid state. Thermal ellipsoids are drawn with 50% probability. High disorder (greyed out atoms) leads to insignificant values of selected bond length and angles.

$[Na(C_{12}H_{24}O_6)][^tBuPH\text{-}BH_2\text{-}^tBuPH]$ (3c):

3c crystallizes from a toluene solution layered by the 3-4-fold amount of pentane at -28 °C as colourless blocks in the monoclinic space group $P2_1/n$. Figure S 4.2 shows the molecular structure of **3c** in solid state.

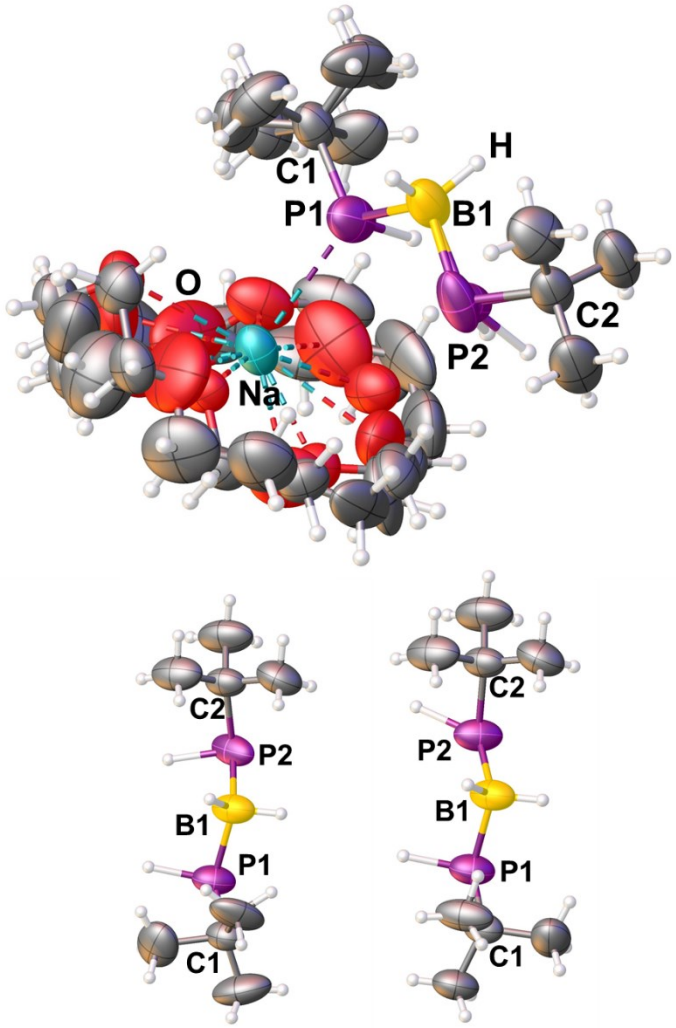

Figure S 4.2. Molecular structure of **3c** in solid state. Thermal ellipsoids are drawn with 50% probability. Selected bond length [Å] and angles [°]: P1-B1: 1.943(4), P1-C1: 1.855(3), P2-B1: 1.954(6) – 1.973(9), P2-C2: 1.85(1) – 1.867(6), ∠(P1-B1-P2): 106.8(3) – 109.7(4), ∠(B1-P1-C1): 108.8(2), ∠(B1-P2-C2): 108.1(2) – 108.2(4), ∠(B1-P1-Na1): 136.5(1). Top: disordered solid state structure of **3c**; bottom: 2 possible conformers of the anionic part of **3c**.

$[Na(C_{12}H_{24}O_6)(thf)_2][^tBuAsH\text{-}BH_2\text{-}^tBuAsH]$ (**4d**$(thf)_2$):

4d$(thf)_2$ crystallizes from a concentrated THF solution at -28 °C as yellow needles in the monoclinic space group *I2/a*. Figure S 4.3 shows the molecular structure of **4d**$(thf)_2$ in solid state.

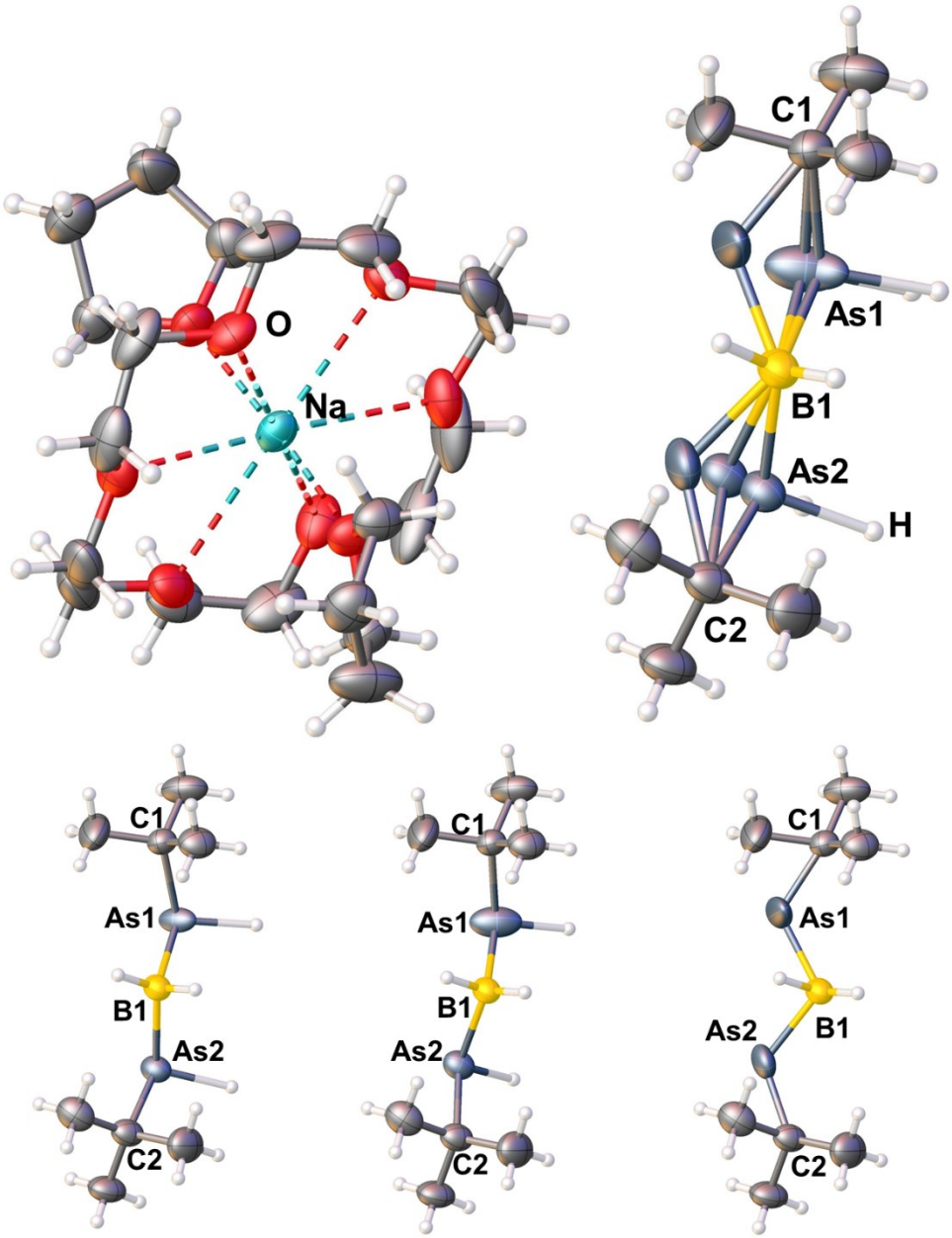

Figure S 4.3. Molecular structure of **4d**$(thf)_2$ in solid state. Thermal ellipsoids are drawn with 50% probability. Selected bond length [Å] and angles [°]: As1-B1: 2.066(4) – 2.066(6), As1-C1: 1.995(4) – 1.997(5), As2-B1: 2.081(3) – 2.100(4), As2-C2: 1.980(4) – 2.041(3), ∠(As1-B1-As2): 100.9(2) – 104.6(2), ∠(B1-As1-C1): 104.7(2) – 104.8(2), ∠(B1-As2-C2): 103.6(1) – 105.0(2). Top: disordered solid state structure of **4d**$(thf)_2$; bottom: 3 possible conformers of the anionic part of **4d**$(thf)_2$; bottom right: lowest occupied anion (6%) omitted for discussion of values and conformation.

$[Na(C_{12}H_{24}O_6)(thf)_2][W(CO)_4(H_2P\text{-}BH_2\text{-}PH_2)]$ $(\mathbf{5}(thf)_2)$:

5$(thf)_2$ crystallizes from a THF solution layered by the 3-4-fold amount of *n*-hexane at -28 °C as clear yellow block in the triclinic space group $P\bar{1}$. Figure S 4.4 shows the molecular structure of **5**$(thf)_2$ in solid state.

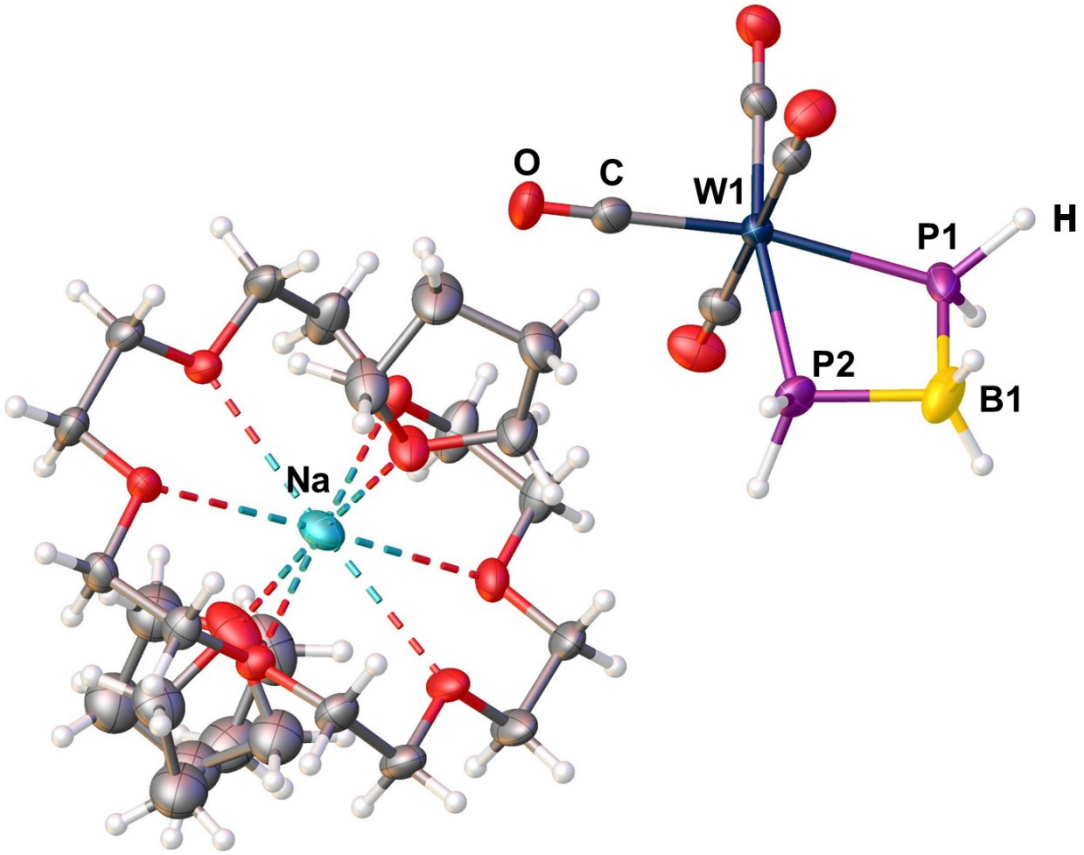

Figure S 4.4. Molecular structure of **5**$(thf)_2$ in solid state. Thermal ellipsoids are drawn with 50% probability. Selected bond length [Å] and angles [°]: P1-B1: 1.982(5), P2-B1: 1.957(4), P1-W1: 2.5531(7), P2-W1: 2.5506(7), ∠(P1-B1-P2): 93.0(1), ∠(P1-W1-P2): 68.08(3), ∠(W1-P1-B1-P2): 12.142.

$([K(C_{12}H_{24}O_6)(thf)_2][W(CO)_4(H_2As\text{-}BH_2\text{-}AsH_2)])_2$ $(6(thf)_4)$:

6$(thf)_4$ crystallizes from a THF solution layered by the 3-4-fold amount of *n*-hexane at -28 °C as clear yellow blocks in the monoclinic space group $P2_1/c$. Figure S 4.5 shows the molecular structure of **6**$(thf)_4$ in solid state.

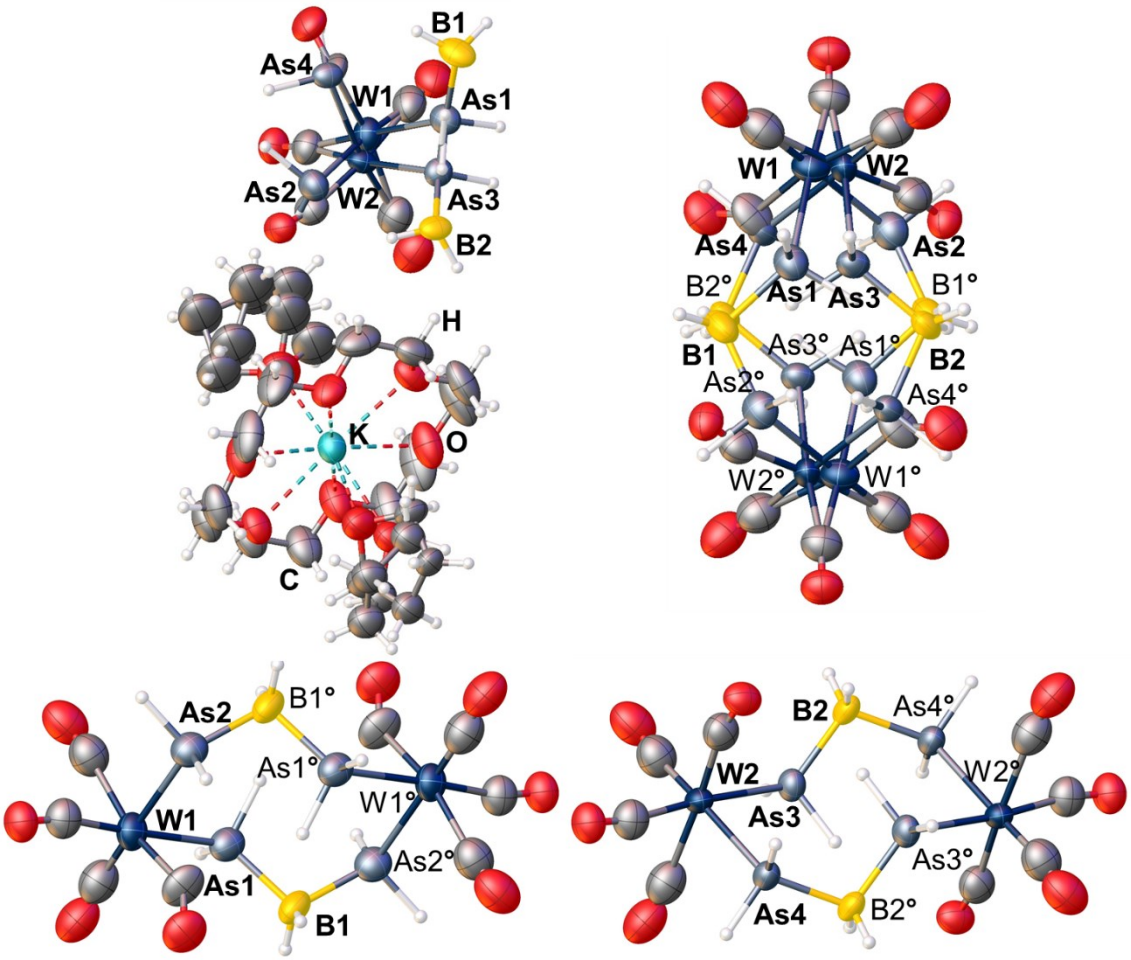

Figure S 4.5. Molecular structure of **6**$(thf)_4$ in solid state. Thermal ellipsoids are drawn with 50% probability. Selected bond length [Å] and angles [°]: As1-B1: 2.06(1), As2-B1: 2.103, As1-W1: 2.641(2), As2-W1: 2.594(2), As3-B2: 2.06(1), As4-B2: 2.089, As3-W2: 2.643(1), As4-W2: 2.666(3), ∠(As1-B1-As2): 105.161, ∠(As1-W1-As2): 89.08(6), ∠(As3-B2-As4): 105.013, ∠(As3-W2-As4): 88.52(5), ∠(W1-As1-B1-As2): 146.784, ∠(W2-As3-B2-As4): 148.850. Top left: disordered solid state structure of **6**$(thf)_4$; top right: disordered grown solid state structure of the anion; atoms labeled with ° are generated by symmetrical operations; bottom: 2 different possible isomers of the anionic part of **6**$(thf)_4$; atoms labeled with ° are generated by symmetrical operations.

$[Na(C_{12}H_{24}O_6)(thf)_2][W(CO)_4(H_2As\text{-}BH_2\text{-}PH_2\text{-}BH_2\text{-}AsH_2)]$ $(7(thf)_2)$:

7$(thf)_2$ crystallizes from a THF solution layered by the 3-4-fold amount of *n*-hexane at -28 °C as clear colourless blocks in the orthorhombic space group $P2_12_12_1$. Figure S 4.6 shows the molecular structure of **7**$(thf)_2$ in solid state.

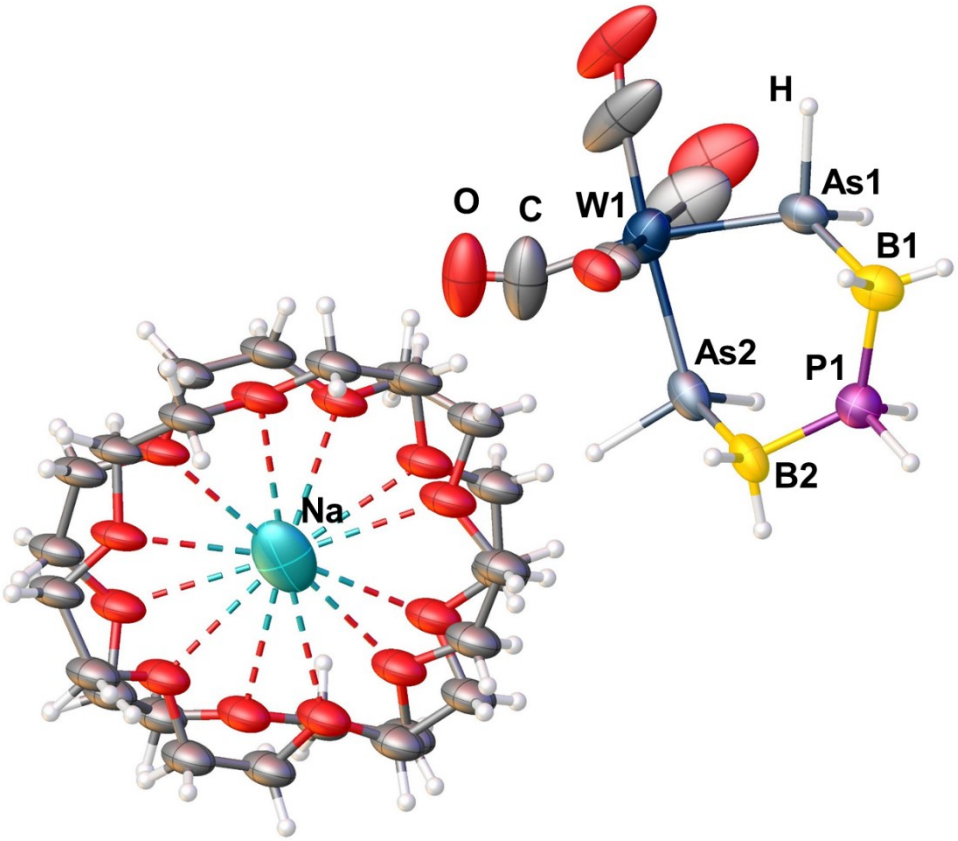

Figure S 4.6. Molecular structure of **7**$(thf)_2$ in solid state. THF-molecules are omitted for heavy disorder and calculated by solvent-mask-order. Thermal ellipsoids are drawn with 50% probability. Selected bond length [Å] and angles [°]: As1-B1: 2.17(4), As2-B2: 2.09(3), P1-B1: 1.99(3), P1-B2: 1.95(3), As1-W1: 2.622(3), As2-W1: 2.627(4), ∠(As1-B1-P1): 103(2), ∠(As2-B2-P1): 107(2), ∠(B1-P1-B2): 125(1), ∠(As1-W1-As2): 85.06(9), ∠(W1-As1-B1-P1): 49.888, ∠(As1-B1-P1-B2): 54.553, ∠(B1-P1-B2-As2): 64.964, ∠(P1-B2-As2-W1): 64.9, ∠(B2-As2-W1-As1): 51.439, ∠(As2-W1-As1-B1): 46.913.

$[Na(C_{12}H_{24}O_6)(thf)_2][W(CO)_4(^tBuPH\text{-}BH_2\text{-}^tBuPH)]$ $(8(thf)_2)$:

8$(thf)_2$ crystallizes from a THF solution layered by the 3-4-fold amount of *n*-hexane at -28 °C as clear yellow prism in the triclinic space group *P1*. Figure S 4.7 shows the molecular structure of **8**$(thf)_2$ in solid state.

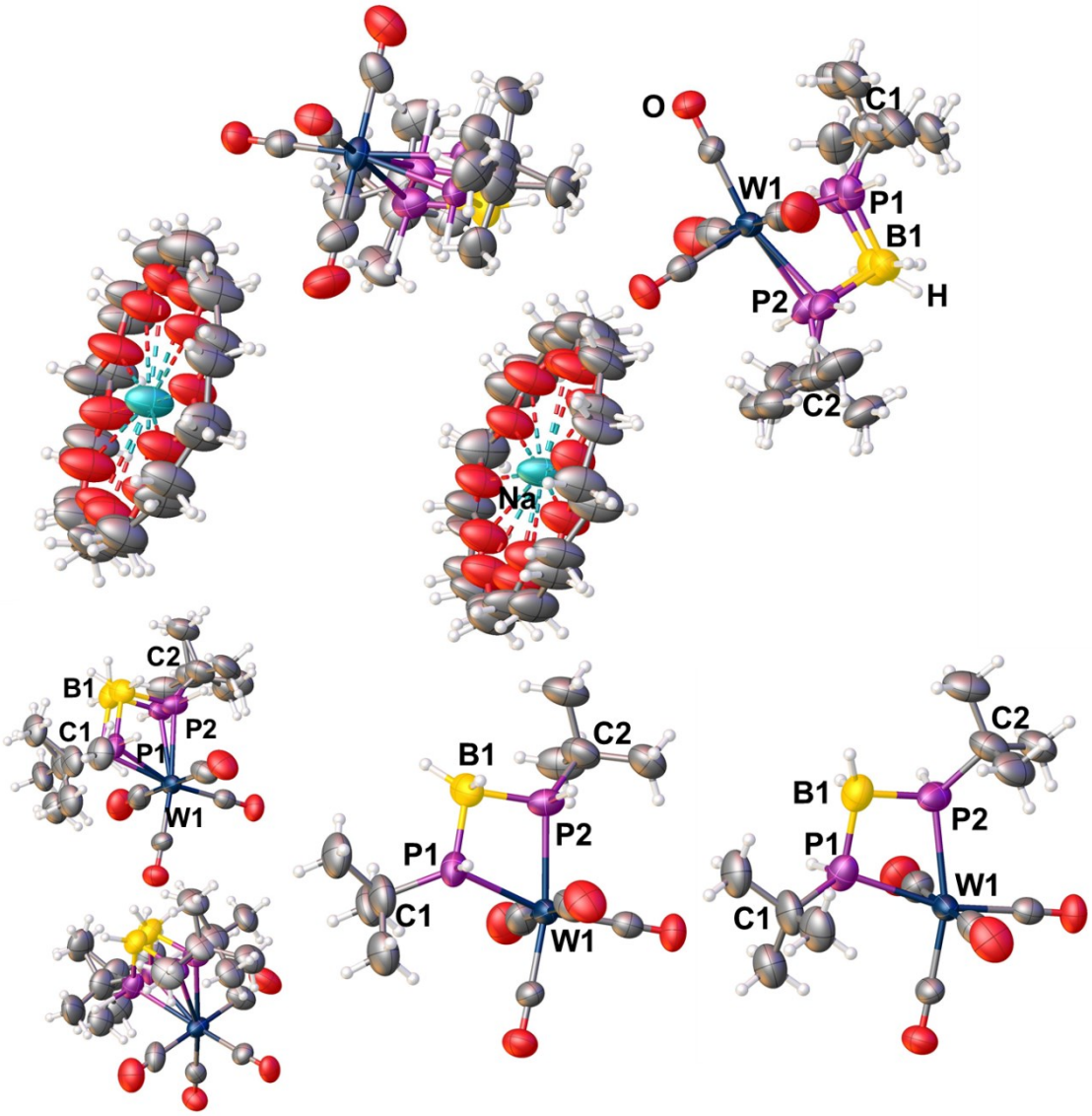

Figure S 4.7. Molecular structure of **8**$(thf)_2$ in solid state. THF-molecules are omitted for heavy disorder and calculated by solvent-mask-order. Thermal ellipsoids are drawn with 50% probability. Selected bond length [Å] and angles [°]: P1-B1: 1.90(1) – 1.91(1), P2-B1: 1.90(1) – 1.91(1), P1-C1: 1.81(3) – 1.83(3), P2-C2: 1.82(3) – 1.85(3), P1-W1: 2.550(5) – 2.570(5), P2-W1: 2.550(5) – 2.574(5), ∠(P1-B1-P2): 92.2(8) – 92.6(8), ∠(C1-P1-B1): 118(2) – 119(2), ∠(C2-P2-B1): 117(1) – 119(1), ∠(P1-W1-P2): 65.1(1), ∠(W1-P1-B1-P2): 11.884 – 15.101. Top: disordered solid state structure of **8**$(thf)_2$; bottom left: 2 independent anions; bottom right: 2 enantiomers of the anionic part of **8**$(thf)_2$.

$[Na(C_{12}H_{24}O_6)(thf)_2][W(CO)_4(^tBuAsH\text{-}BH_2\text{-}^tBuAsH)]$ $(9(thf)_2)$:

9$(thf)_2$ crystallizes from a THF solution layered by the 3-4-fold amount of *n*-hexane at -28 °C as clear yellow prism in the triclinic space group *P1*. Figure S 4.8 shows the molecular structure of **9**$(thf)_2$ in solid state.

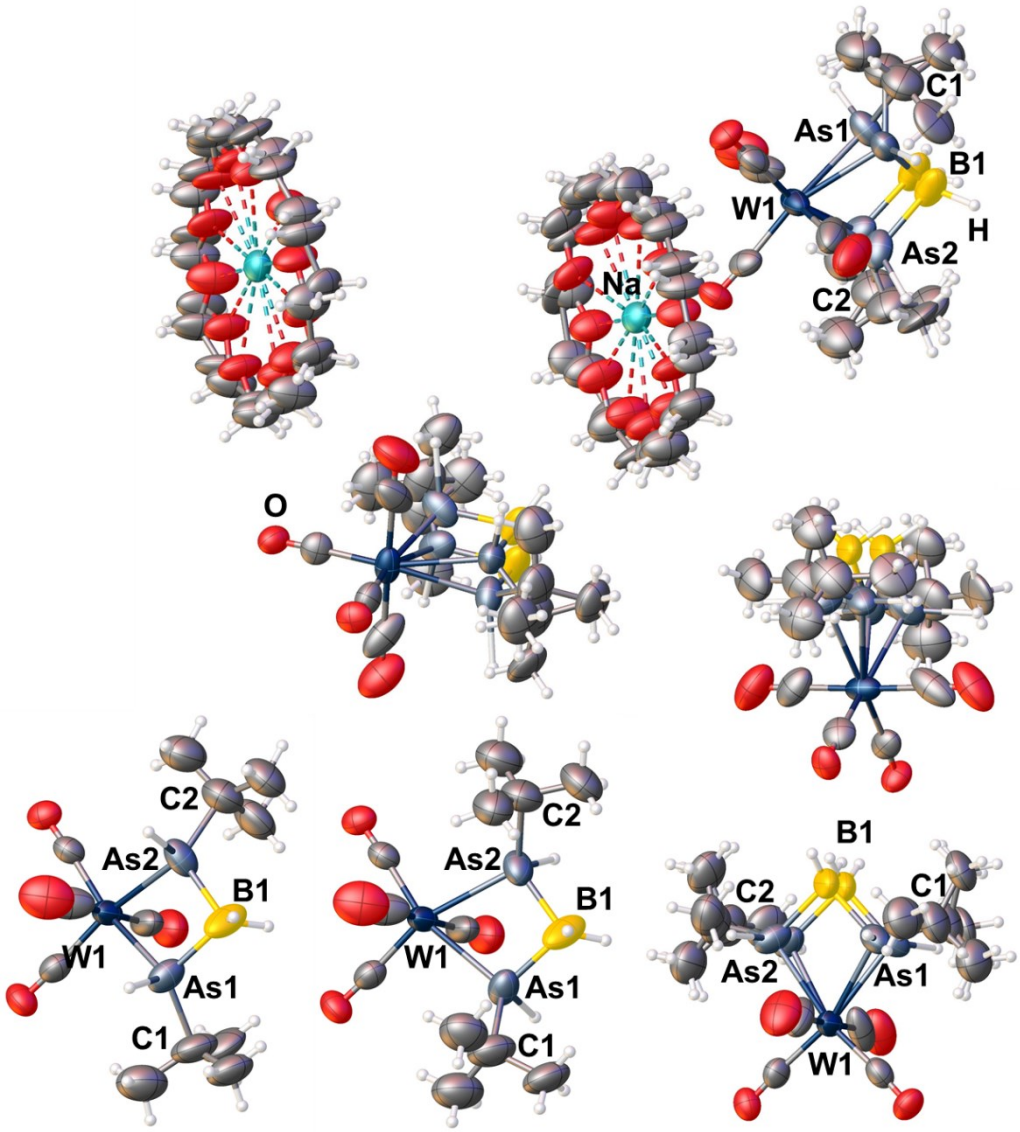

Figure S 4.8. Molecular structure of **9**$(thf)_2$ in solid state. THF-molecules are omitted for heavy disorder and calculated by solvent-mask-order. Thermal ellipsoids are drawn with 50% probability. Selected bond length [Å] and angles [°]: As1-B1: 2.05(2) – 2.06(2), As2-B1: 2.06(2) – 2.07(2), As1-C1: 1.93(5) – 1.99(5), As2-C2: 1.95(5) – 2.00(5), As1-W1: 2.672(3) – 2.682(3), As2-W1: 2.675(3) – 2.685(3), ∠(As1-B1-As2): 91(1), ∠(C1-As1-B1): 115(2) – 118(2), ∠(C2-As2-B1): 114(2) – 117(2), ∠(As1-W1-As2): 66.3(1) – 66.5(1), ∠(W1-As1-B1-As2): 9.185 – 14.812. Top: disordered solid state structure of **9**$(thf)_2$; bottom left: 2 enantiomers of the anionic part of **9**$(thf)_2$; bottom right: 2 independent anions.

$[Cu_2Na_2(thf)_4(H_2P\text{-}BH_2\text{-}PH_2)_4]$ (10):

10 crystallizes from a THF solution layered by the 3-4-fold amount of *n*-hexane at -28 °C as colourless blocks in the orthorhombic space group *Pbcn*. Figure S 4.9 shows the molecular structure of **10** in solid state.

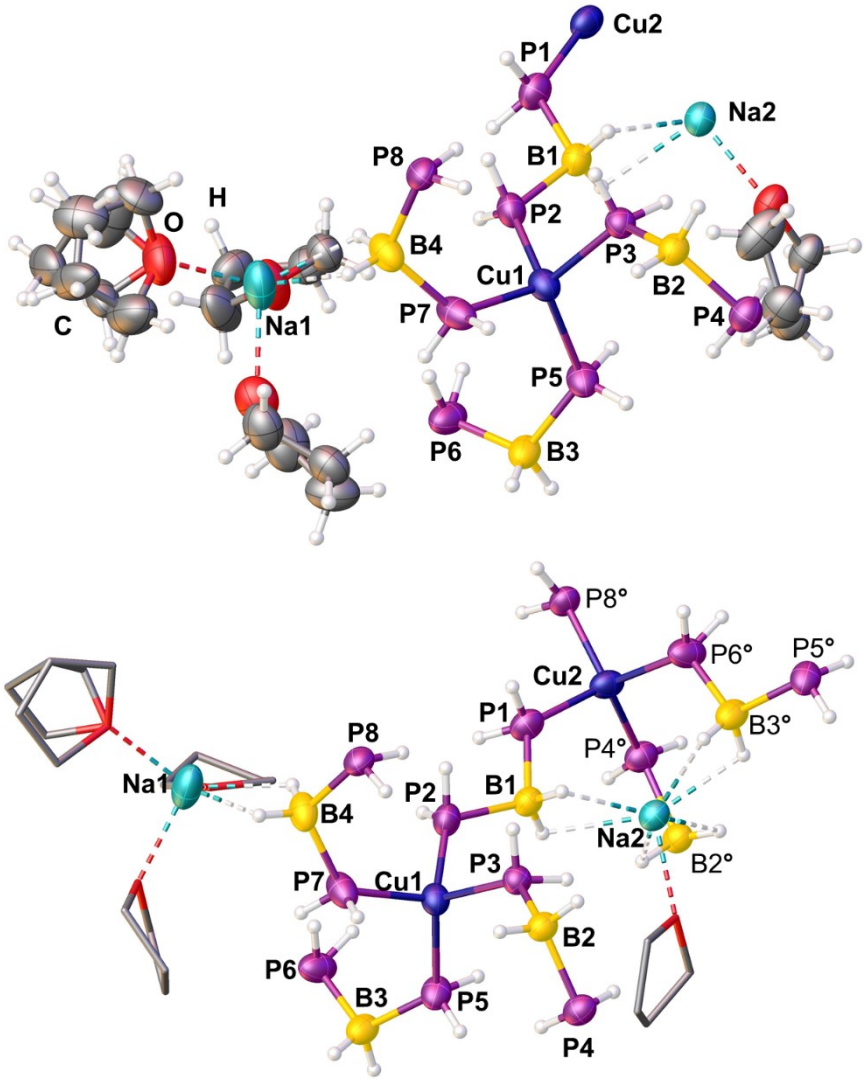

Figure S 4.9. Molecular structure of **10** in solid state. Thermal ellipsoids are drawn with 50% probability. Atoms labeled with ° are generated by symmetrical operations; Selected bond length [Å] and angles [°]: P1-B1: 1.944(8), P2-B1: 1.960(7), P3-B2: 1.952(7), P4-B2: 1.958(7), P5-B3: 1.967(8), P6-B3: 1.965(8), P7-B4: 1.950(9), P8-B4: 1.938(8), Cu1-P1: 2.292(2), Cu1-P3: 2.298(2), Cu1-P5: 2.290(2), Cu1-P7: 2.288(2), Cu2-P2: 2.290(2), Cu2-P4°: 2.300(2), Cu2-P6°: 2.295(2), Cu2-P8°: 2.299(2), Cu2-Na2: 3.375(2), B1-Na2: 2.776(8), H(B1)-Na2: 2.4(2)/ 2.5(2), B2°-Na2: 2.771(7), H(B2°)-Na2: 2.343/ 2.548, B3°-Na2: 2.818, H(B3°)-Na2: 2.288/ 2.490, B4-Na1: 2.678(9), H(B4)-Na1: 2.2(2), ∠(P1-B1-P2): 113.5(3), ∠(P3-B2-P4): 113.7(3), ∠(P5-B3-P6): 113.3(4), ∠(P7-B4-P8): 113.9(4), ∠(P1-Cu1-P3): 102.84(6), ∠(P1-Cu1-P5): 106.60(7), ∠(P1-Cu1-P7): 111.74(8), ∠(P3-Cu1-P5): 118.22(7), ∠(P3-Cu1-P7): 107.57, ∠(P5-Cu1-P7): 109.73(7), ∠(P2-Cu2-P4°): 111.679, ∠(P2-Cu2-P6°): 107.333, ∠(P2-Cu2-P8°): 107.121, ∠(P4°-Cu2-P6°): 112.266, ∠(P4°-Cu2-P8°): 105.80(7), ∠(P6°-Cu2-P8°): 112.595, ∠(P2-Cu2-Na2): 68.45(6), ∠(P4°-Cu2-Na2): 72.596, ∠(P6°-Cu2-Na2): 73.459, ∠(P8°-Cu2-Na2): 173.670. Top: unit cell of the solid state structure of **10**; bottom: grown solid state structure of **10** with focus on environment of Cu- and Na-atoms; hydrogen atoms bonded to carbon are omitted for clarity, THF-molecules are drawn as tubes.

4.5.4 Crystallographic Information

Table S 4.1. Crystallographic data for compounds **3c**$(thf)_2$ and **3c**.

	3c$(thf)_2$	**3c**
Emipirical formula	$C_{28}H_{60}BNaO_8P_2$	$C_{20}H_{46}BNaO_6P_2$
Formula weight *M*	620.50 g/mol	478.31 g/mol
Crystal	clear light yellow needle	clear colourless plate
Crystal size [mm³]	0.286 x 0.269 x 0.154	0.287 x 0.187 x 0.147
Temperature *T*	193.00(10) K	123.0(3) K
Cristal system	monoclinic	monoclinic
Space group	*C2/m*	$P2_1/n$
Unit cell dimensions	*a* = 17.2946(5) Å	*a* = 9.4100(3) Å
	b = 10.8998(3) Å	*b* = 10.7085(3) Å
	c = 9.9671(3) Å	*c* = 27.5932(8) Å
	α = 90°	*α* = 90°
	β = 91.647(3)°	*β* = 92.978(3)°
	γ = 90°	*γ* = 90°
Volume *V*	1878.09(9) Å^3	2776.73(14) Å^3
Formula units *Z*	2	4
Absorption coefficient $\mu_{Cu\text{-}K\alpha}$	1.483 mm^{-1}	1.324 mm^{-1}
Density (calculated) ρ_{calc}	1.097 g/cm^3	1.144 g/cm^3
F(000)	676	1040
Theta range θ_{min} / θ_{max} / θ_{full}	4.438 / 74.275 / 67.684 °	3.999 / 59.870 / 56.650 °
Absorption correction	multi-scan	gaussian
Index ranges	-21 < *h* < 21	-11 < *h* < 11
	-13 < *k* < 13	-13 < *k* < 13
	-11 < *l* < 12	-33 < *l* < 33
Reflections collected	7515	26681
Independent reflections [$I > 2\sigma(I)$]	1804 (R_{int} = 0.0129)	4210 (R_{int} = 0.0295)
Completeness to full θ	1.000	1.000
Transmission T_{min} / T_{max}	0.56537 / 1.00000	0.641 / 1.000
Data / restraints / parameters	1979 / 100 / 187	5538 / 1018 / 496
Goodness-of-fit on F^2 *S*	1.050	1.051
Diffractometer type	GV 50	GV 50
Radiation type (λ)	Cu (1.54184 Å)	Cu (1.39222 Å)
Final *R*-values [$I > 2\sigma(I)$]	R_1 = 0.0713	R_1 = 0.0797
	wR_2 = 0.2362	wR_2 = 0.2389
Final *R*-values (all data)	R_1 = 0.0743	R_1 = 0.0959
	wR_2 = 0.2416	wR_2 = 0.2580
Largest difference hole	-0.331	-0.454
and peak $\Delta\rho$	0.347 eÅ^{-3}	0.742 eÅ^{-3}

Table S 4.2. Crystallographic data for compounds **4d**$(thf)_2$ and **5**$(thf)_2$.

	4d$(thf)_2$	**5**$(thf)_2$
Emipirical formula	$C_{28}H_{61.88}As_2BNaO_8$	$C_{24}H_{46}BNaO_{12}P_2W$
Formula weight *M*	710.29 g/mol	806.20 g/mol
Crystal	clear colourless plate	clear yellow block
Crystal size [mm³]	0.207 x 0.192 x 0.146	0.2 x 0.176 x 0.115
Temperature *T*	123.00(16) K	122.95(18) K
Cristal system	monoclinic	triclinic
Space group	*I2/a*	$P\bar{1}$
Unit cell dimensions	*a* = 17.3533(4) Å	*a* = 9.2213(2) Å
	b = 10.8763(2) Å	*b* = 12.7998(3) Å
	c = 39.4708(10) Å	*c* = 15.0987(3) Å
	α = 90°	*α* = 86.308(2) °
	β = 91.297(2)°	*β* = 80.305(2) °
	γ = 90°	*γ* = 78.250(2)°
Volume *V*	7447.8(3) Å^3	1719.01(7) Å^3
Formula units *Z*	8	2
Absorption coefficient $\mu_{Cu\text{-}K\alpha}$	2.659 mm^{-1}	7.688 mm^{-1}
Density (calculated) ρ_{calc}	1.267 g/cm^3	1.558 g/cm^3
F(000)	3007	812
Theta range θ_{min} / θ_{max} / θ_{full}	4.216 / 74.424 / 67.684 °	3.529 / 74.573 / 67.684°
Absorption correction	gaussian	gaussian
Index ranges	-15 < *h* < 21	-11 < *h* < 11
	-9 < *k* < 13	-15 < *k* < 15
	-47 < *l* < 48	-18 < *l* < 18
Reflections collected	18650	19192
Independent reflections [$I > 2\sigma(I)$]	6655 (R_{int} = 0.0453)	6689 (R_{int} = 0.0231)
Completeness to full θ	0.994	0.993
Transmission T_{min} / T_{max}	0.673 / 1.000	0.394 / 0.668
Data / restraints / parameters	7320 / 68 / 450	6804 / 114 / 425
Goodness-of-fit on F^2 *S*	1.067	1.040
Diffractometer type	GV 50	GV 50
Radiation type (λ)	Cu (1.54184 Å)	CuK_α (1.54184 Å)
Final *R*-values [$I > 2\sigma(I)$]	R_1 = 0.0730	R_1 = 0.0235
	wR_2 = 0.2018	wR_2 = 0.0573
Final *R*-values (all data)	R_1 = 0.0764	R_1 = 0.0239
	wR_2 = 0.2081	wR_2 = 0.0576
Largest difference hole	-0.867	-0.670
and peak $\Delta\rho$	1.410 eÅ^{-3}	1.106 eÅ^{-3}

Table S 4.3. Crystallographic data for compounds **6**(thf)$_4$ and **7**(thf)$_2$.

	6(thf)$_4$	**7**(thf)$_2$
Emipirical formula	$C_{24}H_{46}As_2BKO_{12}W$	$C_{24}H_{50}As_2B_2NaO_{12}PW$
Formula weight *M*	910.21 g/mol	939.91 g/mol
Crystal	clear yellow block	clear colourless block
Crystal size [mm³]	0.342 x 0.245 x 0.16	0.206 x 0.086 x 0.073
Temperature *T*	123.00(10) K	123.0(2) K
Cristal system	monoclinic	orthorhombic
Space group	*P2$_1$/c*	*P2$_1$2$_1$2$_1$*
Unit cell dimensions	*a* = 14.0819(3) Å	*a* = 9.2429(3) Å
	b = 15.1834(3) Å	*b* = 12.9526(5) Å
	c = 17.7987(4) Å	*c* = 31.1175(9) Å
	α = 90°	*α* = 90°
	β = 100.706(2)°	*β* = 90°
	γ = 90°	*γ* = 90°
Volume *V*	3739.29(14) Å^3	3725.4(2) Å^3
Formula units *Z*	4	4
Absorption coefficient $\mu_{Cu\text{-}K\alpha}$	9.109 mm^{-1}	8.678 mm^{-1}
Density (calculated) ρ_{calc}	1.617 g/cm^3	1.676 g/cm^3
F(000)	1800	1864
Theta range θ_{min} / θ_{max} / θ_{full}	3.855 / 74.261 / 67.684°	3.696 / 73.448 / 67.684°
Absorption correction	gaussian	gaussian
Index ranges	-12 < *h* < 17	-11 < *h* < 11
	-16 < *k* < 18	-16 < *k* < 15
	-16 < *l* < 21	-38 < *l* < 38
Reflections collected	18421	41393
Independent reflections [$I > 2\sigma(I)$]	6910 (R_{int} = 0.0266)	6946 (R_{int} = 0.1337)
Completeness to full θ	0.996	0.999
Transmission T_{min} / T_{max}	0.178 / 0.899	0.334 / 0.803
Data / restraints / parameters	7327 / 410 / 507	7370 / 1035 / 462
Goodness-of-fit on F^2 *S*	1.053	1.051
Diffractometer type	GV 50	GV 50
Radiation type (λ)	CuK_α (1.54184 Å)	CuK_α (1.54184 Å)
Final *R*-values [$I > 2\sigma(I)$]	R_1 = 0.0733	R_1 = 0.1201
	wR_2 = 0.2189	wR_2 = 0.3159
Final *R*-values (all data)	R_1 = 0.0750	R_1 = 0.1227
	wR_2 = 0.2215	wR_2 = 0.3189
Largest difference hole	-1.636	-2.521
and peak $\Delta\rho$	1.809 eÅ^{-3}	2.476 eÅ^{-3}
Flack parameter		0.50(5)

Table S 4.4. Crystallographic data for compounds **8**$(thf)_2$ and **9**$(thf)_2$.

	8$(thf)_2$	**9**$(thf)_2$
Emipirical formula	$C_{32}H_{62}BNaO_{12}P_2W$	$C_{32}H_{62}As_2BNaO_{12}W$
Formula weight *M*	918.40 g/mol	1006.30 g/mol
Crystal	clear yellow prism	clear yellow prism
Crystal size [mm³]	0.251 x 0.195 x 0.163	0.18 x 0.158 x 0.145
Temperature *T*	122.9(2) K	122.9(3) K
Cristal system	triclinic	triclinic
Space group	*P1*	*P1*
Unit cell dimensions	*a* = 11.7703(3) Å	*a* = 11.7795(3) Å
	b = 11.77569(14) Å	*b* = 11.7812(3) Å
	c = 17.5594(3) Å	*c* = 17.7202(4) Å
	α = 70.4331(14)°	*α* = 109.368(2)°
	β = 70.4762(18)°	*β* = 109.408(2)°
	γ = 89.9897(13)°	*γ* = 90.007(2)°
Volume *V*	2144.22(7) Å^3	2171.27(10) Å^3
Formula units *Z*	2	2
Absorption coefficient $\mu_{Cu\text{-}K\alpha}$	6.231 mm^{-1}	7.150 mm^{-1}
Density (calculated) ρ_{calc}	1.422 g/cm^3	1.539 g/cm^3
F(000)	940	1012
Theta range θ_{min} / θ_{max} / θ_{full}	4.016 / 74.791 / 67.684°	4.008 / 74.880 / 67.684°
Absorption correction	gaussian	gaussian
Index ranges	-14 < *h* < 14	-14 < *h* < 14
	-14 < *k* < 14	-14 < *k* < 14
	-21 < *l* < 21	-22 < *l* < 21
Reflections collected	59346	46138
Independent reflections [$I > 2\sigma(I)$]	15491 (R_{int} = 0.0419)	15124 (R_{int} = 0.0483)
Completeness to full θ	99.91	0.999
Transmission T_{min} / T_{max}	0.421 / 0.728	0.420 / 0.651
Data / restraints / parameters	16261 / 1539 / 1203	16562 / 1477 / 1140
Goodness-of-fit on F^2 *S*	1.033	1.053
Diffractometer type	GV 50	GV 50
Radiation type (λ)	CuK_α (1.54184 Å)	CuK_α (1.54184 Å)
Final *R*-values [$I > 2\sigma(I)$]	R_1 = 0.0477	R_1 = 0.0581
	wR_2 = 0.1276	wR_2 = 0.1518
Final *R*-values (all data)	R_1 = 0.0490	R_1 = 0.0628
	wR_2 = 0.1296	wR_2 = 0.1566
Largest difference hole	-1.169	-1.129
and peak $\Delta\rho$	1.077 eÅ^{-3}	0.960 eÅ^{-3}
Flack parameter	0.014(16)	0.163(16)

Table S 4.5. Crystallographic data for compounds **10**.

	10
Emipirical formula	$C_{16}H_{56}B_4Cu_2Na_2O_4P_8$
Formula weight *M*	776.66 g/mol
Crystal	clear colourless block
Crystal size [mm³]	0.173 x 0.14 x 0.133
Temperature *T*	122.9(2) K
Cristal system	monoclinic
Space group	$P2_1$
Unit cell dimensions	a = 10.2192(2) Å b = 17.6836(2) Å c = 10.53140(10) Å α = 90° β = 94.106(2)° γ = 90°
Volume *V*	1898.27(5) Å^3
Formula units *Z*	2
Absorption coefficient $\mu_{Cu\text{-}K\alpha}$	4.964 mm^{-1}
Density (calculated) ρ_{calc}	1.359 g/cm^3
F(000)	808
Theta range θ_{min} / θ_{max} / θ_{full}	4.209 / 74.755 / 67.684°
Absorption correction	gaussian
Index ranges	-12 < h < 12 -22 < k < 22 -13 < l < 13
Reflections collected	38551
Independent reflections [$I > 2\sigma(I)$]	7187 (R_{int} = 0.0544)
Completeness to full θ	0.999
Transmission T_{min} / T_{max}	0.425 / 0.615
Data / restraints / parameters	7618 / 227 / 425
Goodness-of-fit on F^2 *S*	1.031
Diffractometer type	GV 50
Radiation type (λ)	CuK_α (1.54184 Å)
Final *R*-values [$I > 2\sigma(I)$]	R_1 = 0.0471 wR_2 = 0.1253
Final *R*-values (all data)	R_1 = 0.0498 wR_2 = 0.1287
Largest difference hole and peak $\Delta\rho$	-0.248 0.632 eÅ^{-3}

4.5.5 NMR Spectroscopy

$[Na(C_{12}H_{24}O_6)(thf)_2][^tBuPH\text{-}BH_2\text{-}^tBuPH]$ (3c(thf)$_2$):

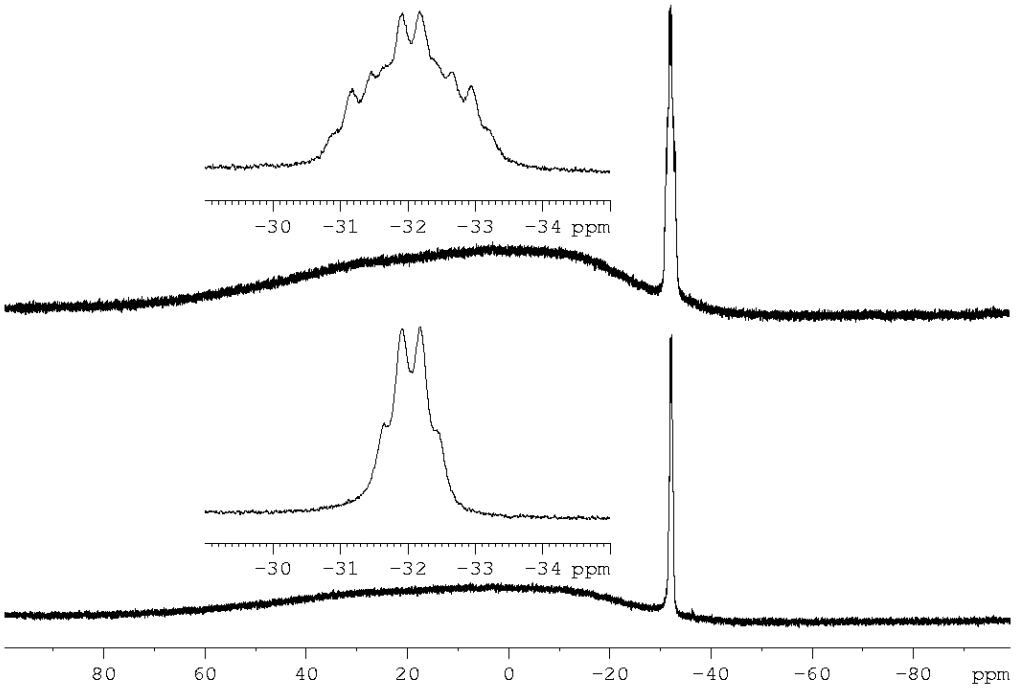

Figure S 4.10. $^{11}B\{^1H\}$ (bottom) and ^{11}B NMR spectrum (top) of **3c** in toluene-d_8.

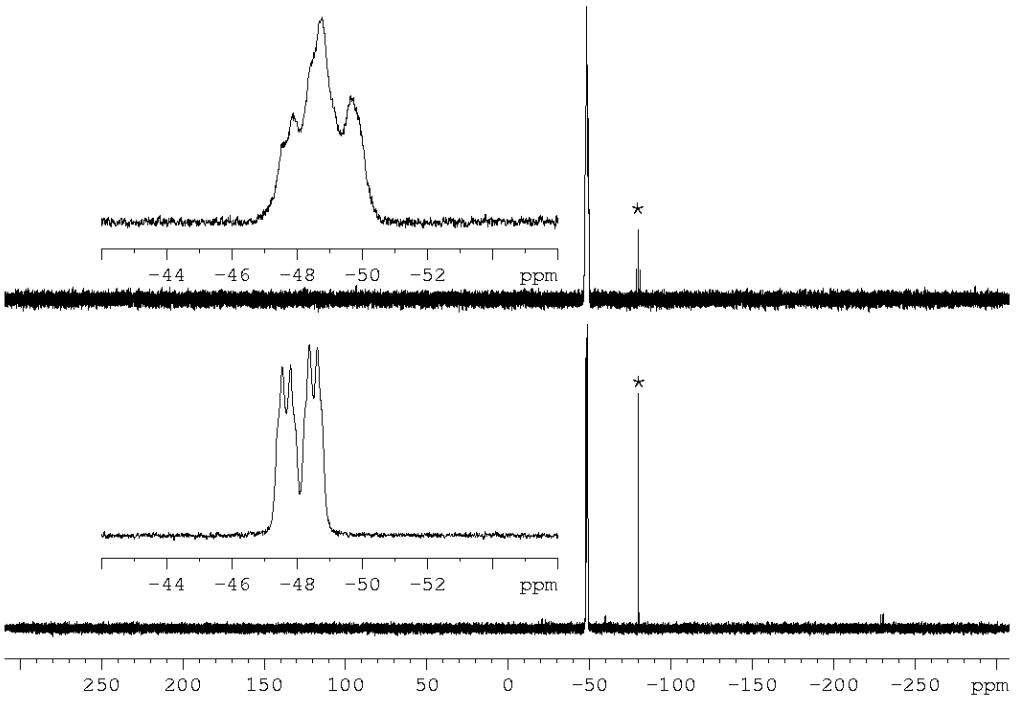

Figure S 4.11. $^{31}P\{^1H\}$ (bottom) and ^{31}P NMR spectrum (top) of **3c** in toluene-d_8.* = $^tBuPH_2$.

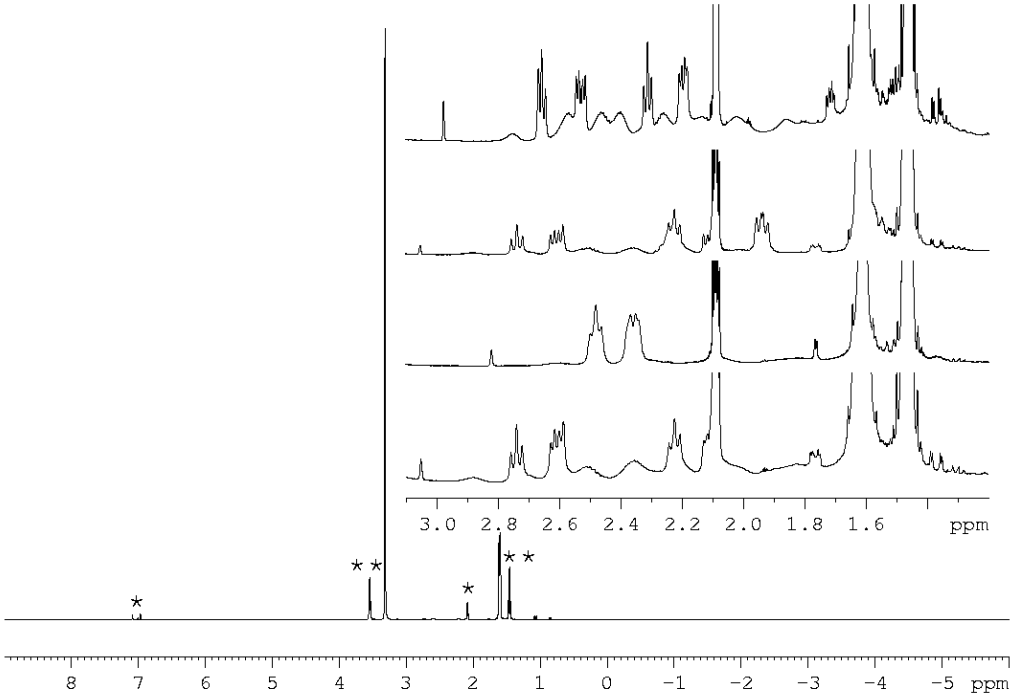

Figure S 4.12. ^{1}H NMR spectrum of **3c** in toluene-d_8. * = solvent (toluene-d_8), ** = THF. Magnified part shows ^{1}H, ^{1}H{^{31}P}, ^{1}H{^{11}B}, ^{1}H (600 MHz) NMR (from bottom to top) of the anion**.**

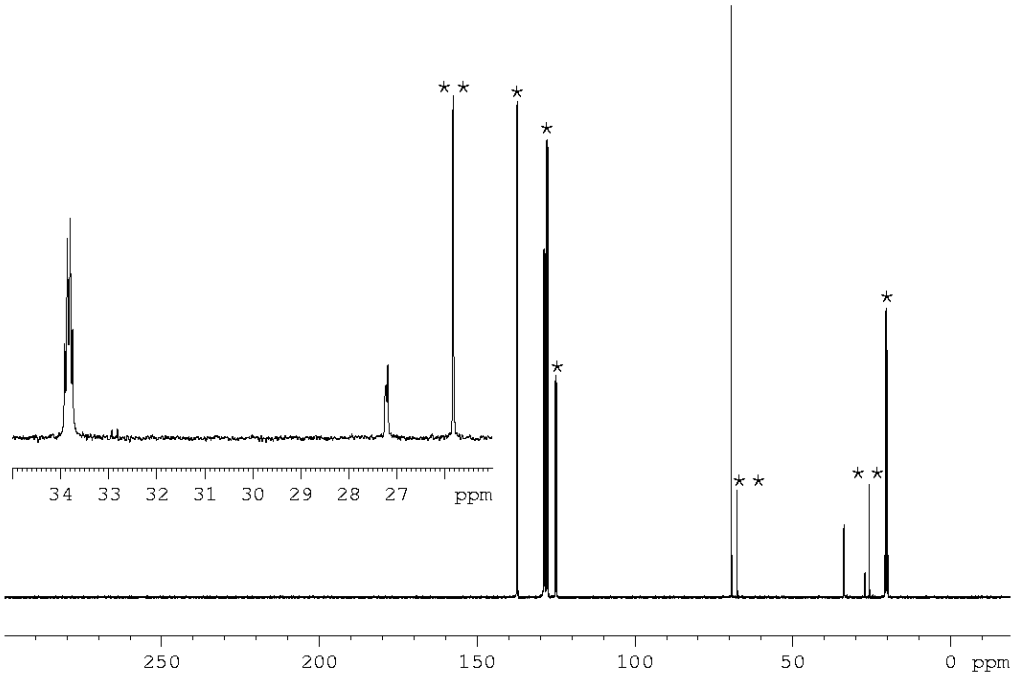

Figure S 4.13. ^{13}C NMR spectrum of **3c** in toluene-d_8. * = solvent (toluene-d_8), ** = THF.

$[Na(C_{12}H_{24}O_6)(thf)_2][^tBuAsH\text{-}BH_2\text{-}^tBuAsH]$ (4d(thf)$_2$):

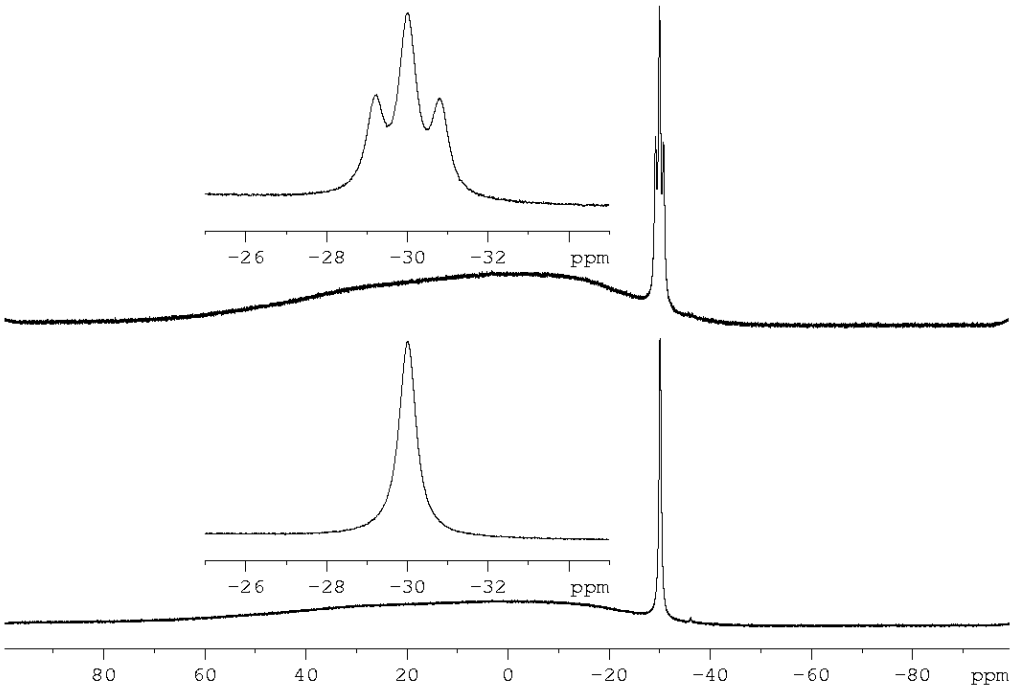

Figure S 4.14. $^{11}B\{^1H\}$ (bottom) and ^{11}B NMR spectrum (top) of **4d** in toluene-d_8.

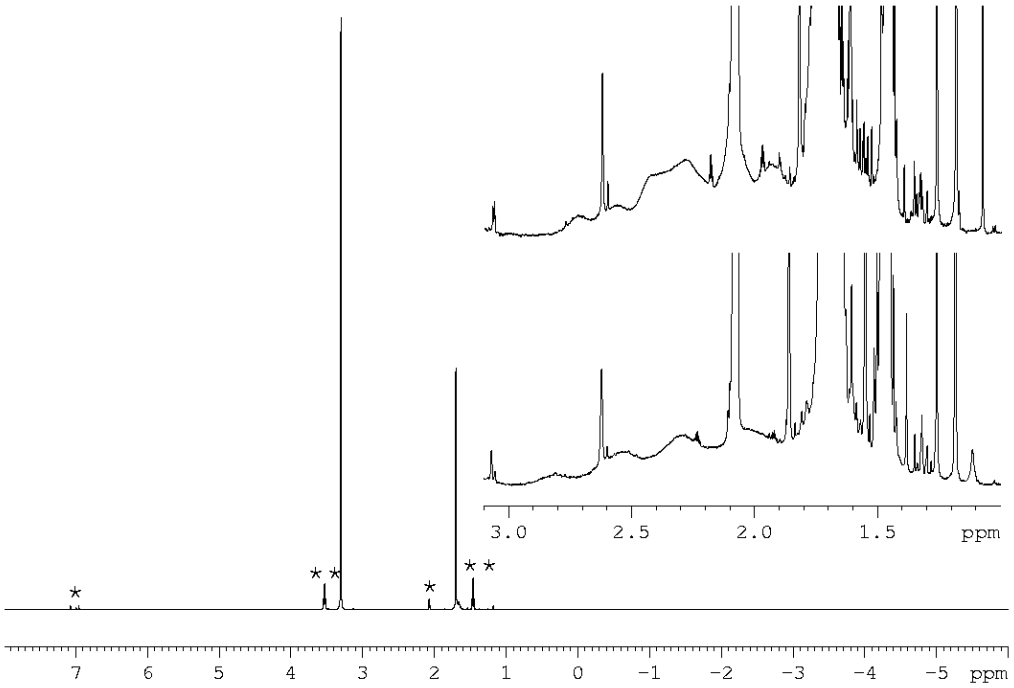

Figure S 4.15. ^1H NMR spectrum of **4d** in toluene-d_8. * = solvent (toluene-d_8), ** = THF. Magnified part shows ^1H, ^1H (600 MHz) NMR (from bottom to top) of the anion.

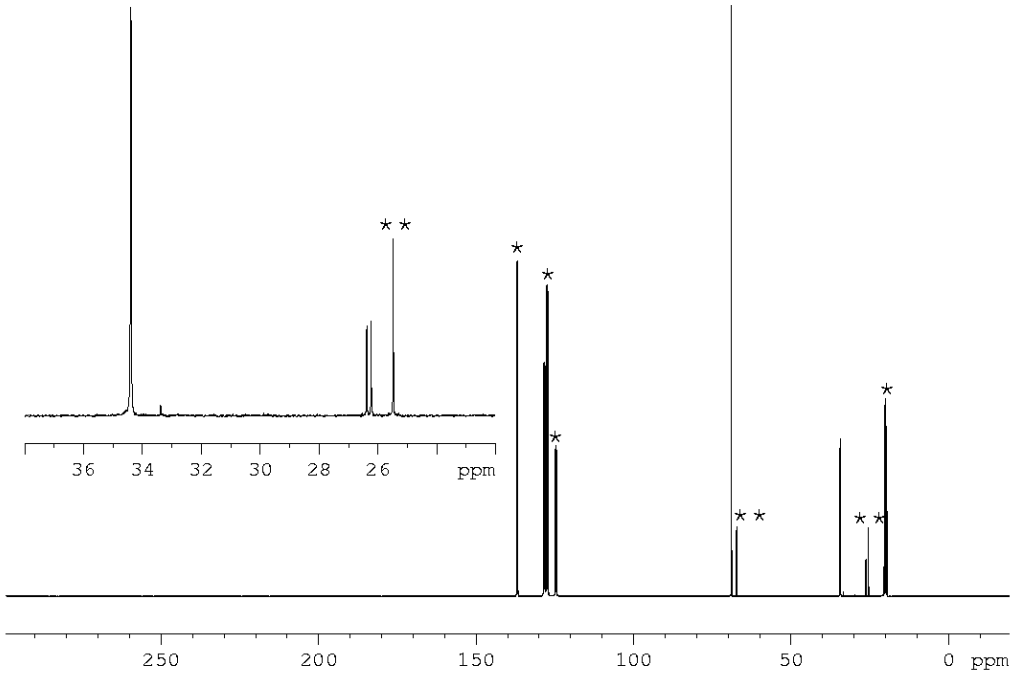

Figure S 4.16. ^{13}C NMR spectrum of **4d** in toluene-d_8. * = solvent (toluene-d_8), ** = THF.

$[Na(C_{12}H_{24}O_6)(thf)_2][W(CO)_4(H_2P\text{-}BH_2\text{-}PH_2)]$ $(5(thf)_2)$:

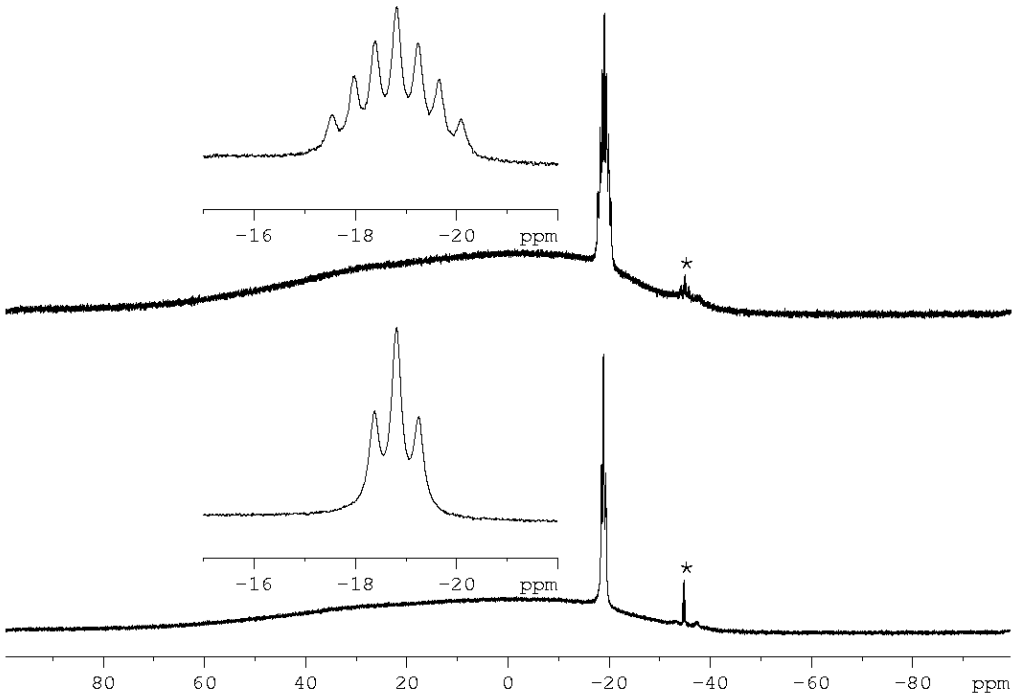

Figure S 4.17. $^{11}B\{^1H\}$ (bottom) and ^{11}B NMR spectrum (top) of **5** in THF-d_8. * = $Na^+[H_2P\text{-}BH_2\text{-}PH_2]^-$.

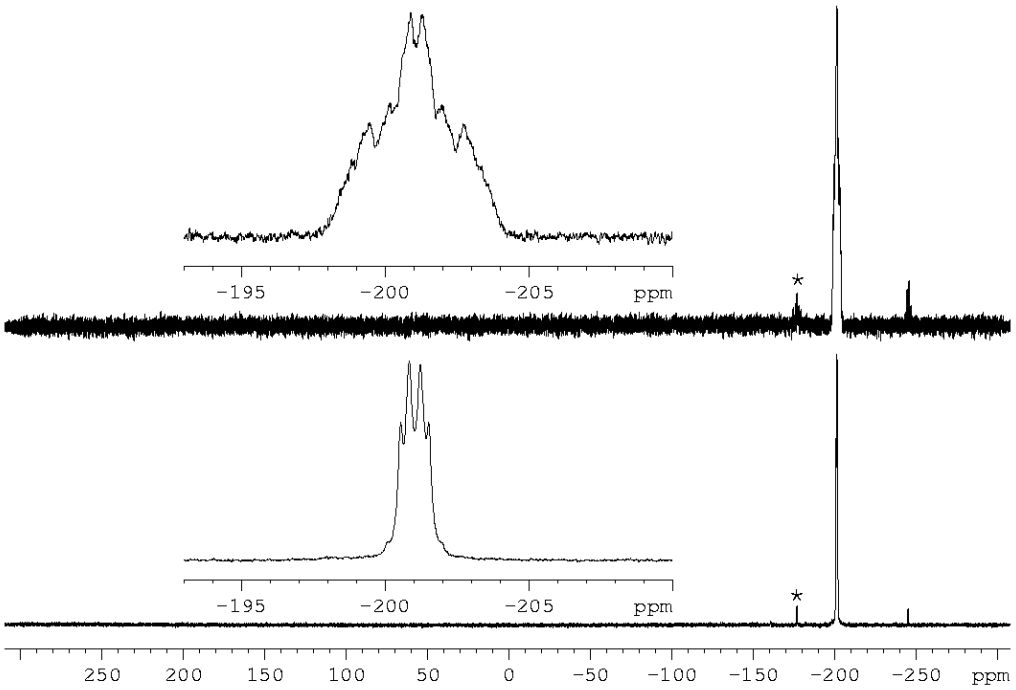

Figure S 4.18. $^{31}P\{^{1}H\}$ (bottom) and ^{31}P NMR spectrum (top) of **5** in THF-d_8. * = $Na^{+}[H_2P\text{-}BH_2\text{-}PH_2]^{-}$.

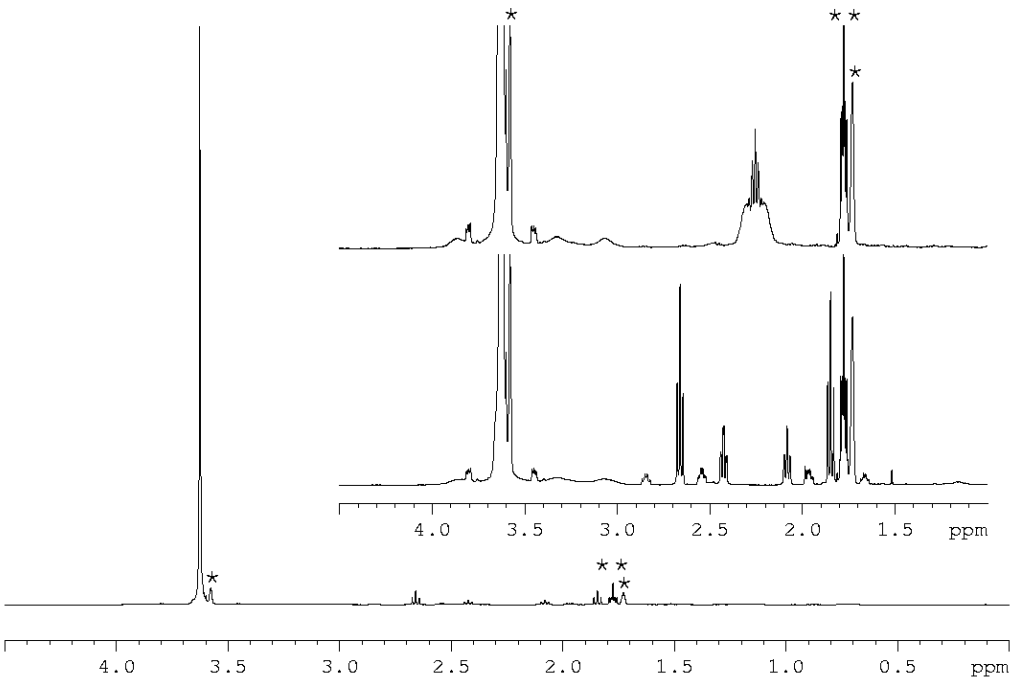

Figure S 4.19. ^{1}H NMR spectrum of **5** in THF-d_8. * = solvent (THF-d_8), ** = solvent (THF). Magnified part shows ^{1}H, $^{1}H\{^{31}P\}$ NMR (from bottom to top) of the anion.

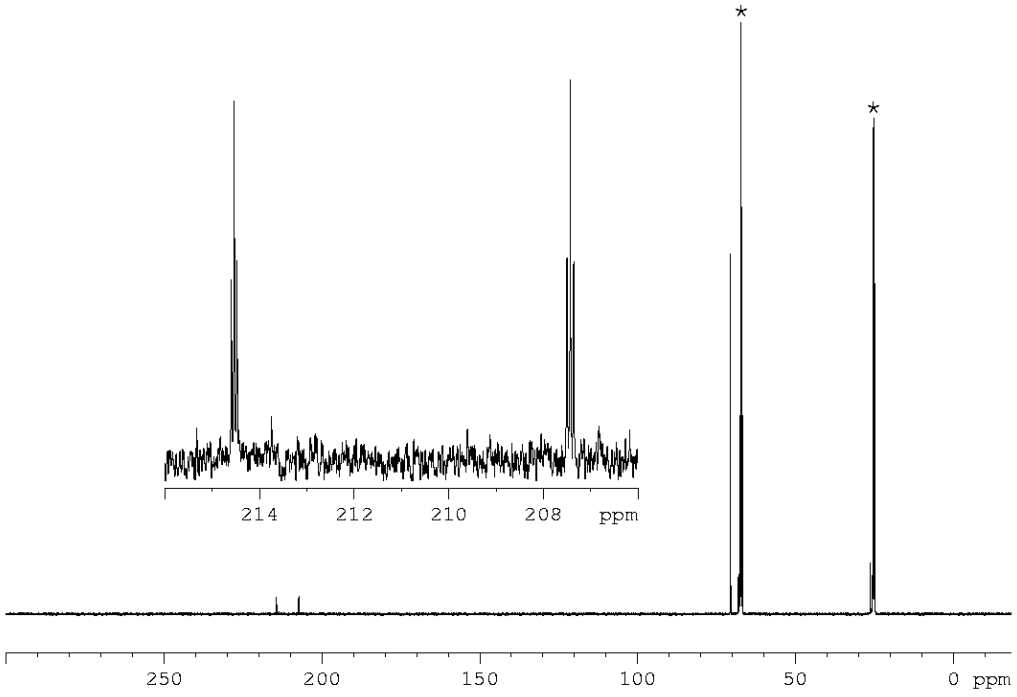

Figure S 4.20. ^{13}C NMR spectrum of **5** in THF-d_8. * = solvent (THF-d_8).

$([Na(C_{12}H_{24}O_6)(thf)_2][W(CO)_4(H_2As\text{-}BH_2\text{-}AsH_2)])_2$ $(6(thf)_4)$:

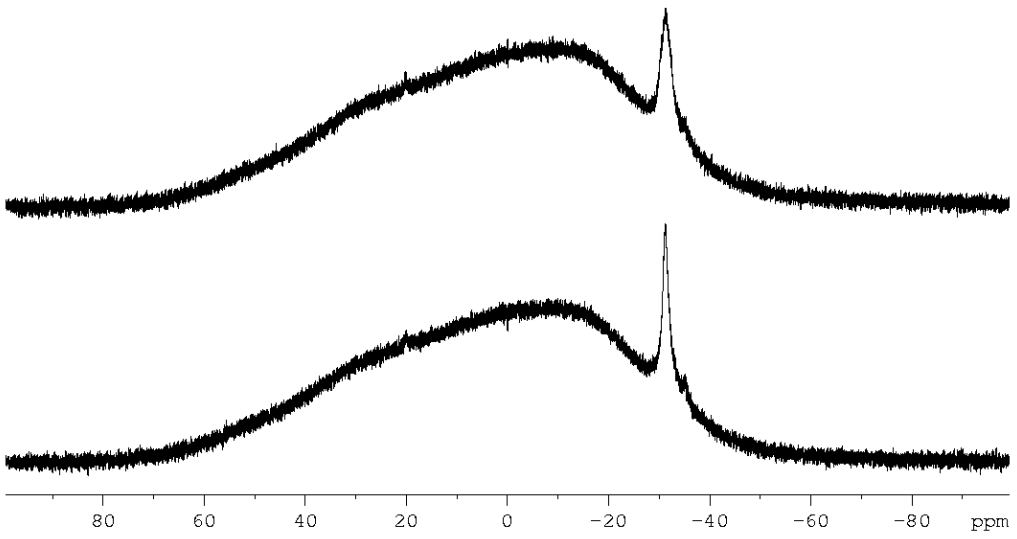

Figure S 4.21. $^{11}B\{^1H\}$ (bottom) and ^{11}B NMR spectrum (top) of **6** in THF-d_8.

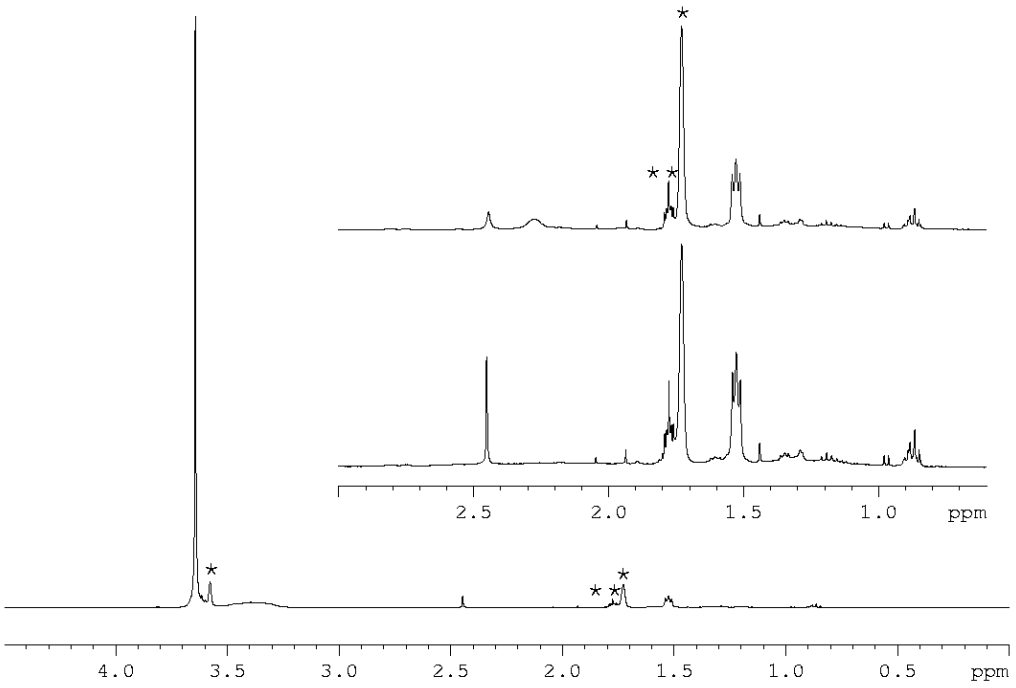

Figure S 4.22. ^{1}H NMR spectrum of **6** in THF-d_8. * = solvent (THF-d_8), ** = solvent (THF). Magnified part shows ^{1}H, $^{1}H\{^{11}B\}$ NMR (from bottom to top) of the anion.

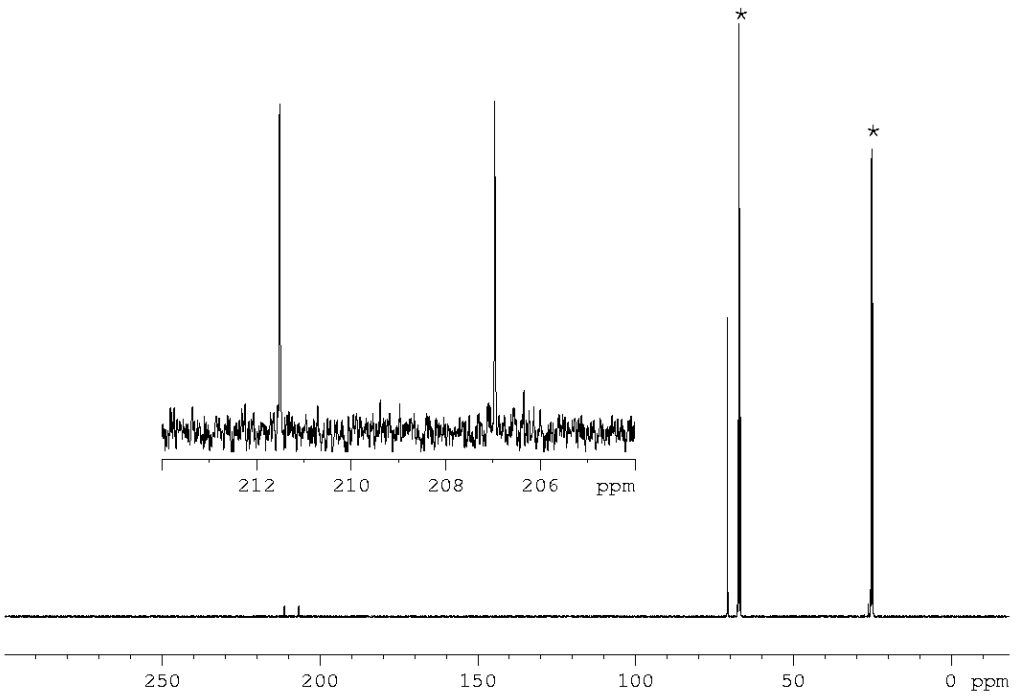

Figure S 4.23. ^{13}C NMR spectrum of **6** in THF-d_8. * = solvent (THF-d_8).

$[Na(C_{12}H_{24}O_6)(thf)_2][W(CO)_4(H_2As\text{-}BH_2\text{-}PH_2\text{-}BH_2\text{-}AsH_2)]$ $(7(thf)_2)$:

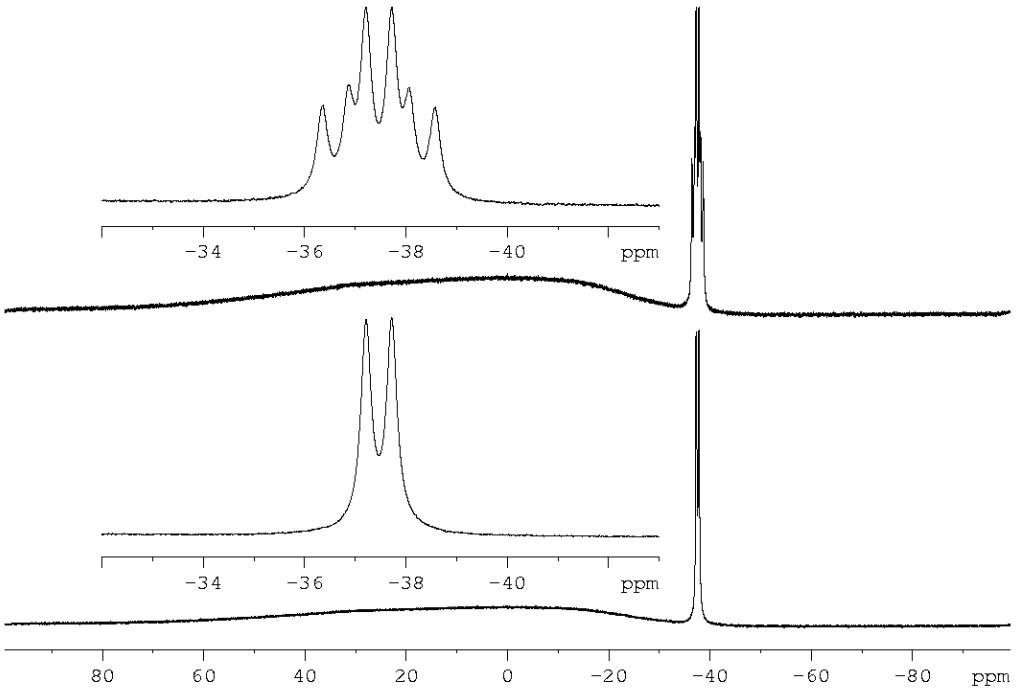

Figure S 4.24. $^{11}B\{^1H\}$ (bottom) and ^{11}B NMR spectrum (top) of **7** in THF-d_8.

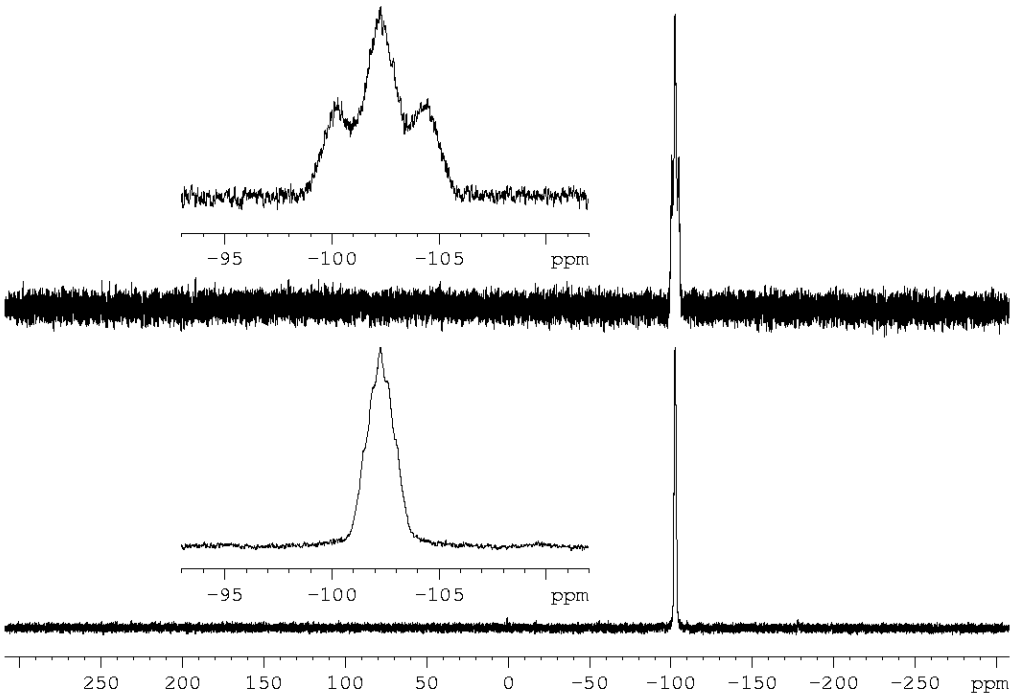

Figure S 4.25. $^{31}P\{^1H\}$ (bottom) and ^{31}P NMR spectrum (top) of **7** in THF-d_8.

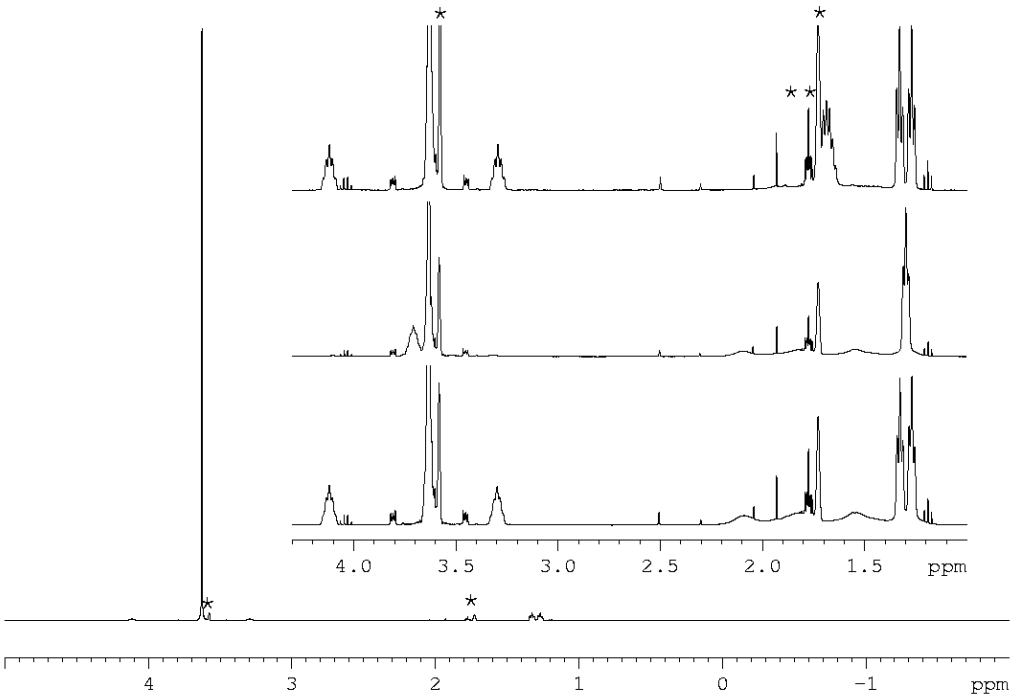

Figure S 4.26. ^{1}H NMR spectrum of **7** in THF-d_8. * = solvent (THF-d_8), ** = solvent (THF). Magnified part shows ^{1}H, $^{1}H\{^{31}P\}$, $^{1}H\{^{11}B\}$ NMR (from bottom to top) of the anion.

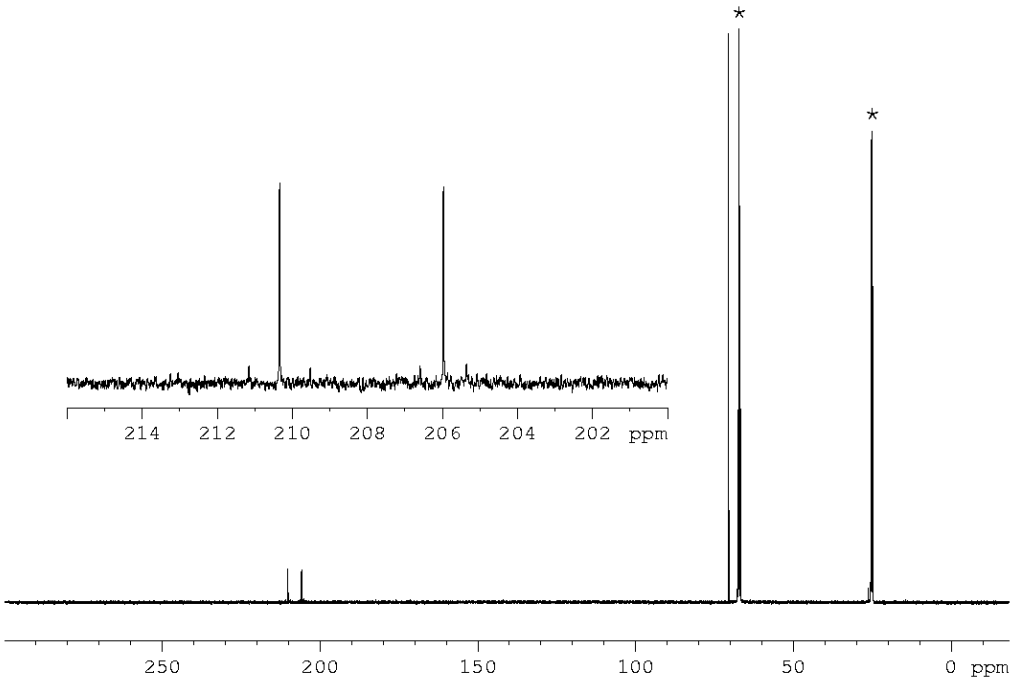

Figure S 4.27. ^{13}C NMR spectrum of **7** in THF-d_8. * = solvent (THF-d_8).

$[Na(C_{12}H_{24}O_6)(thf)_2][W(CO)_4(^tBuPH\text{-}BH_2\text{-}^tBuPH)]$ (**8**(thf)$_2$):

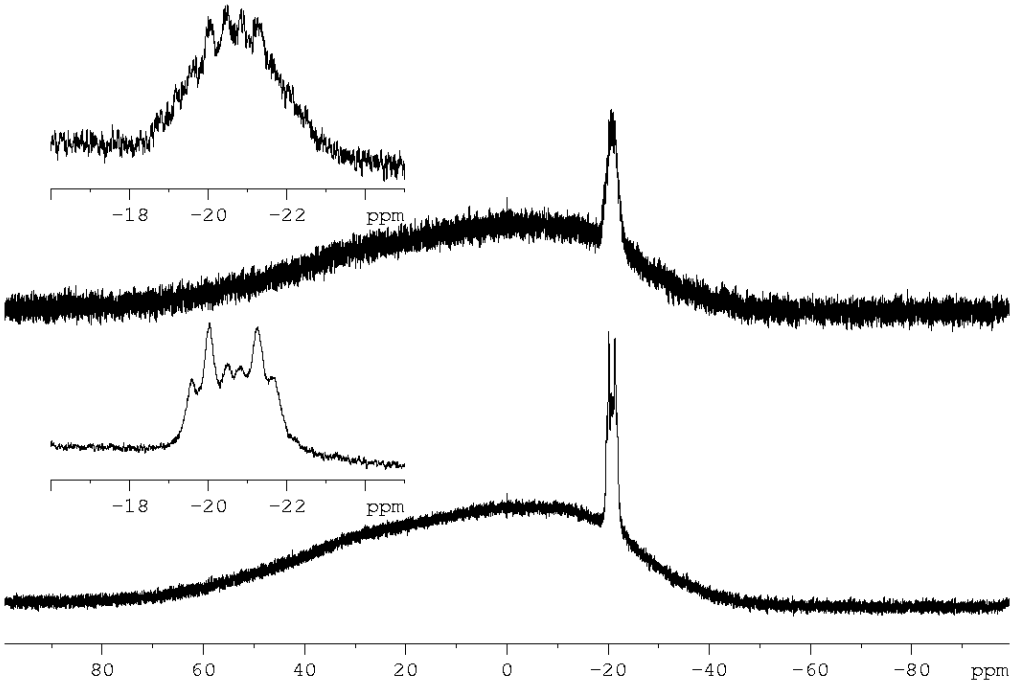

Figure S 4.28. $^{11}B\{^1H\}$ (bottom) and ^{11}B NMR spectrum (top) of **8** in THF-d_8.

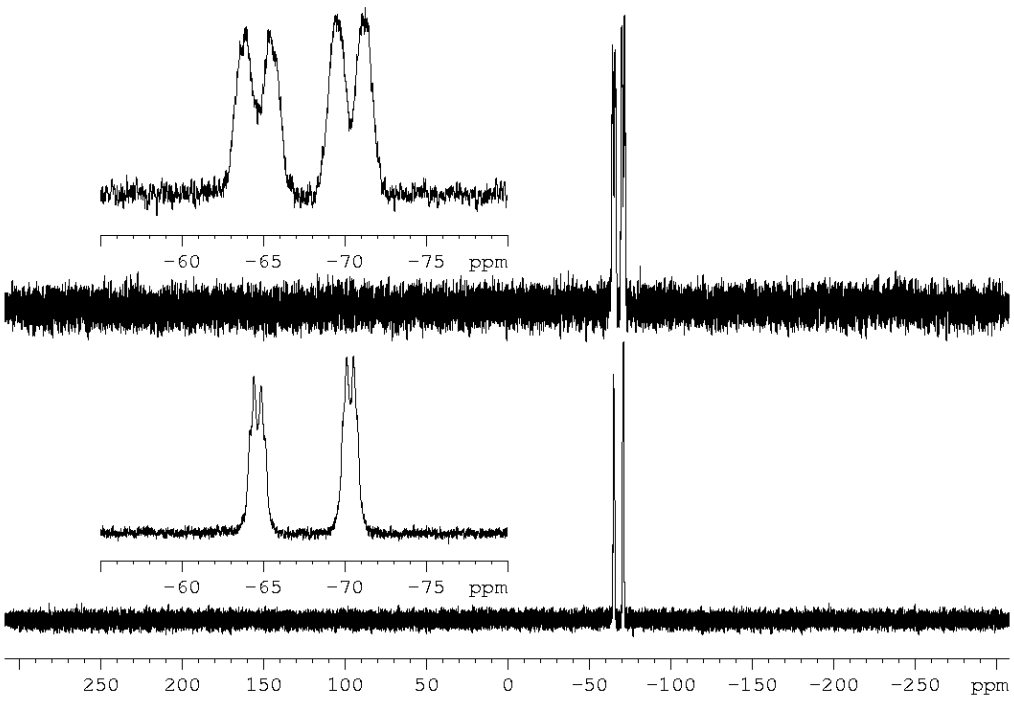

Figure S 4.29. $^{31}P\{^1H\}$ (bottom) and ^{31}P NMR spectrum (top) of **8** in THF-d_8.

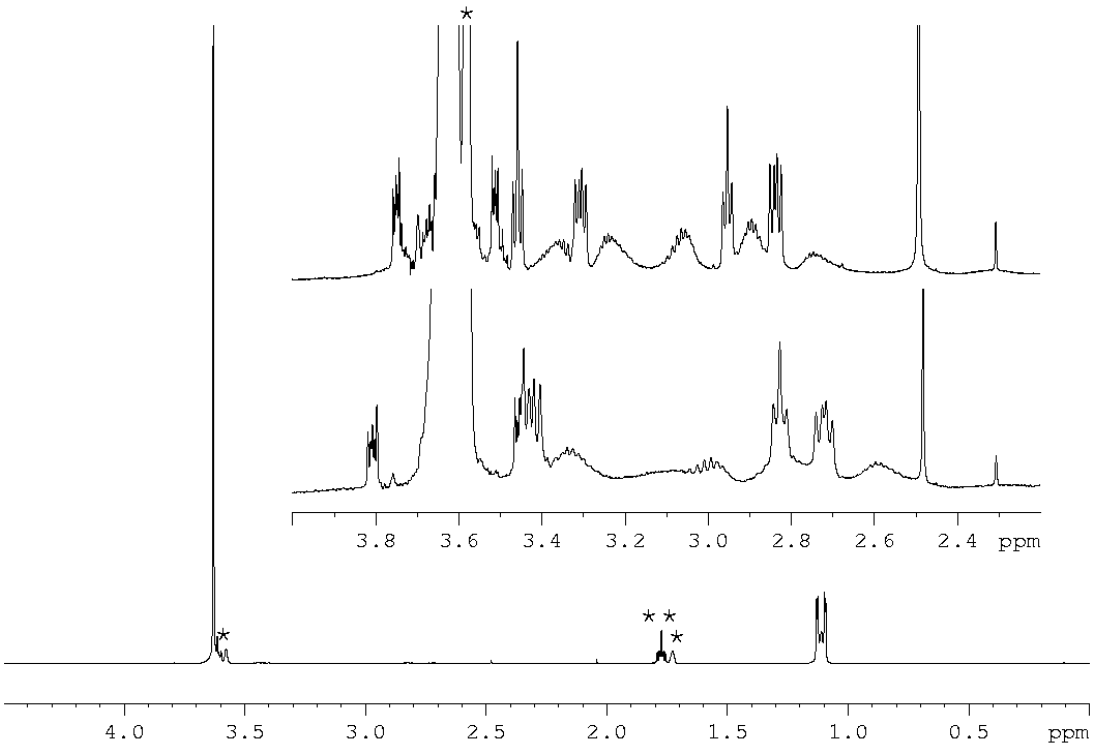

Figure S 4.30. ^{1}H NMR spectrum of **8** in THF-d_8. * = solvent (THF-d_8), ** = solvent (THF). Magnified part shows ^{1}H (400 MHz), ^{1}H NMR (600 MHz) (from bottom to top) of the anion.

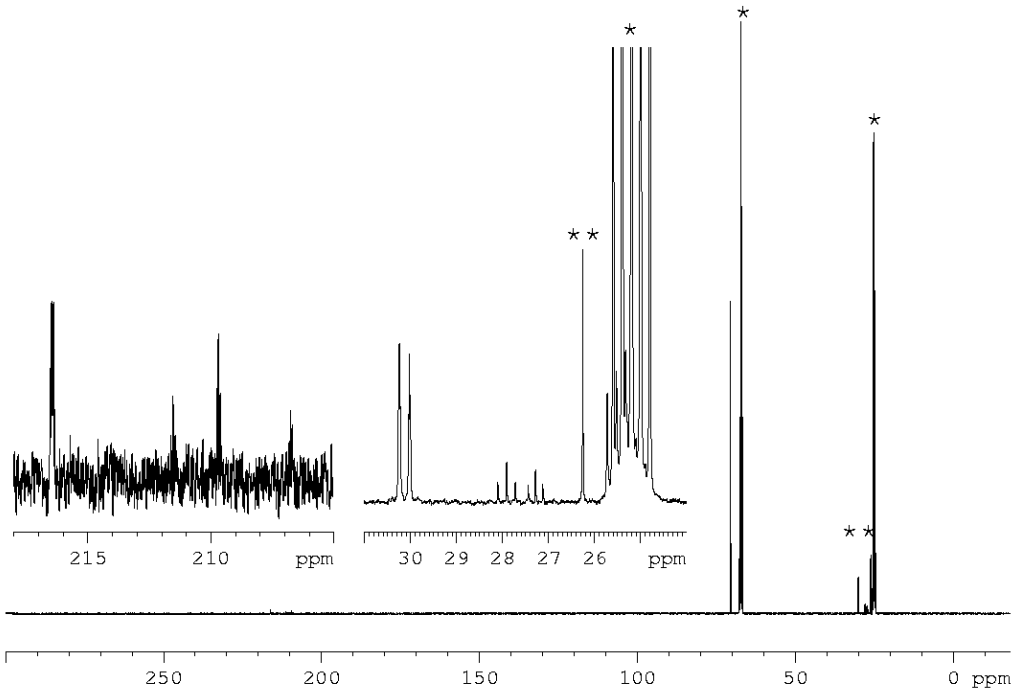

Figure S 4.31. ^{13}C NMR spectrum of **8** in THF-d_8. * = solvent (THF-d_8), ** = solvent (THF).

$[Na(C_{12}H_{24}O_6)(thf)_2][W(CO)_4(^tBuAsH\text{-}BH_2\text{-}^tBuAsH)]$ $(9(thf)_2)$:

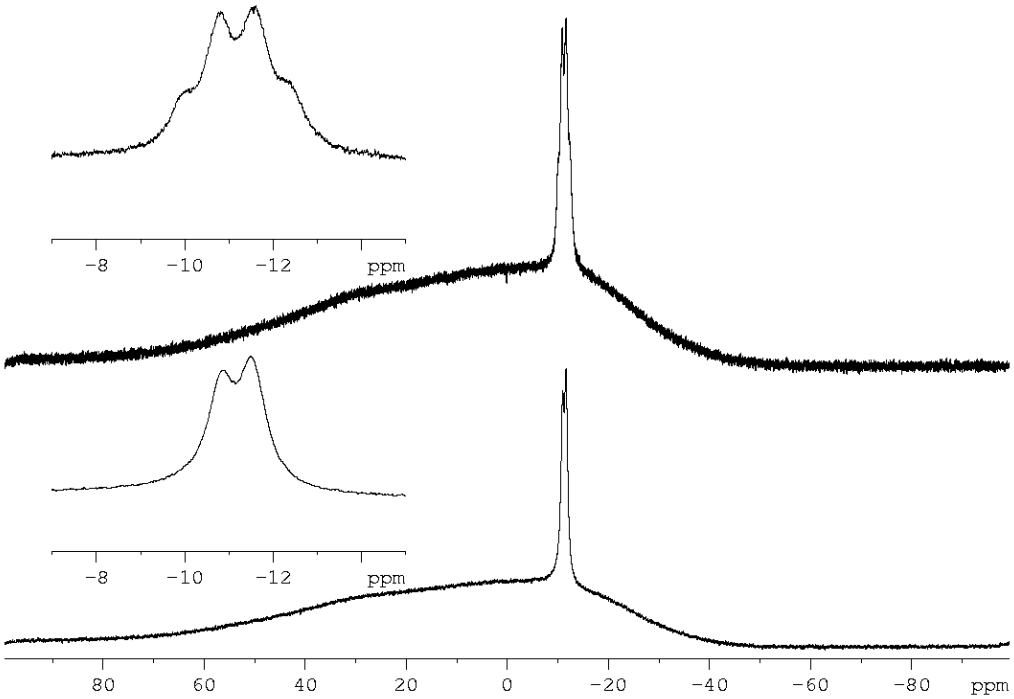

Figure S 4.32. $^{11}B\{^1H\}$ (bottom) and ^{11}B NMR spectrum (top) of **9** in THF-d_8.

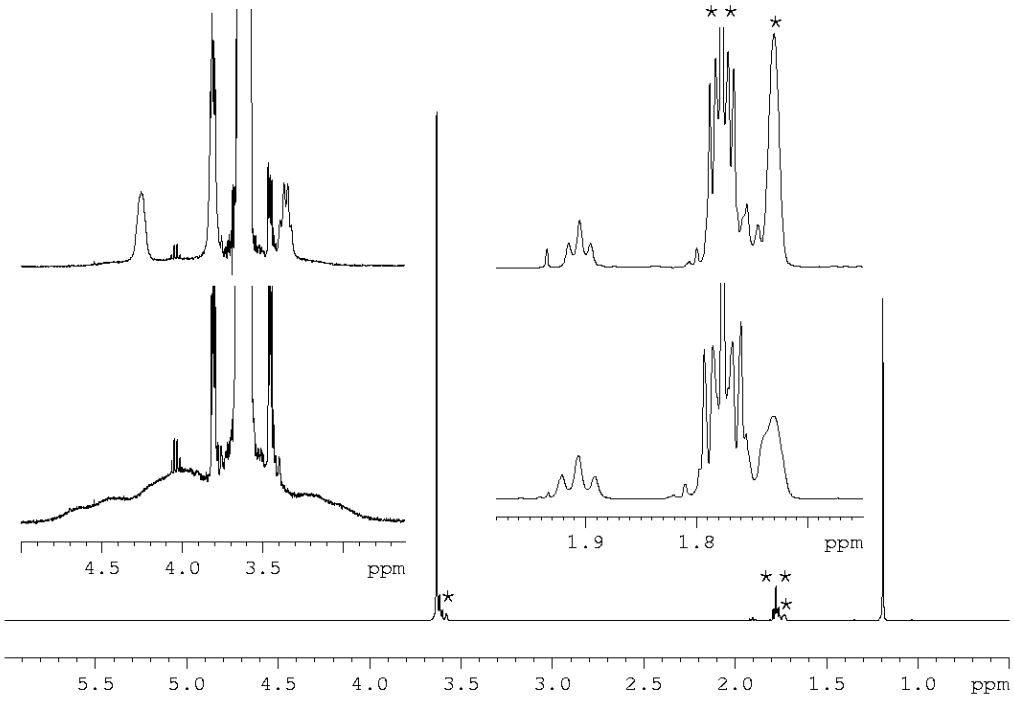

Figure S 4.33. ^1H NMR spectrum of **9** in THF-d_8. * = solvent (THF-d_8), ** = solvent (THF). Magnified part shows left sided ^1H, $^1H\{^{11}B\}$ and right sided ^1H (400 MHz), ^1H NMR (600 MHz) (from bottom to top) of the anion.

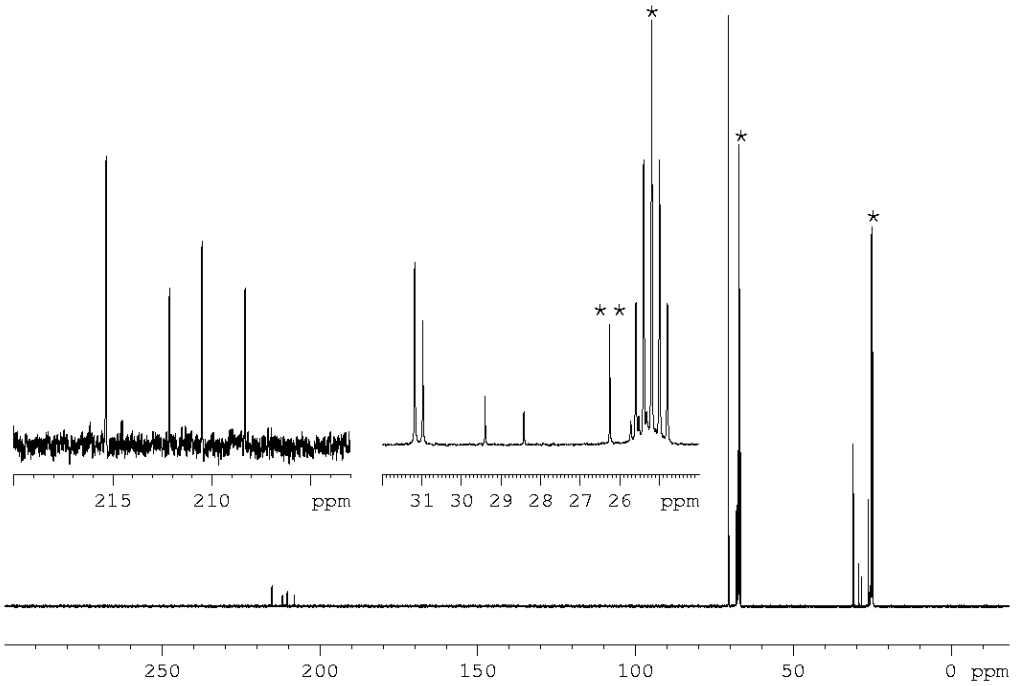

Figure S 4.34. ^{13}C NMR spectrum of **9** in THF-d_8. * = solvent (THF-d_8), ** = solvent (THF).

$[Cu_2Na_2(thf)_4(H_2P\text{-}BH_2\text{-}PH_2)_4]$ (10):

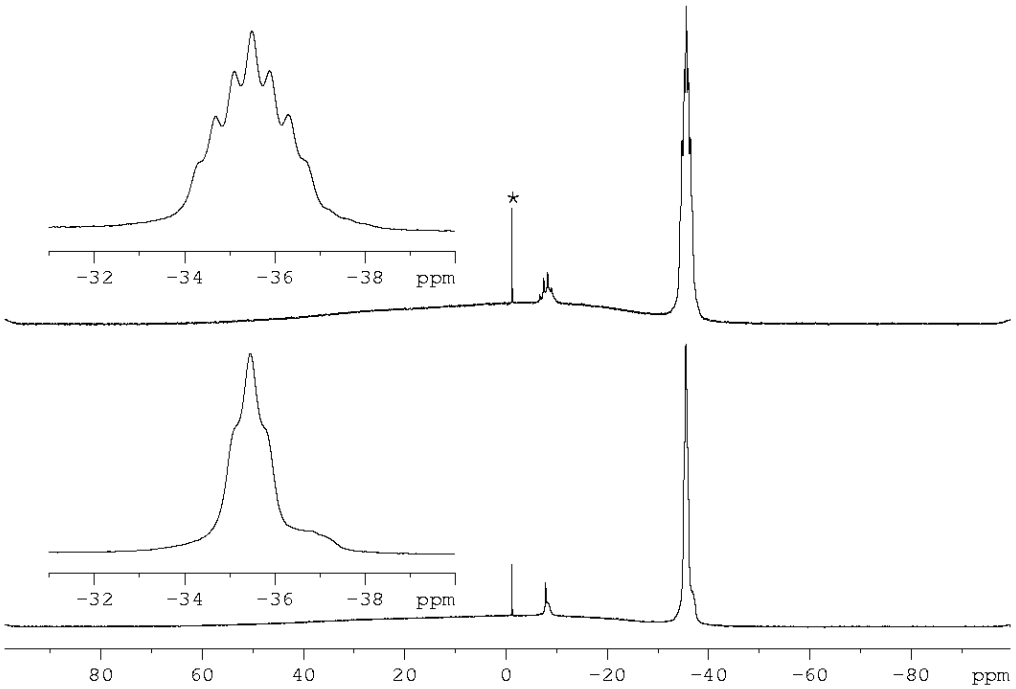

Figure S 4.35. $^{11}B\{^1H\}$ (bottom) and ^{11}B NMR spectrum (top) of **10** in THF + C_6D_6 capillary. * = $[BF_4]^-$.

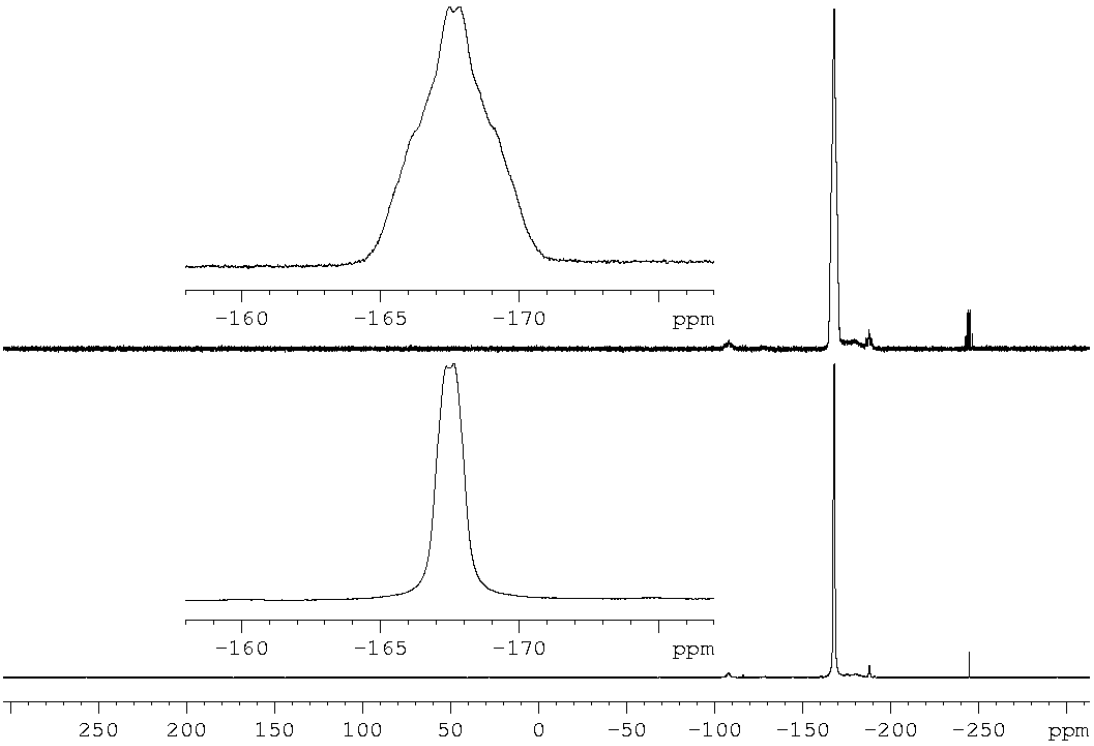

Figure S 4.36. $^{31}P\{^{1}H\}$ (bottom) and ^{31}P NMR spectrum (top) of **10** in THF + C_6D_6 capillary.

$[Cu_2Na_2(^{t}BuPH\text{-}BH_2\text{-}^{t}BuPH)_4]$ (12):

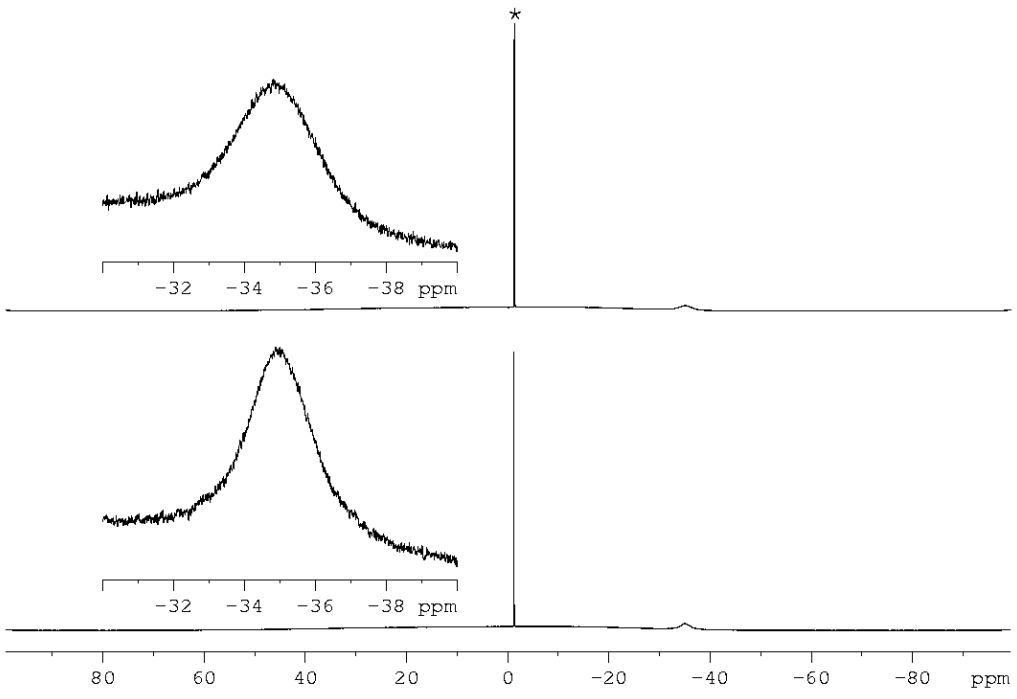

Figure S 4.37. $^{11}B\{^{1}H\}$ (bottom) and ^{11}B NMR spectrum (top) of **12** in THF-d_8. * = $[BF_4]^-$.

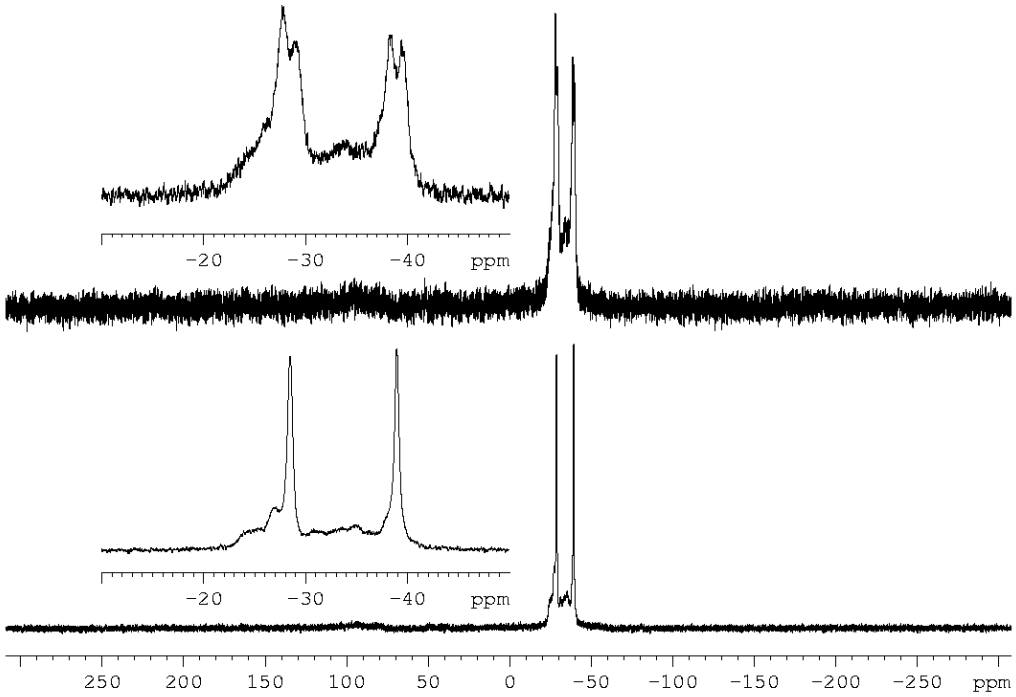

Figure S 4.38. $^{31}P\{^{1}H\}$ (bottom) and ^{31}P NMR spectrum (top) of **12** in THF-d_8.

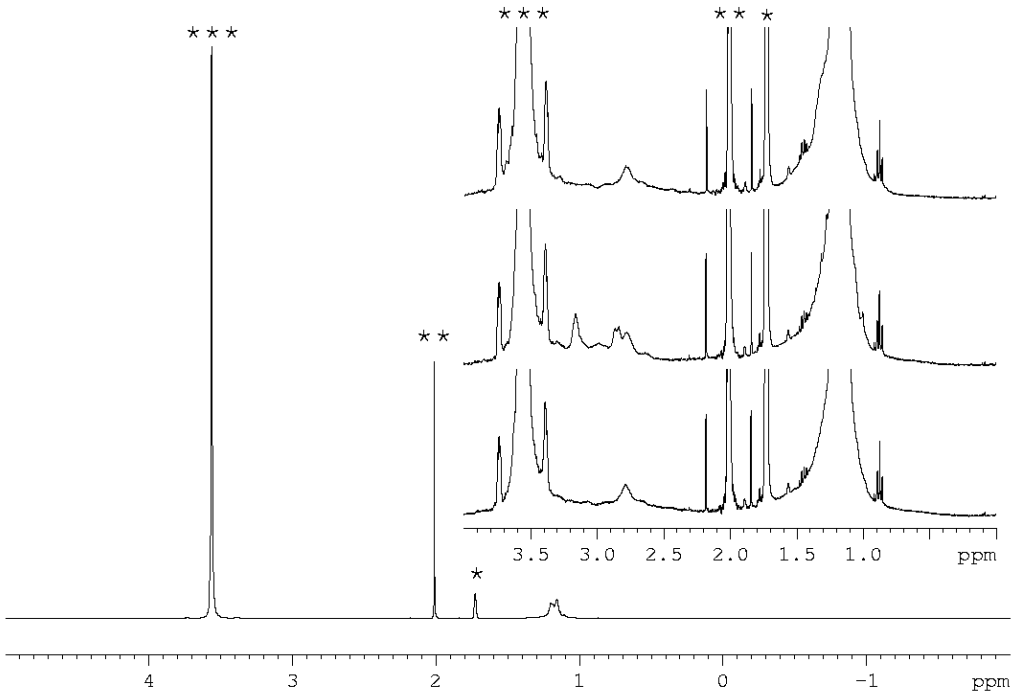

Figure S 4.39. ^{1}H NMR spectrum of **12** in THF-d_8. * = solvent (THF-d_8), ** = CH_3CN, *** = $C_{12}H_{24}O_6$. Magnified part shows ^{1}H, $^{1}H\{^{31}P\}$, $^{1}H\{^{11}B\}$ NMR (from bottom to top) of the anion.

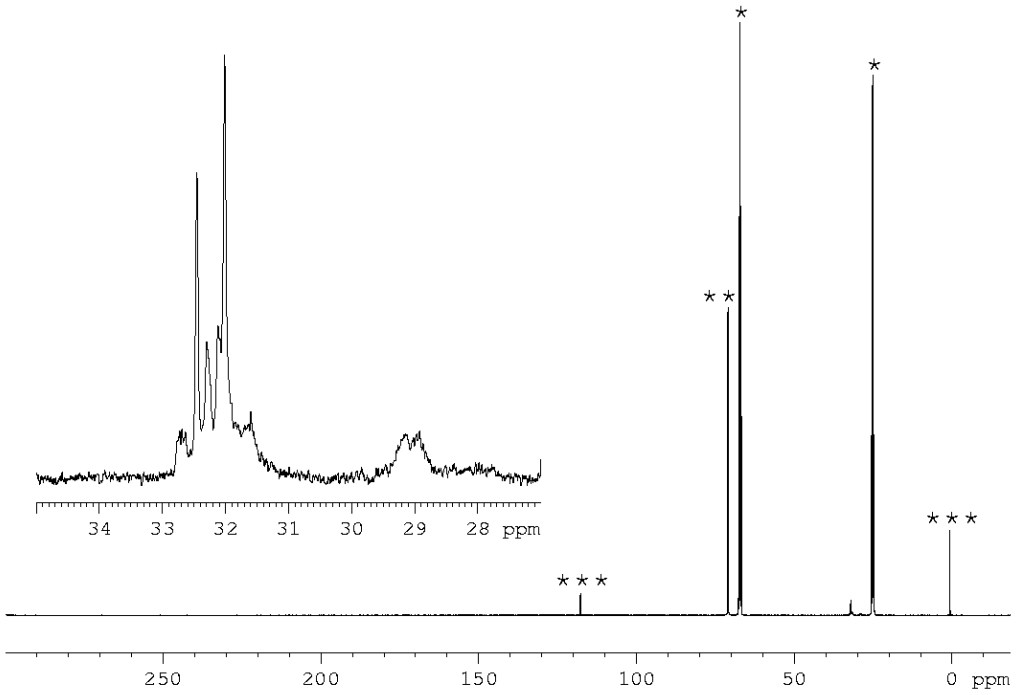

Figure S 4.40. ^{13}C NMR spectrum of **12** in THF-d_8. * = solvent (THF-d_8), ** = $C_{12}H_{24}O_6$, *** = CH_3CN.

$[Cu_2Na_2(^tBuAsH\text{-}BH_2\text{-}^tBuAsH)_4]$ (13):

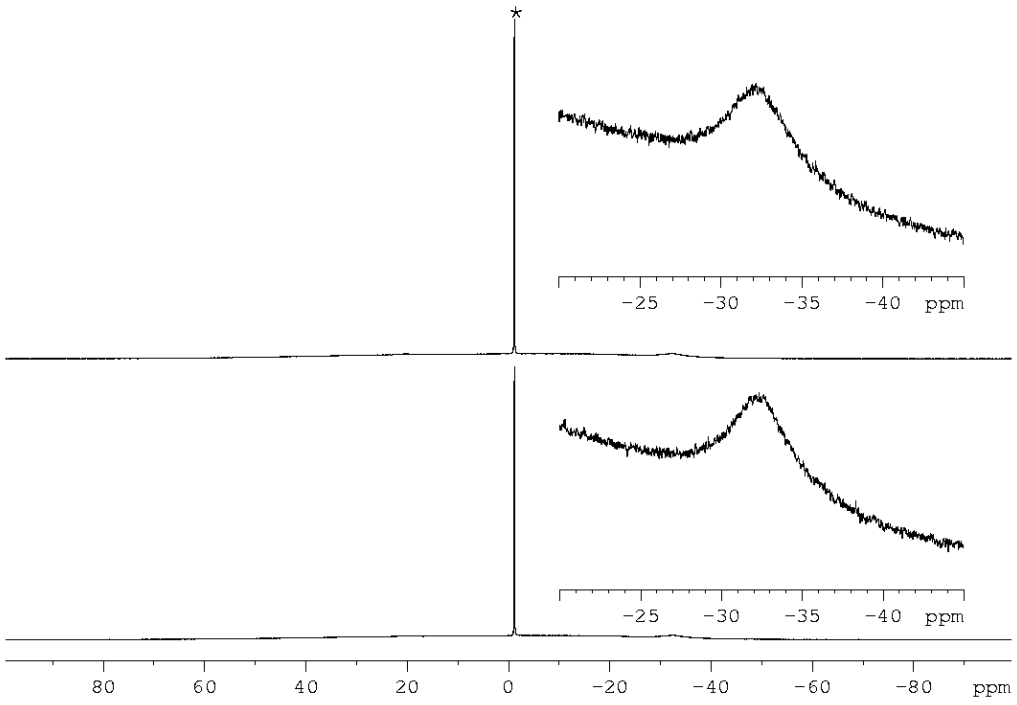

Figure S 4.41. $^{11}B\{^1H\}$ (bottom) and ^{11}B NMR spectrum (top) of **13** in THF-d_8. * = $[BF_4]^-$.

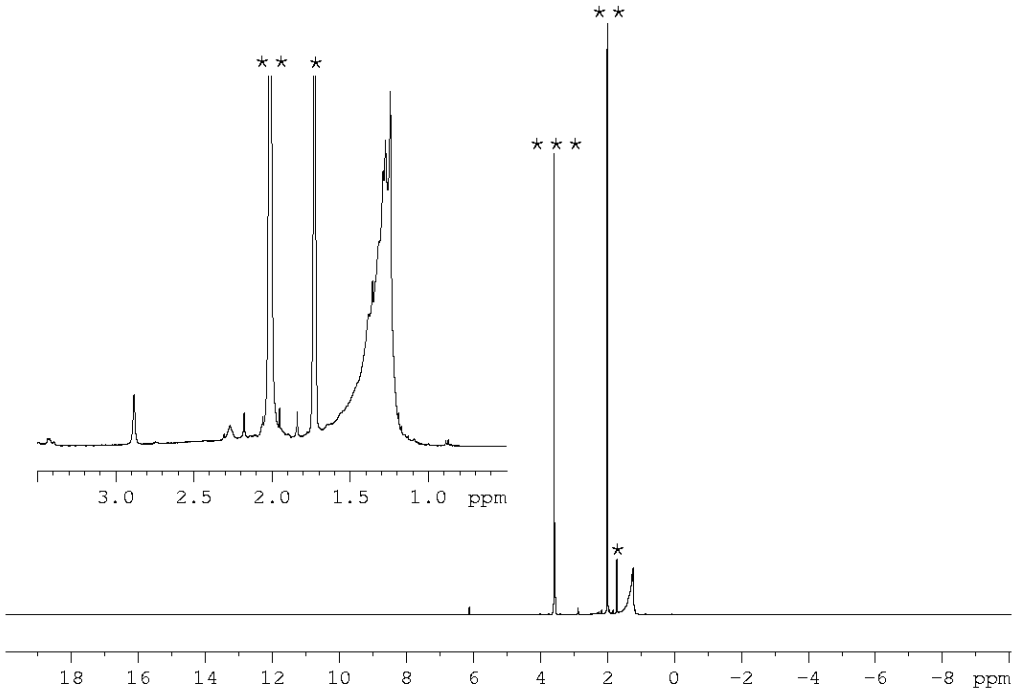

Figure S 4.42. ^{1}H NMR spectrum of **13** in THF-d_8. * = solvent (THF-d_8), ** = CH_3CN, *** = $C_{12}H_{24}O_6$.

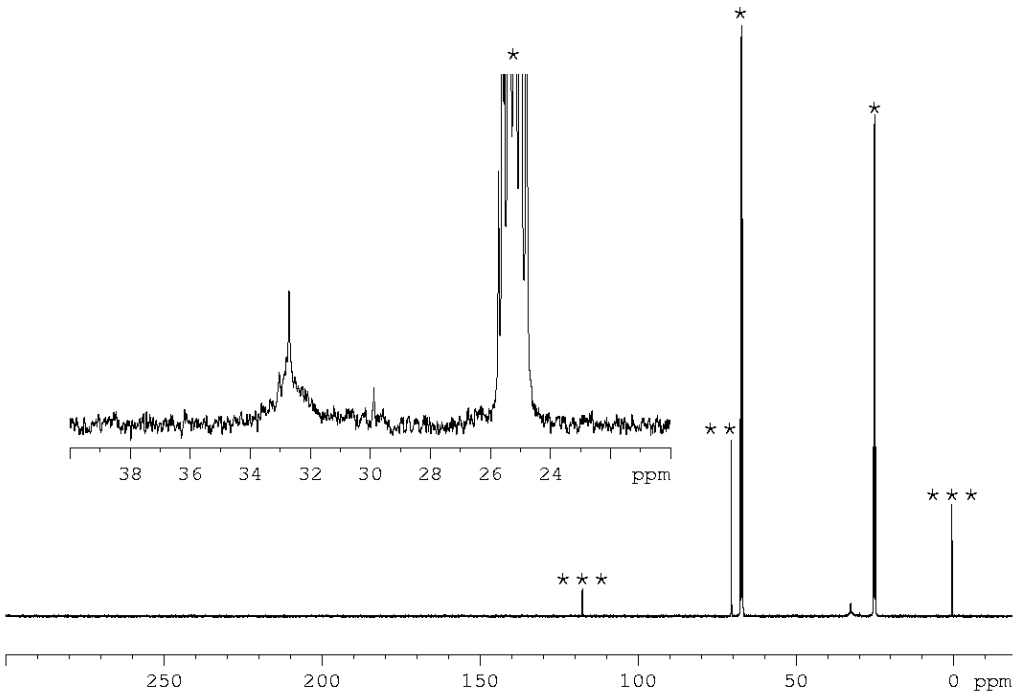

Figure S 4.43. ^{13}C NMR spectrum of **13** in THF-d_8. * = solvent (THF-d_8), ** = $C_{12}H_{24}O_6$, *** = CH_3CN.

4.5.6 Computational Details

For all computations Gaussian 09 program package[11] was used throughout. Density functional theory (DFT) in form of Becke's three-parameter hybrid functional B3LYP[12] with 6-311++G** all electron basis set was employed. For W Effective Core Potential LANL2TZ(f) basis set was used.[13] Basis sets were obtained from the EMSL basis set exchange database.[14] The geometries of the compounds have been fully optimized and verified to be true minima on their respective potential energy surface (PES).

Table S 4.6. Gas phase reaction energies ΔE^{o}_{0}, standard reaction enthalpies ΔH^{o}_{298}, Gibbs energies ΔG^{o}_{298} in kJ·mol^{-1}, and standard reaction entropies ΔS^{o}_{298}, J·mol^{-1}·K^{-1}. B3LYP/6-311++G** (ECP LANL2TZ(f) on W) level of theory.

Reaction	**ΔE^{o}_{0}**	**ΔH^{o}_{298}**	**ΔS^{o}_{298}**	**ΔG^{o}_{298}**
$[W(CO)_4(nbd)] + [PH_2BH_2PH_2]^- = nbd + [W(CO)_4PH_2BH_2PH_2]^-$ (**5**)	-135.2	-131.0	13.3	-135.0
$[W(CO)_4(nbd)] + [AsH_2BH_2AsH_2]^- = nbd + [W(CO)_4AsH_2BH_2AsH_2]^-$	-97.6	-94.8	9.0	-97.5
$2\,[W(CO)_4(nbd)] + 2\,[PH_2BH_2PH_2]^- = 2\,nbd + [(CO)_4W(PH_2BH_2PH_2)_2W(CO)_4]^{2-}$	-162.6	-145.2	-146.2	-101.6
$2\,[W(CO)_4(nbd)] + 2\,[AsH_2BH_2AsH_2]^- = 2\,nbd + [(CO)_4W(AsH_2BH_2AsH_2)_2W(CO)_4]^{2-}$ (**6**)	-104.0	-88.9	-157.2	-42.0

Table S 4.7. Total energies E^{o}_{0}, sum of electronic and thermal enthalpies H^{o}_{298} (Hartree) and standard entropies S^{o}_{298} (cal·mol^{-}1·K^{-1}) for studied compounds. B3LYP/6-311++G** (ECP LANL2TZ(f) on W) level of theory.

Compound	**E^{o}_{0}**	**H^{o}_{298}**	**S^{o}_{298}**
nbd	-271.5500290	-271.416248	70.088
$[W(CO)_4nbd]$	-792.9582322	-792.779242	125.174
$[W(CO)_4PH_2BH_2PH_2]^-$ (**5**)	-1232.7420685	-1232.633264	131.938
$[W(CO)_4AsH_2BH_2AsH_2]^-$	-5021.7352488	-5021.630298	138.848
$[PH_2BH_2PH_2]^-$	-711.2823656	-711.220376	73.662
$[AsH_2BH_2AsH_2]^-$	-4500.289879	-4500.231188	81.6
$[(CO)_4W(PH_2BH_2PH_2)_2W(CO)_4]^{2-}$	-2465.4430704	-2465.222031	222.543
$[(CO)_4W(AsH_2BH_2AsH_2)_2W(CO)_4]^{2-}$ (**6**)	-10043.4357667	-10043.22223	235.791

Table S 4.8. Optimized xyz coordinates (in Angstroms) for studied compounds B3LYP/6-311++G** (ECP LANL2TZ(f) on W) level of theory.

nbd

Atom	x	y	z
H	-1.931152000	1.334516000	-1.021650000
C	-1.242696000	0.666842000	-0.521332000
C	1.242696000	-0.666842000	-0.521332000
C	-1.242696000	-0.666842000	-0.521332000
C	1.242696000	0.666842000	-0.521332000
C	0.000000000	0.000000000	1.356816000
H	-1.931152000	-1.334516000	-1.021650000
H	1.931152000	1.334516000	-1.021650000
H	1.931152000	-1.334516000	-1.021650000
H	-0.898757000	0.000000000	1.977375000
H	0.898757000	0.000000000	1.977375000
C	0.000000000	1.122875000	0.273448000
H	0.000000000	2.158066000	0.610776000
C	0.000000000	-1.122875000	0.273448000
H	0.000000000	-2.158066000	0.610776000

[W(CO)$_4$nbd]

Atom	x	y	z
H	2.040420000	1.333967000	-1.355927000
C	1.211053000	0.692182000	-1.615194000
C	-1.211053000	-0.692182000	-1.615194000
C	1.211053000	-0.692182000	-1.615194000
C	-1.211053000	0.692182000	-1.615194000
C	0.000000000	0.000000000	-3.542694000
H	2.040420000	-1.333967000	-1.355927000
H	-2.040420000	1.333967000	-1.355927000
H	-2.040420000	-1.333967000	-1.355927000
H	0.896995000	0.000000000	-4.167839000
H	-0.896995000	0.000000000	-4.167839000
C	0.000000000	1.125896000	-2.472519000
H	0.000000000	2.161875000	-2.802992000
C	0.000000000	-1.125896000	-2.472519000
H	0.000000000	-2.161875000	-2.802992000
W	0.000000000	0.000000000	0.377786000
C	-1.479262000	0.000000000	1.718874000
C	1.479262000	0.000000000	1.718874000
C	0.000000000	2.036209000	0.631231000
C	0.000000000	-2.036209000	0.631231000
O	0.000000000	3.163773000	0.844707000
O	-2.362536000	0.000000000	2.461479000
O	2.362536000	0.000000000	2.461479000
O	0.000000000	-3.163773000	0.844707000

$[W(CO)_4PH_2\text{-}BH_2\text{-}PH_2]^-$ (5)

Atom	x	y	z
W	-0.014752000	-0.278652000	0.000000000
P	-0.011434000	1.891632000	1.452142000
P	-0.011434000	1.891632000	-1.452142000
O	-0.010387000	-2.437959000	2.290445000
O	-0.010387000	-2.437959000	-2.290445000
O	3.179525000	-0.375569000	0.000000000
O	-3.206203000	-0.385235000	0.000000000
C	-0.011434000	-1.640274000	1.439555000
C	2.023409000	-0.311445000	0.000000000
C	-2.049274000	-0.325285000	0.000000000
C	-0.011434000	-1.640274000	-1.439555000
B	0.320107000	3.229180000	0.000000000
H	-1.191696000	2.225105000	2.166779000
H	-1.191696000	2.225105000	-2.166779000
H	0.894123000	2.092442000	2.527170000
H	0.894123000	2.092442000	-2.527170000
H	1.498263000	3.491180000	0.000000000
H	-0.396984000	4.196575000	0.000000000

$[W(CO)_4AsH_2\text{-}BH_2\text{-}AsH_2]^-$

Atom	x	y	z
W	0.000001000	0.642946000	0.000000000
As	-0.000001000	-1.605875000	1.528806000
As	-0.000001000	-1.605875000	-1.528806000
O	-0.000002000	2.815333000	2.268878000
O	-0.000002000	2.815333000	-2.268878000
O	-3.193384000	0.725260000	0.000000000
O	3.193386000	0.725256000	0.000000000
C	-0.000001000	2.008612000	1.426648000
C	-2.036848000	0.669950000	0.000000000
C	2.036850000	0.669948000	0.000000000
C	-0.000001000	2.008612000	-1.426648000
B	-0.000001000	-3.077676000	0.000000000
H	1.127610000	-1.887282000	2.508005000
H	1.127610000	-1.887282000	-2.508005000
H	-1.127614000	-1.887279000	2.508003000
H	-1.127614000	-1.887279000	-2.508003000
H	-1.014016000	-3.722484000	0.000000000
H	1.014014000	-3.722484000	0.000000000

$[PH_2\text{-}BH_2\text{-}PH_2]^-$

Atom	x	y	z
P	0.000000000	1.728910000	-0.113009000
B	0.000000000	0.000000000	0.898310000
H	-1.037403000	1.501063000	-1.073712000
H	1.037403000	1.501063000	-1.073712000

P	0.000000000	-1.728910000	-0.113009000
H	-0.997163000	0.000000000	1.596780000
H	0.997163000	0.000000000	1.596780000
H	1.037403000	-1.501063000	-1.073712000
H	-1.037403000	-1.501063000	-1.073712000

$[AsH_2\text{-}BH_2\text{-}AsH_2]^-$

Atom	x	y	z
As	0.000000000	1.825760000	-0.061694000
B	0.000000000	0.000000000	1.009344000
H	-1.101438000	1.537578000	-1.091126000
H	1.101438000	1.537578000	-1.091126000
As	0.000000000	-1.825760000	-0.061694000
H	-1.001989000	0.000000000	1.694809000
H	1.001989000	0.000000000	1.694809000
H	1.101438000	-1.537578000	-1.091126000
H	-1.101438000	-1.537578000	-1.091126000

$[(CO)_4W(PH_2\text{-}BH_2\text{-}PH_2)_2W(CO)_4]^{2-}$

Atom	x	y	z
H	-0.323871000	3.187396000	-1.492539000
B	-0.036489000	2.056964000	-1.173453000
H	-0.146041000	1.273806000	-2.076881000
P	-1.272846000	1.530717000	0.301223000
H	-1.591705000	2.761516000	0.933751000
H	-0.450765000	1.060069000	1.358109000
W	-3.410847000	0.022262000	0.056015000
C	-4.989503000	-1.150962000	-0.119166000
P	-1.862987000	-2.013594000	-0.588005000
C	-4.581133000	1.543176000	0.526081000
C	-3.560075000	0.498757000	-1.926301000
C	-3.254073000	-0.479887000	2.018972000
P	1.862987000	2.013593000	-0.588001000
H	2.507467000	2.756973000	-1.613797000
W	3.410847000	-0.022262000	0.056015000
H	1.961811000	3.031110000	0.401292000
B	0.036486000	-2.056973000	-1.173471000
H	-2.507479000	-2.756978000	-1.613790000
H	-1.961800000	-3.031104000	0.401296000
H	0.146039000	-1.273818000	-2.076901000
H	0.323861000	-3.187408000	-1.492553000
P	1.272848000	-1.530726000	0.301203000
H	1.591719000	-2.761527000	0.933721000
H	0.450766000	-1.060094000	1.358096000
C	4.581117000	-1.543191000	0.526078000
C	4.989514000	1.150954000	-0.119146000
C	3.254062000	0.479886000	2.018972000
C	3.560088000	-0.498733000	-1.926307000
O	3.198048000	0.769297000	3.140855000

O	3.708509000	-0.756873000	-3.044218000
O	5.290183000	-2.430362000	0.807636000
O	5.936400000	1.833124000	-0.214689000
O	-3.708493000	0.756926000	-3.044206000
O	-5.936383000	-1.833138000	-0.214718000
O	-5.290202000	2.430348000	0.807631000
O	-3.198061000	-0.769289000	3.140857000

$[(CO)_4W(AsH_2\text{-}BH_2\text{-}AsH_2)_2W(CO)_4]^{2-}$ (6)

Atom	x	y	z
H	0.241144000	3.289259000	1.527646000
B	-0.006129000	2.152134000	1.217569000
H	0.103757000	1.359213000	2.109685000
As	1.343666000	1.618801000	-0.310347000
H	1.666750000	2.951182000	-0.969463000
H	0.485558000	1.131880000	-1.467056000
W	3.589013000	0.084792000	-0.081791000
C	5.179783000	-1.065406000	0.071685000
As	1.992705000	-2.047513000	0.540542000
C	4.735098000	1.625903000	-0.520160000
C	3.730497000	0.529352000	1.906330000
C	3.438144000	-0.380847000	-2.055884000
As	-1.992686000	2.047516000	0.540540000
H	-2.714798000	2.900542000	1.575904000
W	-3.589009000	-0.084768000	-0.081791000
H	-2.065023000	3.103779000	-0.554902000
B	0.006144000	-2.152289000	1.217553000
H	2.714832000	-2.900521000	1.575911000
H	2.065101000	-3.103765000	-0.554906000
H	-0.103790000	-1.359487000	2.109769000
H	-0.241048000	-3.289471000	1.527487000
As	-1.343703000	-1.618873000	-0.310304000
H	-1.666915000	-2.951257000	-0.969351000
H	-0.485618000	-1.132065000	-1.467077000
C	-4.735106000	-1.625877000	-0.520134000
C	-5.179769000	1.065448000	0.071618000
C	-3.438098000	0.380815000	-2.055893000
C	-3.730528000	-0.529257000	1.906342000
O	-3.388788000	0.646733000	-3.182865000
O	-3.874310000	-0.775229000	3.027915000
O	-5.433001000	-2.527152000	-0.783169000
O	-6.137074000	1.733686000	0.154842000
O	3.874260000	0.775367000	3.027895000
O	6.137089000	-1.733637000	0.154949000
O	5.432987000	2.527177000	-0.783211000
O	3.388858000	-0.646797000	-3.182849000

4.5.7 References

[1] C. Marquardt, T. Kahoun, A. Stauber, G. Balázs, M. Bodensteiner ,A. Y. Timoshkin, M. Scheer, *Angew. Chem. Int. Ed.* **2016,** *55*, 14828-14832; *Angew.Chem.* **2016**, *128*, 15048-15052.

[2] R. B. King, A. Fronzaglia, *Inorg. Chem.* **1966**, *5*, 1837-1846; E. Subasi, S. Karahan, A. Ercag, *Russ. J. Coord. Chem+.* **2007**, *33*, 886-890.

[3] W. A. Herrmann, G. Brauer, *Synthetic Methods of Organometallic and Inorganic Chemistry, Vol. 3,* **1996***,* Thieme Publishers, Stuttgart.

[4] A. Tzschach, W. Deylig, *Z. Anorg. Allg. Chem.* **1965**, *336*, 36-41.

[5] C. Marquardt, T. Jurca, K.-C. Schwan, A. Stauber, A. V. Virovets, G. R. Whittell, I. Manners, M. Scheer, *Angew. Chem. Int. Ed.* **2015**, *54*, 13782-13786; *Angew. Chem.* **2015***, 127,* 13986-13991.

[6] CrysAlisPro Software System, Rigaku Oxford Diffraction, (**2017**).

[7] A. Altomare, M. C.Burla, M. Camalli, G. L. Cascarano, C. Giacovazzo, A. Guagliardi, A.G. G. Moliterni, G. Polidori, R. Spagna, *J. Appl. Cryst.* **1999**, *32*, 115-119.

[8] G. M. Sheldrick, ShelXT-Integrated space-group and crystal-structure determination, *Acta Cryst.* **2015**, *A71*, 3-8.

[9] O. V. Dolomanov and L. J. Bourhis and R. J. Gildea and J. A. K. Howard and H. Puschmann, Olex2: A complete structure solution, refinement and analysis program, *J. Appl. Cryst*. **2009**, *42*, 339-341.

[10] G. M. Sheldrick, Crystal structure refinement with ShelXL, *Acta Cryst.* **2015**, *C71*, 3-8.

[11] M. J. Frisch, G. W. Trucks, H. B. Schlegel, G. E. Scuseria, M. A. Robb, J. R. Cheeseman, G. Scalmani, V. Barone, B. Mennucci, G. A. Petersson, H. Nakatsuji, M. Caricato, X. Li, H. P. Hratchian, A. F. Izmaylov, J. Bloino, G. Zheng, J. L. Sonnenberg, M. Hada, M. Ehara, K. Toyota, R. Fukuda, J. Hasegawa, M. Ishida, T. Nakajima, Y. Honda, O. Kitao, H. Nakai, T. Vreven, J. A. Montgomery, Jr., J. E. Peralta, F. Ogliaro, M. Bearpark, J. J. Heyd, E. Brothers, K. N. Kudin, V. N. Staroverov, T. Keith, R. Kobayashi, J. Normand, K. Raghavachari, A. Rendell, J. C. Burant, S. S. Iyengar, J. Tomasi, M. Cossi, N. Rega, J. M. Millam, M. Klene, J. E. Knox, J. B. Cross, V. Bakken, C. Adamo, J. Jaramillo, R. Gomperts, R. E. Stratmann, O. Yazyev, A. J. Austin, R. Cammi, C. Pomelli, J. W. Ochterski, R. L. Martin, K. Morokuma, V. G. Zakrzewski, G. A. Voth, P. Salvador, J. J. Dannenberg, S. Dapprich, A. D. Daniels, O. Farkas, J. B. Foresman, J. V. Ortiz, J. Cioslowski, D. J. Fox, Gaussian 09, Revision E.01, Gaussian, Inc., Wallingford CT, **2013**.

[12] a) A. D. Becke, *J. Chem. Phys.* **1993**, *98*, 5648. b) C. Lee, W. Yang, R.G. Parr, *Phys. Rev. B.* **1988**, *37*, 785.

[13] (a) L. E. Roy, P.J. Hay, R. L. Martin, *J. Chem. Theory Comput.* **2008**, *4*, 1029; (b) A. W. Ehlers, M. Bohme, S. Dapprich, A. Gobbi, A. Hollwarth, V. Jonas, K. F. Kohler, R. Stegmann, A. Veldkamp, G. Frenking, *Chem. Phys. Lett.* **1993**, *208*, 111; (c) P. J. Hay, W. R. Wadt, *J. Chem. Phys.* **1985**, *82*, 299.

[14] (a) D. Feller, *J. Comp. Chem.* **1996**, *17*, 1571-1586; (b) K. L. Schuchardt, B. T. Didier, T. Elsethagen, L. Sun, V. Gurumoorthi, J. Chase, J. Li, T. L. Windus, *J. Chem. Inf. Model.* **2007**, *47*, 1045-1052.

Preface

The following chapter has been compiled for future publication.

Authors

Tobias Kahoun, Christian Marquardt, Michael Bodensteiner, Alexey Y. Timoshkin, A. V. Virovets, Manfred Scheer.

Author contributions

The synthesis and characterization of compounds **4**, **5**, **6**, **8**, **9**, **10**, **11**, **12** were performed by Tobias Kahoun.

The synthesis and characterization of compounds **3**, **7** were performed by Dr. Christian Marquardt. Both compounds have been reported in his PhD-thesis (Regensburg, **2015**).

X-ray structural analyses of **4**$(thf)_2$, **6**$(thf)_2$, **7**$(thf)_2$, **9**, **11**$(thf)_2$, **12**$(thf)_2$ were performed by Tobias Kahoun and Dr. Michael Bodensteiner.

X-ray structural analyses of **3**$(thf)_2$, **7**$(thf)_2$ were performed by Dr. Christian Marquardt and Dr. Alexander V. Virovets. Both compounds have been reported in his PhD-thesis (Regensburg, **2015**).

The manuscript (including supporting information, figures, schemes and graphical abstract) was written by Tobias Kahoun with contributions by Dr. Christian Marquardt (introduction and supporting information).

5 Substituted Anionic Derivatives of Parent Pnictogenylboranes

Tobias Kahoun, Christian Marquardt, Michael Bodensteiner, Alexey Y. Timoshkin, A. V. Virovets, Manfred Scheer.

Abstract: We report on the synthesis and characterization of three membered organosubstituted anionic pnictogenylborane derivatives. Reactions of pnictogenylboranes of the type H_2E-BH_2-NMe_3 (**2a**: E = P, **2b**: E = As) with pnictogen based nucleophiles of the type $ME'H_2$ (E' = P, As) lead to the formation of anionic compounds of the type $M[H_2E$-BH_2-$E'H_2]$ (E = E' = P, M = Na; E = E' = As, M = K; E = P, E' = As, M = Na). Using organosubstituted pnictogen based nucleophiles of the type MER^1R^2 (E = P, As; R^1 = H, R^2 = ^{t}Bu; R^1 = R^2 = Ph) pnictogenylboranes H_2E-BH_2-NMe_3 (**2a**: E = P, **2b**: E = As), with subsequent addition of 18-crown-6 ($C_{12}H_{24}O_6$) results in the asymmetric compounds $[M(C_{12}H_{24}O_6)][H_2E$-$BH_2$-$ER^1R^2]$ (**3**: E = P; R^1 = H, R^2 = ^{t}Bu, M = Na; **4**: E = As; R^1 = H, R^2 = ^{t}Bu, M = Na; **7**: E = P; R^1 = R^2 = Ph, M = Na; **8**: E = As; R^1 = R^2 = Ph, M = K), containing either exclusively phosphorus or arsenic. The corresponding group 15 element mixed derivatives of the type $[M(C_{12}H_{24}O_6)][H_2E'$-$BH_2$-$ER^1R^2]$ (**5**: E = As, E' = P; R^1 = H, R^2 = ^{t}Bu, M = Na; **9**: E = P, E' = As; R^1 = R^2 = Ph, M = Na; **10**: E = As, E' = P; R^1 = R^2 = Ph, M = K) can be obtained by reaction of the appropriate Lewis base stabilized pnictogenylboranes with substituted nucleophiles. Due to side reactions and decomposition of the starting material during the reaction, $[H_2As$-BH_2-^{t}BuPH$]^-$ is only accessible as a BH_3 coordinating derivative in form of $[Na(C_{12}H_{24}O_6)][H_2As$-$BH_2$-^{t}BuPH-$BH_3]$ (**6**). Additionally we report about the synthesis of the diphenyl substituted symmetric compound $[M(C_{12}H_{24}O_6)][Ph_2E$-$BH_2$-$EPh_2]$ (**11**: E = P, M = Na; **12**: E = As, M = K) which can be seen as an inorganic, isostructural and charged analogs of dppm (1,1-Bis(diphenylphosphino)methane) and dpam (1,1-Bis(diphenylarsino)methane). All compounds were characterized by multinuclear NMR spectroscopy, mass spectrometry and IR spectroscopy. Additionally the molecular structure of compounds **3**, **4**, **6**, **7**, **9**, **11** and **12** were determined by X-ray diffraction experiments.

5.1 Introduction

Saturated pnictogen-triel-adducts as inorganic ethane analogs are used as starting material for versatile chemistry. Beside investigations as hydrogen storage materials[1] they reveal to be suitable precursors for catenation. Corresponding oligomers and polymers, containing a group 13/15 backbone, are mainly obtained from saturated group 13/15 adducts of the type H_3B-ER_2H (E = N, P; R = H, alkyl, aryl) undergoing a metal catalyzed dehydrocoupling reaction.[2,3] The demand of catalytical agents can be avoided by using Lewis base (LB) stabilized phosphanylboranes of the type RR'P-BH_2-LB (R = alkyl, aryl) instead of saturated group 13/15 adducts.[4] Such Lewis base stabilized pnictogenylborane derivatives are thoroughly investigated by our group. Beside the hydrogen substituted parent compounds H_2E-BH_2-NMe_3 (E = P (**2a**), As (**2b**), Sb) organosubstituted analogs are also accessible.[4,5,6] Beside serving as substrate for polymerization these compounds reveal to be excellent building blocks for controlled oligomerization. Recently we reported about the synthesis of dimeric pnictogenboranes bearing a H_2P-BH_2-EH_2-BH_2 unit (E = P, As).[7] Focusing on cationic 13/15 oligomers *Miller* and *Muetterties* reported on the synthesis of species containing a E-B-E backbone (**I**).[8] Using Lewis base stabilized pnicrogenylboranes our working group was able to report about similar compounds of the type $[Me_3N$-BH_2-$(ER^1R^2$-$BH_2)_n$-$NMe_3]^+$ (**II**) revealing an elongated 13/15 unit.[5b,9]

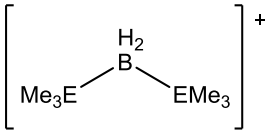

I

E = N, P, As

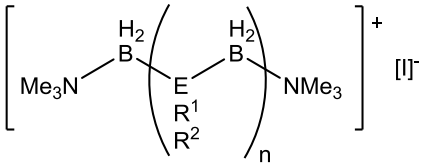

II

E = P, As
R^1 = H, R^2 = ^{t}Bu
R^1 = R^2 = H, Ph
n = 1, 2

Those compounds show a high thermodynamic stability and especially $[Me_3N$-BH_2-AsR^1R^2-BH_2-AsR^1R^2-BH_2-$NMe_3]^+$ (R^1 = R^2 = H, Ph) are unique as they represent the longest linear arsenic boron containing oligomers so far. Anionic compounds with terminal phosphine groups are less investigated. Most of the known examples are represented by branched examples (type **III**[10] and **IV**[11]) whereas our group was able to report the synthesis of linear hydrogen substituted anionic chain like compounds (**V** and **VI**)[12].

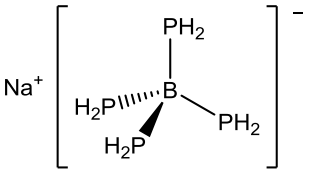

III

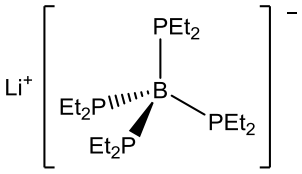

IV

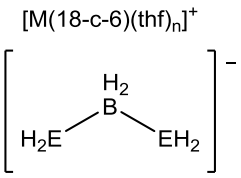

V

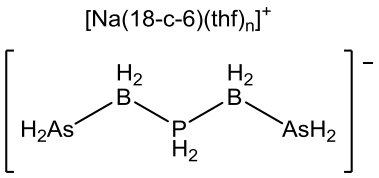

VI

V: E = P, M = Na, n = 2
E = As, M = K, n = 0

Comparable organosubstituted compounds with terminal BH_3 groups (V**II**[13] and V**III**[14]) are accessible by deprotonation of the corresponding phosphane borane adduct and subsequent coordination of one equivalent of BH_3.

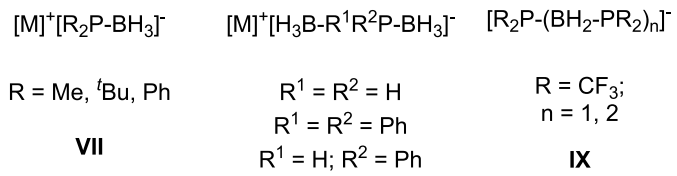

Substituted anionic oligomers with terminal phosphine groups are unknown, except to few examples of the type $[(R_2P(BH_2\text{-}PR_2)_n]^-$ (**IX**) reported by *Burg*.[15] Purification of the obtained products prove challenging as they were only accessible as mixtures and were characterized exclusively by NMR spectroscopy. Additionally to the linear anionic parent compounds (**V**) our group was recently able to report about the synthesis of symmetric compounds with terminal, *tert*-butyl substituted phosphine and arsine groups.[12,6] Therefore, we investigated if the synthetic approach can be expanded to asymmetric organosubsituted derivatives. Here we report about the synthesis and characterisation of the corresponding compounds bearing one hydrogen substituted and one organosubstituted terminal phosphine and arsine group, respectively. Further a synthetic route to inorganic, anionic dppm (1,1-Bis(diphenylphosphino)methane) and dpam (1,1-Bis(diphenylarsino)methane) analogs is presented here.

5.2 Results and Discussion

By reacting pnictogenylborans with hydrogen substituted phosphanides and arsenides, the parent anionic chain like compounds $[H_2E\text{-}BH_2\text{-}EH_2]^-$ (E = P, As) can be obtained.[12] By switching to organosubstituted pnictogenides the corresponding derivatives are accessible. Here it is possible to synthesize asymmetric (**A**, **B**, **C**) and symmetric (**D**) compounds depending on the used Lewis base stabilized pnictogenylborane and pnictogenides (Scheme 5.1). For isolation and crystallization of the compounds the addition of stoichiometric equivalents of 18-crown-6 (X1 = $C_{12}H_{24}O_6$; **3**, **4**, **5**, **6**, **7**, **11**, **12**) or [2.2.2]cryptand (X2 = $C_{18}H_{36}N_2O_6$; **8**, **9**, **10**) to the reaction solutions is inevitable.

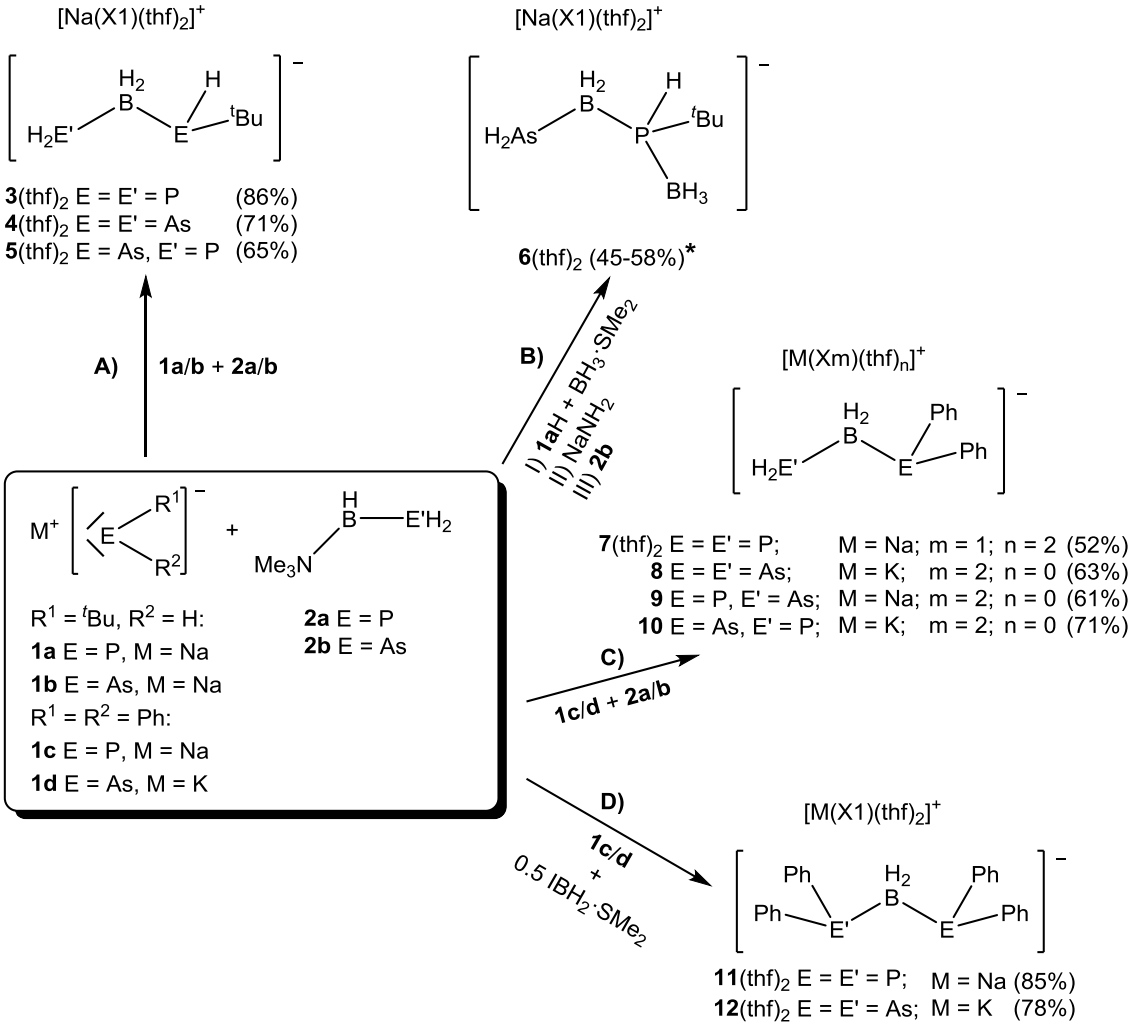

Scheme 5.1. Synthesis of asymmetric (**A** - **C**) and symmetric (**D**) anionic chain like compounds; * variable content of THF. Yields are given in parentheses. X1 = 18-crown-6 ($C_{12}H_{24}O_6$); X2 = [2.2.2]cryptand ($C_{18}H_{36}N_2O_6$).

Sonication of Na^{t}BuPH (**1a**) with $H_2P\text{-}BH_2\text{-}NMe_3$ (**2a**) leads to the formation of the corresponding product $Na[H_2P\text{-}BH_2\text{-}^t\text{BuPH}]$. After addition of equivalent amounts of 18-crown-6 $[Na(C_{12}H_{24}O_6)][H_2P\text{-}BH_2\text{-}^t\text{BuPH}]$ (**3**, Scheme 5.1) can be isolated. The analog arsenic based compound

$[Na(C_{12}H_{24}O_6)][H_2As\text{-}BH_2\text{-}^tBuAsH]$ (**4**, Scheme 5.1) as well as $[Na(C_{12}H_{24}O_6)][H_2P\text{-}BH_2\text{-}^tBuAsH]$ (**5**, Scheme 5.1) are accessible by reaction of **1b** with **2b** and **2a** at room temperature, respectively.

The apparently simple reaction of Na^tBuPH (**1a**) with $H_2As\text{-}BH_2\text{-}NMe_3$ (**2b**) does not lead to the desired product $Na[H_2As\text{-}BH_2\text{-}^tBuPH]$. Instead the formation of $^tBuPH_2$ and decomposition of $H_2As\text{-}BH_2\text{-}NMe_3$ (**2b**) has been observed. Reaction of the nucleophile $Na[^tBuPH\text{-}BH_3]$ with $H_2As\text{-}BH_2\text{-}NMe_3$ (**2b**) results in the formation of the desired product $Na[H_2As\text{-}BH_2\text{-}^tBuPH\text{-}BH_3]$ which is isolated as compound **6** (**B**, Scheme 5.1) after addition of equivalent amounts of 18-crown-6. The nucleophile $Na[^tBuPH\text{-}BH_3]$ is accessible by coordination of BH_3 towards $^tBuPH_2$ (**1a**) using $BH_3\text{-}SMe_2$ and subsequent metalation with $NaNH_2$ (**B**, Scheme 5.1).[16]

The described synthetic procedure of so far presented anionic chain like compounds is similar for diphenyl substituted derivatives (**C**, Scheme 5.1). To obtain $[Na(C_{12}H_{24}O_6)][H_2P\text{-}BH_2\text{-}PPh_2]$, a solution of $H_2P\text{-}BH_2\text{-}NMe_3$ (**2a**) is sonicated with $NaPPh_2$ (**1c**). Addition of 18-crown-6 to the reaction solution leads to formation of $[Na(C_{12}H_{24}O_6)][H_2P\text{-}BH_2\text{-}PPh_2]$ (**7**, Scheme 5.1). The arsenic based analog compound $[K(C_{18}H_{36}N_2O_6)][H_2As\text{-}BH_2\text{-}AsPh_2]$ (**8**, Scheme 5.1) as well as the phosphorus and arsenic mixed compound $[K(C_{18}H_{36}N_2O_6)][H_2P\text{-}BH_2\text{-}AsPh_2]$ (**10**, Scheme 5.1) are only accessible by reaction of the corresponding starting meterials (**8**: **2b** + **1d**; **10**: **2a** + **1d**) at 60 C° (**8**) and 70 °C (**10**), respectively. For the synthesis of compounds $[Na(C_{18}H_{36}N_2O_6)][H_2As\text{-}BH_2\text{-}PPh_2]$ (**9**, Scheme 5.1) the addition of $NaPPh_2$ (**1c**) to $H_2As\text{-}BH_2\text{-}NMe_3$ (**2b**) at room temperature is sufficient. Adding 18-crown-6 instead of [2.2.2]cryptand to reaction solutions of compound **8**-**10** results in oily products.

After the addition of diphenyl-pnictogenylboranes $Ph_2E\text{-}BH_2\text{-}NMe_3$ (E = P, As) to diphenyl substituted pnictogen based nucleophiles $MEPh_2$ (**1c**, E = P, M = Na; **1d**, E = As, M = K) no reaction has been observed, despite various reaction conditions have been tested. Adding **1c** and **1d** to a solution of $IBH_2\text{-}SMe_2$ in a 2:1 stoichiometry at -80 °C and allowing to reach room temperature leads to the expected product $Na[Ph_2P\text{-}BH_2\text{-}PPh_2]$ and $K[Ph_2As\text{-}BH_2\text{-}AsPh_2]$, respectively (**D**, Scheme 5.1). Addition of equivalent amounts of 18-crown-6 to the reaction solutions results in formation of the compounds **11** and **12**.

According to heteronuclear NMR spectroscopy of the crude reaction solutions, compounds **4, 8**, **9**, **10** and **12** are accessible without the formation of side products. For compound **6** the additional formation of the anionic species $[H_3B\text{-}^tBuPH\text{-}BH_3]^-$ can be observed. During the synthesis of compounds **5** and **11** signals related to minor inpurities that are not further determind can be detected. Samples of the purified and isolated compounds **3**-**12** are investigated by heteronuclear NMR spectroscopy. In the ^{31}P NMR spectra of the *tert*-butyl substituted compounds **3** and **5** the signals related to the PH_2 groups are slightly high field shifted compared to the parent compound $[H_2P\text{-}BH_2\text{-}PH_2]^-$. This shift is even stronger for the diphenyl substituted compounds **7** and **10**. In the ^{11}B NMR spectra an analog trend can

be observed for the signals of the BH_2 groups compared to the parent compounds $[H_2E\text{-}BH_2\text{-}EH_2]^-$ (E = P, As). While the *tert*-butyl substituted derivatives **3**, **4** and **5** reveal only a slight shift to the lower field, the diphenyl substituted derivatives **7**, **8**, **9** and **10** again show a significantly greater shift to the higher field.[12] For compound **6** the shift is reversed to the observed trend, here the signal of the BH_2 group occurs at -36.6 ppm (Table 5.1).

Table 5.1. NMR parameters of compounds **3** - **12** and $[H_2E\text{-}BH_2\text{-}EH_2]^-$ (E = P, As)[12].

Compound	$\delta(^{31}P)$ P^aH_2 [ppm]	$\delta(^{31}P)$ $P^bR^1R^2$ [ppm]	$^1J_{P,H}$ $^a/^b$ [Hz]	$\delta(^{11}B)$ B^aH_2 [ppm]	$\delta(^{11}B)$ B^bH_3 [ppm]	$^1J_{B,H}$ $^a/^b$ [Hz]	$^1J_{B,P}$ $^a/^b$ [Hz]
$[H_2P\text{-}BH_2\text{-}PH_2]^-$	-175.0	-	172.0	-34.7	-	99	26
$[H_2As\text{-}BH_2\text{-}AsH_2]^-$	-	-	-	-34.5	-	106	-
3	-188.8	-32.9	173 / 177	-33.8	-	97 / -	27 / -
4	-	-	-	-32.6	-	105 / -	-
5	-189.3	-	174 / -	-32.9	-	100 / -	26 / -
6	-	5.7	- / 302	-36.6	-40.5	102 / 93	69 / 56
7	-203.3	-15.2	173 / -	-29.1	-	98 / -	-
8	-	-	-	-28.0	-	106 / -	-
9	-	-16.7	-	-28.9	-	100 / -	-
10	-202.9	-	174 / -	-28.0	-	99 / -	23 / -
11	-	-27.7	-	-21.1	-	95 / -	-
12	-	-	-	-19.6	-	102 / -	-

For all compounds the $^1J_{B,H}$ coupling constants are similar to the values of the parent compounds $[H_2E\text{-}BH_2\text{-}EH_2]^-$ (E = P, As). Contrary to this the values of the $^1J_{P,H}$ and $^1J_{B,P}$ coupling constants of **6** are increased compared to the other compounds as well as $[H_2E\text{-}BH_2\text{-}EH_2]^-$ (E = P, As) (Table 5.1). This deviation can be explained by the cooridination of the additional BH_3 group.

While the terminal PH_2 groups of compounds **7** and **10** each occur as a broad doublet ($^1J_{H,P}$ = 173 Hz (**7**), 174 Hz (**10**)) in the ^1H NMR spectra, the signals of each PH_2 group belonging to **3** and **5** show two sets of signals in form of broad doublets. This effect is caused by the chiral center located at the *tert*-butyl substituted pnictogen atom in **3** and **5**, indicating two enationmers.[6] A similar effect can be observed for the pnictogen bonded hydrogen atom belonging to the ^{t}BuAsH group in compound **5**. Despite the chirality of compounds **3**-**6** only the signals of the BH_2 groups belonging to compounds **4** and **6** occur as a doublet of signals. The signals of the terminal AsH_2 groups in compounds **4**, **6**, **8** and **9** occur as multiplets in a slightly negative ppm range (-0.16 ppm (**4**), -0.08 ppm (**6**), -0.23 ppm (**8**), -0.26 ppm (**9**)), indicating the hydridic character of the hydrogen atoms.

Crystals of the products can be obtained by storing saturated THF-solution layered with *n*-hexane (**3**, **4**, **5**, **6**), diethyl ether (**8**, **9**, **10**, **11**, **12**) or storing saturated THF/*n*-hexane solutions (**7**) at -28 °C. Single crystals suitable for X-ray diffraction could be obtained for compounds **3**, **4**, **6**, **7**, **9**, **11** and **12**.

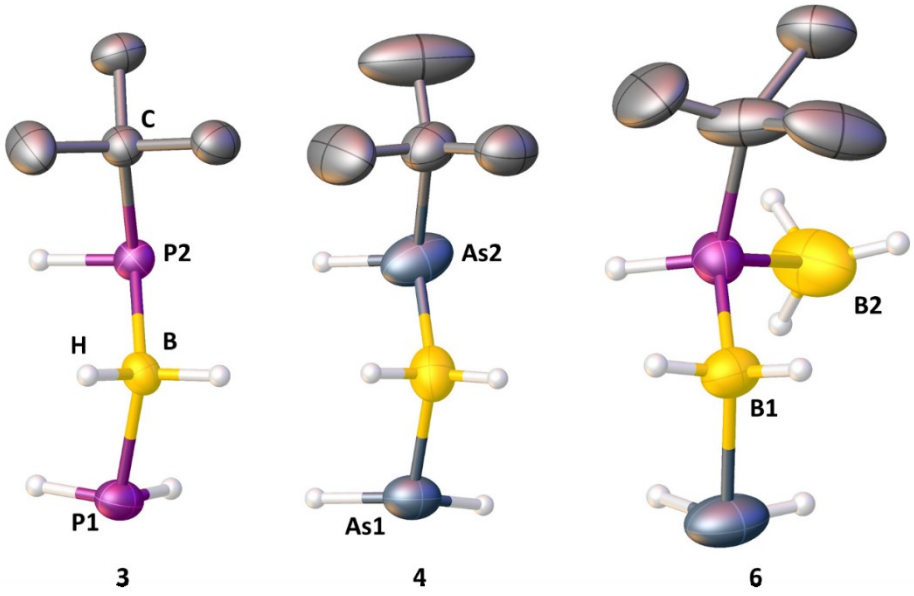

Figure 5.1 Molecular structure of the anions in **3**, **4** and **6**. Hydrogen atoms bond to carbon and cation are omitted for clarity. Thermal ellipsoids are drawn with 50% probability. Selected bond length [Å] and angles [°]: **3**: P1-B 1.975(2) – 1.979(2), P2-B 1.951(3) – 2.037(7), P1-B-P2 107.8(2) – 112.3(1), B1-P2-C1 103.1(3) – 106.9(1); **4:** As1-B 2.022(6) – 2.065(5), As2-B 2.073(6) – 2.122(5), As1-B-As2 105.7(3) – 108.7(2), B1-As2-C1 103.1(2) – 105.0(2); **6:** As-B 2.079(3), P-B 1.917(4) – 1.969(4), P-B2: 1.941(8) – 1.950(8), As-B1-P 108.5(2) – 111.5(2), B1-P-C 108.1(2) – 110.6(2), B1-P-B2 115.5(4) – 117.8(4).

Compounds **3**, **4** and **6** crystalize in the centrosymmetric space group $P\bar{1}$. The solid state structures of **3**, **4** and **6** show disorder revealing two enantiomers. A ratio of 60:40 can be determined for the two enantiomers *R*:*S* in case of **3** and **4**. For **6** a ratio of 51:49 can be determined.

Table 5.2. Selected bond lengths and angles of compound **3**, **4**, **6**. For convenience the corresponding bond lengths and angles in the parent compounds $[H_2E\text{-}BH_2\text{-}EH_2]^-$[12], $Me_3N\text{-}BH_2\text{-}^t BuPH\text{-}BH_3$[17] and $[^t BuEH\text{-}BH_2\text{-}^t BuEH]^-$ (E = P, As)[6] are also given (labeling according to Figure 5.1).

Compound	E1-B1 [Å]	E2-B1 [Å]	E1-B1-E2 [°]	B1-E2-C [°]	E2-B2 [Å]	B1-E2-B2 [°]
$[H_2P\text{-}BH_2\text{-}PH_2]^-$ (E = P)	1.960(3) – 1.963(3)	-	110.4(1)	-	-	-
$[^t BuPH\text{-}BH_2\text{-}^t BuPH]^-$ (E = P)	-	1.943(4) – 1.973(9)	106.8(3) – 109.7(4)	108.1(2) – 108.8(2)	-	-
3 (E = P)	1.975(2) – 1.979(2)	1.951(3) – 2.037(7)	107.8(2) – 112.3(1)	103.1(3) – 106.9(1)	-	-
$BH_3\text{-}^t BuPH\text{-}BH_2\text{-}NMe_3$ (E = P)	-	1.964(2)	-	105.25(8)	1.946(2)	122.61(9)
6 (E = P)	2.079(3)	1.917(4) – 1.969(4)	108.5(2) – 111.5(2)	108.1(2) – 110.6(2)	1.941(8) – 1.950(8)	115.5(4) – 117.8(4)
$[H_2As\text{-}BH_2\text{-}AsH_2]^-$ (E = As)	2.062(2) – 2.126(2)	-	109.47(2) – 110.99(2)	-	-	-
$[^t BuAsH\text{-}BH_2\text{-}^t BuAsH]^-$ (E = As)	-	2.066(4) – 2.100(4)	100.9(2) – 104.6(2)	103.6(1) – 105.0(2)	-	-
4 (E = As)	2.022(6) – 2.065(5)	2.073(6) – 2.122(5)	105.7(3) – 108.7(2)	103.1(2) – 105.0(2)	-	-

Comparing the determined pnictogen boron bond lengths in compound **3**, **4** and **6** with literature known compounds, all values are quite similar. The E1-B1-E2 angle in compound **3**, **4** and **6** are closer to the values of the parent compounds $[H_2E\text{-}BH_2\text{-}EH_2]^-$ than to the acute angles of the substituted derivatives $[^t\text{BuEH-}BH_2\text{-}^t\text{BuEH}]^-$ (E = P, As) (Table 5.2).[12,6]

Due to the synperiplanar arrangement of the two *tert*-butyl groups within the compounds $[^t\text{BuEH-}BH_2\text{-}^t\text{BuEH}]^-$ (E = P, As) a reduction of the E-B-E angle is favored to increase the distance between the sterically demanding substituents. In compound **3**, **4** and **6**, with only one organic substituent, the angle is more relaxed. This effect can also be observed by comparing the values of the B-P-C angle in compound **3** with $[^t\text{BuPH-}BH_2\text{-}^t\text{BuPH}]^-$.[6] In compound **4** the analog angle is almost identical to the one of $[^t\text{BuAsH-}BH_2\text{-}^t\text{BuAsH}]^-$.[6] This can be explained by larger distance between the substituents resulting from the longer pnictogen boron bonds. For **6** the B1-P-B2 angle is slightly reduced compared to the corresponding angle in $Me_3N\text{-}BH_2\text{-}^t\text{BuPH-}BH_3$ (Table 5.2).[17]

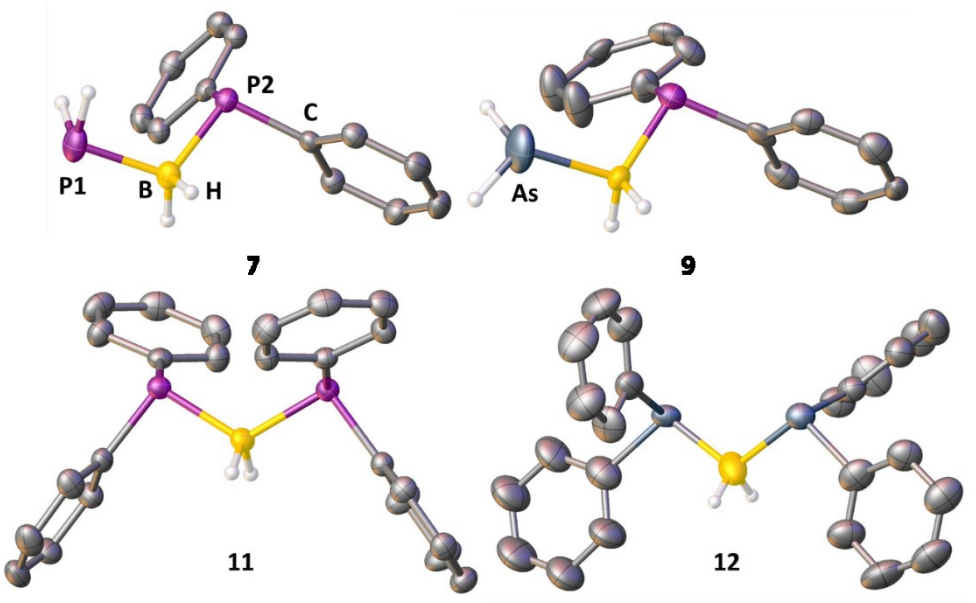

Figure 5.2. Molecular structure of the anions of **7** and **9**. Hydrogen atoms bond to carbon and cation are omitted for clarity. Thermal ellipsoids are drawn with 50% probability. Selected bond length [Å] and angles [°]: **7**: P1-B 1.973(2), P2-B 1.965(2), P1-B-P2 111.36(8); **9**: As-B 2.02(3) – 2.12(3), P-B 1.88(2) – 1.97(1), As-B-P 111.3(5) – 122.0(1); **11**: P-B 1.976(3) – 1.982(3), P-B-P 118.3(1); **12**: As-B 1.928(8) – 2.014(7), As-B-As 114.5(5) – 119.9(5).

While in compound **7** the P1-B bond length is slightly elongated in comparison to the parent compound $[H_2P\text{-}BH_2\text{-}PH_2]^-$, the $AsH_2\text{-}BH_2$ bond in **9** is quite similar to the one in $[H_2As\text{-}BH_2\text{-}AsH_2]^-$.[12] The bond length between the substituted phosphine (PPh_2) and borane groups (BH_2) in compound **7**, **9** and **11** are very close to values known from $Ph_2P\text{-}BH_2\text{-}NMe_3$ and $[H_2P\text{-}BH_2\text{-}PH_2]^-$.[4,12] The $Ph_2As\text{-}BH_2$ bond length in compound **12** is slightly shortened in comparison to $Ph_2As\text{-}BH_2\text{-}NMe_3$ (Table 5.3).[5b]

Table 5.3. Selected bond lengths and angles of compound **7**, **9**, **11**, **12**. For convenience the corresponding bond lengths and angles in the parent compounds $[H_2E\text{-}BH_2\text{-}EH_2]^-$ (E = P, As)[12] and $Ph_2E\text{-}BH_2\text{-}NMe_3$ (E = P[4], As[5b]) are also given (labeling according to Figure 5.2).

Compound	$EH_2\text{-}BH_2$ [Å]	$Ph_2E\text{-}B$ [Å]	E-B-E [°]
$[H_2P\text{-}BH_2\text{-}PH_2]^-$	1.960(3) – 1.963(3)	-	110.4(1)
$Ph_2P\text{-}BH_2\text{-}NMe_3$	-	1.975(2)	112.4(2)
7	1.983(2)	1.965(2)	111.36(8)
9	2.02(3) – 2.12(3)	1.88(2) – 1.97(1)	111.3(5) – 114.5(6)[18]
11	-	1.976(3) – 1.982(3)	118.3(1)
$[H_2As\text{-}BH_2\text{-}AsH_2]^-$	2.062(2) – 2.126(2)	-	109.47(2) – 110.99(2)
$Ph_2As\text{-}BH_2\text{-}NMe_3$	-	2.098(8)	111.2(5)
12	-	1.928(8) – 2.014(7)	114.5(5) – 119.9(5)

The angle between the pnictogen atoms in compound **7** is in between the values of the parent compound $[H_2P\text{-}BH_2\text{-}PH_2]^-$ and $Ph_2P\text{-}BH_2\text{-}NMe_3$.[12,4] The molecular structure of compound **9** reveals an E-B-E angle with values between 111.3(5) - 114.5(6)° which indicates a slightly widening according to $[H_2P\text{-}BH_2\text{-}PH_2]^-$ and the corresponding Lewis base stabilized pnicotgenylborane.[12,4] For compounds **11** and **12** the E-B-E angles are stronger widend than in $[H_2E\text{-}BH_2\text{-}EH_2]^-$ and $Ph_2E\text{-}BH_2\text{-}NMe_3$ (E = P, As) what is owed the sterically demanding phenyl substituents on both pnictogen atoms (Table 5.3).[12,4,5b] In the solid state for all compounds a synclinal arrangement along the $BH_2\text{-}ER^1R^2$-axis can be observed. Additionally an antiperiplanar arrangement along the $EH_2\text{-}BH_2$ axis can be observed for compounds **3**, **4**, **6** and **7**, while the solid state structure of **9** reveals a synclinal conformation instead. Further an antiperiplanar conformation can be observed along the ^{t}BuPH-BH_3-axis of compound **6**.

5.3 Conclusion

Reacting Lewis base stabilized pnictogenylboranes with substituted pnictogenid salts leads to the linear, three membered, anionic chain like compounds in good yields. Depending on the combination of the starting material not only phosphorus or arsenic containing compounds but also derivatives containing both different pnictogen atoms are accessible in an easy way. Offering two coordination sites on both pnictogen atoms the here presented asymmetric compounds **3**, **4**, **5**, **6**, **7**, **8**, **9**, **10** are interesting candidates for coordination chemistry. Additionally the synthesis of the first 1,1-Bis(diphenylphosphino)borate (**11**) and 1,1-Bis(diphenylarsino)borate (**12**) is presented. Compounds **11** and **12** are isostructural to dppm (1,1-Bis(diphenylphosphino)methane) and dpam (1,1-Bis(diphenylarsino)methane). As negatively charged inorganic analogs of these established ligands compounds **11** and **12** are promising alternatives offering different properties. The coordination behavior of these compounds is in focus of current investigations.

5.4 References

[1] a) C. W. Hamilton, R. T. Baker, A. Staubitz, I. Manners, *Chem. Soc. Rev.* ***2009,*** *38,* 279-293; b) A. Staubitz, A. P. M. Robertson, I. Manners, *Chem. Rev.* **2010**, *110*, 4079-4124.

[2] a) B. L. Dietrich, K. I. Goldberg, D. M. Heinekey, T. Autrey, J. C. Linehan, *Inorg. Chem.* **2008**, *47*, 8583-8585; b) R. Dallanegra, A. P. M. Robertson, A. B. Chaplin, I. Manners, A. S. Weller, *Chem. Commun.* **2011**, *47*, 3763-3765; c) A. Staubitz, M. E. Sloan, A. P. M. Robertson, A. Friedrich, S. Schneider, P. J. Gates, J. S. a. d. Günne, I. Manners, *J. Am. Chem. Soc.* **2010**, *132*, 13332-13345; d) A. Staubitz, A. P. M. Robertson, M. E. Sloan, I. Manners, *Chem. Rev.* **2010**, *110*, 4023 – 4078; e) V. Pons, R. T. Baker, *Angew. Chem. Int. Ed.* **2008**, *47*, 9600-9602; f) H. Dorn, J. M. Rodezno, B. Brunnhöfer, E. Rivard, J. A. Massey, I. Manners, *Macromolecules*, **2003**, *36*, 291-297; g) H. Dorn, R. A. Singh, J. A. Massey, A. J. Lough, I. Manners, *Angew. Chem. Int. Ed.* **1999**, *22*, 3321-3323; *Angew. Chem.* **1990**, *111*, 3540-3543.

[3] a) H. Dorn, R. A. Singh, J.A. Massey, A. J. Lough, I. Manners, *Angew. Chem. Int. Ed.* **1999**, *38*, 3321-3323; b) T. Oshiki, T. Imamoto, *Bull. Chem. Soc. Jpn.* **1990**, *63*, 2846-2849.

[4] C. Marquardt, T. Jurca, K.-C. Schwan, A. Stauber,A. V. Virovets, G. R. Whittell, I. Manners, M. Scheer, *Angew. Chem. Int. Ed.* **2015**, *54*, 13782-13786; *Angew. Chem.* **2015**, *54*, 13986-13991.

[5] a) C. Marquardt, A. Adolf, A. Stauber, M. Bodensteiner, A. V. Virovets, A. Y. Timoshkin, M. Scheer, *Chem. Eur. J.* **2013**, 19, 11887-11891; b) O. Hegen, A. V. Virovets, A. Y. Timoshkin, M. Scheer, *Chem. Eur. J.* **2018**, *24*, 16521-16525; c) C. Marquardt, O. Hegen, M. Hautmann, G. Balázs, M. Bodensteienr, A. V. Virovets, A. Y. Timoshkin, M. Scheer, *Angew. Chem. Int. Ed.* **2015**, *54*, 13122-13125; *Angew. Chem.* **2015**, *127*, 13315-13318.

[6] See **chapter 4**; compounds ^{t}BuAsH-BH$_2$-NMe$_3$ (**4**), [Na(C$_{12}$H$_{24}$O$_6$)][^{t}BuPH-BH$_2$-^{t}BuPH] (**3c**) and [Na(C$_{12}$H$_{24}$O$_6$)][^{t}BuAsH-BH$_2$-^{t}BuAsH] (**4d**).

[7] O. Hegen, C. Marquardt, A. Y. Timoshkin, M. Scheer, *Angew. Chem. Int. Ed.* **2017**, *56*, 12783-12787; *Angew. Chem.* **2017**, *129*, 12959-12963.

[8] N. E. Miller, E. L. Muetterties, *J. Am. Chem. Soc.* **1964**, *86*, 1033-1038.

[9] a) C. Marquardt, C. Thoms, A. Stauber, G. Balazs, M. Bodensteiner, M. Scheer, *Angew. Chem. Int. Ed.* 2014, 53, 3727-3730; b) C. Marquardt, G. Balázs, J. Baumann, A. V. Virovets, M. Scheer, *Chem. Eur. J.* **2017**, *23*, 11423-11429.

[10] M. Baudler, C. Block, *Z. anorg. allg. Chem.* **1988**, *567*, 7-12.

[11] G. Fritz, F. Pfannerer, *Z. anorg. allg. Chem.* **1970**, *373*, 30-35.

[12] C. Marquardt, T. Kahoun, A. Stauber, G. Balázs, M. Bodensteiner ,A. Y. Timoshkin, M. Scheer, *Angew. Chem. Int. Ed.* **2016,** *55*, 14828-14832; *Angew. Chem.* **2016**, *128*, 15048-15052.

[13] a) F. Dornhaus, M. Bolte, H.-W. Lerner, M. Wagner, *Eur. J. Inorg. Chem.* **2006**, *24*, 5138 – 3147, b) H. C. Miller, E. L. Muetterties, US 2999864, **1961**.

[14] a) R. E. Hester, E. Mayer, *Spectrochim. Acta Mol. and Biomol. Spectrosc.* **1967**, 23, 2218-2220. b) M. R. Anstey, M. T. Corbett, E. H. Majzoub, J. G. Cordaro, *Inorg. Chem.* **2010**, 49, 8197–8199. c) E. Mayer, A. W. Laubengayer, *Monatsh. Chem.* **1970**, 101, 1138-1144. d) F. Dornhaus, M. Bolte, H.-W. Lerner, M. Wagner, *Eur. J. Inorg. Chem.* **2006**, 24, 1777–1785.

[15] A. B. Burg, *Inorg. Chem.* **1978**, *3*, 593-599.

[16] Using a teflon coated stirring bar turns it black and the reaction solution green. A glass coated stirring bar is used instead. As a side product the formation of $Na[H_3B\text{-}^tBuPH\text{-}BH_3]^-$ can be observed.

[17] C. Marquardt, T. Kahoun, J. Baumann, A. Y. Timoshkin, M. Scheer, *Z. Anorg. Allg. Chem.* **2017**, *643*, 1326-1330.

[18] Due to high disorder in the molecular structure of compound **9** the values of the E-B-E angle varies over a large range. The angle with a value of 122.0(1)° is omitted from discussion.

5.5 Experimental Section

5.5.1 Synthetic Procedures

All manipulations were performed under an atmosphere of dry argon/ nitrogen using standard glove-box and Schlenk techniques. All solvents were degassed and purified by standard procedures. The compounds $H_2E\text{-}BH_2\text{-}NMe_3$ (E = P, As)[1], $KAsPh_2$[2], were prepared according to literature procedures. Other chemicals were obtained from STREM Chemicals, INC. (PPh_2H). $NaPPh_2$ was firstly synthesised in 2015 without further characterisation.[3]

The NMR spectra were recorded on either an Avance 400 spectrometer (**3**, **4**, **5**, **6**, **7**, **8**, **9**, **10**, **11**, **12**) (^{1}H: 400.13 MHz, ^{31}P: 161.976 MHz, ^{11}B: 128.378 MHz, ^{13}C{^{1}H}: 100.623 MHz) with δ [ppm] referenced to external $SiMe_4$ (^{1}H, ^{13}C), H_3PO_4 (^{31}P), $BF_3{\cdot}Et_2O$ (^{11}B) or an **Avance III HD 600** spectrometer (**4**) (^{1}H: 600.13 MHz).

IR spectra were recorded either on a DIGILAB (FTS 800) FT-IR spectrometer (**3**, **5**, **6**, **7**, **8**) or a Thermo Scientific (NICOLET iS 5, iD1 Transmission) FT-IR spectrometer (**4**, **9**, **10**, **11**, **12**) with $\tilde{\nu}$ [cm^{-1}]. Mass spectra were recorded either on a ThermoQuest Finnigan TSQ 7000 (**3**, **7**; Mass-Spectrometry-Department, University of Regensburg) or a Waters/Micromass LCT-TOF classic (**4**, **5**, **6**, **8**, **9**, **10**, **11**, **12**; Mass Spectrometer in Working group) (ESI-MS).

The C, H, N analyses were measured on an Elementar Vario EL III apparatus (**3**, **4**, **5**, **6**, **7**, **8**, **9**, **10**, **11**, **12**).

General remarks for C, H, N analyses:

C, H, N analyses were carried out repeatedly. Different amounts of coordinating THF have been found in nearly all cases. Total removal of the THF was not always possible, however C, H, N analyses are in good agreement with the expected values considering a varying THF-content (0.5 % tolerance).

Synthesis of $NaPPh_2$ (**1c**): 1.74 mL (1.860 g, 10 mmol) Ph_2PH is added to a suspension of 390 mg (10.00 mmol) $NaNH_2$ in 10 mL THF at -50°C. The solution is stirred for 5 h at room temperature, until all $NaNH_2$ is consumed. A clear red solution is obtained which is degassed three times to remove NH_3. The solution is used as a 1 M stock solution of $NaPPh_2$ in THF.

Yield of [$NaPPh_2$]: (100 %, according to ^{31}P NMR).

^{31}P NMR (C_6D_6, 25 °C): δ = -27.2 (s, PPh_2).

$^{31}P\{^{1}H\}$ NMR (C_6D_6, 25 °C): δ = -27.2 (s, PPh_2).

Synthesis of $[Na(C_{12}H_{24}O_6)(thf)_2][H_2P\text{-}BH_2\text{-}^tBuPH]$ (**3**$(thf)_2$):

A solution of 106 mg (1.00 mmol) $H_2P\text{-}BH_2\text{-}NMe_3$ in 2 mL toluene is added to a solution of 112 mg (1.00 mmol) Na^tBuPH in 20 ml THF. After sonication of the mixture for 2.5 h, the solution is filtrated onto 264 mg (1.00 mmol) solid $C_{12}H_{24}O_6$ (18-crown-6). The solution is layered with 60 mL of *n*-hexane. **3**$(thf)_2$ crystallizes at 4 °C as colourless blocks. The solvent is decanted, the crystals are separated, washed with cold *n*-hexane (0 °C, 3 × 5 mL) and dried *in vacuo*.

Yield of $[Na(C_{12}H_{24}O_6)(thf)_{0.15}][H_2P\text{-}BH_2\text{-}^tBuPH]$ (**3**$(thf)_{0.15}$): 374 mg (86%).

^{1}H NMR (THF-d_8, 25 °C): δ = 0.65 (dm, $^{1}J_{Ha,P}$ = 173 Hz, 1H, PH^aH^b), 0.79 (dm, $^{1}J_{Hb,P}$ = 173 Hz, 1H, PH^aH^b), 1.07 (d, $^{3}J_{H,P}$ = 9 Hz, ^{t}Bu), 1.22 (m, 2H, BH_2), 1.76 (dm, $^{1}J_{H,P}$ = 177 Hz, 1H, ^{t}BuPH), 3.64 (s, 24H, $C_{12}H_{24}O_6$).

^{31}P NMR (THF-d_8, 25 °C): δ = -188.0 (t, br, $^{1}J_{P,H}$ = 173 Hz, PH_2), –32.9 (d, br, $^{1}J_{P,H}$ = 177 Hz, P^{t}BuH).

$^{31}P\{^{1}H\}$ NMR (THF-d_8, 25 °C): δ = -188.8 (m, PH_2), –32.9 (m, P^{t}BuH).

^{11}B NMR (THF-d_8, 25 °C): δ = -33.8 (tt, $^{1}J_{B,P}$ = 27 Hz, $^{1}J_{B,H}$ = 97 Hz, BH_2).

$^{11}B\{^{1}H\}$ NMR (THF-d_8, 25 °C): δ = -33.8 (t, $^{1}J_{B,P}$ = 27 Hz, BH_2).

$^{13}C\{^{1}H\}$ NMR (THF-d_8, 25 °C): δ = 27.2 (dd, $^{1}J_{C,P}$ =15 Hz, $^{3}J_{C,P}$ = 5 Hz, $\underline{C}(CH_3)_3$), 33.8 (d, $^{2}J_{C,P}$ = 10 Hz, CH_3), 70.6 (s, $C_{12}H_{24}O_6$).

IR (KBr): $\tilde{\nu}$ = 2902 (vs, CH), 2316 (s, br, BH), 2240 (s, PH), 1975 (w), 1627 (br, w), 1471 (m), 1464 (m),1353 (s), 1285 (m), 1251 (s), 1109 (vs, CO), 962 (s), 837 (m), 711 (w), 530 (w).

ESI-MS (THF) anion: *m/z* = 135 (48 %, $[H_2P\text{-}BH_2\text{-}^tBuPH]^-$), 181 (100 %,$[PH_2\text{-}BH_2\text{-}H_2P\text{-}BH_2\text{-}^tBuPH]^-$), 227 (15%, $[H^tBuP\text{-}BH_2\text{-}PH_2\text{-}BH_2\text{-}PH_2\text{-}BH_2\text{-}PH_2]^-$).

Elemental analysis (%) calculated for $C_{16}H_{38}BNaO_6P_2(thf)_{0.15}$ (**3**$(thf)_{0.15}$): C: 46.00, H: 9.12; found: C: 46.06, H: 9.02.

Synthesis of $[Na(C_{12}H_{24}O_6)(thf)_2][H_2As\text{-}BH_2\text{-}^tBuAsH]$ (**4**$(thf)_2$):

A solution of 79 mg (0.50 mmol) $H_2As\text{-}BH_2\text{-}NMe_3$ in 1 ml toluene is added to a solution of 78 mg (0.50 mmol) Na^tBuAsH in 5 ml THF at room temperature and stirred for 16 h. The solution is filtrated onto 125 mg (0.47 mmol) solid $C_{12}H_{24}O_6$ (18-crown-6) and layered with 25 ml *n*-hexane. **4**$(thf)_2$

crystallizes at -28 °C as colorless blocks. The solvent is decanted, the crystals are separated, washed with cold *n*-hexane (-30 °C, 3 x 10 ml) and dried *in vacuo*.

Yield of $[Na(C_{12}H_{24}O_6)(thf)_{0.75}][H_2As\text{-}BH_2\text{-}^tBuAsH]$ (**4**$(thf)_{0.75}$): 186 mg (71%).

^{1}H NMR (THF-d_8, 25 °C): δ = -0.16 (m, 2H, AsH_2), 1.16 (m, 1H, ^{t}BuAsH), 1.17 (s, 9H, ^{t}Bu), 1.33 (m, 1H, BH^aH^b), 1.60 (m, 1H, BH^aH^b), 3.64 (s, 24H, $C_{12}H_{24}O_6$).

^{11}B NMR (THF-d_8, 25 °C): δ = -32.6 (t, $^1J_{B,H}$ = 105 Hz, BH_2).

^{11}B{^{1}H} NMR (THF-d_8, 25 °C): δ = -32.6 (s, BH_2).

^{13}C{^{1}H} NMR (THF-d_8, 25 °C): δ = 26.2 (s, $C(CH_3)_3$), 34.6 (s, CH_3), 70.6 (s, $C_{12}H_{24}O_6$).

IR (KBr): $\tilde{\nu}$ = 2901 (vs, CH), 2746 (vw), 2724 (vw), 2692 (vw), 2354 (s, BH), 2045 (s, AsH), 1736 (vw), 1689 (vw), 1608 (w), 1581 (w), 1470 (m), 1454 (m), 1413 (w), 1352 (vs), 1299 (w), 1284 (w), 1249 (m), 1108 (vs, CO), 962 (s), 836 (m), 789 (vw), 770 (vw), 726 (vw), 659 (vw), 589 (vw), 529 (vw), 479 (vw).

ESI-MS (THF) anion: *m/z* = 222.9 (100%, $[H_2As\text{-}BH_2\text{-}^tBuAsH]^-$).

Elemental analysis (%) calculated for $C_{16}H_{38}As_2BNaO_6(thf)_{0.75}$ (**4**$(thf)_{0.75}$): C: 40.44, H: 7.86; found: C: 40.41, H: 7.72.

Synthesis of $[Na(C_{12}H_{24}O_6)(thf)_2][H_2P\text{-}BH_2\text{-}^tBuAsH]$ (**5**$(thf)_2$):

A solution of 52 mg (0.50 mmol) $H_2P\text{-}BH_2\text{-}NMe_3$ in 1 ml toluene is added to a solution of 78 mg (0.50 mmol) Na^{t}BuAsH in 5 ml THF at room temperature and stirred for 16 h. The solution is filtrated onto 127 mg (0.48 mmol) solid $C_{12}H_{24}O_6$ (18-crown-6) and layered with 20 ml of *n*-hexane. **5**$(thf)_2$ crystallizes at -28 °C as colorless blocks. The solvent is decanted, the crystals are separated, washed with cold *n*-hexane (-30 °C, 2 x 10 ml) and dried *in vacuo*.

Yield of $[Na(C_{12}H_{24}O_6)(thf)_{0.2}][H_2P\text{-}BH_2\text{-}^tBuAsH]$ (**5**$(thf)_{0.2}$): 150 mg (65%).

^{1}H NMR (THF-d_8, 25 °C): δ = 0.84 (dm, $^1J_{Ha,P}$ = 174 Hz, 1H, PH^aH^b), 0.93 (dm, $^1J_{Hb,P}$ = 174 Hz, 1H, PH^aH^b), 1.06 (m, 0.5H, AsH^a), 1.15 (m, 0.5H, AsH^b), 1.15 (q, br, $^1J_{H,B}$ = 100 Hz, 2H, BH_2), 1.17 (s, 9H, ^{t}Bu), 3.64 (s, $C_{12}H_{24}O_6$).

^{31}P NMR (THF-d_8, 25 °C): δ = -189.3 (tm, $^1J_{P.H}$ = 174 Hz, PH_2).

^{31}P{^{1}H} NMR (THF-d_8, 25 °C): δ = -189.3 (q, $^1J_{P.B}$ = 26 Hz, PH_2).

^{11}B NMR (THF-d_8, 25 °C): δ = -32.9 (td, $^1J_{B,H}$ = 100 Hz, $^1J_{B,P}$ = 26 Hz, BH_2).

$^{11}B\{^1H\}$ NMR (THF-d_8, 25 °C): δ = -32.9 (d, $^1J_{B,P}$ = 26 Hz, BH_2).

$^{13}C\{^1H\}$ NMR (THF-d_8, 25 °C): δ = 34.1 (s, $\underline{C}(CH_3)_3$), 34.7 (s, CH_3), 70.6 (s, $C_{12}H_{24}O_6$).

ESI-MS (THF) anion: *m/z* = 179.0 (100%, $[H_2P\text{-}BH_2\text{-}^t\text{BuAsH}]^-$), 225.0 (15%, $H_2P\text{-}BH_2\text{-}^t\text{BuAsH-}BH_2\text{-}PH_2]^-$)

Elemental analysis (%) calculated for $C_{16}H_{38}AsBNaO_6P(thf)_{0.2}$ (**5**$(thf)_{0.2}$): C: 41.94, H: 8.30; found: C: 42.09, H: 8.23.

Synthesis of $Na^tBuPH\text{-}BH_3$:

0.1 ml (76 mg, 1.00 mmol) $BH_3\text{-}SMe_2$ are added to a solution of 0.13 ml (90 mg, 1.00 mmol) $^t\text{BuPH}_2$ in 3 ml THF at room temperature and stirred for 16 h. Subsequently 32 mg (1.33 mmol) NaH are added and the suspension is stirred for 16 h. The suspension is filtrated and degassed three times to remove H_2.

Yield of $Na^tBuPH\text{-}BH_3$: (91%, according to ^{31}P NMR).

^{31}P NMR (THF + C_6D_6-cappilary, 25 °C): δ = -58.2 (d, br, $^1J_{P,H}$ = 192 Hz, ^{t}BuPH).

$^{31}P\{^1H\}$ NMR (THF + C_6D_6-cappilary, 25 °C): δ = -58.2 (q, , $^1J_{P,B}$ = 33 Hz, ^{t}BuPH).

^{11}B NMR (THF + C_6D_6-cappilary, 25 °C): δ = -37.8 (qd, $^1J_{B,H}$ = 87 Hz, $^1J_{B.P}$ = 33 Hz, BH_3).

$^{11}B\{^1H\}$ NMR (THF + C_6D_6-cappilary, 25 °C): δ = -37.8 (d, $^1J_{B.P}$ = 33 Hz, BH_3).

Synthesis of $[Na(C_{12}H_{24}O_6)(thf)_2][H_2As\text{-}BH_2\text{-}^t\text{BuPH-}BH_3]$ (**6**$(thf)_2$):

150 mg (1.00 mmol) $H_2As\text{-}BH_2\text{-}NMe_3$ in 1 ml toluene are added to a solution of 115 mg (0.91 mmol) $Na[^t\text{BuPH-}BH_3]$ and stirred for 16 h at room temperature. The solution is filtrated onto 225 mg (0.85 mmol) $C_{12}H_{24}O_6$ and all volatiles are removed *in vacuo*. The residue is dissolved in 4 ml THF and layered with 20 ml of *n*-hexane. **6**$(thf)_2$ cristallizes at -30 °C as colorless blocks. The solvent is decanted, the crystals are separated, washed with cold *n*-hexane (-30 °C, 2 x 5 ml) and dried *in vacuo*. **6**$(thf)_2$ is an oil at room temperature. The formation of $Na[H_3B\text{-}^t\text{BuPH-}BH_3]$ as a side product can be observed.

Yield of $[Na(C_{12}H_{24}O_6)(thf)_n][H_2As\text{-}BH_2\text{-}^t\text{BuPH-}BH_3]$ (**6**$(thf)_n$): 237 mg (58%, n = 0; 45%, n = 2).

^1H NMR (THF-d_8, 25 °C): δ = -0.08 (dm, 2H, AsH_2), 0.35 (q, br, $^1J_{H,B}$ = 93 Hz, 3H, BH_3), 1.02 (q, br, $^1J_{H,B}$ = 102 Hz, 1H, $B\underline{H}^aH^b$),1.08 (d, $^4J_{H,P}$ = 11 Hz, 9H, $^t\underline{Bu}$), 1.21 (q, br, $^1J_{H,B}$ = 102 Hz, 1H, $BH^a\underline{H}^b$), 3.10 (dm, $^1J_{H,P}$ = 302 Hz, 1H, $^t\text{BuP}\underline{H}$), 3.63 (s, 24 H, $C_{12}H_{24}O_6$).

^{31}P NMR (THF-d_8, 25 °C): δ = 5.7 (d, $^1J_{P,H}$ = 302 Hz, ^{t}BuPH).

$^{31}P\{^{1}H\}$ NMR (THF-d_8, 25 °C): δ = 5.7 (m, ^{t}BuPH).

^{11}B NMR (THF-d_8, 25 °C): δ = -40.5 (qd, $^{1}J_{B,P}$ = 56 Hz, $^{1}J_{B,H}$ = 93 Hz, BH_3), -36.6 (td, $^{1}J_{B,P}$ = 69 Hz, $^{1}J_{B,H}$ = 102 Hz, BH_2).

$^{11}B\{^{1}H\}$ NMR (THF-d_8, 25 °C): δ = -40.5 (d, $^{1}J_{B,P}$ = 56 Hz, BH_3), -36.6 (d, $^{1}J_{B,P}$ = 69 Hz, BH_2).

$^{13}C\{^{1}H\}$ NMR (THF-d_8, 25 °C): δ = 27.0 (d, $^{1}J_{C,P}$ = 25 Hz, $\underline{C}(CH_3)_3$), 29.3 (d, $^{2}J_{C,P}$ = 2 Hz, CH_3), 70.6 (s, $C_{12}H_{24}O_6$).

ESI-MS (THF) anion: *m/z* = 179.0 (10%, $[H_2As\text{-}BH_2\text{-}^{t}BuPH]^-$), 193.0 (100 %, $[H_2As\text{-}BH_2\text{-}^{t}BuPH\text{-}BH_3]^-$).

Synthesis of $[Na(C_{12}H_{24}O_6)(thf)_2][H_2P\text{-}BH_2\text{-}PPh_2]$ (**7**$(thf)_2$):

A solution of 106 mg (1.00 mmol) $H_2P\text{-}BH_2\text{-}NMe_3$ in 2 mL toluene is added to a solution of 208 mg (1.00 mmol) $NaPPh_2$ in 20 ml THF. After sonication of the mixture for 2.5 h, the solution is filtrated onto 264 mg (1.00 mmol) solid $C_{12}H_{24}O_6$ (18-crown-6). After removal of all volatiles *in vacuo* **7** is dissolved in 5 mL THF and filtrated again. The solvent is removed *in vacuo* and 20 mL *n*-hexane are added to the white solid. THF is added drop wise until a clear colourless solution is obtained. **7**$(thf)_2$ crystallizes at -28 °C as colourless blocks. The solvent is decanted, the crystals are separated, washed with cold *n*-hexane (0 °C, 3 × 5 mL) and dried *in vacuo*. **7**$(thf)_2$ is a colourless waxy solid/oil at room temperature.

Yield of $[Na(C_{12}H_{24}O_6)(thf)_{1.1}][H_2P\text{-}BH_2\text{-}PPh_2]$ (**7**$(thf)_{1.1}$]): 310 mg (52%).

^{1}H NMR (THF-d_8, 25 °C): δ = 0.71 (d, $^{1}J_{H,P}$ = 173 Hz, 2H, PH_2), 1.50 (q, $^{1}J_{H,B}$ = 100 Hz, 2H, BH_2). 3.56 (s, 24H, $C_{12}H_{24}O_6$), 6.86 (m, 2H, *p*-Ph), 6.97 (m, 4H, *m*-Ph), 7.44 (m, 4H, *o*-Ph).

^{31}P NMR (THF-d_8, 25 °C): δ = -203.3 (t, $^{1}J_{P,H}$ = 173 Hz, PH_2), -15.2 (s, PPh_2).

$^{31}P\{^{1}H\}$ NMR (THF-d_8, 25 °C): δ = -203.3 (s, br, PH_2), -15.2 (s, PPh_2).

^{11}B NMR (THF-d_8, 25 °C): δ = -29.1 (tm, $^{1}J_{B,H}$ = 98 Hz, BH_2).

$^{11}B\{^{1}H\}$ NMR (THF-d_8, 25 °C): δ = -29.1 (s, br, BH_2).

$^{13}C\{^{1}H\}$ NMR (THF-d_8, 25 °C): δ = 70.6 (s, $C_{12}H_{24}O_6$), 124.1 (s, *p*-Ph), 126.8 (d, $^{3}J_{C,P}$ = 5 Hz, *m*-Ph), 134.7 (d, $^{2}J_{C,P}$ = 14 Hz, *o*-Ph), 150.8 (dd, $^{1}J_{C,P}$ = 26 Hz, $^{3}J_{P,C}$ = 4 Hz, *i*-Ph).

IR (film, NaCl):): $\tilde{\nu}$ = 2910 (vs, CH), 2876 (vs, CH), 2320 (s, br, BH), 2267 (s, PH), 1959 (w), 1894 (w), 1821 (vw), 1620 (w), 1579 (m), 1474 (s), 1455 (m), 1431 (m), 1353 (s), 1297 (m), 1250 (m), 1107 (vs, CO), 1027 (m), 957 (s), 835 (m), 741 (m), 700 (s), 591 (m), 542 (w), 507 (w), 417 (w).

ESI-MS (THF) anion: *m/z* = 185 (34%, $[PPh_2]^-$), 231 (100%, $[H_2P\text{-}BH_2\text{-}Ph_2P]^-$), 277 (12 %, $[H_2P\text{-}BH_2\text{-}Ph_2P\text{-}BH_2\text{-}PH_2]^-$).

Elemental analysis (%) calculated for $C_{25}H_{38}BNaO_6P_2(thf)_{1.1}$ (**7**$(thf)_{1.1}$]): C: 57.04, H: 7.89; found: C: 57.11, H: 7.79.

Synthesis of $[K(C_{18}H_{36}N_2O_6)][H_2As\text{-}BH_2\text{-}AsPh_2]$ (**8**)

A solution of 75 mg (0.50 mmol) $H_2As\text{-}BH_2\text{-}NMe_3$ in 1 ml toluene is added to a solution of 156 mg (0.50 mmol) $KAsPh_2(C_4H_8O_2)_{0.625}$ in 5 ml THF and is stirred for 16 h at 60 °C. The reaction liquid is filtrated on 170 mg (0.45 mmol) solid $C_{18}H_{26}N_2O_6$ ([2.2.2]cryptand) and layered with 25 ml of diethyl ether. **8** crystallizes at -28 °C as thinn orange plates. The solvent is decanted, the crystals are separated, washed with cold diethyl ether (-30 °C, 3 x 5 ml) and dried *in vacuo*.

Yield of $[K(C_{18}H_{36}N_2O_6)][H_2As\text{-}BH_2\text{-}AsPh_2]$ (**8**): 233 mg (63%).

^{1}H NMR (THF-d_8, 25 °C): δ = -0.23 (m, 2H, AsH_2), 1.73 (q, br, $^1J_{H,B}$ = 106 Hz, 2H, BH_2), 2.53 (t, $^3J_{H,H}$ = 5 Hz, 12H, CH_2N), 3.52 (t, $^3J_{H,H}$ = 5 Hz, 12H, CH_2O), 3.57 (s, 12H, $(CH_2)_2O$), 6.88 (tm, $^3J_{H,H}$ = 7 Hz, 2H, *p*-Ph), 6.95 (tm, $^3J_{H,H}$ = 7 Hz, 4H, *m*-Ph), 7.53 (dm, $^3J_{H,H}$ = 8 Hz, 4H, *o*-Ph).

^{11}B NMR (THF-d_8, 25 °C): δ = -28.0 (t, $^1J_{B,H}$ = 106 Hz, BH_2).

^{11}B{^{1}H} NMR (THF-d_8, 25 °C): δ = -28.0 (s, BH_2).

^{13}C{^{1}H} NMR (THF-d_8, 25 °C): δ = 54.9 (s, CH_2N), 68.5 (s, CH_2O), 71.3 (s, $(CH_2)_2O$), 124.6 (s, *p*-Ph), 127.1 (s, *m*-Ph), 135.7 (s, *o*-Ph), 151.2 (s, *i*-Ph).

IR (KBr): $\tilde{\nu}$ = 3055 (w), 3043 (w), 2961 (m, CH), 2884 (s, CH), 2815 (m, CH) 2758 (vw), 2739 (vw), 2359 (m, BH), 2332 (m, BH), 2039 (m, AsH), 1652 (vw), 1635 (vw)m 1577 (vw), 1475 (m), 1445 (m), 1354 (s), 1299 (m), 1259 (m), 1242 (vw), 1131 (s), 1104 (vs, CO), 1082 (s), 949 (s), 931 (m), 831 (w), 738 (w), 699 (w), 574 (vw), 526 (vw).

ESI-MS (THF) anion: *m/z* = 318.9 (100%, $[H_2As\text{-}BH_2\text{-}AsPh_2]^-$).

Elemental analysis (%) calculated for $C_{30}H_{50}AsBKN_2O_6P$ (**8**): C: 49.03, H: 6.86, N: 3.81; found: C: 48.97, H: 6.94, N: 4.16.

Synthesis of $[Na(C_{18}H_{36}N_2O_6)][H_2As\text{-}BH_2\text{-}PPh_2]$ (**9**):

A solution of 177 mg (1.0 mmol) $NaPPh_2$ in 1 ml THF is added to a solution of 148 mg (1.0 mmol) $H_2As\text{-}BH_2\text{-}NMe_3$ in 4 ml THF. After stirring for 16 h at room temperature the reaction liquid is filtrated onto 339 mg (0.9 mmol) solid $C_{18}H_{36}N_2O_6$ ([2.2.2]cryptand). The solution is layered with 20 ml *n*-hexane. **9** crystallizes at -30 °C as orange blocks. The solvent is decanted, the crystals are separated, dried *in vacuo* and dissolved in 5 ml THF. The obtained solution is layered with 20 ml diethyl ether. **9** crystallizes at -30 °C as colourless blocks. The solvent is decanted, the crystals are separated, washed with cold diethyl ether (-30 °C, 2 x 10 ml) and dried *in vacuo*.

Yield of $[Na(C_{18}H_{36}N_2O_6)][H_2As\text{-}BH_2\text{-}PPh_2]$ (**9**): 368 mg (61%).

^{1}H NMR (THF-d_8, 25 °C): δ = -0.26 (m, 2H, AsH_2), 1.69 (q, br, $^1J_{H,B}$ = 100 Hz, 2H, BH_2), 2.60 (t, $^3J_{H,H}$ = 5 Hz, 12H, NCH_2), 3.54 (t, $^3J_{H,H}$ = 5 Hz, 12H, OCH_2), 3.57 (s, 12H, $O(CH_2)_2O$), 6.89 (m, 2H, *p*-Ph), 7.00 (m, 4H, *m*-Ph), 7.47 (m, 4H, *o*-Ph).

^{31}P NMR (THF-d_8, 25 °C): δ = -16.7 (s, br, PPh_2).

^{31}P{^{1}H} NMR (THF-d_8, 25 °C): δ = -16.7 (m, PPh_2).

^{11}B NMR (THF-d_8, 25 °C): δ = -28.9 (t, $^1J_{B,H}$ = 100 Hz, BH_2).

^{11}B{^{1}H} NMR (THF-d_8, 25 °C): δ = -28.9 (m, BH_2).

^{13}C{1H} NMR (THF-d_8, 25 °C): δ = 53.7 (s, NCH_2), 68.4 (s, OCH_2) , 69.3 (s, $O(CH_2)_2O$), 124 .3 (s, *p*-Ph), 126.9 (d, $^3J_{C,P}$ = 5 Hz, *m*-Ph), 134.7 (d, $^2J_{C,P}$ = 14 Hz, *o*-Ph), 150.8 (d, $^1J_{C,P}$ = 25 Hz, *i*-Ph).

IR (KBr): $\tilde{\nu}$ = 3058 (w, CH), 2960 (s, CH), 2911 (s, CH), 2863 (s, CH), 2811 (s, CH), 2755 (w, CH), 2733 (w, CH), 2698 (w, CH), 2311 (s, BH), 2221 (w), 2050 (m, AsH), 1945 (vw), 1913 (vw), 1869 (vw), 1818 (vw), 1660 (vw), 1580 (w), 1561 (vw), 1466 (s), 1455 (s), 1438 (m), 1432 (m), 1397 (vw), 1378 (vw), 1355 (s), 1301 (s), 1268 (m), 1235 (w), 1176 (w), 1131 (s), 1100 (vs), 1090 (vs), 1073 (s), 1053 (m), 1036 (s), 1005 (m), 973 (w), 926 (vs), 846 (vw), 819 (s), 745 (m), 730 (m), 699 (s), 659 (w), 583 (w), 563 (m), 532 (vw), 508 (m), 468 (w), 419 (vw).

ESI-MS (THF) anion: *m*/*z* = 275 (100%, $[H_2As\text{-}BH_2\text{-}PPh_2]^-$), 365 (40%, $[H_2As\text{-}BH_2\text{-}PPh_2\text{-}BH_2\text{-}AsH_2]^-$).

Elemental analysis (%) calculated for $C_{30}H_{50}AsBN_2NaO_6P$ (**9**): C: 53.42, H: 7.47, N: 4.15; found: C: 53.40, H: 7.21, N: 4.13.

Synthesis of $[K(C_{18}N_2H_{36}O_6)][H_2P\text{-}BH_2\text{-}AsPh_2]$ (**10**):

A solution of 105 mg (1.00 mmol) $H_2P\text{-}BH_2\text{-}NMe_3$ in 2 ml toluene is added to a solution of 323 mg (1.00 mmol) $KAsPh_2(C_4H_8O_2)_{0.625}$ in 4 ml THF and stirred for 16 h at 70 °C. The reaction liquid is filtrated on 370 mg (0.98 mmol) solid $C_{18}N_2H_{36}O_6$ ([2.2.2]cryptand) and layered with 25 ml diethyl ether. **10** crystallizes at -28 °C as thinn red plates. The solvent is decanted, the crystals are separated, washed with cold diethyl ether (-30 °C, 3 x 5 ml) and dried *in vacuo*.

Yield of $[K(C_{18}N_2H_{36}O_6)][H_2P\text{-}BH_2\text{-}AsPh_2]$ (**10**): 481 mg (71%).

^{1}H NMR (THF-d_8, 25 °C): δ = 0.82 (dm, $^1J_{H,P}$ = 174 Hz, 2H, PH_2), 1.59 (q, br, $^1J_{H,B}$ = 99 Hz, 2H, BH_2), 2.51 (t, $^3J_{H,H}$ = 5 Hz, 12H, CH_2N), 3.50 (t, $^3J_{H,H}$ = 5 Hz, 12H, CH_2O), 3.54 (s, 12H, $O(CH_2)_2O$), 6.88 (tm, $^3J_{H,H}$ = 7 Hz, 2H, *p*-Ph), 6.96 (tm, $^3J_{H,H}$ = 7 Hz, 4H, *m*-Ph), 7.53 (dm, $^3J_{H,H}$ = 7 Hz, 4H, *o*-Ph).

^{31}P NMR (THF-d_8, 25 °C): δ = -202.9 (tm, br, $^1J_{P,H}$ = 174 Hz, PH_2).

^{31}P{^{1}H} NMR (THF-d_8, 25 °C): δ = -202.9 (m, PH_2).

^{11}B NMR (THF-d_8, 25 °C): δ = -28.0 (td, $^1J_{B,H}$ = 99 Hz, $^1J_{B,P}$ = 23 Hz, BH_2).

^{11}B{^{1}H} NMR (THF-d_8, 25 °C): δ = -28.0 (d, $^1J_{B,P}$ = 23 Hz, BH_2).

^{13}C{^{1}H} NMR (THF-d_8, 25 °C): δ = 54.8 (s, CH_2N), 68.4 (s, CH_2O), 71.2 (s, $(CH_2)_2O$), 124.5 (s, *p*-Ph), 126.9 (s, *m*-Ph), 135.6 (s, *o*-Ph), 151.0 (s, *i*-Ph).

IR (KBr): $\tilde{\nu}$ = 3043 (vw), 2960 (w, CH), 2881 (m, CH), 2814 (m, CH) 2758 (vw), 2727 (vw), 2325 (w, BH), 2261 (w, PH), 1634 (vw), 1575 (vw), 1558 (vw), 1475 (m), 1461 (w), 1443 (w), 1354 (m), 1298 (w), 1259 (w), 1242 (vw), 1172 (vw), 1131 (s), 1103 (vs, CO), 1083 (s), 1023 (vw), 949 (m), 931 (m), 887 (vw), 831 (w), 741 (w), 698 (w), (vw), 571 (vw), 526 (vw), 482 (vw), 463 (vw).

ESI-MS (THF) anion: *m/z* = 274.9 (100%, $[H_2P\text{-}BH_2\text{-}AsPh_2]^-$).

Elemental analysis (%) calculated for $C_{30}H_{50}AsBKN_2O_6P$ (**10**): C: 52.15, H: 7.30, N: 4.05; found: C: 52.26, H: 6.77, N: 3.93.

Synthesis of $[Na(C_{12}H_{24}O_6)(thf)_2][Ph_2P\text{-}BH_2\text{-}PPh_2]$ (**11**$(thf)_2$):

A solution of 202 mg (1.00 mmol) $IBH_2\text{-}SMe_2$ in 1 ml toluene is added to a solution of 410 mg (2.00 mmol) $NaPPh_2$ in 8 ml thf at -80 °C. The solution is stirred for 16 h while allowed to reach room temperature. The yellow reaction liquid is filtrated on 185 mg (0.70 mmol) solid $C_{12}H_{24}O_6$ (18-crown-6) and layered with 25 ml diethyl ether. **11**$(thf)_2$ crystallizes at -30 °C as colorless blocks. The solvent is

decanted, the crystals are separated, washed with cold diethyl ether (-30 °C, 2 x 5 ml) and dried *in vacuo*.

Yield of $[Na(C_{12}H_{24}O_6)][Ph_2P\text{-}BH_2\text{-}PPh_2]$ (**11**$(NaI)_{0.07}$): 405 mg (85%).

^{1}H NMR (THF-d_8, 25 °C): δ = 2.07 (m, 2H, BH_2), 3.48 (s, 24 H, $C_{12}H_{24}O_6$), 6.84 (m, 4H, *p*-Ph), 6.93 (m, 8H, *m*-Ph), 7.50 (m, 8H, *o*-Ph).

^{31}P NMR (THF-d_8, 25 °C): δ = -27.7 (m, PPh_2).

^{31}P{^{1}H} NMR (THF-d_8, 25 °C): δ = -27.7 (m, PPh_2).

^{11}B NMR (THF-d_8, 25 °C): δ = -21.1 (s, br, BH_2).

^{11}B{^{1}H} NMR (THF-d_8, 25 °C): δ = -21.1 (t, $^1J_{B,H}$ = 95 Hz, BH_2).

^{13}C{^{1}H} NMR (THF-d_8, 25 °C): δ = 70.5 (s, $C_{12}H_{24}O_6$), 124.2 (s, *p*-Ph), 126.8 (t, $^3J_{C,P}$ = 3 Hz, *m*-Ph), 134.9 (t, $^2J_{C,P}$ = 9 Hz, *o*-Ph), 150.9 (t, $^1J_{C,P}$ = 8 Hz, *i*-Ph).

IR (KBr): $\tilde{\nu}$ = 3062 (m), 3043 (m), 2907 (s, CH), 2872 (m), 2749 (vw), 2720 (vw), 2686 (vw), 2388 (vw), 2304 (m, BH), 2217 (vw), 1950 (vw), 1878 (vw), 1802 (vw), 1755 (vw), 1578 (m), 1568 (vw), 1473 (s), 1453 (m), 1430 (m), 1352 (s), 1297 (w), 1289 (w), 1249 (m), 1178 (vw), 1105 (vs, CO), 1061 (s), 1026 (m), 960 (s), 947 (s), 862 (vw), 834 (m), 743 (s), 697 (s), 627 (vw), 502 (m), 472 (vw).

ESI-MS (THF) anion: *m/z* = 383.1 (100%, $[Ph_2P\text{-}BH_2\text{-}PPh_2]^-$), 581.1 (20 %, $[Ph_2P\text{-}BH_2\text{-}PPh_2\text{-}BH_2\text{-}PPh_2]^-$).

Elemental analysis (%) calculated for $C_{36}H_{46}As_2BKO_6(NaI)_{0.07}$ (**11**$(NaI)_{0.07}$): C: 63.49, H: 6.80; found: C: 63.26, H: 6.82.

Synthesis of $[K(C_{12}H_{24}O_6)(thf)_2][Ph_2As\text{-}BH_2\text{-}AsPh_2]$ (**12**$(thf)_2$):

A solution of 78 mg (0.50 mmol) $BrBH_2\text{-}SMe_2$ in 1 ml toluene is added to a solution of 326 mg (1.00 mmol) $KAsPh_2\cdot(C_4H_8O_2)_{0.625}$ in 5 ml thf at -80 °C. The solution is stirred for 16 h while allowed to reach room temperature. The reaction liquid is filtrated on 264 mg (1.00 mmol) solid $C_{12}H_{24}O_6$ (18-crown-6) and layered with 30 ml diethyl ether. **12**$(thf)_2$ crystallizes at -30 °C as colorless blocks. The solvent is decanted, the crystals are separated, washed with cold diethyl ether (-30 °C, 2 x 4 ml) and dried *in vacuo*.

Yield of $[K(C_{12}H_{24}O_6)][Ph_2As\text{-}BH_2\text{-}AsPh_2]$ (**12**): 302 mg (78%).

^{1}H NMR (THF-d_8, 25 °C): δ = 2.23 (m, 2H, BH_2), 3.48 (s, 24 H, $C_{12}H_{24}O_6$), 6.87 (m, 4H, *p*-Ph), 6.93 (m, 8H, *m*-Ph), 7.55 (m, 8H, *o*-Ph).

^{11}B NMR (THF-d_8, 25 °C): δ = -19.6 (t, $^{1}J_{B,H}$ = 102 Hz, BH_2).

^{11}B{^{1}H} NMR (THF-d_8, 25 °C): δ = -19.6 (s, BH_2).

^{13}C{^{1}H} NMR (THF-d_8, 25 °C): δ = 70.9 (s, $C_{12}H_{24}O_6$), 124.6 (s, *p*-Ph), 126.9 (s, *m*-Ph), 135.7 (s, *o*-Ph), 150.5 (s, *i*-Ph).

IR (KBr): $\tilde{\nu}$ = 3058 (m), 3046 (m), 2986 (w), 2945 (m), 2905 (s, CH), 2869 (s), 2824 (m), 2800 (w), 2744 (vw), 2714 (vw), 2686 (vw), 2334 (s, BH), 2221 (vw), 1965 (vw), 1875 (vw), 1812 (vw), 1575 (s), 1471 (s), 1451 (m), 1430 (s), 1350 (vs), 1298 (w), 1283 (m), 1248 (s), 1176 (vw), 1104 (vs, CO), 1022 (m), 998 (vw), 960 (vs), 908 (s), 834 (s), 745 (s), 743 (s), 698 (vs) 662 (vw), 529 (vw), 513 (vw), 486 (w), 458 (vw).

ESI-MS (THF) anion: *m/z* = 470.9 (100%, $[Ph_2As\text{-}BH_2\text{-}AsPh_2]^-$), 713.0 (8 %, $[Ph_2As\text{-}BH_2\text{-}AsPh_2\text{-}BH_2\text{-}AsPh_2]^-$).

Elemental analysis (%) calculated for $C_{36}H_{46}As_2BKO_6$ (**12**): C: 55.83, H: 5.98; found: C: 55.79, H: 5.89.

5.5.2 X-ray Diffraction Analysis

The X-ray diffraction experiments were performed either on a GV50 diffractometer with TitanS2 detector (**3**$(thf)_2$, **4**$(thf)_2$, **6**$(thf)_2$, **11**$(thf)_2$, **12**$(thf)_2$) or a Gemini R Ultra CCD diffractometer with AtlasS2 detector (**7**$(thf)_2$, **9**) from Rigaku Oxford Diffraction (formerly Agilent Technologies) applying Cu-$K\alpha$ radiation (λ = 1.54178 Å) (**3**$(thf)_2$, **4**$(thf)_2$, **6**$(thf)_2$, **7**$(thf)_2$, **9**, **11**$(thf)_2$, **12**$(thf)_2$). The measurements were performed either at 123 K (**3**$(thf)_2$, **4**$(thf)_2$, **6**$(thf)_2$, **7**$(thf)_2$, **11**$(thf)_2$, **12**$(thf)_2$) or at 293 K (**9**). Crystallographic data together with the details of the experiments are given in the Table S 5.1 - Table S 5.4 (see below).

A Numerical absorption correction based on gaussian integration was performed over a multifaceted crystal model (**3**$(thf)_2$, **4**$(thf)_2$, **6**$(thf)_2$, **11**$(thf)_2$, **12**$(thf)_2$), an analytical numeric absorption correction using a multifaceted crystal model based on expressions derived by R.C. Clark & J.S. Reid[4] (**7**$(thf)_2$, **9**) or an empirical absorption correction using spherical harmonics as implemented in SCALE3/ ABSPACK (CrysAlisPro software by Rigaku Oxford Diffraction).[5]

All structures were solved using SIR97[6], SHELXT[7] and OLEX^2[8]. Least square refinements against F^2 in anisotropic approximation were done using SHELXL[9].

All non-hydrogen atoms were refined anisotropically. The hydrogen positions of the methyl groups were located geometrically and refined riding on the carbon atoms. Hydrogen atoms belonging to BH2, PH2 and AsH2 groups were located from the difference Fourier map and refined without constraints (**12**$(thf)_2$) or with restrained X–H (X = B, P, As) distances (**3**$(thf)_2$, **4**$(thf)_2$, **6**$(thf)_2$, **7**$(thf)_2$, **9**, **11**$(thf)_2$).

5.5.3 Solid State Structures

$[Na(C_{12}H_{24}O_6)(thf)_2][H_2P\text{-}BH_2\text{-}^tBuPH]$ (**3**$(thf)_2$):

3$(thf)_2$ crystallizes from a THF solution layered by the 3-4-fold amount of *n*-hexane at 4 °C as colourless blocks in the triclinic space group $P\overline{1}$. Figure S 5.1 shows the molecular structure of **3**$(thf)_2$ in solid state.

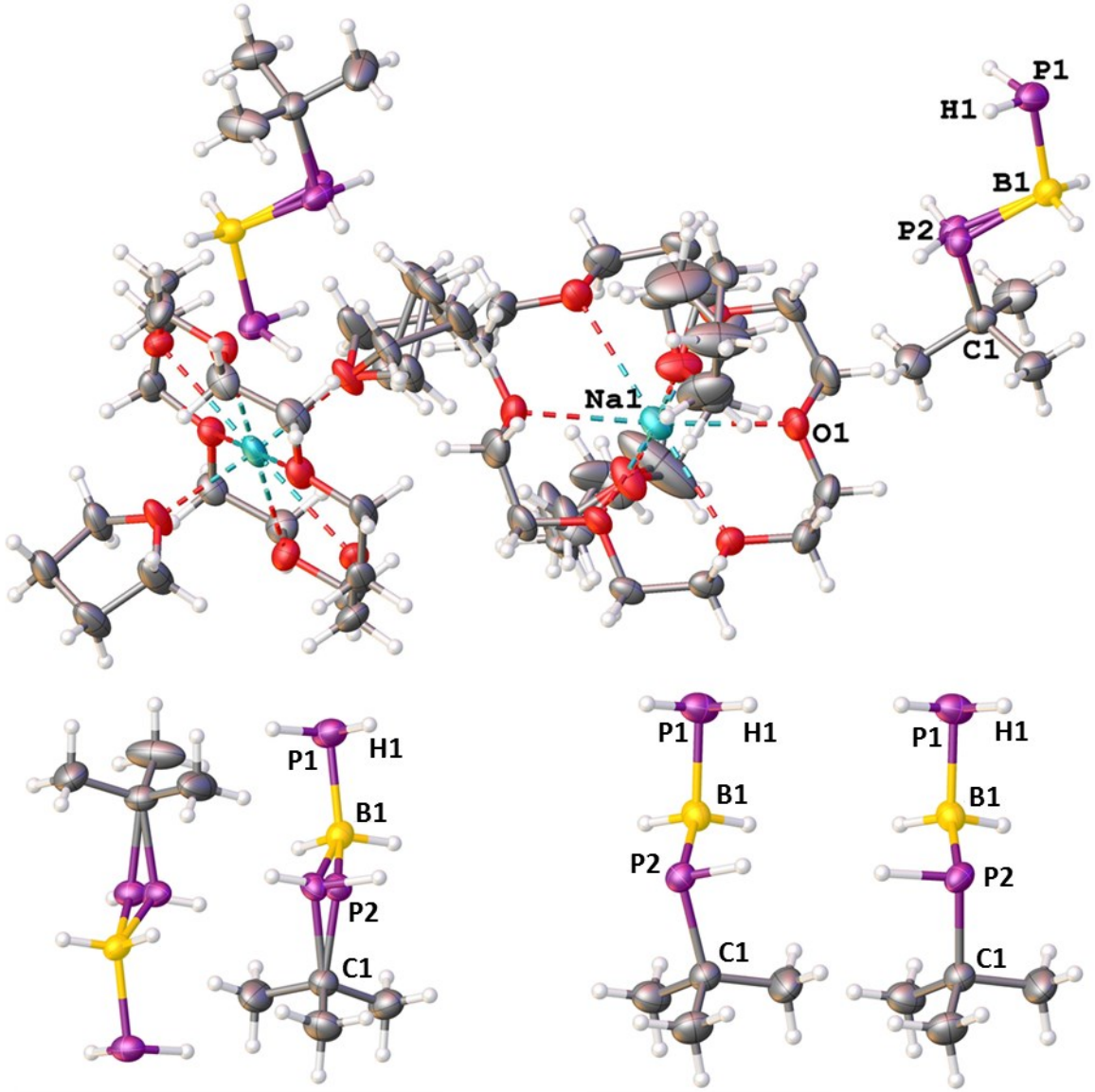

Figure S 5.1. Molecular structure of **3**$(thf)_2$ in solid state. Thermal ellipsoids are drawn with 50% probability. Selected bond length [Å] and angles [°]: P1-B1: 1.975(2) – 1.979(2), P2-B1: 1.951(3) – 2.037(7), P2-C1: 1.893(5) – 1.898(3), ∠(P1-B1-P2): 107.8(2) – 112.3(1), ∠(B1-P2-C1): 103.1(3) – 106.9(1). Top: disordered solid state structure of **3**$(thf)_2$; bottom left: 2 independent anions; bottom right: 2 enantiomers of the anionic part of **3**$(thf)_2$.

$[Na(C_{12}H_{24}O_6)(thf)_2][H_2As\text{-}BH_2\text{-}^tBuAsH]$ $(4(thf)_2)$:

4$(thf)_2$ crystallizes from a THF solution layered by the 3-4-fold amount of *n*-hexane at -28 °C as colourless blocks in the triclinic space group $P\bar{1}$. Figure S 5.2 shows the molecular structure of **4**$(thf)_2$ in solid state.

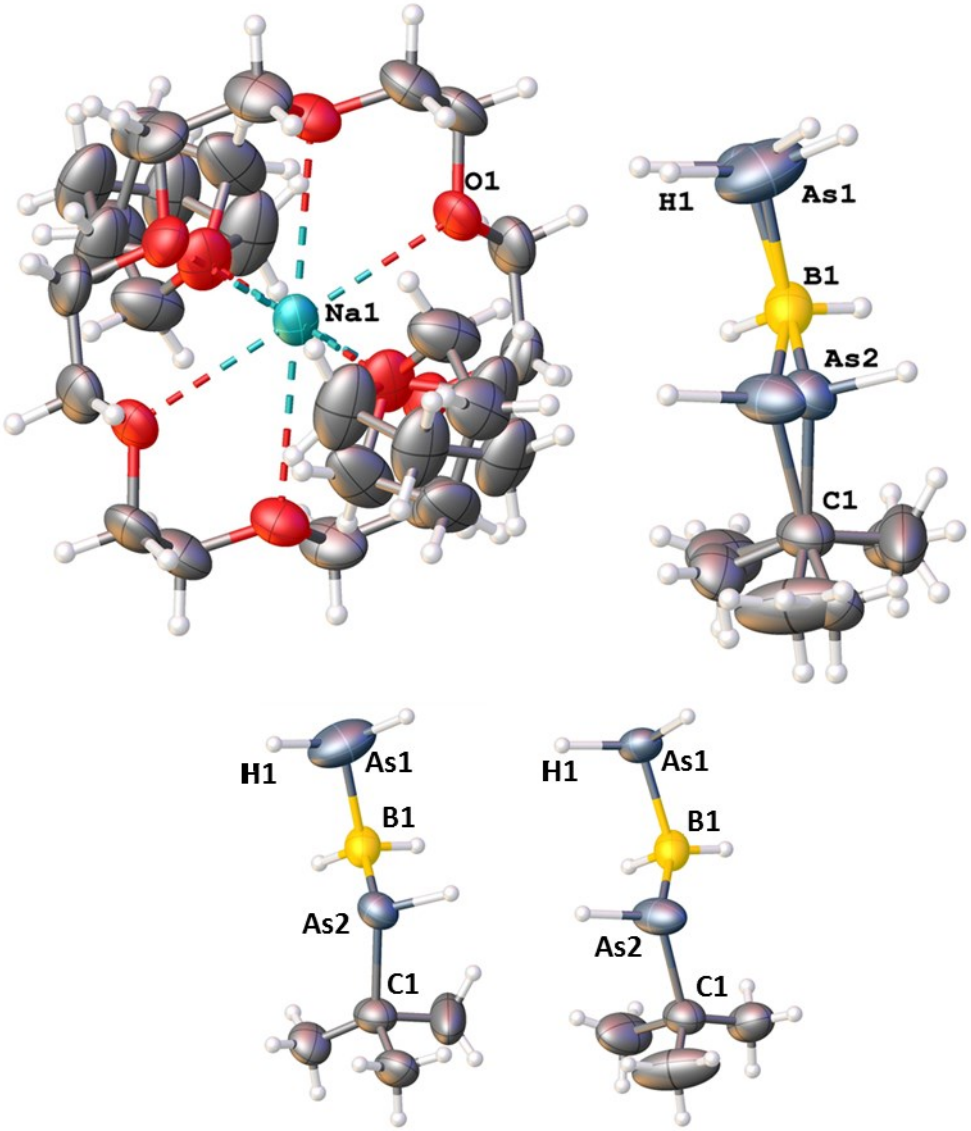

Figure S 5.2. Molecular structure of **4**$(thf)_2$ in solid state. Thermal ellipsoids are drawn with 50% probability. Selected bond length [Å] and angles [°]: As1-B1: 2.022(6) – 2.065(5), As2-B1: 2.073(6) – 2.122(5), As2-C1: 2.005(5) – 2.010(4), ∠(As1-B1-As2): 105.7(3) – 108.7(2), ∠(B1-As2-C1): 103.1(2) – 105.0(2). Top: disordered solid state structure of **4**$(thf)_2$; bottom: 2 enantiomers of the anionic part of **4**$(thf)_2$.

$[Na(C_{12}H_{24}O_6)(thf)_2][H_2As\text{-}BH_2\text{-}^tBuPH\text{-}BH_3]$ (6(thf)$_2$):

6(thf)$_2$ crystallizes from a THF solution layered by the 3-4-fold amount of *n*-hexane at -28 °C as colourless blocks in the triclinic space group $P\bar{1}$. Figure S 5.3 shows the molecular structure of **6**(thf)$_2$ in solid state.

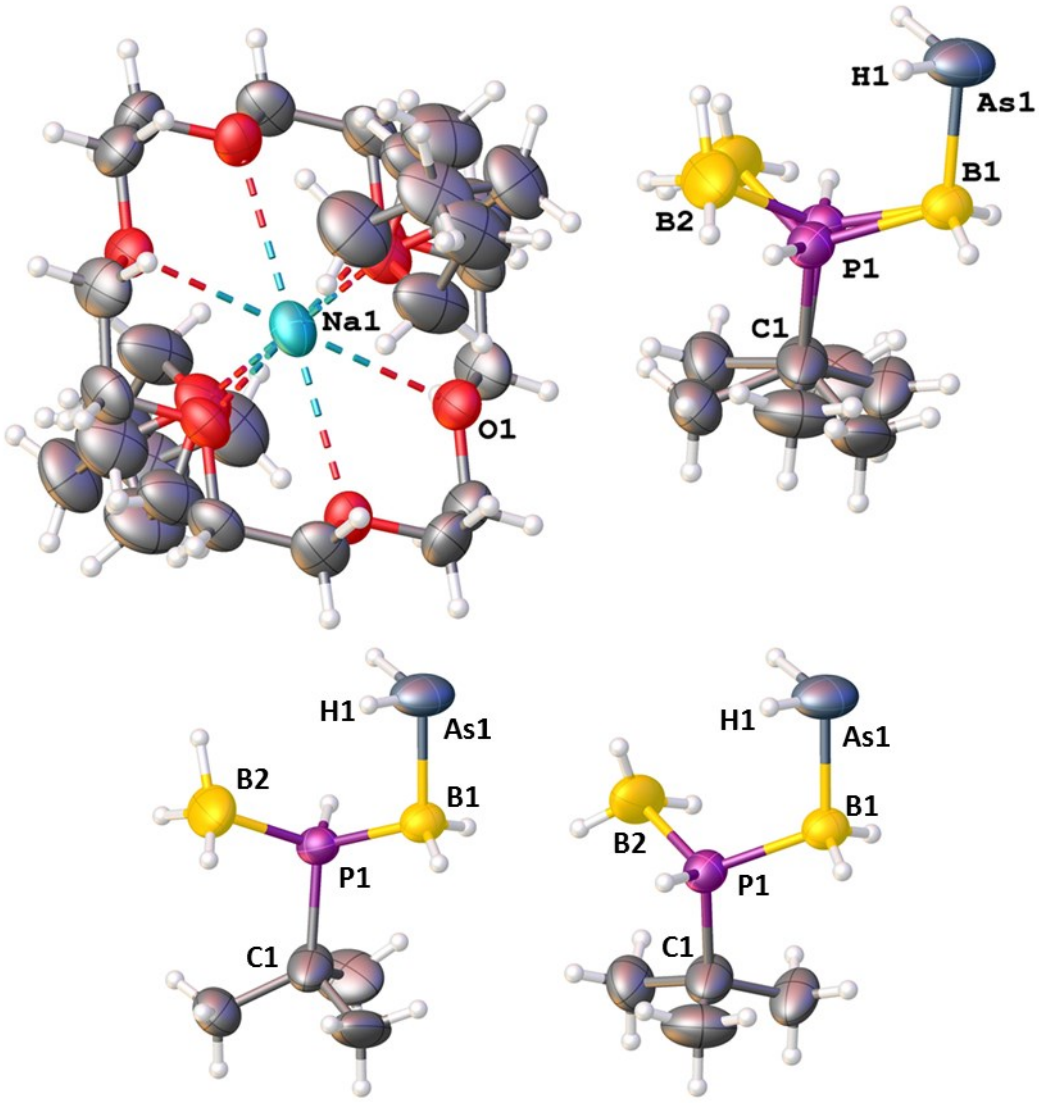

Figure S 5.3. Molecular structure of **6**(thf)$_2$ in solid state. Thermal ellipsoids are drawn with 50% probability. Selected bond length [Å] and angles [°]: As1-B1: 2.079(3), P1-B1: 1.917(4) – 1.969(4), P1-C1: 1.824(4) – 1.935(4), P1-B2: 1.941(8) – 1.950(8), ∠(As1-B1-P1): 108.5(2) – 111.5(2), ∠(B1-P1-C1): 108.1(2) – 110.6(2), ∠(B1-P1-B2): 115.5(4) – 117.8(4), ∠(B2-P1-C1): 103.8(4) – 106.5(3). Top: disordered solid state structure of **6**(thf)$_2$; bottom: 2 enantiomers of the anionic part of **6**(thf)$_2$.

$[Na(C_{12}H_{24}O_6)(thf)_2][H_2P\text{-}BH_2\text{-}PPh_2]$ $(7(thf)_2)$:

7$(thf)_2$ crystallizes from a THF/*n*-hexane mixture at -28 °C as colourless blocks in the orthorhombic space group *Pccn*. Figure S 5.4 shows the molecular structure of **7**$(thf)_2$ in solid state.

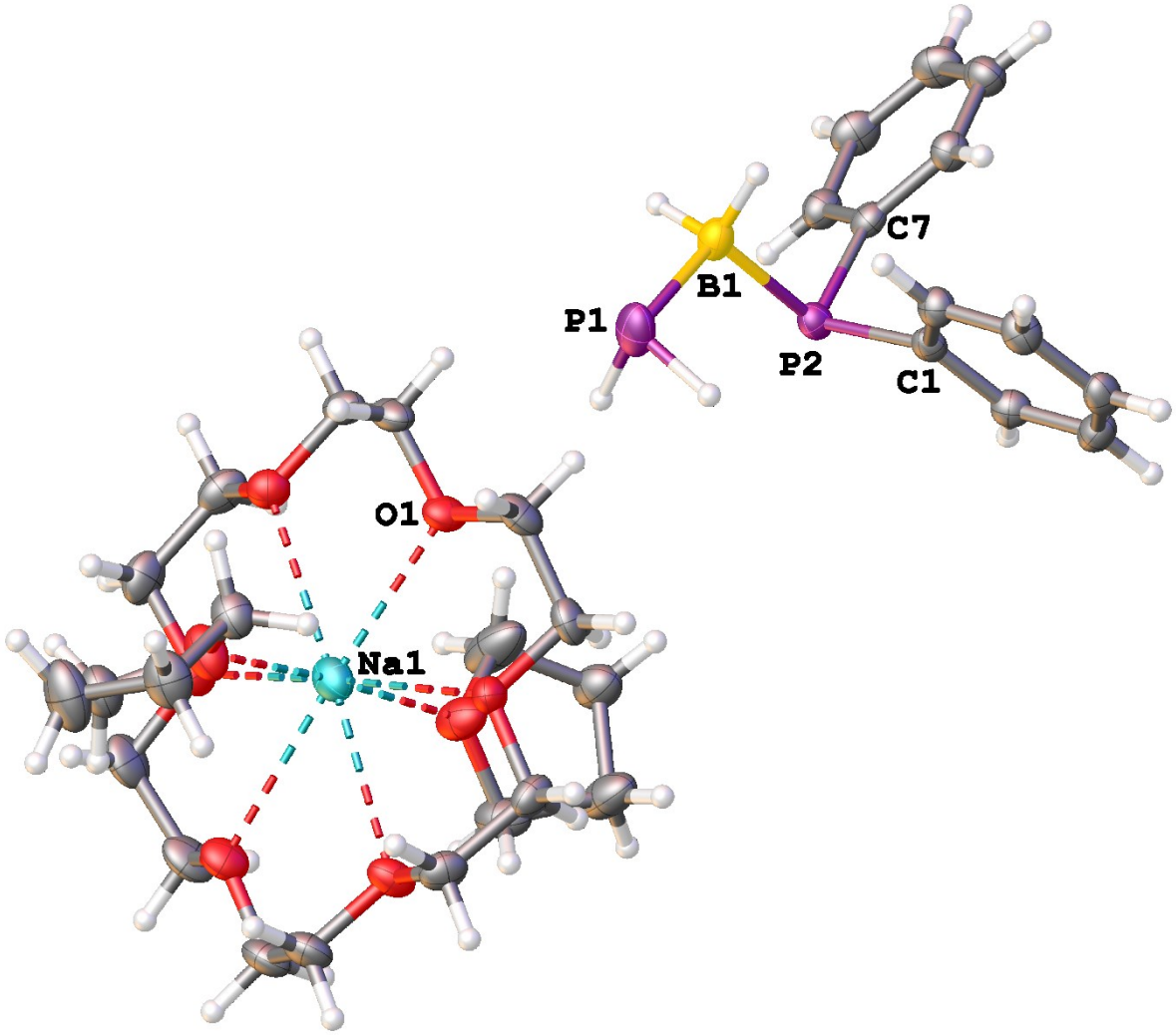

Figure S 5.4. Molecular structure of **7**$(thf)_2$ in solid state. Thermal ellipsoids are drawn with 50% probability. Selected bond length [Å] and angles [°]: P1-B1: 1.973(2), P2-B1: 1.965(2), P2-C1: 1.847(1), P2-C7: 1.841(1), ∠(P1-B1-P2): 111.36(8), ∠(B1-P2-C1): 105.56(6), ∠(B1-P2-C7): 101.63(6), ∠(C1-P2-C7): 100.95(6).

$[Na(C_{18}H_{36}N_2O_6)][H_2As\text{-}BH_2\text{-}PPh_2]$ (9):

9 crystallizes from a THF solution layered by the 3-4-fold amount of *n*-hexane at -28 °C as colourless blocks in the orthorhombic space group *Pbcn*. Figure S 5.5 shows the molecular structure of **9** in solid state.

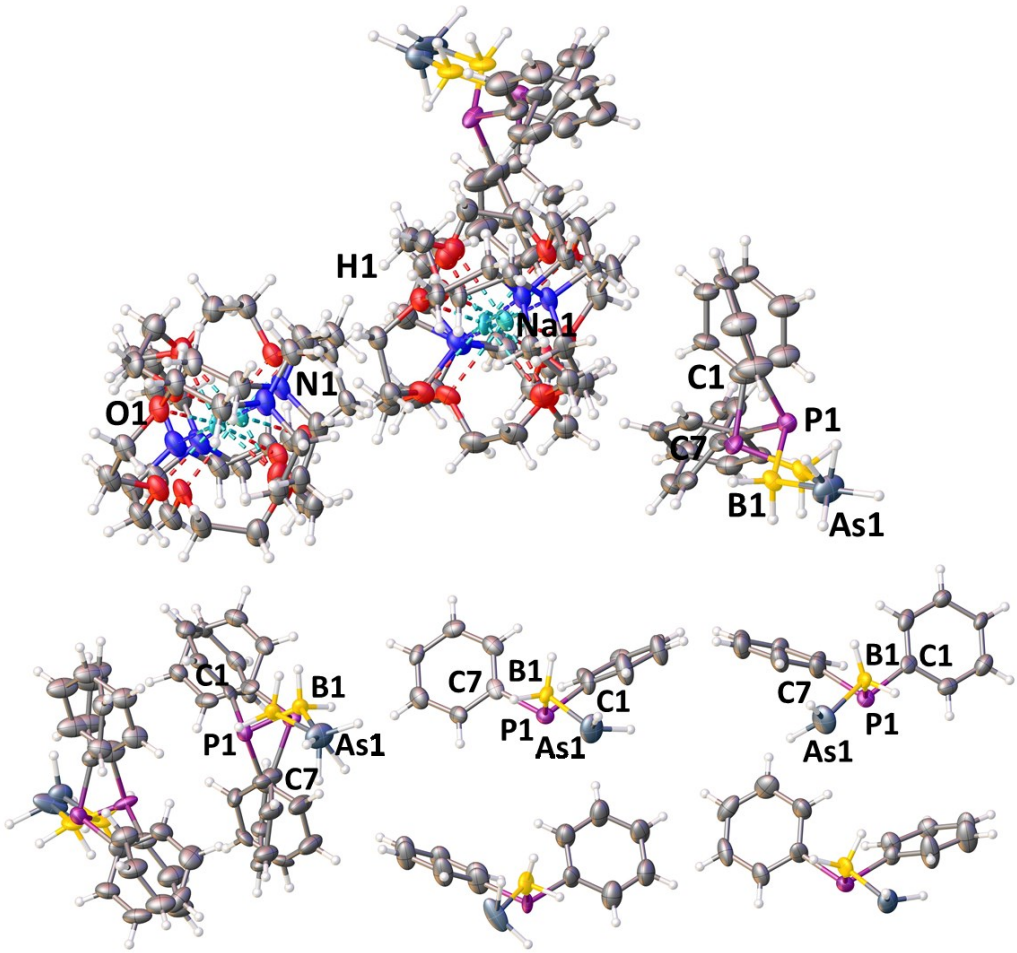

Figure S 5.5. Molecular structure of **9** in solid state. Thermal ellipsoids are drawn with 50% probability. Selected bond length [Å] and angles [°]: As-B1: 2.02(3) – 2.12(3), P1-B1: 1.88(2) – 1.97(1), P1-C1/C7: 1.83(2) – 1.92(2), ∠(As-B1-P1): 111.3(5) – 122.0(1), ∠(B1-P1-C1/C7): 101.1(4) – 109.6(1), ∠(C1-P1-C7): 97.3(1) – 103.9(1). Top: highly disordered solid state structure of **9**; bottom left: 2 independent anions; bottom right: 4 different possible conformers of the anionic part of **9**.

$[Na(C_{12}H_{24}O_6)(thf)_2][Ph_2P\text{-}BH_2\text{-}PPh_2]$ (**11**$(thf)_2$):

11$(thf)_2$ crystallizes from a THF solution layered by the 3-4-fold amount of diethyl ether at -28 °C as colourless blocks in the orthorhombic space group *Pbc2₁*. Figure S 5.6 shows the molecular structure of **11**$(thf)_2$ in solid state.

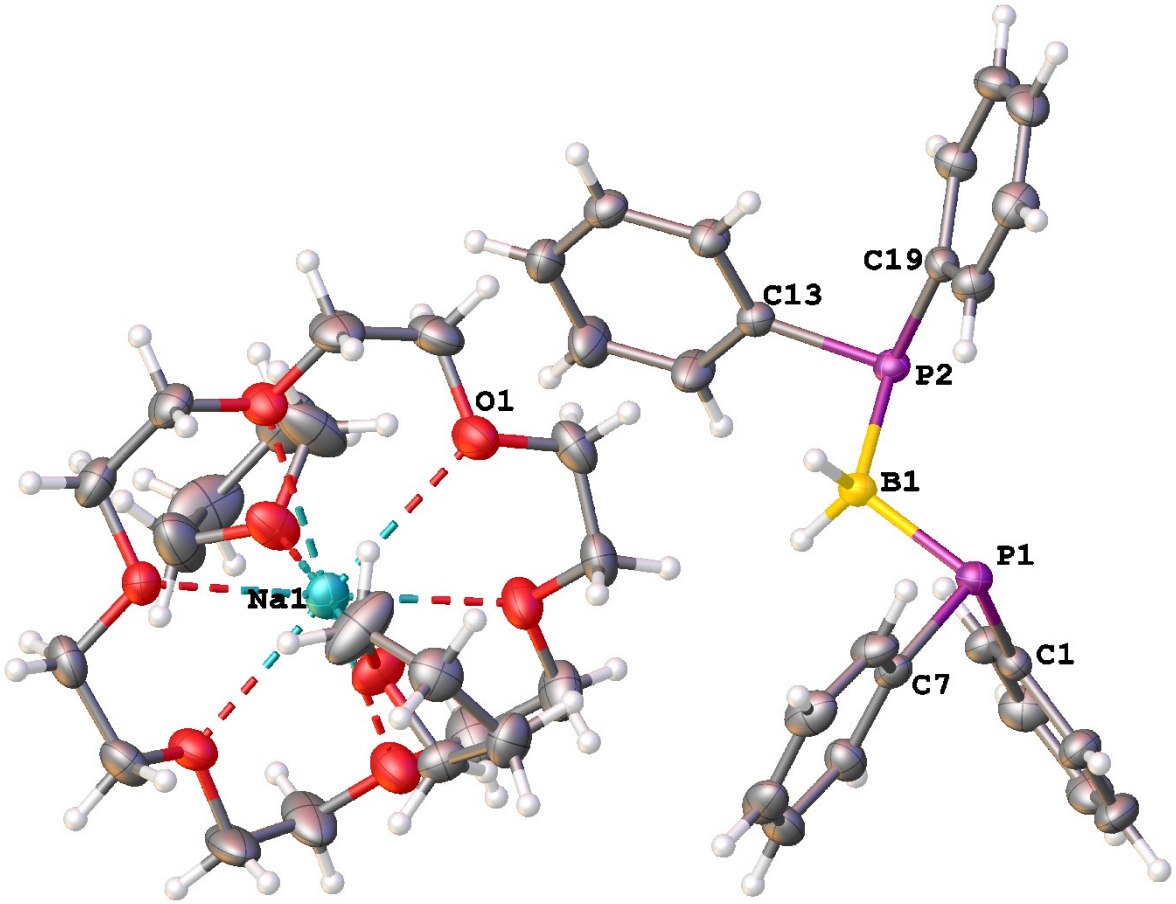

Figure S 5.6. Molecular structure of **11**$(thf)_2$ in the solid state. Thermal ellipsoids are drawn with 50% probability. Selected bond length [Å] and angles [°]: P1-B1: 1.976(3), P1-C1: 1.842(3), P1-C7: 1.843(2), P2-B1: 1.982(3), P2-C13: 1.845(2), P2-C19: 1.834(3), ∠(P1-B1-P2): 118.3(1), ∠(B1-P1-C1): 107.5(1), ∠(B1-P1-C7): 96.7(1), ∠(B1-P2-C13): 96.9(1), ∠(B1-P2-C19): 107.0(1), ∠(C1-P1-C7): 99.7(1), ∠(C13-P2-C19): 99.9(1).

$[K(C_{12}H_{24}O_6)(thf)_2][Ph_2As\text{-}BH_2\text{-}AsPh_2]$ (**12**$(thf)_4$):

12$(thf)_4$ crystallizes from a THF solution layered by the 3-4-fold amount of diethyl ether at -28 °C as colourless plates in the orthorhombic space group *Pna2₁*. Figure S 5.7 shows the molecular structure of **12**$(thf)_4$ in solid state.

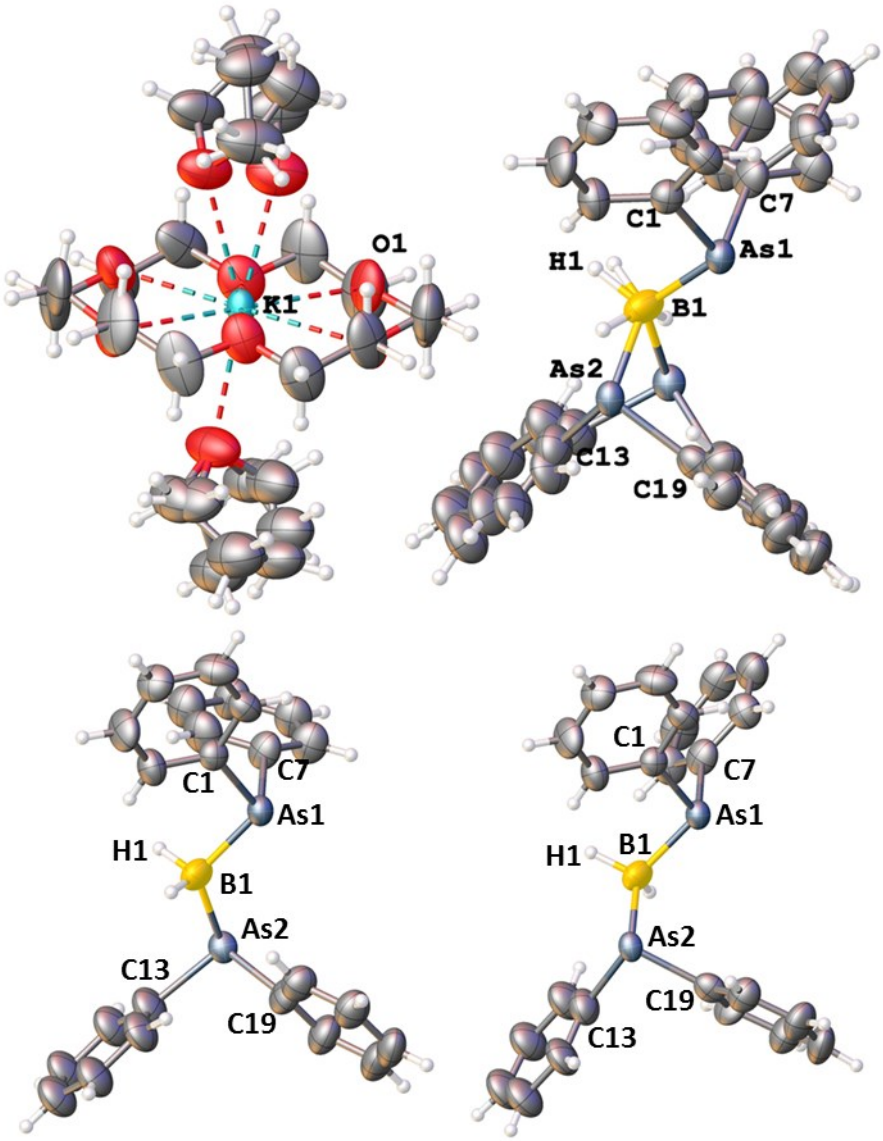

Figure S 5.7. Molecular structure of **12**$(thf)_4$ in solid state. Two THF-molecules in the cell are omitted for heavy disorder and calculated by solvent-mask-order. Thermal ellipsoids are drawn with 50% probability. Selected bond length [Å] and angles [°]: As1-B1: 2.014(7), As1-C1: 1.960(8), As1-C7: 1.965(7), As2-B1: 1.928(8) – 2.009(8), As2-C13: 1.96(2) – 2.02(2), As2-C19: 2.00(1) – 2.01(2), ∠(As1-B1-As2): 114.5(5) – 119.9(5), ∠(B1-As1-C1): 104.2(3), ∠(B1-As1-C7): 105.0(4), ∠(B1-As2-C13): 105.6(1) – 106.4(4), ∠(B1-As2-C19): 104.7(4) – 109.6(1), ∠(C1-As1-C7): 95.2(3), ∠(C13-P2-C19): 97.0(6) – 99.7(1). Top: disordered solid state structure of **12**$(thf)_4$; bottom: 2 possible conformers of the anionic part of **12**$(thf)_4$.

5.5.4 Crystallographic Information

Table S 5.1. Crystallographic data for compounds **3**$(thf)_2$ and **4**$(thf)_2$.

	3$(thf)_2$	**4**$(thf)_2$
Emipirical formula	$C_{24}H_{54}BNaO_8P_2$	$C_{24}H_{54}As_2BNaO_8$
Formula weight *M*	566.41 g/mol	654.31 g/mol
Crystal	clear colourless block	clear colourless block
Crystal size [mm³]	0.198 x 0.139 x 0.115	0.206 x 0.135 x 0.107
Temperature *T*	123(2) K	123.01(12) K
Cristal system	triclinic	triclinic
Space group	$P\bar{1}$	$P\bar{1}$
Unit cell dimensions	*a* = 9.1081(2) Å *b* = 18.5819(5) Å *c* = 19.5284(5) Å *α* = 88.080(2)° *β* = 85.232(2)° *γ* = 79.598(2)°	*a* = 9.3511(6) Å *b* = 10.4566(6) Å *c* = 18.6365(11) Å *α* = 87.953(5)° *β* = 80.059(5)° *γ* = 68.250(5)°
Volume *V*	3238.96(14) Å^3	1666.35(18) Å^3
Formula units *Z*	4	2
Absorption coefficient $\mu_{Cu\text{-}K\alpha}$	1.675 mm^{-1}	2.927 mm^{-1}
Density (calculated) ρ_{calc}	1.162 g/cm^3	1.304 g/cm^3
F(000)	1232	688
Theta range θ_{min} / θ_{max} / θ_{full}	2.418 / 73.743 / 67.679 °	4.555 / 75.372 / 67.684 °
Absorption correction	gaussian	gaussian
Index ranges	-9 < *h* < 11 -17 < *k* < 22 -22 < *l* < 24	-11 < *h* < 11 -12 < *k* < 10 -23 < *l* < 23
Reflections collected	20740	12982
Independent reflections [$I > 2\sigma(I)$]	8966 (R_{int} = 0.0377)	5666 (R_{int} = 0.0355)
Completeness to full θ	0.985	0.999
Transmission T_{min} / T_{max}	0.805 / 0.866	0.690 / 1.000
Data / restraints / parameters	12383 / 0 / 825	6576 / 230 / 460
Goodness-of-fit on F^2 *S*	0.941	1.032
Gerätetyp	GV50	GV 50
Strahlungsart (λ)	Cu (1.54178 Å)	Cu (1.54184 Å)
Final *R*-values [$I > 2\sigma(I)$]	R_1 = 0.0513 wR_2 = 0.1341	R_1 = 0.0669 wR_2 = 0.1888
Final *R*-values (all data)	R_1 = 0.0655 wR_2 = 0.1402	R_1 = 0.0732 wR_2 = 0.1967
Largest difference hole and peak $\Delta\rho$	-0.345 0.423 eÅ^{-3}	-0.615 0.926 eÅ^{-3}

Table S 5.2. Crystallographic data for compounds **6**$(thf)_2$ and **7**$(thf)_2$.

	6$(thf)_2$	**7**$(thf)_2$
Emipirical formula	$C_{24}H_{57}AsB_2NaO_8P$	$C_{32}H_{54}BNaO_8P_2$
Formula weight *M*	624.19 g/mol	662.49 g/mol
Crystal	clear colourless block	clear colourless block
Crystal size [mm³]	0.214 x 0.164 x 0.089	0.5517 x 0.1493 x 0.1165
Temperature *T*	123.0(2) K	122.9(4) K
Cristal system	triclinic	orthorhombic
Space group	$P\bar{1}$	*Pccn*
Unit cell dimensions	*a* = 9.4763(5) Å	*a* = 19.86405(18) Å
	b = 10.3756(5) Å	*b* = 19.2682(2) Å
	c = 18.8170(9) Å	*c* = 19.23470(16) Å
	α = 88.515(4)°	*α* = 90°
	β = 81.081(4)°	*β* = 90°
	γ = 70.892(4)°	*γ* = 90°
Volume *V*	1726.44(16) Å^3	7361.98(12) Å^3
Formula units *Z*	2	8
Absorption coefficient $\mu_{Cu\text{-}K\alpha}$	2.203 mm^{-1}	1.552 mm^{-1}
Density (calculated) ρ_{calc}	1.201 g/cm^3	1.195 g/cm^3
F(000)	668	2848
Theta range θ_{min} / θ_{max} / θ_{full}	2.378 / 74.852 / 67.684 °	3.937 / 67.095 / 67.095 °
Absorption correction	gaussian	analytical
Index ranges	-11 < *h* < 11	-19 < *h* < 23
	-9 < *k* < 12	-20 < *k* < 22
	-23 < *l* < 23	-21 < *l* < 22
Reflections collected	12941	42140
Independent reflections [$I > 2\sigma(I)$]	5551 (R_{int} = 0.0225)	6023 (R_{int} = 0.0302)
Completeness to full θ	0.987	0.996
Transmission T_{min} / T_{max}	0.856 / 0.932	0.582 / 0.884
Data / restraints / parameters	6670 / 294 / 505	6546 / 4 / 413
Goodness-of-fit on F^2 *S*	1.037	1.036
Gerätetyp	GV 50	Gemini Ultra
Strahlungsart (λ)	Cu (1.54184 Å)	Cu (1.54184 Å)
Final *R*-values [$I > 2\sigma(I)$]	R_1 = 0.0526	R_1 = 0.0321
	wR_2 = 0.1331	wR_2 = 0.847
Final *R*-values (all data)	R_1 = 0.0623	R_1 = 0.0349
	wR_2 = 0.1414	wR_2 = 0.0872
Largest difference hole	-0.890	-0.310
and peak $\Delta\rho$	0.404 eÅ^{-3}	0.340 eÅ^{-3}

Table S 5.3. Crystallographic data for compounds **9**$(thf)_2$ and **11**$(thf)_2$.

	9$(thf)_2$	**11**$(thf)_2$
Emipirical formula	$C_{30}H_{50}AsBN_2NaO_6P$	$C_{44}H_{62}BNaO_8P_2$
Formula weight *M*	674.41 g/mol	814.67 g/mol
Crystal	clear colourless block	clear colourless block
Crystal size [mm³]	0.28 x 0.114 x 0.101	0.288 x 0.2 x 0.195
Temperature *T*	293(2) K	122.99(10) K
Cristal system	orthorhombic	orthorhombic
Space group	*Pbcn*	$Pbc2_1$
Unit cell dimensions	*a* = 17.3350(3) Å	*a* = 18.8526(3) Å
	b = 43.0418(10) Å	*b* = 15.2039(2) Å
	c = 20.2779(4) Å	*c* = 15.5312(3) Å
	α = 90°	*α* = 90°
	β = 90°	*β* = 90°
	γ = 90°	*γ* = 90°
Volume *V*	15130.0(5) Å^3	4451.77(13) Å^3
Formula units *Z*	16	4
Absorption coefficient $\mu_{Cu\text{-}K\alpha}$	2.036 mm^{-1}	1.381 mm^{-1}
Density (calculated) ρ_{calc}	1.184 g/cm^3	1.216 g/cm^3
F(000)	5696	1744
Theta range θ_{min} / θ_{max} / θ_{full}	3.508 / 66.796 / 66.796 °	2.344 / 74.392 / 67.684 °
Absorption correction	analytical	gaussian
Index ranges	-12 < *h* < 20	-20 < *h* < 23
	-49 < *k* < 49	-15 < *k* < 18
	-23 < *l* < 21	-18 < *l* < 14
Reflections collected	67801	21839
Independent reflections [$I > 2\sigma(I)$]	8480 (R_{int} = 0.0791)	7685 (R_{int} = 0.0336)
Completeness to full *θ*	0.967	0.996
Transmission T_{min} / T_{max}	0.594 / 0.816	0.622 / 1.000
Data / restraints / parameters	12999 / 3200 / 1412	7952 / 1 / 514
Goodness-of-fit on F^2 *S*	1.025	1.014
Gerätetyp	Gemini ultra	GV 50
Strahlungsart (*λ*)	Cu (1.54184 Å)	Cu (1.54184 Å)
Final *R*-values [$I > 2\sigma(I)$]	R_1 = 0.1230	R_1 = 0.0341
	wR_2 = 0.3143	wR_2 = 0.0907
Final *R*-values (all data)	R_1 = 0.1605	R_1 = 0.0352
	wR_2 = 0.3403	wR_2 = 0.0919
Largest difference hole	-0.575	0.264
and peak *Δρ*	1.534 eÅ^{-3}	-0.164 eÅ^{-3}
Flack parameter		0.52(2)

Table S 5.4. Crystallographic data for compounds **12**$(thf)_4$.

	12$(thf)_4$
Emipirical formula	$C_{52}H_{78}As_2BKO_{10}$
Formula weight *M*	1062.89 g/mol
Crystal	clear colourless plate
Crystal size [mm³]	0.233 x 0.16 x 0.078
Temperature *T*	122.95(18) K
Cristal system	orthorhombic
Space group	*Pna2₁*
Unit cell dimensions	*a* = 21.7386(3) Å *b* = 11.14057(14) Å *c* = 22.2758(3) Å *α* = 90° *β* = 90° *γ* = 90°
Volume *V*	5394.77(13) Å^3
Formula units *Z*	4
Absorption coefficient $\mu_{Cu\text{-}K\alpha}$	2.653 mm^{-1}
Density (calculated) ρ_{calc}	1.131 g/cm^3
F(000)	2240
Theta range θ_{min} / θ_{max} / θ_{full}	3.969 / 80.208 / 67.684 °
Absorption correction	gaussian
Index ranges	-26 < *h* < 22 -13 < *k* < 13 -25 < *l* < 26
Reflections collected	28058
Independent reflections [$I > 2\sigma(I)$]	9778 (R_{int} = 0.0360)
Completeness to full θ	0.997
Transmission T_{min} / T_{max}	0.700 / 0.950
Data / restraints / parameters	10190 / 1559 / 699
Goodness-of-fit on F^2 *S*	1.045
Gerätetyp	GV 50
Strahlungsart (λ)	Cu (1.54184 Å)
Final *R*-values [$I > 2\sigma(I)$]	R_1 = 0.0647 wR_2 = 0.1798
Final *R*-values (all data)	R_1 = 0.0662 wR_2 = 0.1815
Largest difference hole and peak $\Delta\rho$	1.498 -0.714 eÅ^{-3}
Flack parameter	0.16(3)

5.5.5 NMR Spectroscopy

$[Na(C_{12}H_{24}O_6)(thf)_2][H_2P\text{-}BH_2\text{-}^tBuPH]$ $(3(thf)_2)$:

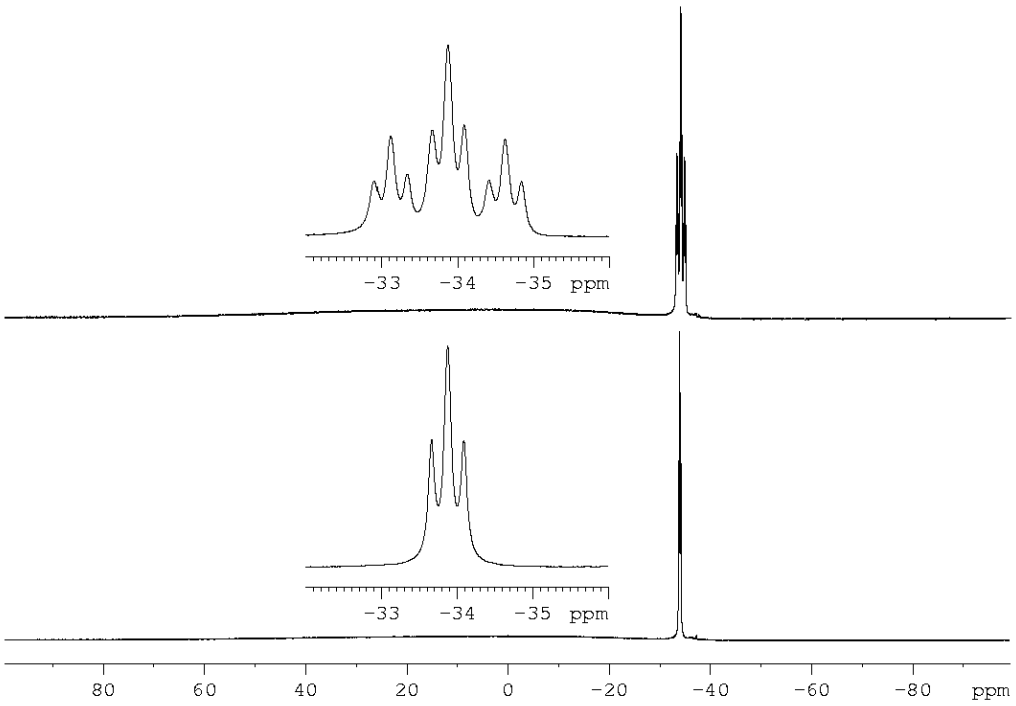

Figure S 5.8. $^{11}B\{^1H\}$ (bottom) and ^{11}B NMR spectrum (top) of **3** in THF-d_8.

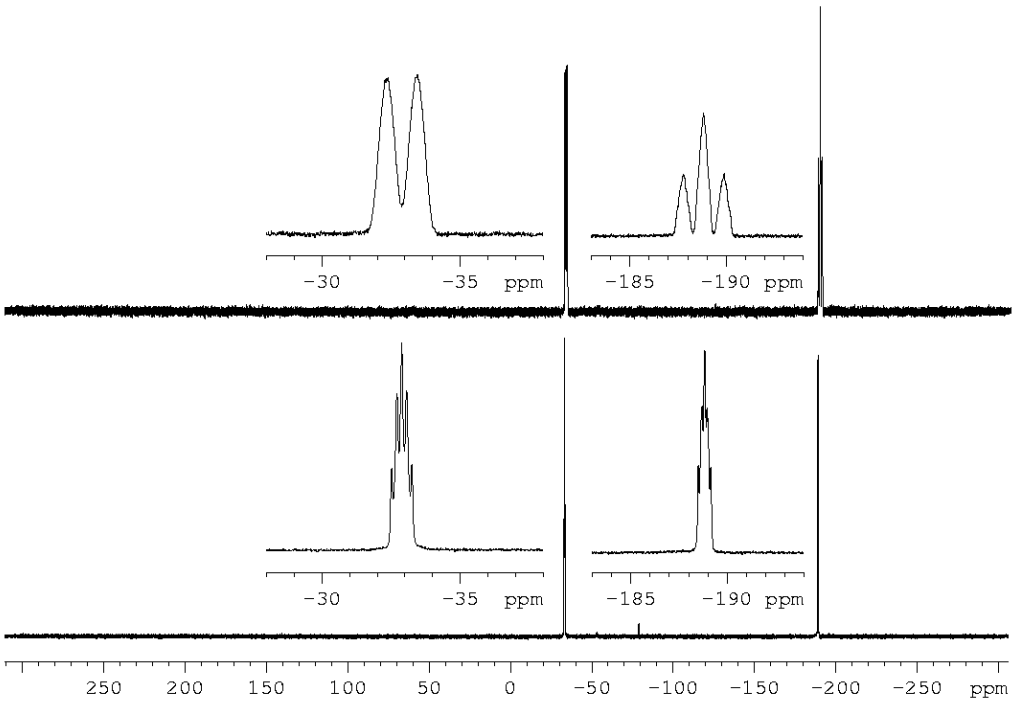

Figure S 5.9. $^{31}P\{^1H\}$ (bottom) and ^{31}P NMR spectrum (top) of **3** in THF-d_8.

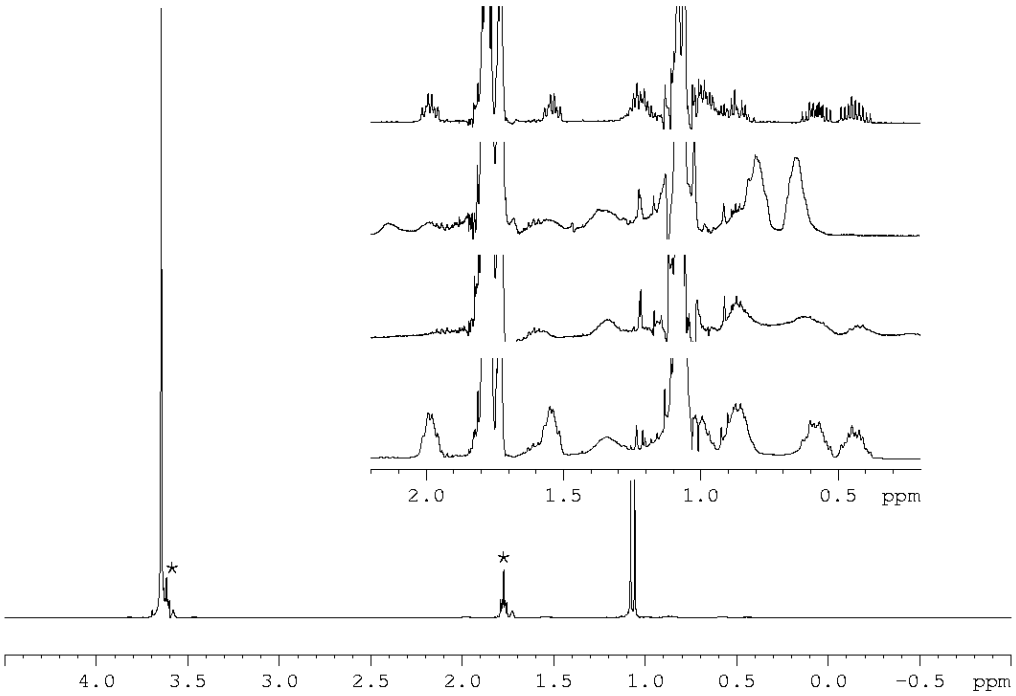

Figure S 5.10. ^{1}H NMR spectrum of **3** in THF-d_8. * = solvent (THF-d_8).
Magnified part shows ^{1}H, ^{1}H{^{31}P} (^{t}BuP<u>H</u>), ^{1}H{^{31}P} (P<u>H^{a}H^{b}</u>), ^{1}H{^{11}B} NMR (from bottom to top) of the anion.

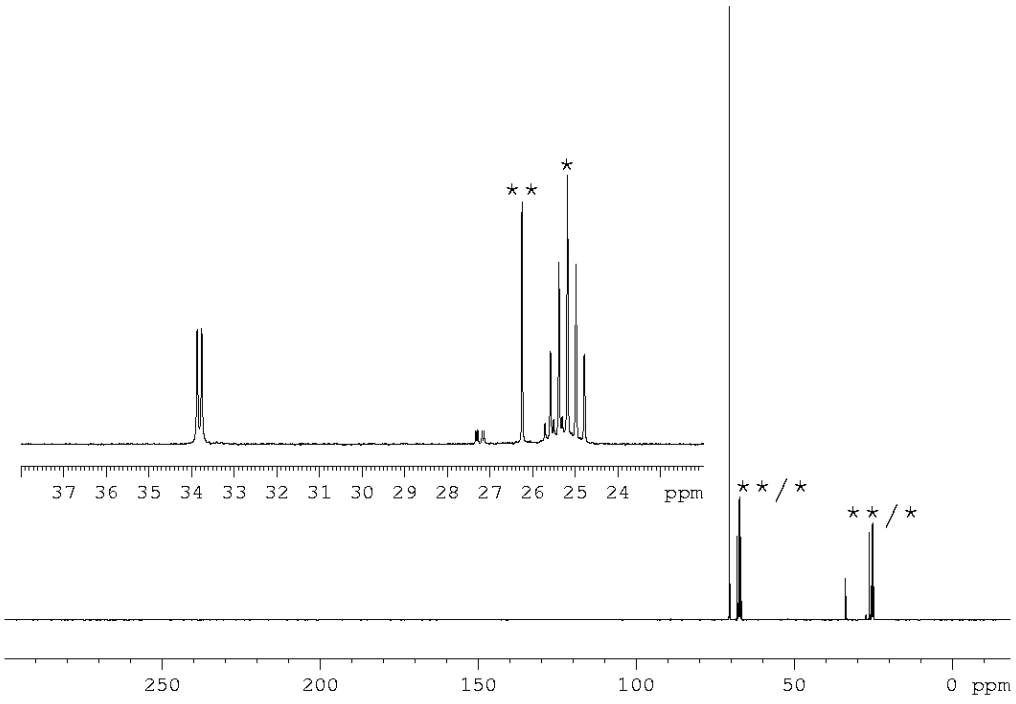

Figure S 5.11. ^{13}C NMR spectrum of **3** in THF-d_8. * = solvent (THF-d_8), ** = solvent (THF).

$[Na(C_{12}H_{24}O_6)(thf)_2][H_2As\text{-}BH_2\text{-}^tBuAsH]$ $(4(thf)_2)$:

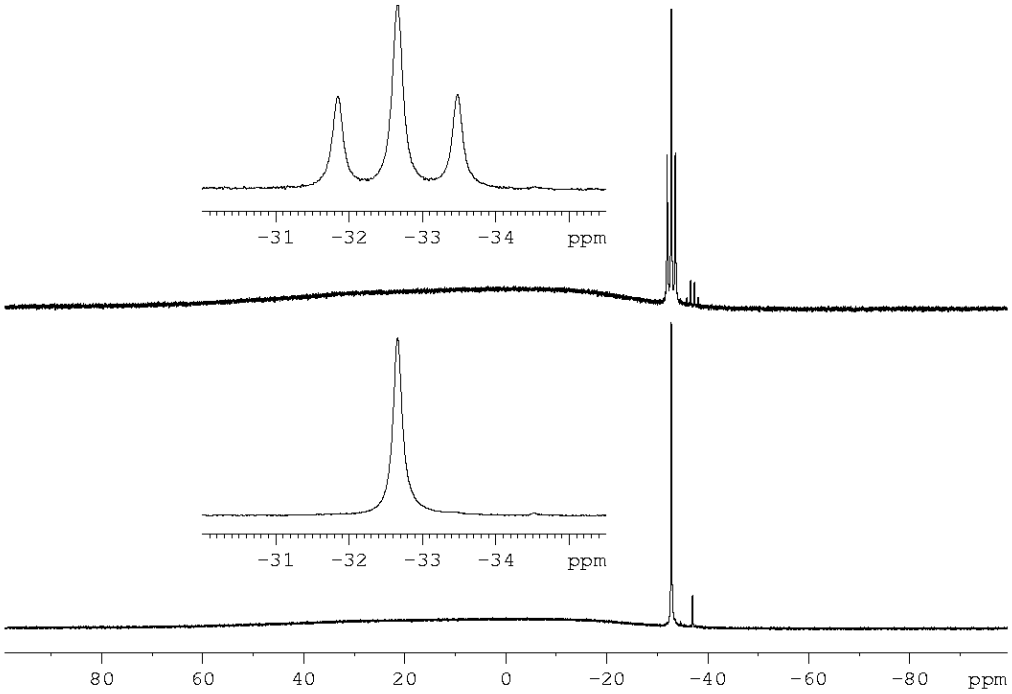

Figure S 5.12. $^{11}B\{^1H\}$ (bottom) and ^{11}B NMR spectrum (top) of **4** in THF-d_8.

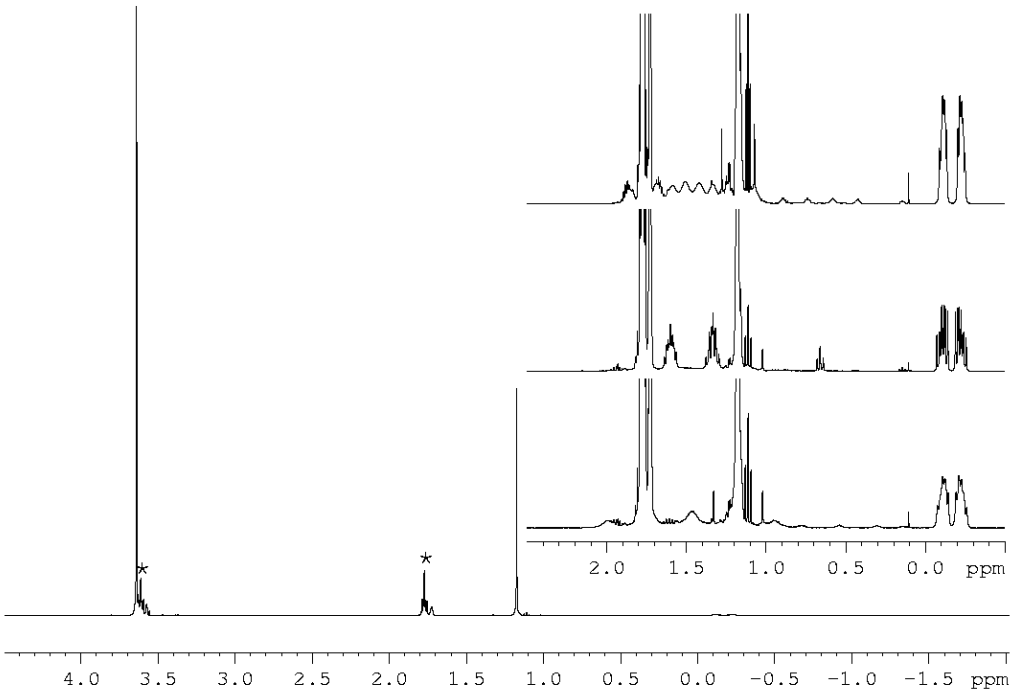

Figure S 5.13. ^1H NMR spectrum of **4** in THF-d_8. * = solvent (THF-d_8).
Magnified part shows ^1H, $^1H\{^{11}B\}$, ^1H (600 MHz) NMR (from bottom to top) of the anion.

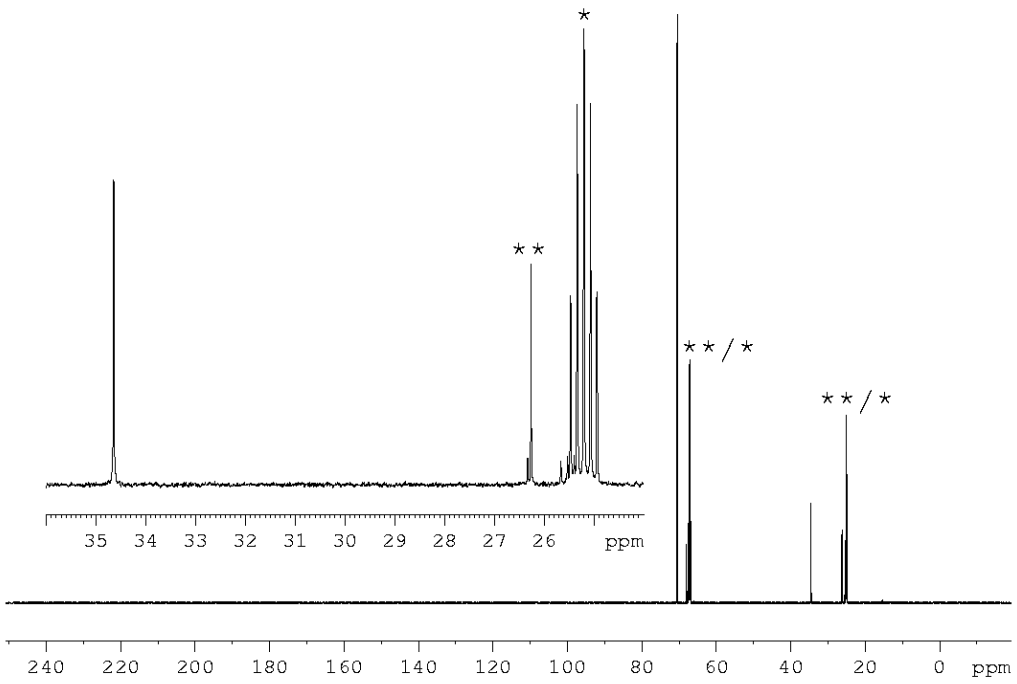

Figure S 5.14. ^{13}C NMR spectrum of **4** in THF-d_8. * = solvent (THF-d_8), ** = solvent (THF).

$[Na(C_{12}H_{24}O_6)(thf)_2][H_2P\text{-}BH_2\text{-}^tBuAsH]$ (5(thf)$_2$):

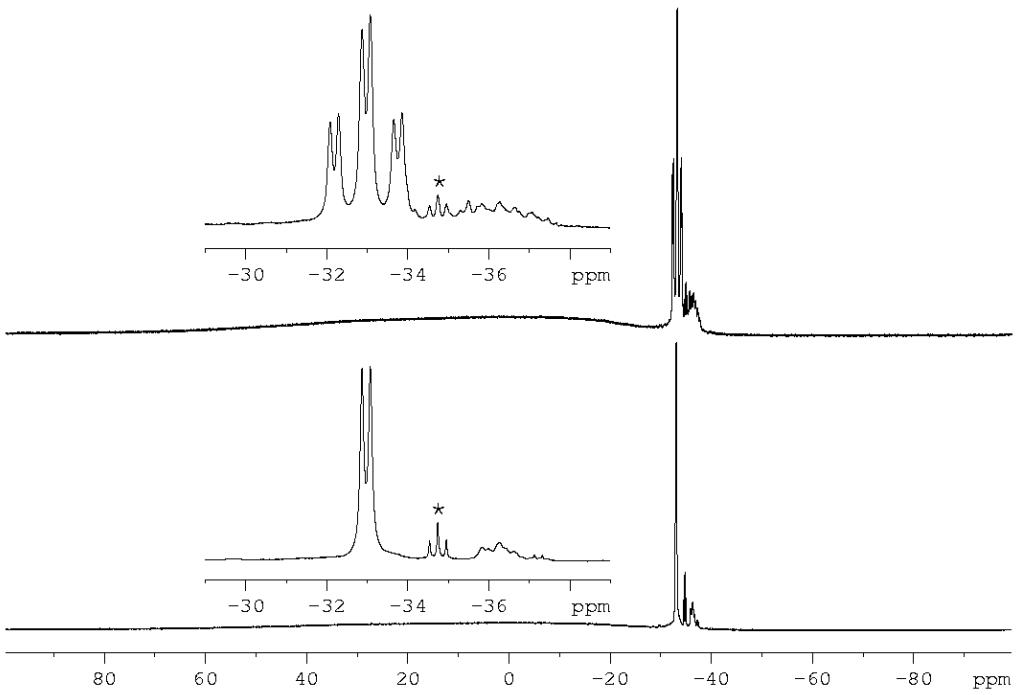

Figure S 5.15. $^{11}B\{^1H\}$ (bottom) and ^{11}B NMR spectrum (top) of **5** in THF-d_8. * = $[H_2P\text{-}BH_2\text{-}PH_2]^-$.

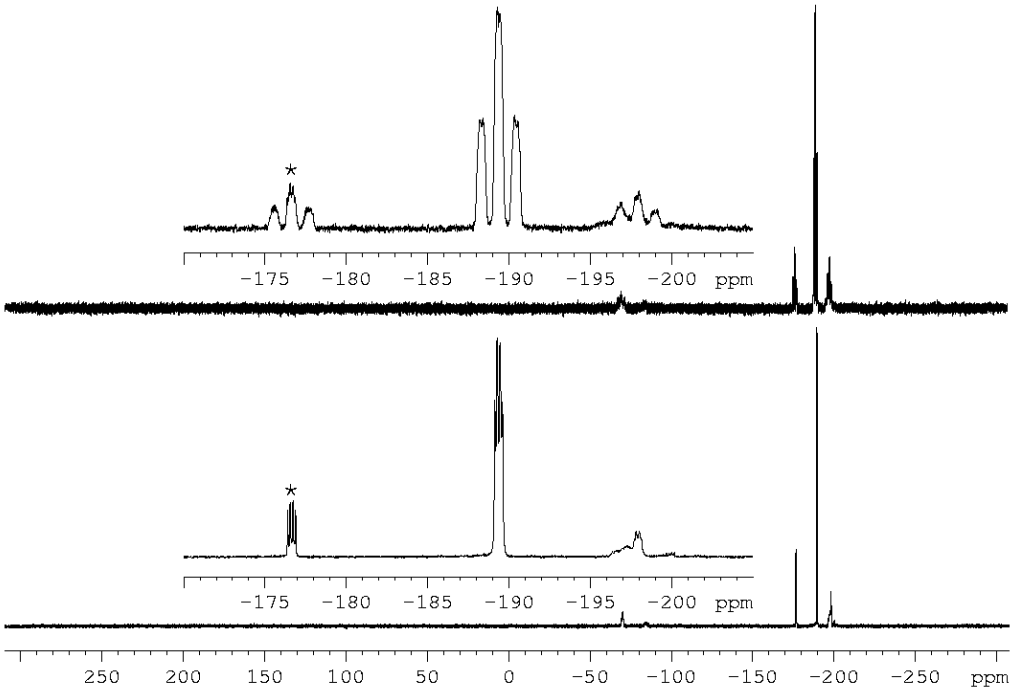

Figure S 5.16. $^{31}P\{^{1}H\}$ (bottom) and ^{31}P NMR spectrum (top) of **5** in THF-d_8. * = $[H_2P\text{-}BH_2\text{-}PH_2]^-$.

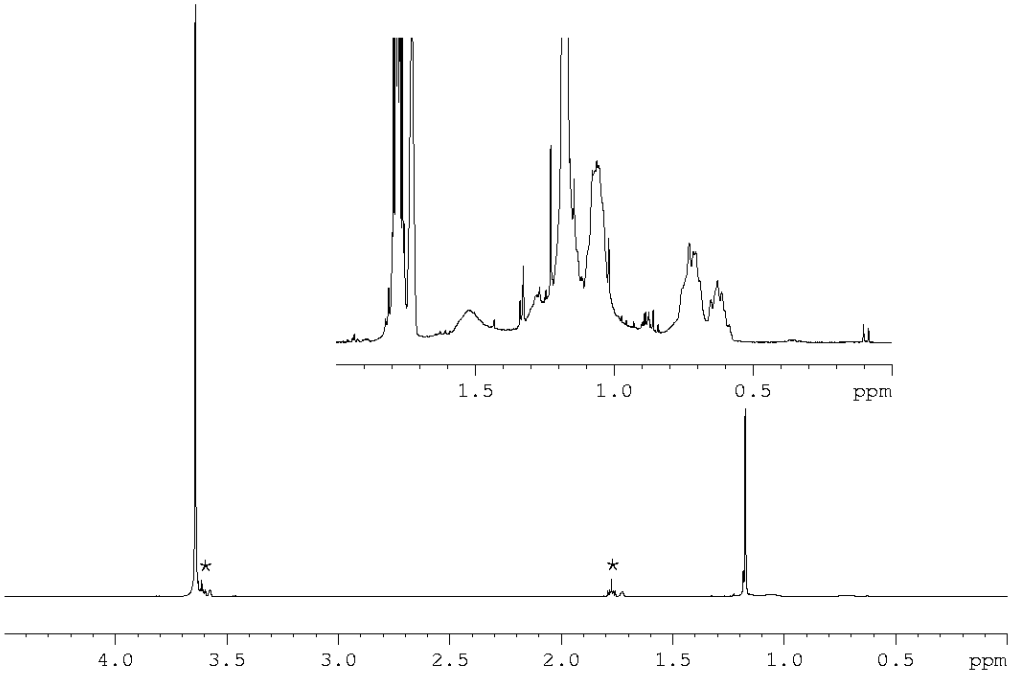

Figure S 5.17. ^{1}H NMR spectrum of **5** in THF-d_8. * = solvent (THF-d_8).

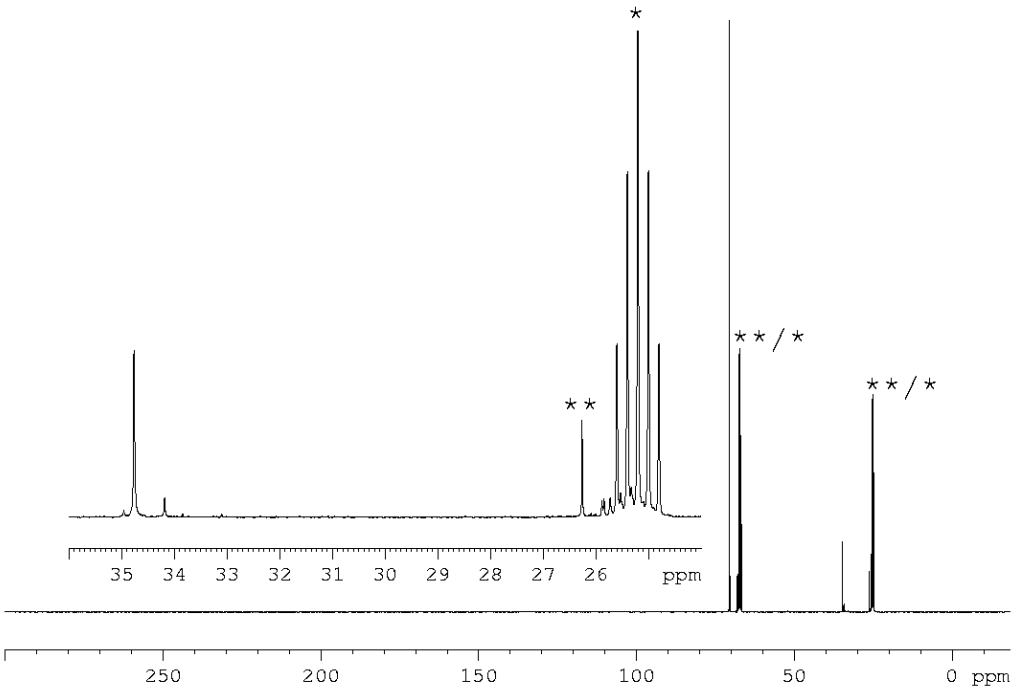

Figure S 5.18. ^{13}C NMR spectrum of **5** in THF-d_8. * = solvent (THF-d_8), ** = solvent (THF).

$[Na(C_{12}H_{24}O_6)(thf)_2][H_2As\text{-}BH_2\text{-}^tBuPH\text{-}BH_3]$ (**6**(thf)$_2$):

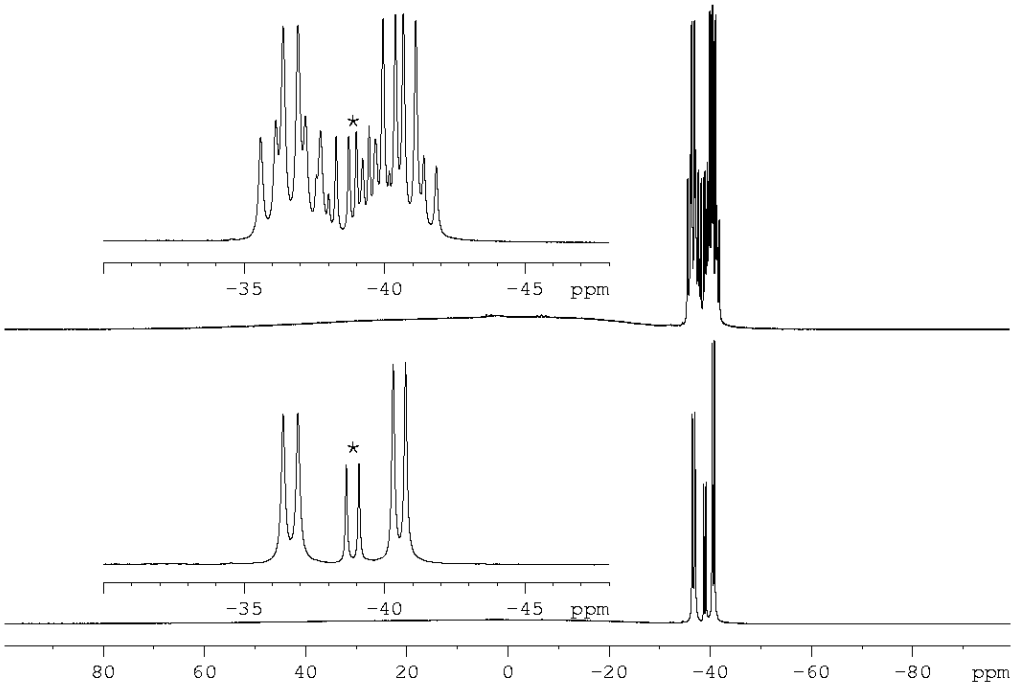

Figure S 5.19. $^{11}B\{^1H\}$ (bottom) and ^{11}B NMR spectrum (top) of **6** in THF-d_8. * = $[H_3B\text{-}^tBuPH\text{-}BH_3]^-$.

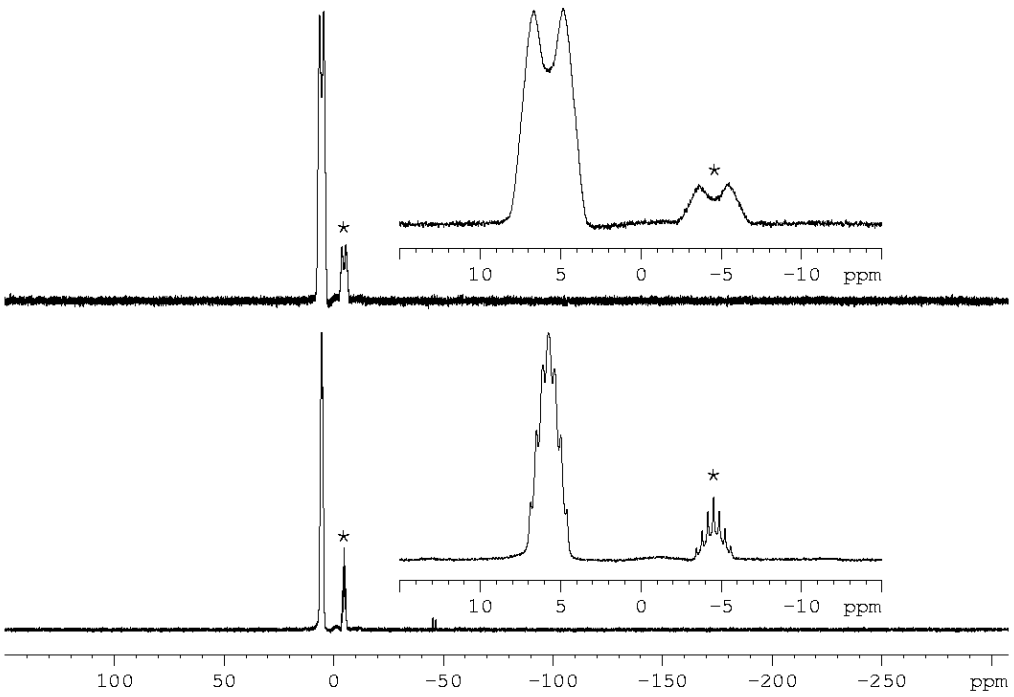

Figure S 5.20. $^{31}P\{^{1}H\}$ (bottom) and ^{31}P NMR spectrum (top) of **6** in THF-d_8. * = $[H_3B\text{-}^{t}BuPH\text{-}BH_3]^-$.

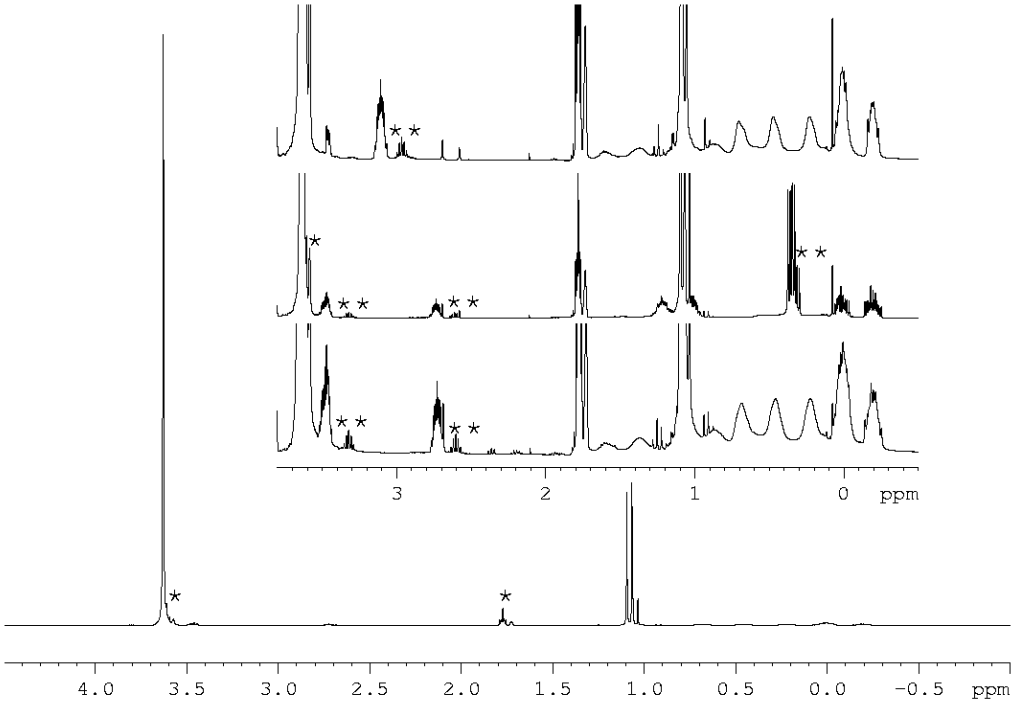

Figure S 5.21. ^{1}H NMR spectrum of **6** in THF-d_8. * = solvent (THF-d_8), ** = $[H_3B\text{-}^{t}BuPH\text{-}BH_3]^-$. Magnified part shows ^{1}H, $^{1}H\{^{11}B\}$, $^{1}H\{^{31}P\}$ NMR (from bottom to top) of the anion.

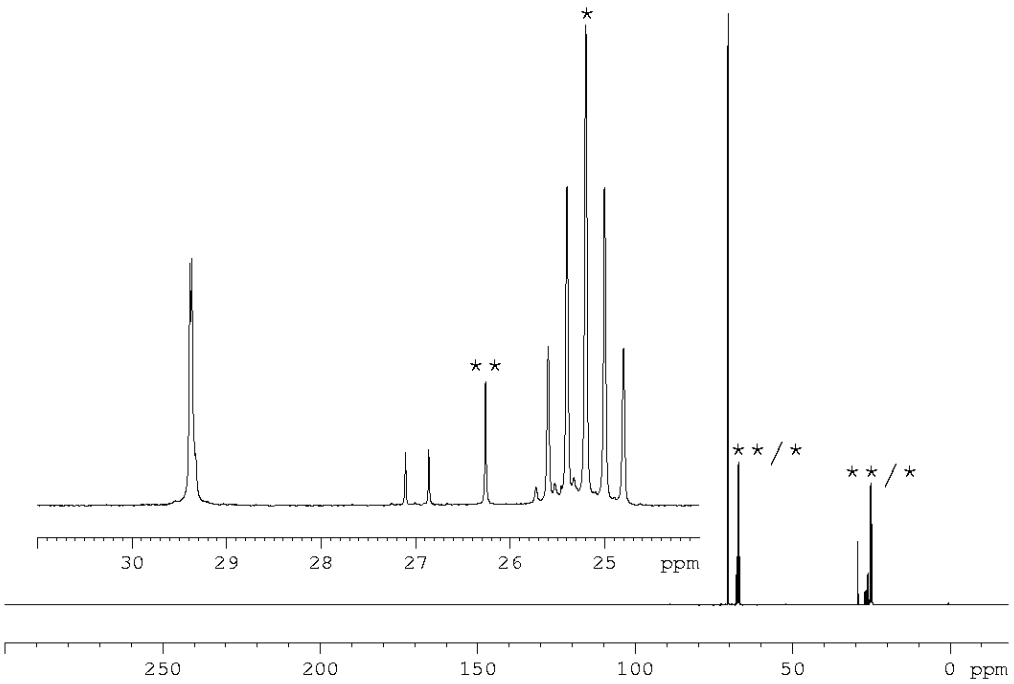

Figure S 5.22. ^{13}C NMR spectrum of **6** in THF-d_8. * = solvent (THF-d_8), ** = solvent (THF).

$[Na(C_{12}H_{24}O_6)(thf)_2][H_2P\text{-}BH_2\text{-}PPh_2]$ $(7(thf)_2)$:

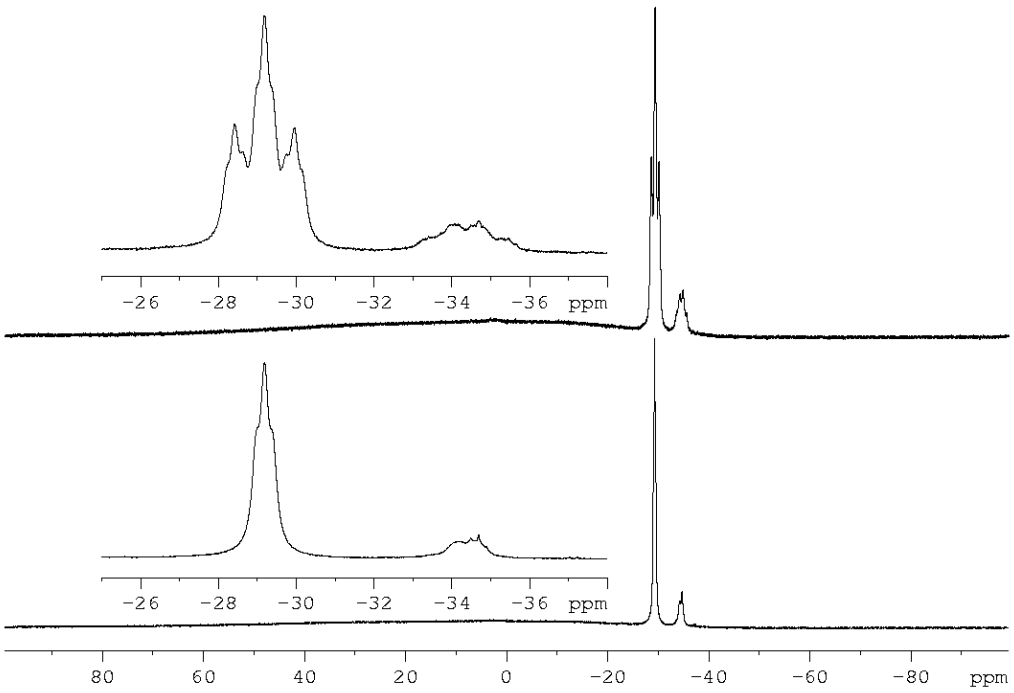

Figure S 5.23. $^{11}B\{^1H\}$ (bottom) and ^{11}B NMR spectrum (top) of **7** in THF-d_8.

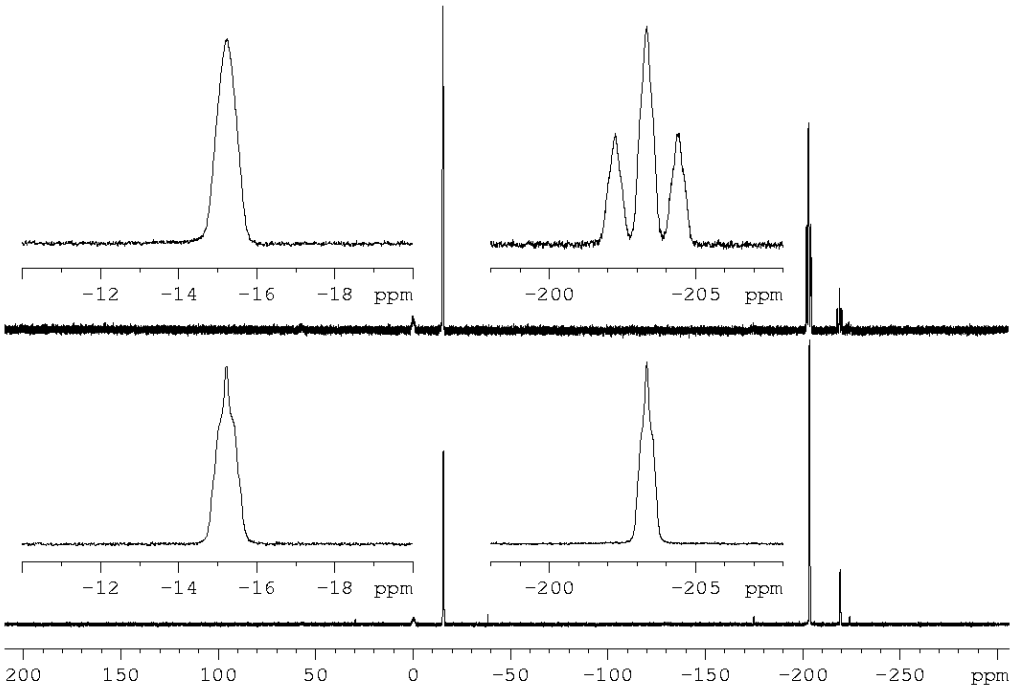

Figure S 5.24. $^{31}P\{^{1}H\}$ (bottom) and ^{31}P NMR spectrum (top) of **7** in THF-d_8.

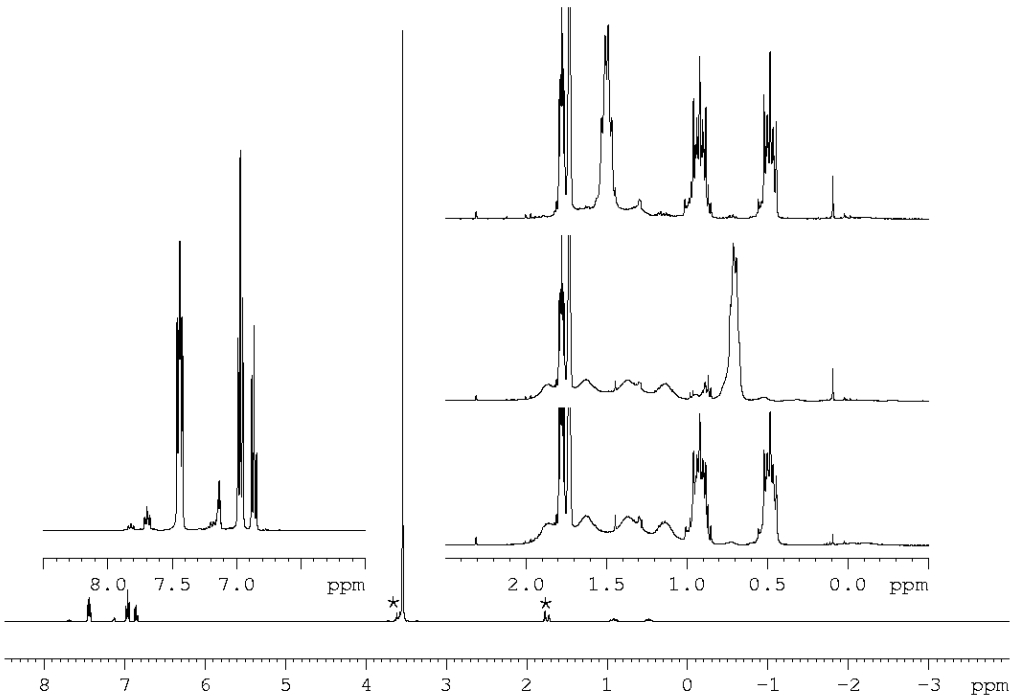

Figure S 5.25. ^{1}H NMR spectrum of **7** in THF-d_8. * = solvent (THF-d_8).
Magnified part shows ^{1}H, $^{1}H\{^{31}P\}$, $^{1}H\{^{11}B\}$ NMR (right, from bottom to top) of the anion.

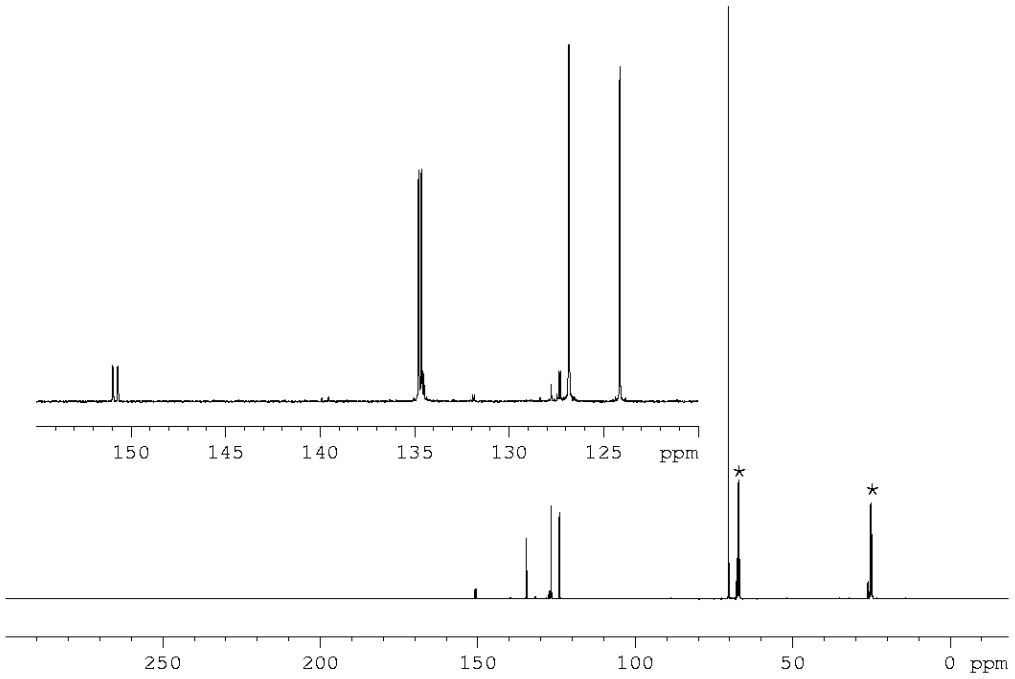

Figure S 5.26. ^{13}C NMR spectrum of **7** in THF-d_8. * = solvent (THF-d_8).

$[K(C_{12}H_{24}O_6)(thf)_2][H_2As\text{-}BH_2\text{-}AsPh_2]$ $(8(thf)_2)$:

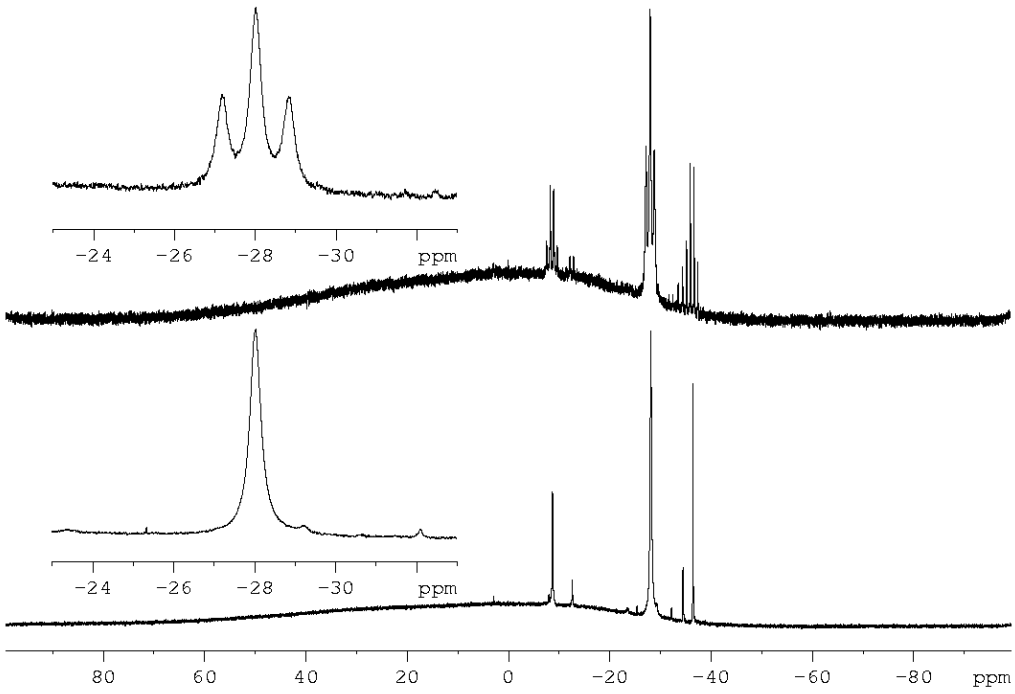

Figure S 5.27. $^{11}B\{^1H\}$ (bottom) and ^{11}B NMR spectrum (top) of **8** in THF-d_8.

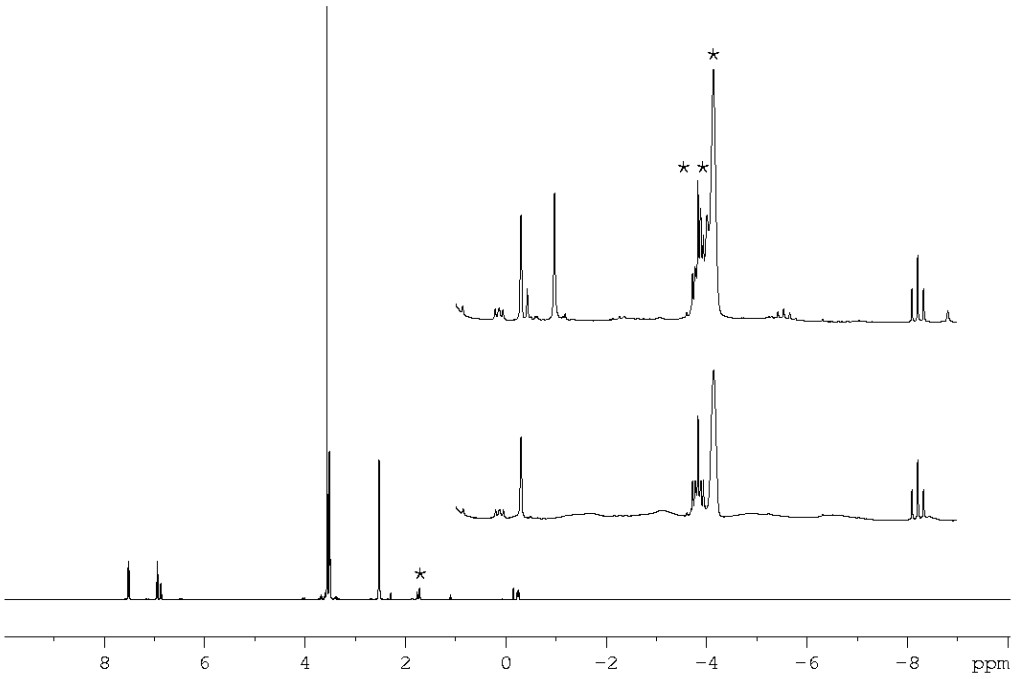

Figure S 5.28. ^{1}H NMR spectrum of **8** in THF-d_8. * = solvent (THF-d_8), ** solvent (THF). Magnified part shows ^{1}H, ^{1}H{^{11}B} NMR (from bottom to top) of the anion.

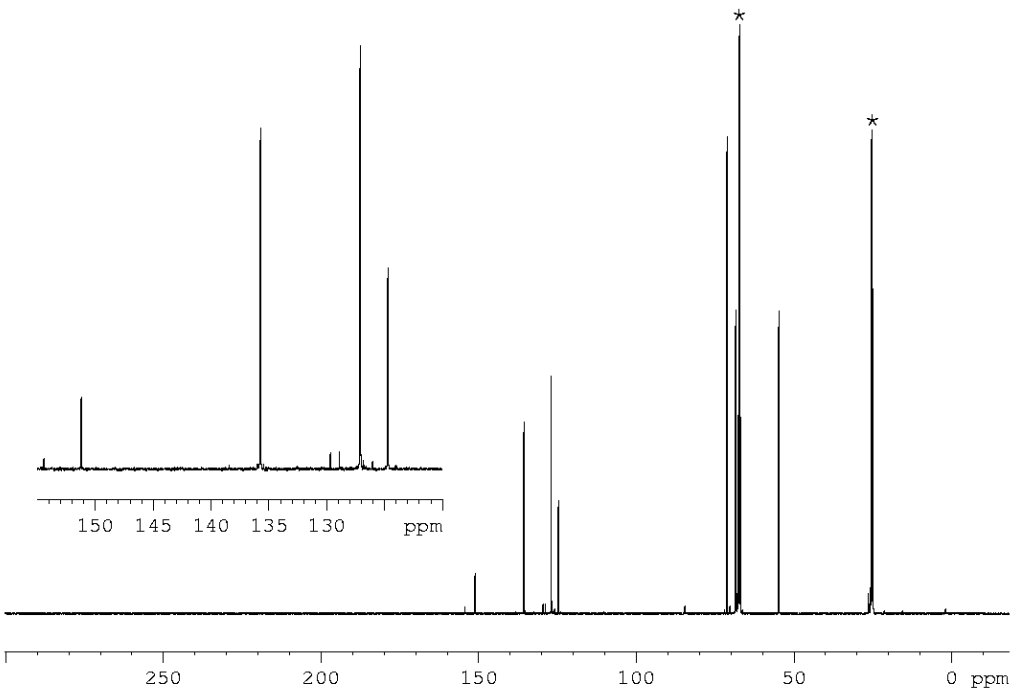

Figure S 5.29. ^{13}C NMR spectrum of **8** in THF-d_8. * = solvent (THF-d_8).

$[Na(C_{18}H_{36}N_2O_6)][H_2As\text{-}BH_2\text{-}PPh_2]$ (9):

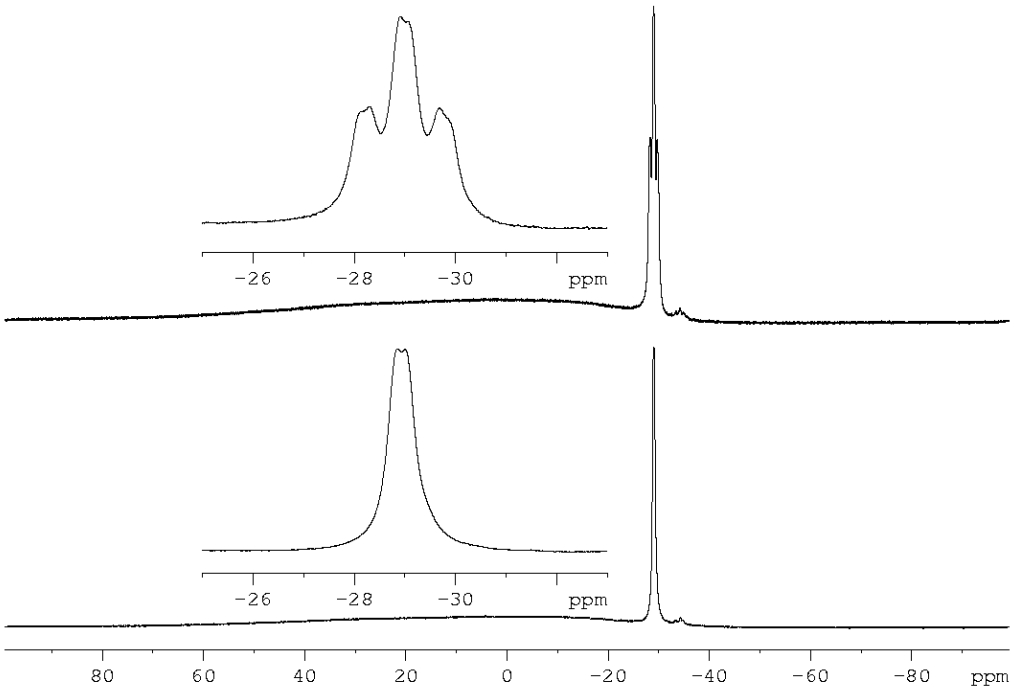

Figure S 5.30. $^{11}B\{^1H\}$ (bottom) and ^{11}B NMR spectrum (top) of **9** in THF-d_8.

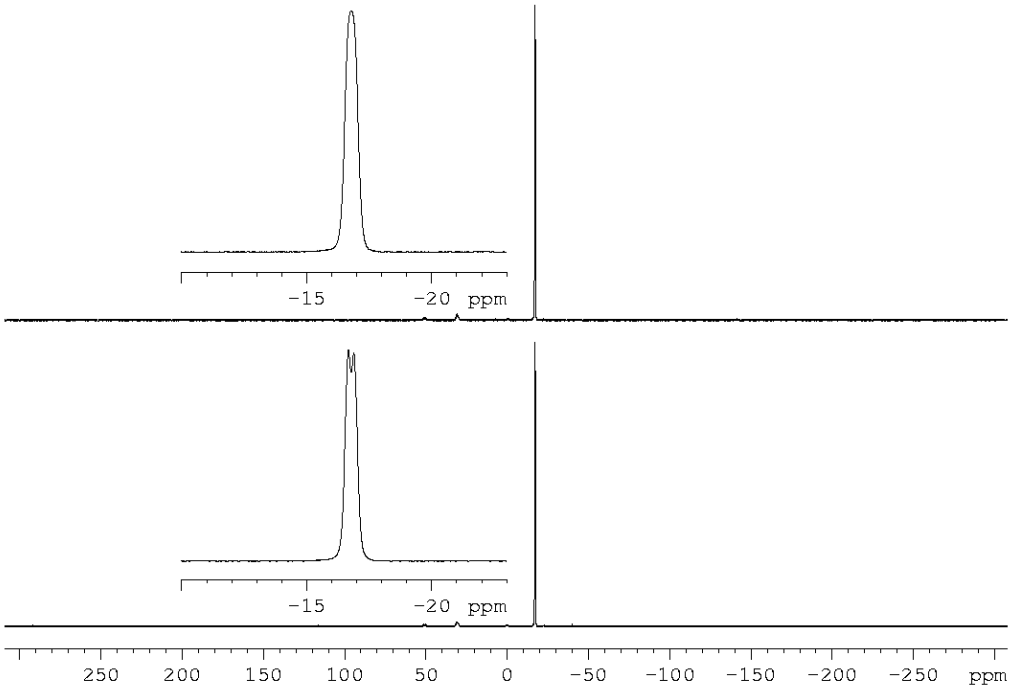

Figure S 5.31. $^{31}P\{^1H\}$ (bottom) and ^{31}P NMR spectrum (top) of **9** in THF-d_8.

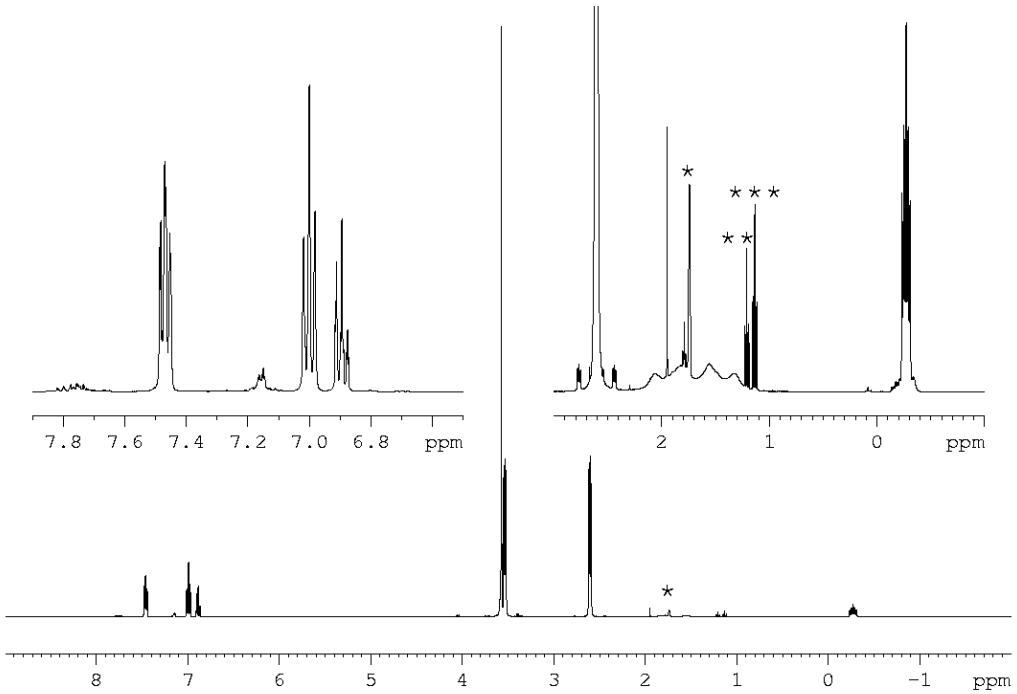

Figure S 5.32. ^{1}H NMR spectrum of **9** in THF-d_8. * = solvent (THF-d_8), ** = ethyl acetate, *** = diethyl ether.

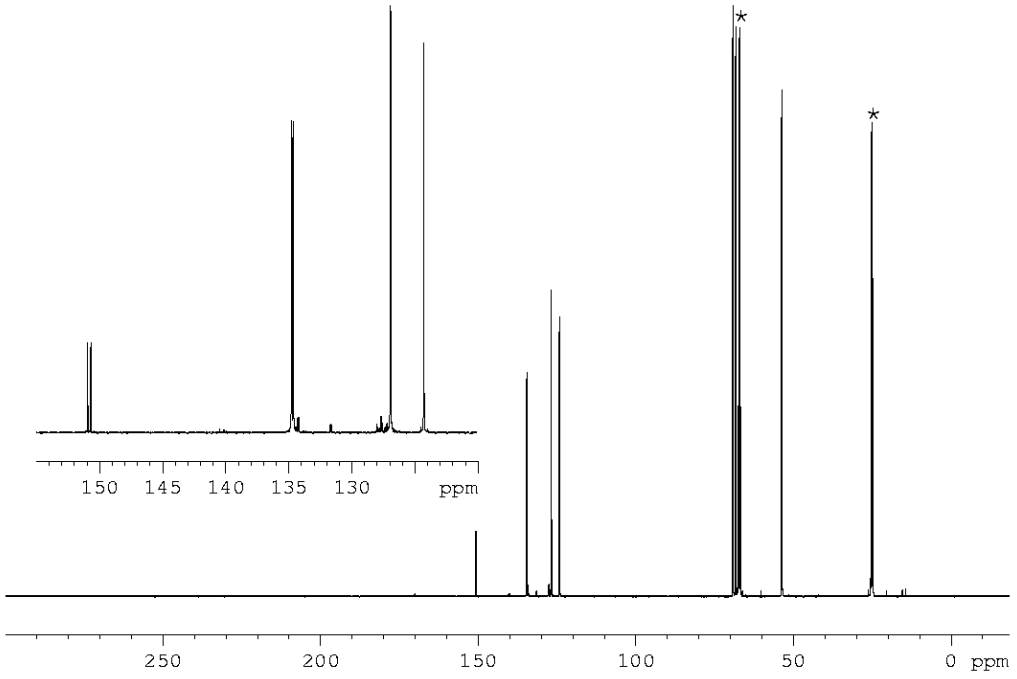

Figure S 5.33. ^{13}C NMR spectrum of **9** in THF-d_8. * = solvent (THF-d_8).

$[K(C_{18}H_{36}N_2O_6)][H_2P\text{-}BH_2\text{-}AsPh_2]$ (10):

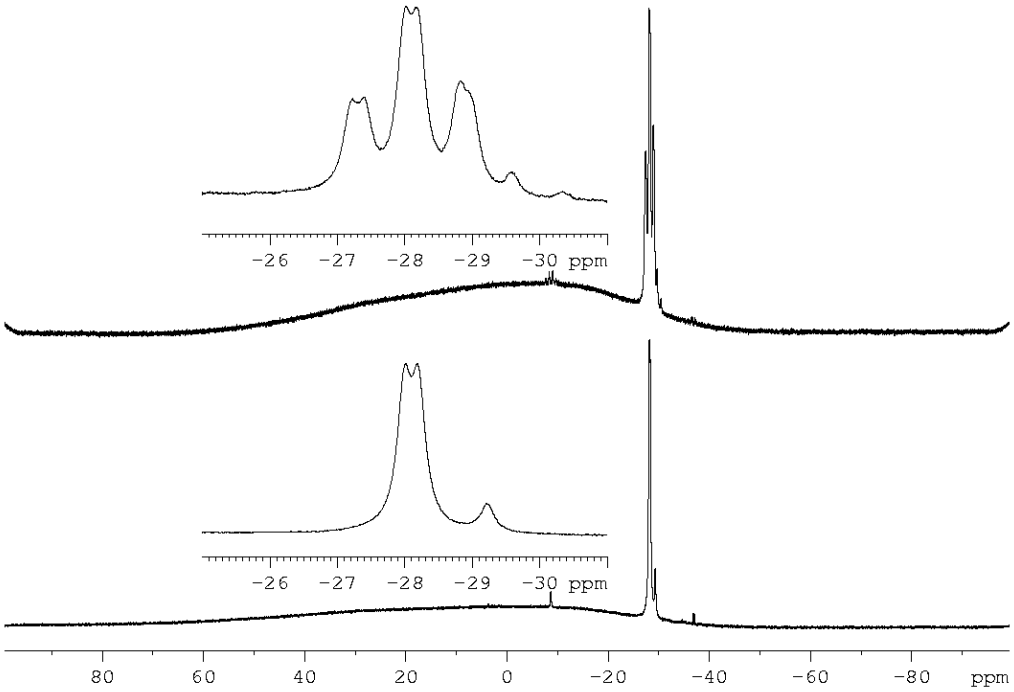

Figure S 5.34. $^{11}B\{^1H\}$ (bottom) and ^{11}B NMR spectrum (top) of **10** in THF-d_8.

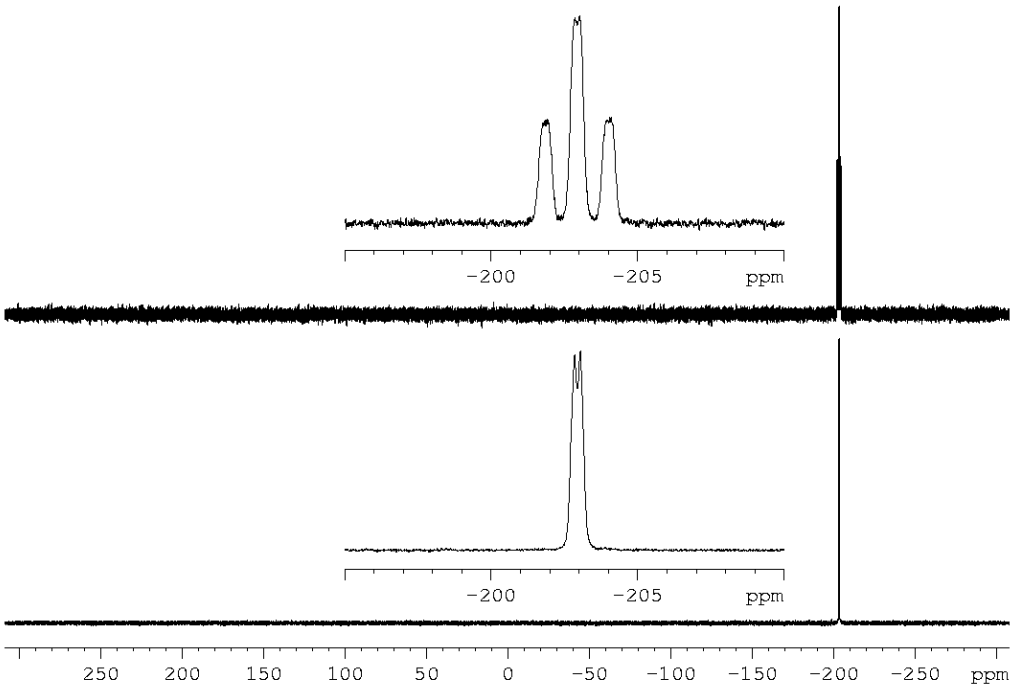

Figure S 5.35. $^{31}P\{^1H\}$ (bottom) and ^{31}P NMR spectrum (top) of **10** in THF-d_8.

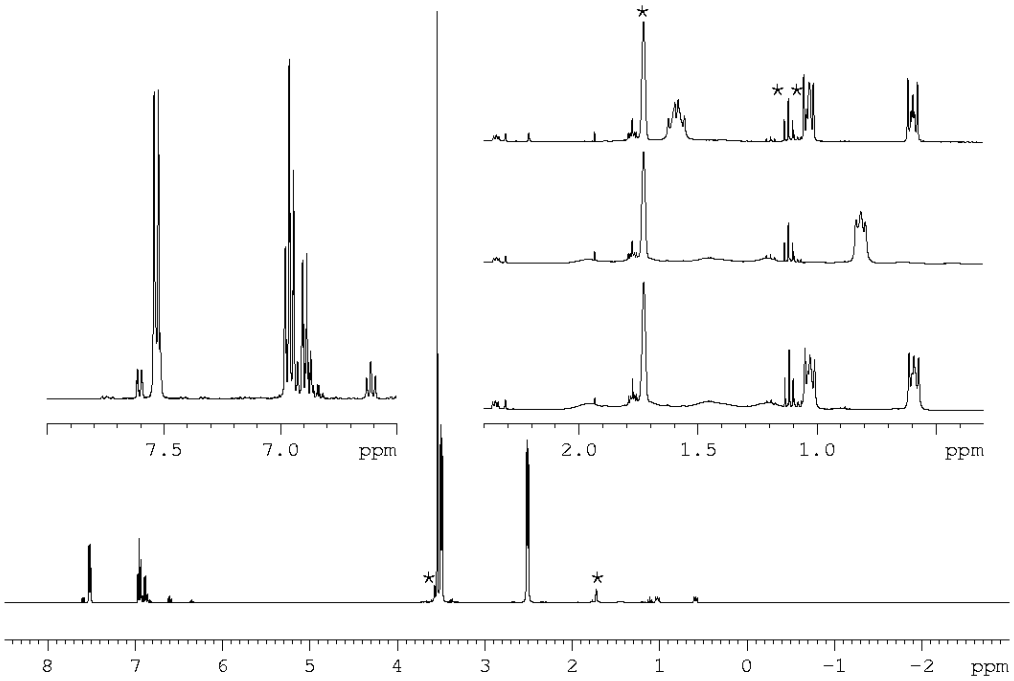

Figure S 5.36. ^{1}H NMR spectrum of **10** in THF-d_8. * = solvent (THF-d_8), ** = diethyl ether. Magnified part shows ^{1}H, ^{1}H{^{31}P}, ^{1}H{^{11}B} NMR (right, from bottom to top) of the anion.

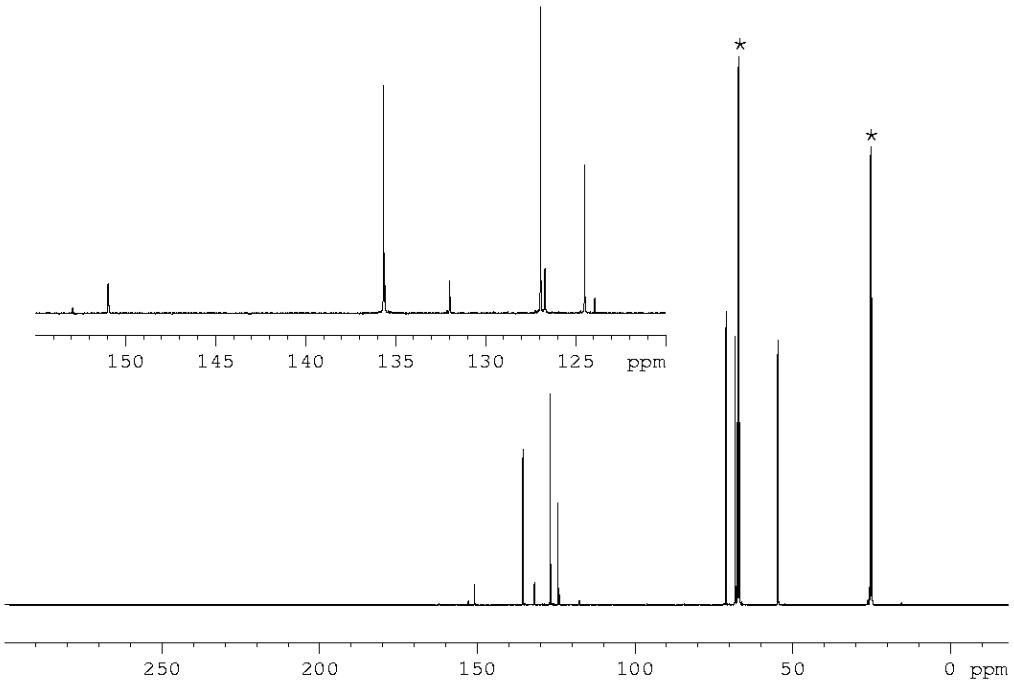

Figure S 5.37. ^{13}C NMR spectrum of **10** in THF-d_8. * = solvent (THF-d_8).

$[Na(C_{12}H_{24}O_6)(thf)_2][Ph_2P\text{-}BH_2\text{-}PPh_2]$ $(11(thf)_2)$:

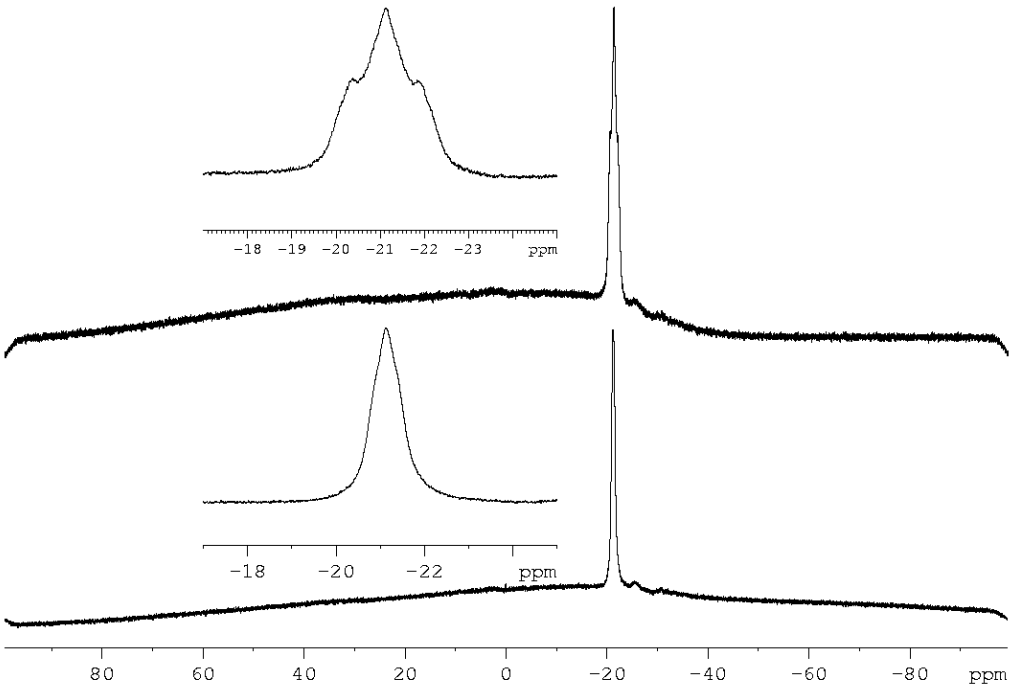

Figure S 5.38. $^{11}B\{^1H\}$ (bottom) and ^{11}B NMR spectrum (top) of **11** in THF-d_8.

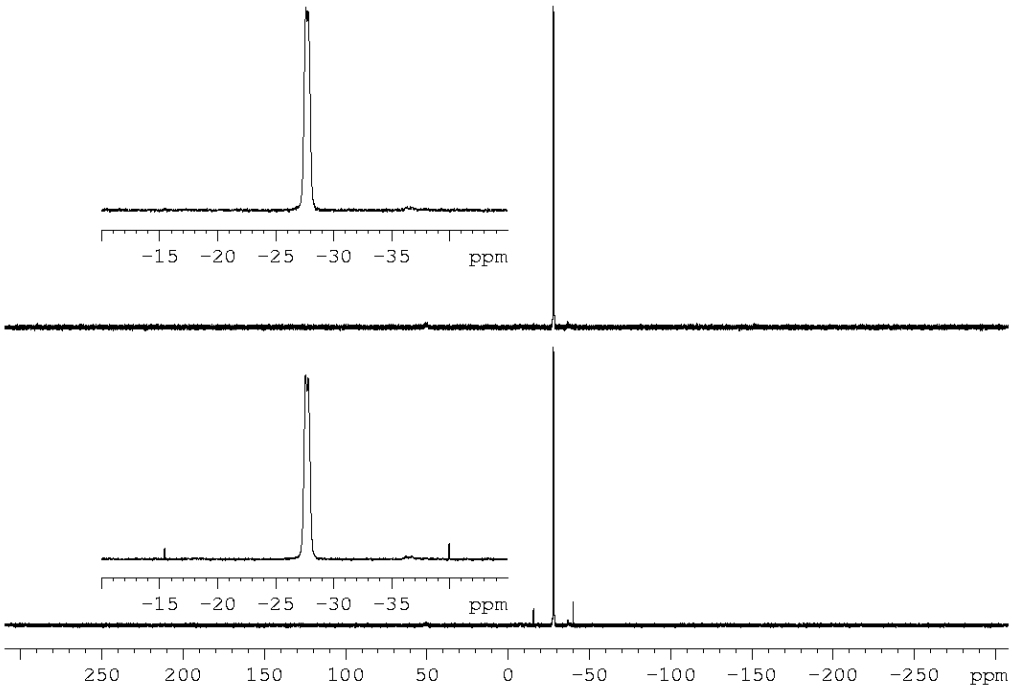

Figure S 5.39. $^{31}P\{^1H\}$ (bottom) and ^{31}P NMR spectrum (top) of **11** in THF-d_8.

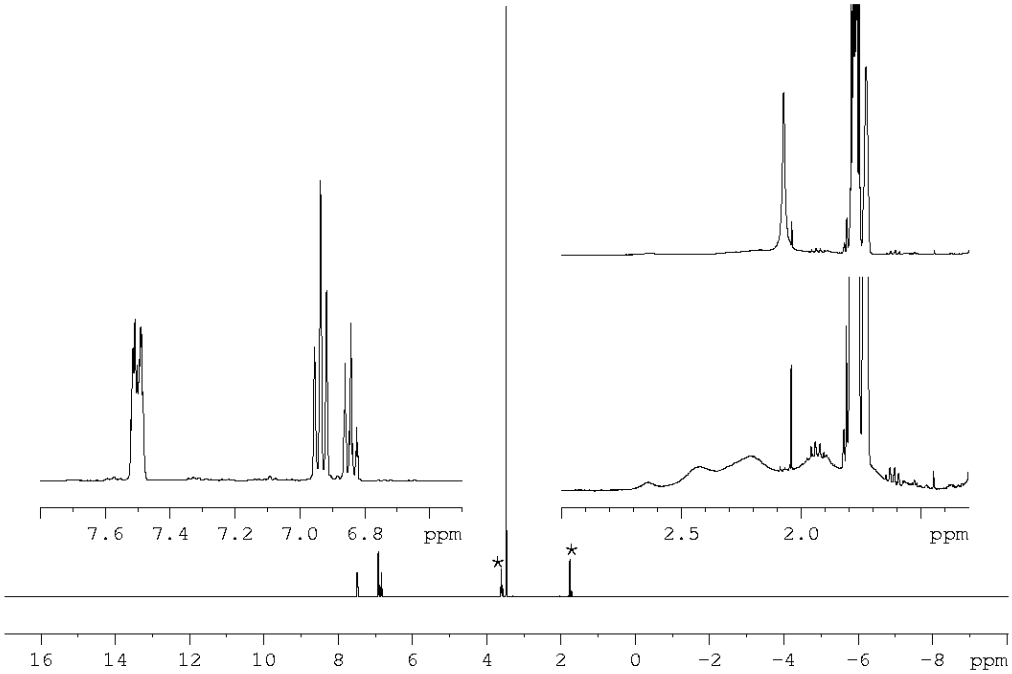

Figure S 5.40. ^{1}H NMR spectrum of **11** in THF-d_8. * = solvent (THF-d_8).
Magnified part shows ^{1}H, ^{1}H{^{11}B} NMR (right, from bottom to top) of the anion.

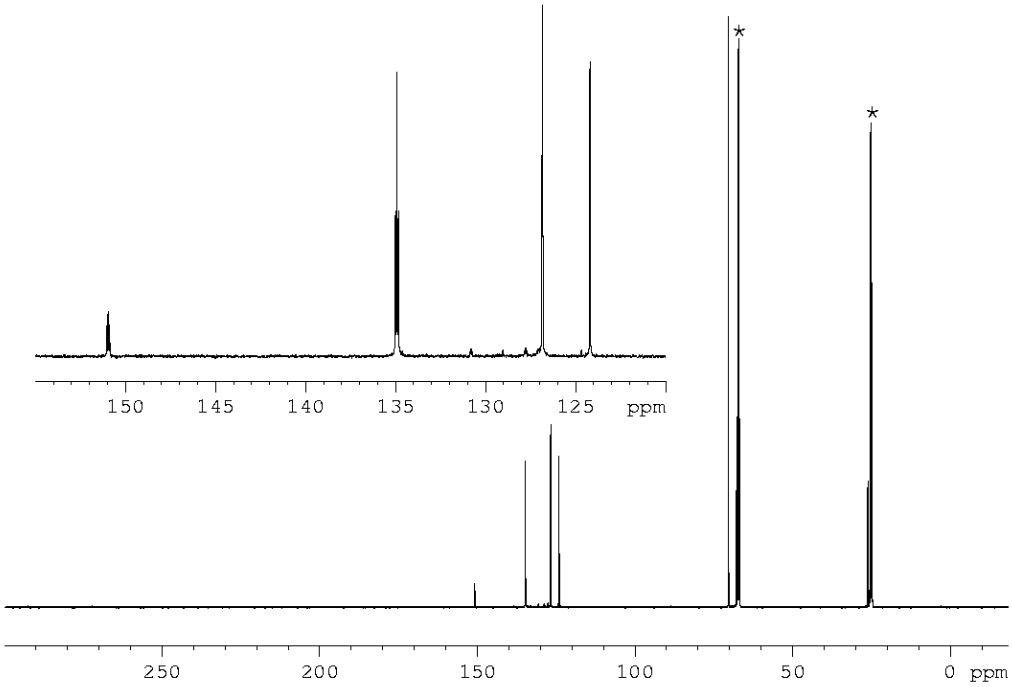

Figure S 5.41. ^{13}C NMR spectrum of **11** in THF-d_8. * = solvent (THF-d_8).

$[K(C_{12}H_{24}O_6)(thf)_2][Ph_2As\text{-}BH_2\text{-}AsPh_2]$ $(12(thf)_2)$:

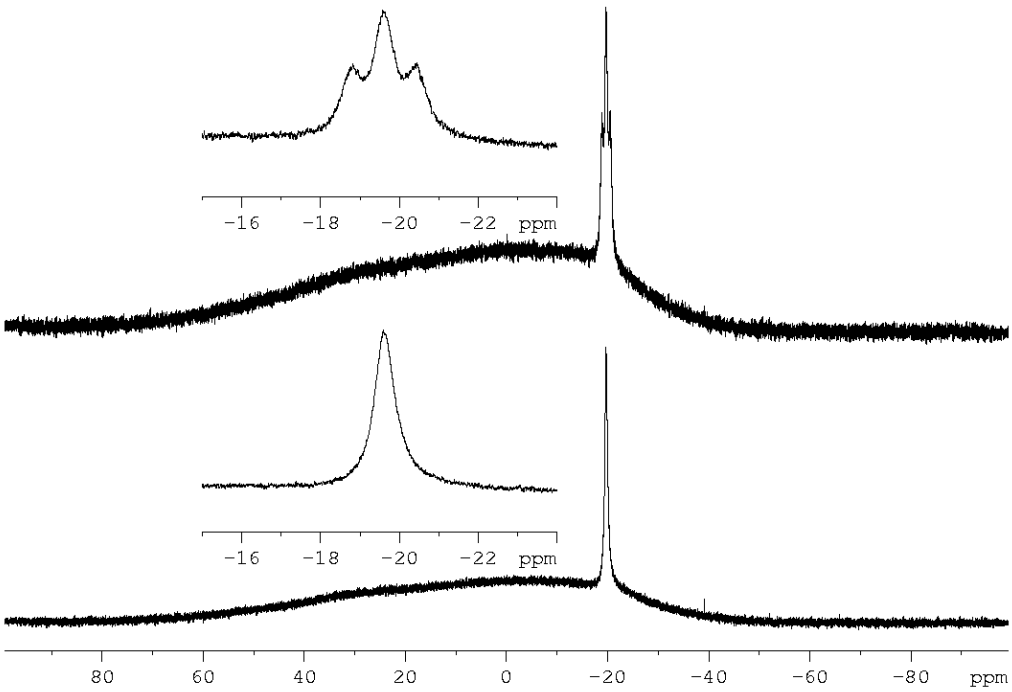

Figure S 5.42. $^{11}B\{^1H\}$ (bottom) and ^{11}B NMR spectrum (top) of **12** in THF-d_8.

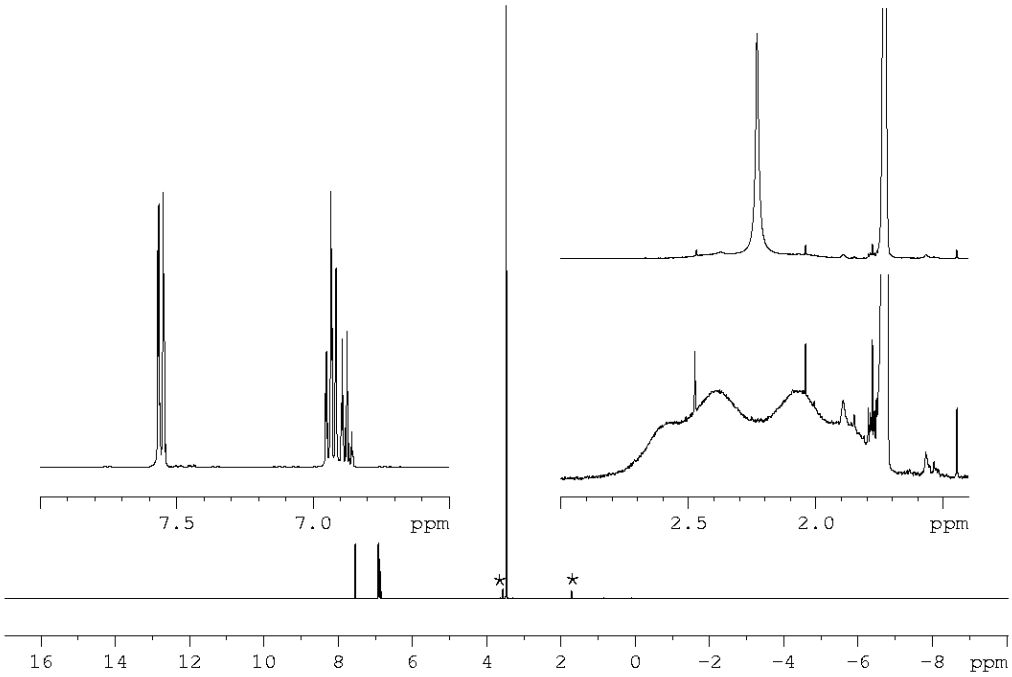

Figure S 5.43. ^1H NMR spectrum of **12** in THF-d_8. * = solvent (THF-d_8).
Magnified part shows ^1H, $^1H\{^{11}B\}$ NMR (right, from bottom to top) of the anion.

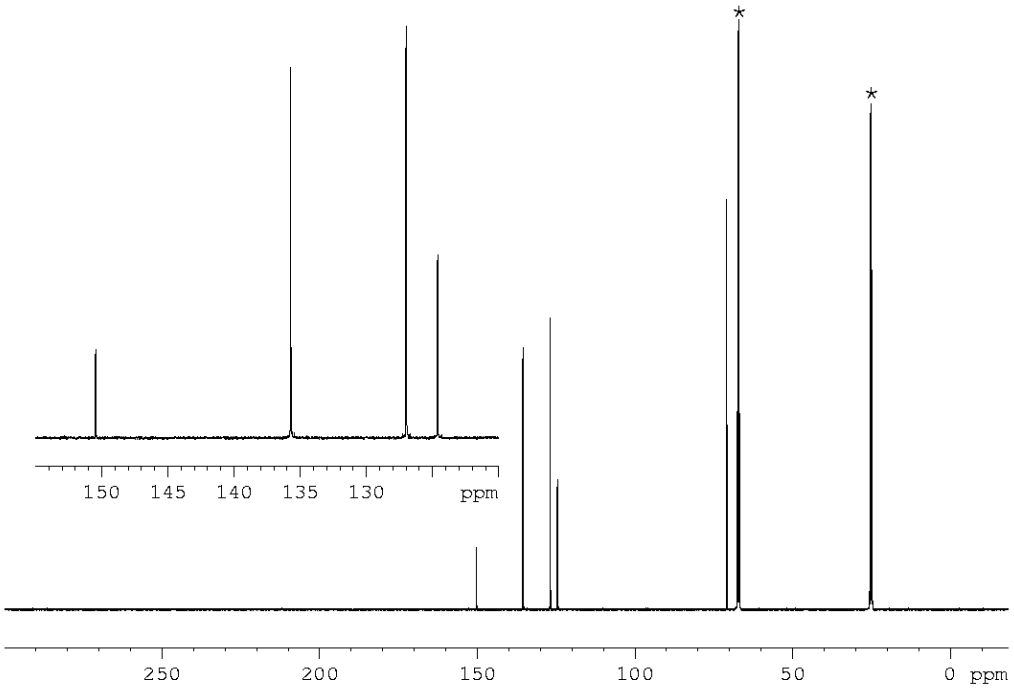

Figure S 5.44. ^{13}C NMR spectrum of **12** in THF-d_8. * = solvent (THF-d_8).

5.5.6 References

[1] C. Marquardt, A. Adolf, A. Stauber, M. Bodensteiner, A. V. Virovets, A. Y. Timoshkin, M. Scheer, *Chem. Eur. J.* **2013***, 19*, 11887-11891.

[2] A. Tzschach, W. Lange, *Chem. Ber.* **1962**, *95*, 1360-1366. The obtained $KAsPh_2$ contains 0.625 equivalents of 1,4-Dioxane.

[3] C. Marquardt, T. Jurca, K.-C. Schwan, A. Stauber, A. V. Virovets, G. R. Whittell, I. Manners, M. Scheer, *Angew. Chem. Int. Ed.* **2015**, *54*, 13782-13786; *Angew. Chem.* **2015***, 127,* 13986-13991.

[4] Clark, R. C. & Reid, J. S., *Acta Cryst.* **1995**, *A51*, 887-897.

[5] Agilent Technologies **2014-2017**, CrysAlisPro Software system, different versions, Agilent Technologies UK Ltd, Oxford, UK.

[6] A. Altomare, M. C.Burla, M. Camalli, G. L. Cascarano, C. Giacovazzo, A. Guagliardi, A.G. G. Moliterni, G. Polidori, R. Spagna, *J. Appl. Cryst.* **1999**, *32*, 115-119.

[7] G.M. Sheldrick, ShelXT-Integrated space-group and crystal-structure determination, *Acta Cryst.* **2015**, *A71*, 3-8.

[8] O.V. Dolomanov and L.J. Bourhis and R.J. Gildea and J.A.K. Howard and H. Puschmann, Olex2: A complete structure solution, refinement and analysis program, *J. Appl. Cryst.* **2009**, *42*, 339-341.

[9] Sheldrick, G.M., Crystal structure refinement with ShelXL, *Acta Cryst.* **2015**, *C71*, 3-8.

Preface

The following chapter has been compiled for future publication.

Authors

Tobias Kahoun, Christian Marquardt, Michael Bodensteiner, Alexey Y. Timoshkin, A. V. Virovets, Manfred Scheer.

Author contributions

The synthesis and characterization of compounds **3**, **4**, **5** were performed by Tobias Kahoun.
The synthesis and characterization of compounds **2** was performed by Dr. Christian Marquardt. This compound has been reported in his PhD-thesis (Regensburg, **2015**).

X-ray structural analyses of **3**$(thf)_2$, **4**$(thf)_2$, **5**$(thf)_2$ were performed by Tobias Kahoun and Dr. Michael Bodensteiner.
X-ray structural analyses of **2**$(thf)_2$ was performed by Dr. Christian Marquardt and Dr. Alexander V. Virovets. This compound has been reported in his PhD-thesis (Regensburg, **2015**).

DFT-calculations were performed by Prof. Dr. Alexey Y. Timoshkin (St. Petersburg State University).

The manuscript (including supporting information, figures, schemes and graphical abstract) was written by Tobias Kahoun with contributions by Dr. Christian Marquardt (supporting information).

6 Five Membered Substituted Anionic Derivatives of Parent Pnictogenylboranes

Tobias Kahoun, Christian Marquardt, Michael Bodensteiner, A. V. Virovets, Manfred Scheer.

Abstract: We report on the synthesis and characterization of anionic five membered organosubstituted pnictogenylborane derivatives. The reaction of three membered substituted anionic pnictogenylborane derivatives of the type $[Na(C_{12}H_{24}O_6)][H_2E\text{-}BH_2\text{-}PR^1R^2]$ (**1a**: E = P, $R^1 = R^2$ = Ph; **1b**: E = As, $R^1 = R^2$ = Ph; **1c**: E = P, R^1 = H, $R^2 = {}^t$Bu) with parent trimethylamine (NMe_3) stabilized pnictogenylboranes $H_2E\text{-}BH_2\text{-}NMe_3$ leads to an elongation of the pnictogen boron backbone. The formation of the corresponding anionic five membered chain like compounds $[Na(C_{12}H_{24}O_6)][H_2P\text{-}BH_2\text{-}PPh_2\text{-}BH_2\text{-}PH_2]$ (**2**), $[Na(C_{12}H_{24}O_6)][H_2As\text{-}BH_2\text{-}PPh_2\text{-}BH_2\text{-}AsH_2]$ (**3**), $[Na(C_{12}H_{24}O_6)][H_2P\text{-}BH_2\text{-}PPh_2\text{-}BH_2\text{-}AsH_2]$ (**4**) and $[Na(C_{12}H_{24}O_6)][H_2P\text{-}BH_2\text{-}{}^t\text{BuPH}\text{-}BH_2\text{-}PH_2]$ (**5**) can be observed.

All compounds were characterized by single crystal X-ray diffractions as well as by multinuclear NMR spectroscopy, mass spectrometry and IR spectroscopy.

6.1 Introduction

Beside carbon based organic substrates like ethylene, monomeric compounds containing group 13 and 15 atoms reveal to be suitable alternatives for polymerizations. Over the last decades the interest in catenation of such compounds increases. Especially ethane analog inorganic monomers like ammonia borane (H_3N-BH_3) or substituted derivatives are used as substrates in metal catalyzed dehydrocoupling reactions.[1] Despite the lower thermal stability H_3P-BH_3 was successfully polymerized using catalytical amounts of $B(C_6F_5)_3$.[2] High molecular weight polymers containing a P-B backbone are accessible by metal catalyzed dehydrocoupling reactions using saturated organosubsituted phosphinoboranes as substrates.[3] A route to a catalyst free polymerization was achieved by our group using organosubstiuted Lewis base stabilized phosphanylboranes as building blocks.[4] These unsaturated monomers tend to spontaneous head to tail polymerization. Corresponding polymers containing an arsenic boron backbone are completely unknown so far. Lower molecular weight oligomers containing at least a six membered nitrogen boron backbone are clearly dominated by cyclic compounds like borazine.[5] Beside synthesis of functionalized borazine derivatives (**I**)[6], the group of *Pringle* reported about the synthesis of an inorganic version of the triphenylphosphine by linking three borazinyl substituents to a phosphorus atom (**II**)[7].

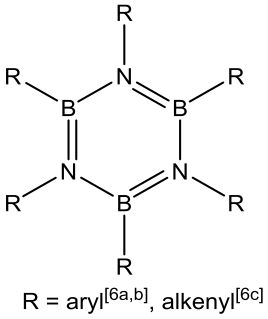

I

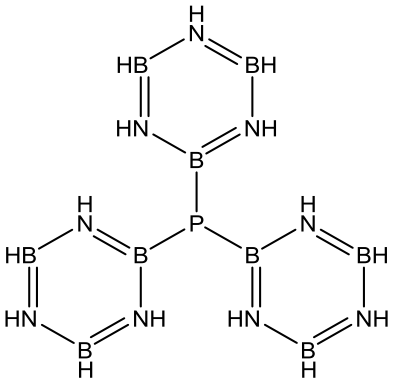

II

The hydrogen substituted phosphorus containing borazin analog compound, the boraphosphinine, is unknown so far. Due to thermal instability investigations of this compound are restricted to theoretical studies.[8] An isolable boraphosphinine derivative (**III**) is accessible by substitution of all hydrogen atoms with bulkier organic residues.[9] An alternative synthetic route using less bulkier amine substituents is reported by *Nöth* and *Paine* (**IV**).[10]

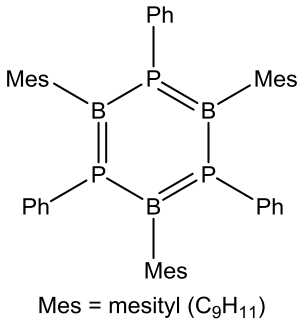

Mes = mesityl (C_9H_{11})

III

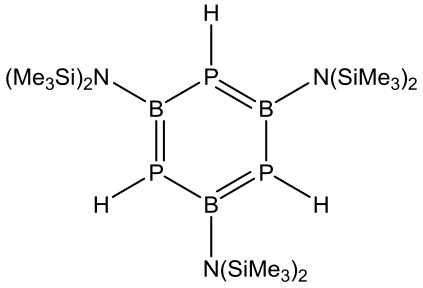

IV

Focusing on linear oligomers containing at least a five membered E-B-E-B-E backbone (E = N[11], E = P[12]) only few example are known in literature. In case of arsenic and boron containing oligomers neither cyclic nor linear containing compounds are known of this length with exception of the cationic species $[Me_3N\text{-}BH_2\text{-}AsR^1R^2\text{-}BH_2\text{-}AsR^1R^2\text{-}BH_2\text{-}NMe_3]I$ (R^1 = R^2 = H, Ph)[13] and an anionic chain like compound $Na[H_2As\text{-}BH_2\text{-}PH_2\text{-}BH_2\text{-}AsH_2]$.[14] The anionic five membered compound is accessible by reaction of Lewis base stabilized arsanylborane with the three membered anionic species $Na[H_2As\text{-}BH_2\text{-}PH_2]$. We recently reported about the synthesis of corresponding three membered organosubstituted compounds of the type $M[H_2E\text{-}BH_2\text{-}ER^1R^2]$ (E = P, As; R^1 = H, ^{t}Bu, Ph; R^2 = H, Ph; M = Na, K).[15] Therefore, we perfomed investigations for the elongation of the 13/15 backbone of such organosubstituted compounds with Lewis base stabilized pnictogenylboranes. Here we present the controlled synthesis of linear, five membered anionic chain like compounds containing terminal arsine groups.

6.2 Result and Discussion

Reaction of $H_2E\text{-}BH_2\text{-}NMe_3$ (E = P, As) with nucleophiles of type $NaPR^1R^2$ (R^1 = R^2 = Ph, R^1 = H, R^2 = ^{t}Bu) with subsequent addition of 18-crown-6 ($C_{12}H_{24}O_6$) leads to formation of the three membered asymmetric anionic chain like compounds $[Na(C_{12}H_{24}O_6)][H_2E\text{-}BH_2\text{-}PR^1R^2]$ (**1a**: E = P, R^1 = R^2 = Ph; **1b**: E = As, R^1 = R^2 = Ph; **1c**: E = P, R^1 = H, R^2 = ^{t}Bu).[15] Adding equivalent amounts of $H_2E\text{-}BH_2\text{-}NMe_3$ (E = P, As) to solutions of **1a**, **1b** and **1c** the desired five membered derivatives are accessible in moderate to good yields.

Sonication of **1a** and **1b** with one equivalent of Lewis base stabilized phosphanyl- and arsanylborane, respectively, leads to the formation of compounds **2** and **3**. Stirring solutions of **1a** and **1c** with one

equivalent of $H_2As\text{-}BH_2\text{-}NMe_3$ at room temperature is sufficient for the formation of compounds **4** and **5** (Scheme 6.1).

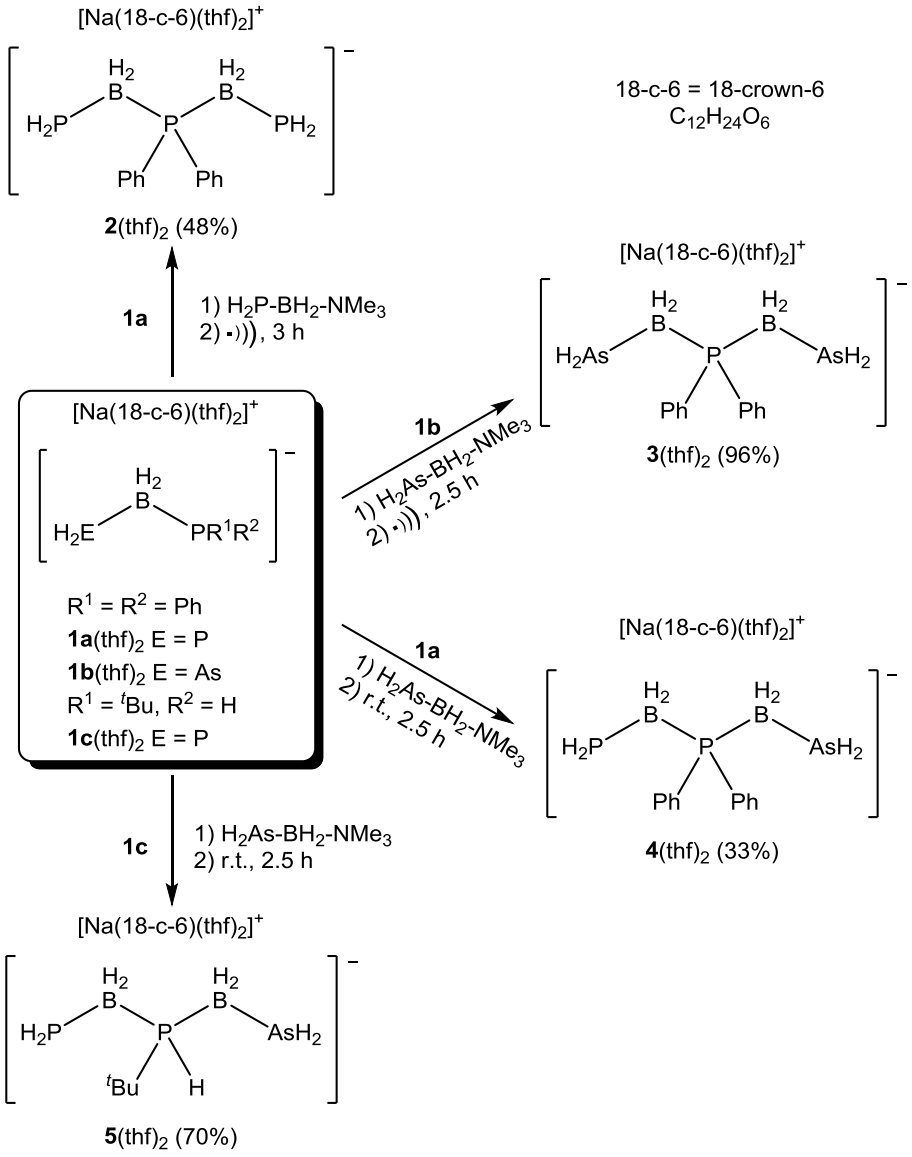

Scheme 6.1. Reaction of substituted three membered chain like compounds with Lewis base stabilized pnictogenylboranes. Isolated yields are given in parentheses. 18-c-6 = 18-Crown-6 ($C_{12}H_{24}O_6$).

According to heteronuclear NMR spectroscopy of the crude reaction solutions, compounds **2**, **3** and **4** are generated very selectively. During the synthesis of **5** the formation of minor side products can be observed. The ^{31}P NMR spectra of the isolated products reaveal that compared to their three membered precursors **1a**-**c**, the signals attributed to the PPh_2 group of compound **2**-**4** are shifted to the lower field by approximately 16 ppm. In case of the *tert*-butyl substituted derivative **5** the observed low field shift is more accentuated (40 ppm). Reactions of **1a**-**1c** with equivalent amounts of $H_2E\text{-}BH_2\text{-}NMe_3$ (E = P, As) lead to substitution of NMe_3 under formation of a new phosphorus boron

bond. Due to this new bond the electron density of the centered phosphorus atom is lowered resulting in the observed low field shift of the corresponding signal. Contrary to the shift of the signal attributed to the substituted secondary phosphine, the signals of the terminal PH_2 groups of compound **2** and **4** are shifted to the higher field (by approximately 17 ppm) in comparison to the starting material. The signal related to the PH_2 group of compound **5** reveals a slightly reduced shift (approximately 14 ppm) compared to compounds **2** and **4**. In the ^{11}B NMR spectra for all products a low field shift of the signals related to the BH_2 groups can be detected (Table 6.1).

Table 6.1. NMR parameters of compounds **2**-**5** compared to **1a**-**c**; $[H_2P^b\text{-}B^cH_2\text{-}P^aR^1R^2\text{-}B^dH_2\text{-}AsH_2]^-$; A: $R^1 = R^2 = Ph$; B: $R^1 = {}^tBu$, $R^2 = H$.

Compound		$P^aR^1R^2$ [ppm]	P^bH_2 [ppm]	$^1J_{P,H}{}^{a}/^{b}$ [Hz]	$B^{c/d}H_2$ [ppm]	$^1J_{B,H}{}^{c}/^{d}$ [Hz]	$^1J_{B,P}{}^{c}/^{d}$ [Hz]
A	**1a**	-15.2	-203.3	173	-29.1 / -	98	-
	1b	-16.7	-	-	-28.9 / -	100	-
	2	0.1	-219.4	181	-34.4 / -	-	-
	3	0.2	-	-	-34.5 / -	98	69
	4	-0.6	-221.1	179	-32.3 - -36.7	-	-
B	**1c**	-32.9	-188.8	177 / 173	-33.8 / -	97	27
	5	13.1	-203.4	180	-37.5 / 37.0	98 / 98	68 / 64

In the ^1H NMR spectra of compounds **2** and **4** the signals of the PH_2 groups occure at approximately 0.74 ppm, as broad doublets with similar coupling constants (**2**: $^1J_{H,P} = 181$ Hz, **4**: $^1J_{H,P} = 179$ Hz). The signals of the AsH_2 groups of compounds **3** and **4** can be observed at approximately -0.21 ppm indicating a hydridic character. The shift of the signals attributed to the BH_2 groups of compounds **2** and **3** slightly differs (**2**: 1.51 ppm, **3**: 1.65 ppm). This deviation can be explained by the different substituents as the terminal PH_2 groups in case of **2** and the AsH_2 groups for **3**. Compound **4** shows two BH_2 groups, one neighbored to a PH_2 group and one to an AsH_2 group, leading to one signal for each group. The shift of both BH_2 group signals is similar to the values found for compounds **2** and **3** (**2**: 1.51 ppm, **3**: 1.65 ppm, **4**: 1.51 ppm + 1.63 ppm).

Due to the chirality of compound **5** two sets of signals can be observed within the ^1H NMR spectrum indicating two enantiomers. The signal of the PH_2 group occur as two broad doublets with a slight shift to the low field in comparison to the analog signals of compounds **2** and **4** (**5**: 0.9 + 1.03 ppm, **2**: 0.74 ppm, **4**: 0.75 ppm). Beside the shape in form of two multiplets additionally a low field shift can be observed for the AsH_2 group in **5** compared to **3** and **4** (**5**: 0.00 ppm, **3**: -0.20 ppm, **4**: -0.22 ppm). For the two signals attributed to the BH_2 groups of **5** a slight high field shift occur (signals located at 1.1 ppm) in comparison to compounds **2**, **3** and **4**, respectively.

Single crystals suitable for X-ray diffraction experiments are obtained for all compounds by either storing saturated THF/ *n*-hexane solutions (**2**), saturated THF solutions (**3**) or THF solutions layered with

n-hexane (**4**, **5**) at -28 °C. The solid state structure of the anionic part of compounds **2**-**5** are shown in Figure 6.1.

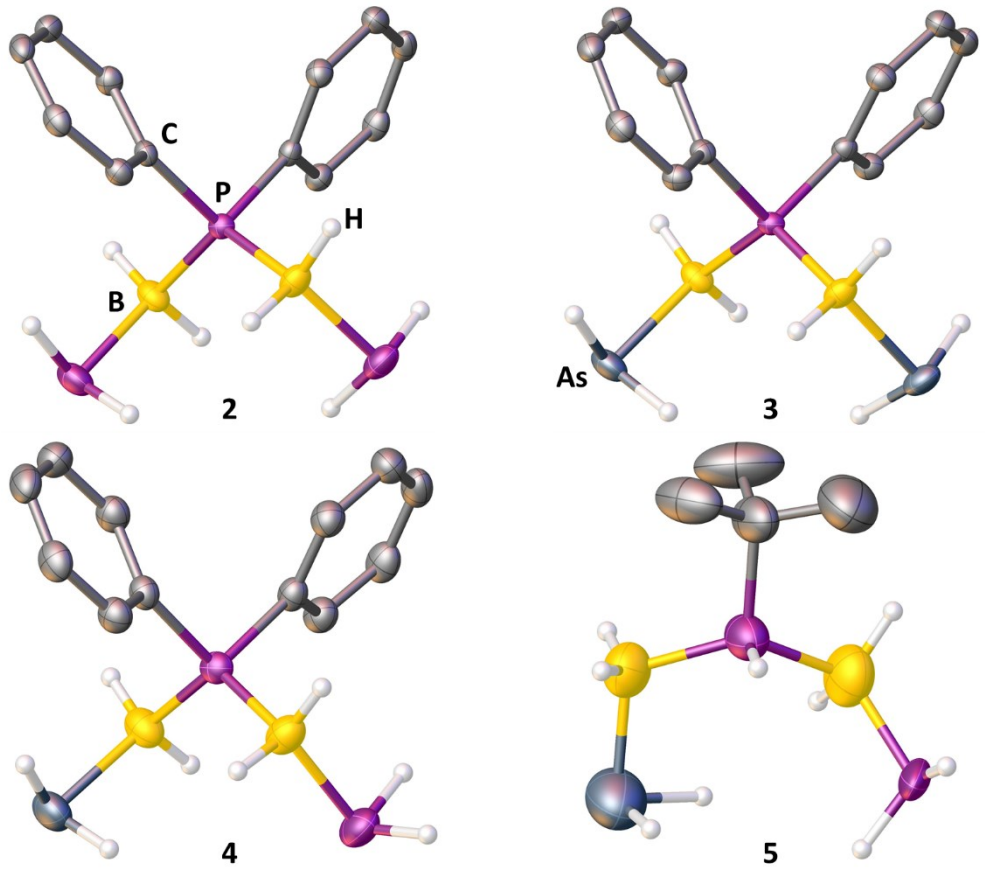

Figure 6.1. Molecular structures of the anions of **5**-**9** in the solid state. Hydrogen atoms bonded to carbon and counter ions are omitted for clarity. Thermal ellipsoids are drawn with 50% probability. Selected bond length [Å] and angles [°]: **2**: P-B 1.940(2) – 1.965(2), P-B-P 113.1(1), B-P-B 121.124; **3**: As-B 2.071(2), P-B 1.940(2), As-B-P 113.08(8); B-P-B 121.332; **4**: As-B 2.032(6), P-B 1.944(3) – 1.99(1), As-B-P 114.3(2), P-B-P 112.2(5), B-P-B 120.902; **5**: As-B 1.995(8), P-B 1.902(5) – 1.909(5), As-B-P 112.5(4), P-B-P 119.7(4), B-P-B 122.998.

Compound **5** crystalizes in the centrosymmetric space group *C*2/c. In the solid state structure two enantiomers *R*:*S* can be observed due to disorder. A 50:50 ratio of the enantiomers is determind. In Figure 6.1 only the *S* enantiomer is shown. The determined geometrical parameters of compound **2**-**4** are very similar to those of the starting material **1a** and **1b** with regards to bond lengths and angles. In comparison to compound **1c** as well as to compounds **2**-**4** in compound **5** a shortened distance between the terminal phosphine group and the neighbored BH_2 group as well as the terminal arsine group and its neighbored BH_2 group can be observed. Additionally the P-B-P angle in compound **5** is widened by approximately 6° while the As-B-P angle is comparable to the values of **1b**, **3** and **4** (Table 6.2).[15]

Table 6.2. Comparison of selected bond length and angles of starting material (**1a**-**c**) and corresponding products (**2**-**5**); A: $R^1 = R^2 = Ph$, B: $R^1 = {}^tBu$, $R^2 = H$)[15].

Compound		H_2P-B	H_2As-B	PR^1R^2-B	P-B-P	As-B-P
A	**1a**	1.973(2)	-	1.965(2)	111.36(8)	-
	2	1.965(2)	-	1.940(2)	113.1(1)	-
	3	-	2.071(2)	1.940(2)	-	113.08(8)
	1b	-	2.02(3) – 2.12(3)	1.88(2) – 1.97(1)	-	111.3(5) – 114.5(6)[16]
	4	1.99(1)	2.032(6)	1.944(3)	112.2(5)	114.3(2)
B	**1c**	1.975(2) – 1.979(2)	-	1.951(3) – 2.037(7)	107.8(2) – 112.3(1)	-
	5	1.909(5)	1.995(8)	1.902(5) – 1.908(5)	119.7(4)	112.5(4)

The solid state structure of compounds **2**-**4** reveal an antiperiplanar arrangement along the EH_2-BH_2 axis (E = P, As). Additionally a synclinal conformation can be observed along the BH_2-PPh_2 axis. Compound **5** reveals an all-antiperiplanar arrangement along all pncitogen boron axis.

In the ESI-MS (anion mode) spectra the molecular ion peak corresponding to the anion for each compound has been detected.

Sonication or heating of **1c** with one equivalent of Lewis base stabilized phosphanylborane does not lead to the desired product $[H_2P\text{-}BH_2\text{-}{}^tBuPH\text{-}BH_2\text{-}PH_2]^-$. According to the ^{31}P NMR spectrum of the reaction mixture only the formation of side- and decomposition products could be observed. Despite variating purification methods the identification or isolation of the reaction products was not successful. Therefore DFT calculation are performed to get a deeper insight to the energetics of the reaction. The reaction energies in the gas phase for both reactions indicate an exothermic reaction progress with -53.3 $kJ{\cdot}mol^{-1}$ for $[H_2P\text{-}BH_2\text{-}{}^tBuPH\text{-}BH_2\text{-}PH_2]^-$ and -56.9 $kJ{\cdot}mol^{-1}$ for $[H_2P\text{-}BH_2\text{-}{}^tBuPH\text{-}BH_2\text{-}AsH_2]^-$ (**5** anion), respectively. According to the difference of only 3.6 $kJ{\cdot}mol^{-1}$ the formation of $[H_2P\text{-}BH_2\text{-}{}^tBuPH\text{-}BH_2\text{-}PH_2]^-$ should be energetically favoured. With focus on the used Lewis base stabilized pnictogenylboranes a possible explanation for the different reaction products can be found. Calculations reveal, Lewis base stabilized phosphanylborane being more stable than its arsenic containing derivate.[17] The experimental approach proves that for the formation of **5** stirring of $H_2As\text{-}BH_2\text{-}NMe_3$ with **1c** at room temperature is sufficient. Under same reaction conditions no reaction can be observed with Lewis base stabilized phosphanylborane. Very probably harsher reaction conditions which are necessary for the reaction of **1c** with $H_2P\text{-}BH_2\text{-}NMe_3$ result in the formation of side products instead. Due to the lack of the corresponding starting material $[H_2As\text{-}BH_2\text{-}{}^tBuPH]^-$ the synthesize of $[H_2As\text{-}BH_2\text{-}{}^tBuPH\text{-}BH_2\text{-}AsH_2]^-$ have been excluded from the beginning.[15]

6.3 Conclusion

In summary, a simple synthetic route is shown here to obtain oraganosubstituted five membered 13/15 oligomers. Beside compound **2** revealing a pure phosphorus boron backbone, similar compounds are accessible bearing one (**4**, **5**) or two (**3**) terminal arsine groups. The here presented compounds **2**, **3**, **4** and **5** are a substantial contribution to enlarge the variety of linear inorganic oligomers containing at least a five membered 13/15 backbone. Additionally compounds **3**, **4** and **5** enlarge the number of 13/15 oligomers containing at least one terminal arsine group. Bearing two coordination sites in form of terminal phosphine and arsine groups, respectively, these compounds are promising chelating ligands as well as linkers. The coordination behavior of the here presented five membered, organosubstituted, anionic pnictogenylborane derivatives is part of current investigations.

6.4 References

[1] a) C.A. Jaska, K. Temple, A. J. Lough, I. Manners, *Chem. Commun.* **2001**, 962-963; b) C.A. Jaska, K. Temple, A. J. Lough, I. Manners, *J. Am. Chem. Soc.* **2003**, *125*, 9424-9434.

[2] J.-M. Denis, H. Forintos, H. Szelke, L. Toupet, T.-N. Pham, P.-J. Madec, A.-C. Gaumonz, *Chem. Commun.* **2003**, 54-55.

[3] a) H. Dorn, R. A. Singh, J. A. Massey, A. J. Lough, I. Manners, *Angew. Chem. Int. Ed.* **1999**, *38*, 3321-3323, *Angew. Chem.* **1999**, *111*, 3540-3543; b) T. N. Hooper, A. S. Weller, N. A. Beattie, S. A. Macgregor, *Chem. Sci.* **2016**, *7*, 2414-2426.

[4] C. Marquardt, T. Jurca, K.-C. Schwan, A. Stauber,A. V. Virovets, G. R. Whittell, I. Manners, M. Scheer, *Angew. Chem. Int. Ed.* **2015**, *54*, 13782-13786.

[5] A. Stock, E. Pohland, *Ber. Dtsch. Chem. Ges.* **1926**, *59*, 2215-2223.

[6] a) M. Schwarz, M. Garnica, F. Fasano, N. Demitri, D. Bonifazi. W. Auwärter, *Chem. Eur. J.* **2018**, *24*, 9565-9571; b) C. W. Chang, Y. Nabae, S. Kuroki, T. Hayakawa, M.-a. Kakimoto, S. Miyata, *Chem. Lett.* **2012**, *41*, 923-925; c) J. Haberecht, A. Krummland, F. Breher, B. Gebhardt, H. Rüegger, R. Nesper, H. Grützmacher, *Dalton Trans.* **2003**, *11*, 2126-2132.

[7] A. D. Gorman, J. A. Bailey, N. Fey, T. A. Young, H. A. Sparkes, P. G. Pringle, *Angew. Chem. Int. Ed.* **2018**, *57*, 15802-15806; *Angew. Chem.* **2018**, *130*, 16028-16032.

[8] N. Matsunaga, T. R. Cundari, M. W. Schmidt, M. S. Gordon, *Theor. Chim. Acta* **1992**, *83*, 57-68; A. S. Lisovenko, A. Y. Timoshkin, *Russ. J. Gen. Chem.* **2011**, *81*, 831-839; A. S. Lisovenko, A. Y. Timoshkin, *Russ. Chem. B+.* **2015**, *64*, 2573-2585.

[9] H. V. Rasika Dias, P. P. Power, *J. Am. Chem. Soc.* **1989**, *111*, 144-148.

[10] D. Dou, M. Westerhausen, G. L. Wood, G. Linti, E. N. Duesler, H. Nöth, R. T. Paine, *Chem. Ber.* **1993**, *126*, 379-397.

[11] a) H. Nöth, H. Vahrenkamp, *Chem. Ber.* **1966**, *99*, 1049-1067; H. Nöth, H. Vahrenkamp, *J. Organomet. Chem.* **1968**, *12*, 23-36; b) W. C. Ewing, P. J. Carroll, L. G. Sneddon, *Inorg. Chem.* **2013**, *52*, 10690-10697; c) W. C. Ewing, A. Marchione, D. W. Himmelberger, P. J. Carroll, L. G. Sneddon, *J. Am. Chem. Soc.* **2011**, *133*, 17093-17099;

[12] a) M. Baudler, C. Block, H. Budzikiewicz, H. Muenster, *Z. Anorg. Allg. Chem.* **1989**, *569*, 7-15; b) A. B. Burg, *Inorg. Chem.* **1978**, *17*, 593-599; c) I. Tsuneo, T. Oshiki, *Tetrahedron Lett.* **1989**, *30*, 383-384.

[13] C. Marquardt, G. Balázs, J. Baumann, A. V. Virovets, M. Scheer*, Chem. Eur. J.* **2017**, *23*, 11423-11429; O. Hegen, A. V. Virovets, A. Y. Timoshkin, M. Scheer, *Chem. Eur. J.* **2018**, *24*, 16521-16525.

[14] C. Marquardt, T. Kahoun, A. Stauber, G. Balázs, M. Bodensteiner , A. Y. Timoshkin, M. Scheer, *Angew. Chem. Int. Ed.* **2016,** *55*, 14828-14832; *Angew. Chem.* **2016**, *128*, 15048-15052.

[15] See **chapter 5**; compounds $[Na(C_{12}H_{24}O_6)][H_2P\text{-}BH_2\text{-}PPh_2]$ (**7**), $[Na(C_{12}H_{24}O_6)][H_2As\text{-}BH_2\text{-}PPh_2]$ (**9**), $[Na(C_{12}H_{24}O_6)][H_2P\text{-}BH_2\text{-}^tBuPH]$ (**3**), $[Na(C_{12}H_{24}O_6)][H_2As\text{-}BH_2\text{-}^tBuPH\text{-}BH_3]$ (**6**).

[16] Due to disorder within the molecular structure the value of value of 122.0(1) is omitted for discussion.

[17] C. Marquardt, A. Adolf, A. Stauber, M. Bodensteiner, A. V. Virovets, A. Y. Timoshkin, M. Scheer, *Chem. Eur. J.* **2013**, *19*, 11887-11891.

6.5 Experimental Section

6.5.1 Synthetic Procedures

All manipulations were performed under an atmosphere of dry argon/ nitrogen using standard glove-box and Schlenk techniques. All solvents were degassed and purified by standard procedures. The compounds $H_2E\text{-}BH_2\text{-}NMe_3$ (E = P, As)[1], $[Na(C_{12}H_{24}O_6)][H_2P\text{-}BH_2\text{-}PPh_2]$,[2] $[Na(C_{12}H_{24}O_6)][H_2As\text{-}BH_2\text{-}PPh_2]$,[2] $[Na(C_{12}H_{24}O_6)][H_2P\text{-}BH_2\text{-}^tBuPH]$,[2] were prepared according to literature procedures.

The NMR spectra were recorded on an Avance 400 spectrometer (**2**, **3**, **4**, **5**) (^{1}H: 400.13 MHz, ^{31}P: 161.976 MHz, ^{11}B: 128.378 MHz, ^{13}C{^{1}H}: 100.623 MHz) with δ [ppm] referenced to external $SiMe_4$ (^{1}H, ^{13}C), H_3PO_4 (^{31}P), $BF_3{\cdot}Et_2O$ (^{11}B).

IR spectra were recorded either on a DIGILAB (FTS 800) FT-IR spectrometer (**2**, **3**) or a Thermo Scientific (NICOLET iS 5, iD1 Transmission) FT-IR spectrometer (**4**, **5**) with $\tilde{\nu}$ [cm^{-1}]. Mass spectra were recorded either on a ThermoQuest Finnigan TSQ 7000 (**2**, **3**; Mass-Spectrometry-Department, University of Regensburg) or a Waters/Micromass LCT-TOF classic (**4**, **5**; Mass Spectrometer in Working group) (ESI-MS).

The C, H, N analyses were measured on an Elementar Vario EL III apparatus (**2**, **3**, **4**, **5**).

General remarks for C, H, N analyses:

C, H, N analyses were carried out repeatedly. Different amounts of coordinating THF have been found in nearly all cases. Total removal of the THF was not always possible, however C, H, N analyses are in good agreement with the expected values considering a varying THF-content (0.5 % tolerance).

Synthesis of $[Na(C_{12}H_{24}O_6)(thf)_2][H_2P\text{-}BH_2\text{-}Ph_2P\text{-}BH_2\text{-}PH_2]$ (**2**$(thf)_2$):

A solution of 27 mg (0.25 mmol) $H_2PBH_2{\cdot}NMe_3$ in 0.5 mL toluene is added to a solution of 130 mg (0.25 mmol) $[Na(C_{12}H_{24}O_6)][H_2P\text{-}BH_2\text{-}PPh_2]$ in 8 ml THF. After sonication of the mixture for 3 h, the solution is filtrated and all volatiles are removed under reduced pressure. The remaining solid is dissolved in 5 mL of THF and filtrated again. The solvent is removed and 20 mL of *n*-hexane are added to the white solid. THF is added drop wise until a clear colourless solution is obtained. **2**$(thf)_2$ crystallises at -28 °C as colourless plates. The supernatant is decanted, the remaining crystals are washed with cold *n*-hexane (0 °C, 3 × 5 mL) and dried *in vacuo*.

Yield of $[Na(C_{12}H_{24}O_6)][H_2P\text{-}BH_2\text{-}Ph_2P\text{-}BH_2\text{-}PH_2]$(**2**): 70 mg (48 %).

^{1}H NMR (THF-d_8, 25 °C): δ = 0.74 (dm, $^1J_{H,P}$ = 181 Hz, 4H, PH_2), 1.51 (q, $^1J_{H,B}$ = 105 Hz, 4H, BH_2), 3.60 (s, 24H, $C_{12}H_{24}O_6$), 7.08-7.19 (m, 6H, *m*- & *p*-Ph) 7.69 (m, 4H, *o*-Ph).

^{11}B NMR (THF-d_8, 25 °C): δ = -34.4 (m, BH_2).

^{11}B{^{1}H} NMR (THF-d_8, 25 °C): δ = -34.4 (m, BH_2).

^{31}P NMR (THF-d_8, 25 °C): δ = -219.4 (tm, $^1J_{H,P}$ = 181 Hz, 2P, PH_2), 0.1 (s, br, 1P, PPh_2).

^{31}P{^{1}H} NMR (THF-d_8, 25 °C): δ = -219.4 (m, 2P, PH_2), 0.1 (s, br, 1P, PPh_2).

^{13}C NMR (THF-d_8, 25 °C): δ = 70.6 (s, $C_{12}H_{24}O_6$), 127.3 (d, *m*-Ph, $^3J_{P,C}$ = 8 Hz), 127.7 (d, *p*-Ph, $^4J_{P,C}$ = 2 Hz), 134.6 (d, *o*-Ph, $^2J_{P,C}$ = 6 Hz), 139.8 (d, *i*-Ph, $^1J_{P,C}$ = 36 Hz).

IR (KBr): $\tilde{\nu}$ = 2902 (vs, CH), 2826 (s, CH), 2747 (w), 2375 (s, br, BH), 2356 (s, br, BH), 2332 (s, PH), 2279 (s, PH), 1622 (vw), 1479 (w), 1477 (w) 1453 (m), 1434 (w), 1352 (s), 1284 (w), 1251 (m), 1113 (vs, CO), 1028 (w), 965 (s), 837 (m), 791 (w), 775 (vw), 742 (m), 723 (w), 702 (m), 615 (vw), 531 (w), 496 (w), 466 (w), 435 (vw).

ESI-MS (THF): anion: *m/z* = 230 (75%, $[Ph_2P(BH_2\text{-}PH_2)_n]^-$ (n = 1)), 277 (100 %, $[Ph_2P(BH_2\text{-}PH_2)_n]^-$ (n = 2)), 323 (100 %, $[Ph_2P(BH_2\text{-}PH_2)_n]^-$ (n = 3)).

Elemental analysis (%) calculated for $C_{24}H_{42}B_2NaO_6P_3$ (**2**): C: 51.04, H: 7.50; found: C: 51.14, H: 7.56.

Synthesis of $[Na(C_{12}O_6H_{24})(thf)_2][H_2As\text{-}BH_2\text{-}PPh_2\text{-}BH_2\text{-}AsH_2]$ (**3**$(thf)_2$):

A solution of 521 mg (3.5 mmol) $H_2As\text{-}BH_2{\cdot}NMe_3$ in 3.5 mL toluene is added to a solution of 1124 mg (2.0 mmol) $[Na(C_{12}O_6H_{24})][H_2As\text{-}BH_2\text{-}PPh_2]$ in 10 mL THF. After sonication of the mixture for 2.5 h, the colourless solution is filtrated. After concentration **3**$(thf)_2$ crystallizes at -30 °C as colourless blocks. The supernatant is decanted, the remaining crystals are washed with cold *n*-hexane (-30 °C, 7 x 5 mL) and dried *in vacuo*.

Yield of $[Na(C_{12}O_6H_{24})(thf)_{0.5}][H_2As\text{-}BH_2\text{-}PPh_2\text{-}BH_2\text{-}AsH_2]$ (**3**$(thf)_{0.45}$): 1.32 g (96%).

^{1}H NMR (THF-d_8, 25°C): δ = -0.20 (m, 4H, AsH_2), 1.65 (q, br, $^1J_{H,B}$ = 98 Hz, 4H, BH_2), 3.58 (s, $C_{12}O_6H_{24}$, 24H), 7.13 (m, 6H, *o*-Ph, *m*-Ph), 7.70 (m, 2H, *p*-Ph).

^{11}B NMR (THF-d_8, 25°C): δ = -34.5 (dt, $^1J_{B,H}$ = 98 Hz, $^1J_{B,P}$ = 69 Hz, BH_2).

^{11}B{^{1}H} NMR (THF-d_8, 25°C): δ = -34.5 (d, $^1J_{B,P}$ = 69 Hz, BH_2).

^{31}P NMR (THF-d_8, 25°C): δ = 0.2 (s, PPh_2).

$^{31}P\{^{1}H\}$ NMR (THF-d_8, 25°C): δ = 0.2 (s, PPh_2).

$^{13}C\{^{1}H\}$ NMR (THF-d_8, 25°C): δ = 70.5 (s, $C_{12}O_6H_{24}$), 127.3 (d, *m*-Ph $^{3}J_{C,P}$ = 8 Hz), 127.8 (d, *p*-Ph $^{4}J_{C,P}$ = 2 Hz), 134.4 (d, *o*-Ph, $^{2}J_{C,P}$ = 6 Hz), 139.8 (d, *i*-Ph, $^{1}J_{C,P}$ = 37 Hz).

IR (KBr): $\tilde{\nu}$ = 3051 (w), 2900 (s, CH), 2825 (w), 2746 (vw), 2396 (s, BH), 2374 (s, BH), 2343 (s, BH), 2221 (m, PH), 2079 (m, AsH), 1974 (vw), 1618 (vw), 1479 (m), 1471 (w), 1452 (w), 1434 (m), 1352 (s), 1305 (w), 1284 (w), 1249 (m), 1111 (vs, CO), 1029 (w), 965 (s), 837 (m), 760 (m), 730 (m), 703 (s), 593 (w), 502 (w), 463 (w), 429 (w).

ESI-MS (THF): anion: *m*/*z* = 364.9 (100%, $[H_2As\text{-}BH_2\text{-}PPh_2\text{-}BH_2\text{-}AsH_2]^-$), 274.8 (17%, $[AsH_2\text{-}BH_2\text{-}PPh_2]^-$).

Elemental analysis (%) calculated for $C_{24}H_{42}As_2B_2NaO_6P(thf)_{0.5}$ (**3**$(thf)_{0.5}$): C: 45.33, H: 6.73; found: C: 45.50, H: 6.54.

Synthesis of $[Na(C_{12}H_{24}O_6)(thf)_2][H_2P\text{-}BH_2\text{-}PPh_2\text{-}BH_2\text{-}AsH_2]$ (**4**$(thf)_2$)

A solution of 104 mg (0.50 mmol) $NaPh_2$ in 4 ml THF is added to a solution of 53 mg (0.50 mmol) $H_2P\text{-}BH_2\text{-}NMe_3$ in 1 ml toluene at room temperature. After sonication of the mixture for 6 h a solution of 75 mg (0.50 mmol) $H_2As\text{-}BH_2\text{-}NMe_3$ in 1 ml toluene is added and stirred for 16 h at room temperature. The reaction liquid is filtrated on 119 mg (0.45 mmol) $C_{12}H_{24}O_6$ and layered with 25 ml of *n*-hexane. **4**$(thf)_2$ crystallizes at -30 °C as colorless blocks. The supernatant is decanted, the remaining crystals are washed with cold *n*-hexane (-30 °C, 2 x 5 ml) and dried *in vacuo*.

Yield of $[Na(C_{12}H_{24}O_6)][H_2P\text{-}BH_2\text{-}PPh_2\text{-}BH_2\text{-}AsH_2]$ (**4**$(thf)_{0.2}$): 104 mg (33%).

^{1}H NMR (THF-d_8, 25 °C): δ = -0.22 (m, 2H, AsH_2), 0.75 (dm, br, $^{1}J_{H,P}$ = 179 Hz, 2H, PH_2), 1.51 (q, br, $^{1}J_{H,B}$ = 96 Hz, 2H, BH_2), 1.63 (q, br, $^{1}J_{H,B}$ = 96 Hz, 2H, BH_2), 3.60 (s, 24 H, $C_{12}H_{24}O_6$), 7.11 (m, 4H, *m*-Ph), 7.13 (m, 2H, *p*-Ph), 7.69 (m, 4H, *o*-Ph).

^{11}B NMR (THF-d_8, 25 °C): δ = -32.3 - -36.7 (m, $BH_2\text{-}PH_2$, $BH_2\text{-}AsH_2$).

$^{11}B\{^{1}H\}$ NMR (THF-d_8, 25 °C): δ = -32.3 - -36.7 (m, $BH_2\text{-}PH_2$, $BH_2\text{-}AsH_2$).

^{31}P NMR (THF-d_8, 25 °C): δ = -221.1 (t, $^{1}J_{P,H}$ = 179 Hz, PH_2), -0.6 (s, br, PPh_2).

$^{31}P\{^{1}H\}$ NMR (thf-d_8, 25 °C): δ = -221.1 (d, $^{1}J_{P,B}$ = 27 Hz, PH_2), -0.6 (s, br, PPh_2).

$^{13}C\{^{1}H\}$ (THF-d_8, 25 °C): δ = 70.6 (s, $C_{12}H_{24}O_6$), 127.2 (d, $^{3}J_{C,P}$ = 8 Hz, *m*-Ph), 127.7 (t, $^{4}J_{C,P}$ = 2 Hz, *p*-Ph), 134.5 (d, $^{2}J_{C,P}$ = 7 Hz, *o*-Ph), 139.8 (d, $^{1}J_{C,P}$ = 36 Hz, *i*-Ph).

IR (KBr): $\tilde{\nu}$ = 3072 (vw), 3051 (vw), 2901 (s), 2826 (w), 2800 (vw), 2743 (vw), 2714 (vw), 2686 (vw), 2370 (s, PH), 2336 (s, PH), 2280 (m, BH), 2223 (vw), 2076 (s, AsH), 1976 (vw), 1616 (vw), 1482 (m), 1471 (m), 1452 (s), 1351 (s), 1305 (vw), 1284 (w), 1249 (m), 1182 (vw), 1112 (vs), 1028 (w), 965 (s), 836 (m), 784 (w), 754 (w), 736 (m), 720 (m), 702 (s), 678 (w), 612 (vw), 533 (vw), 503 (w), 464 (m), 431 (vw).

ESI-MS (THF): anion: *m/z* = 275.0 (100%, $[H_2As\text{-}BH_2\text{-}PPh_2]^-$), 321.1 (80 %, $[H_2P\text{-}BH_2\text{-}PPh2\text{-}BH_2\text{-}AsH_2]^-$).

Elemental analysis (%) calculated for $C_{24}H_{42}AsB_2NaO_6P_2(thf)_{0.2}$ (**4**$(thf)_{0.2}$): C: 47.85, H: 7.05; found: C: 48.19, H: 6.87.

Synthesis of $[Na(C_{12}H_{24}O_6)(thf)_2][H_2P\text{-}BH_2\text{-}^t BuPH\text{-}BH_2\text{-}AsH_2]$ (**5**$(thf)_2$):

A solution of 104 mg (0.70 mmol) $H_2As\text{-}BH_2\text{-}NMe_3$ in 1 ml toluene is added to a solution of 95 mg (0.70 mmol) $Na[^t BuPH\text{-}BH_2\text{-}PH_2]$ in 4 ml THF and stirred for 16 h at room temperature. The solution is filtrated on 185 mg (0.70 mmol) $C_{12}H_{24}O_6$ and layered with 20 ml of *n*-hexane. **5**$(thf)_2$ crystallizes at -30 °C as brown blocks. The supernatant is decanted, the remaining crystals are washed with cold *n*-hexane (-30 °C, 2 x 5 ml) and dried *in vacuo*. **5** is an oil at room temperature.

Yield of $[Na(C_{12}H_{24}O_6)][H_2P\text{-}BH_2\text{-}^t BuPH\text{-}BH_2\text{-}AsH_2]$ (**5**): 252 mg (70 %).

^{1}H NMR (THF-d_8, 25 °C): δ = 0.00 (m, 2H, AsH_2), 0.90 (dm, $^1J_{H,P}$ = 180 Hz, 1H, PH^aH^b), 1.03 (dm, $^1J_{H,P}$ = 180 Hz, 1H, PH^aH^b), 0.55 - 1.70 (m, br, PH_2-BH_2 & AsH_2-BH_2), 1.13 (d, $^4J_{H,H}$ = 11 Hz, 9H, ^{t}BuPH), 3.24 (dm, $^1J_{H,P}$ = 306 Hz, 1H, ^{t}BuPH), 3.63 (s, 24 H, $C_{12}H_{24}O_6$).

^{11}B NMR (THF-d_8, 25 °C): δ = -37.5 (tt, $^1J_{B,H}$ = 98 Hz, $^1J_{B,P}$ = 68 Hz, BH_2-PH_2), -37.0 (td, $^1J_{B,H}$ = 98 Hz, $^1J_{B,P}$ = 64 Hz, BH_2-AsH_2).

^{11}B{^{1}H} NMR (THF-d_8, 25 °C): δ = -37.5 (t, $^1J_{B,P}$ = 68 Hz, BH_2-PH_2), -37.0 (d, $^1J_{B,P}$ = 64 Hz, BH_2-AsH_2).

^{31}P NMR (THF-d_8, 25 °C): δ = -203.4 (tm, $^1J_{P,H}$ = 180 Hz, PH_2), 13.1 (dm, $^1J_{P,H}$ = 306 Hz, ^{t}BuPH).

^{31}P{^{1}H} NMR (THF-d_8, 25 °C): δ = -203.4 (m, PH_2), 13.1 (m, ^{t}BuPH).

^{13}C{^{1}H} NMR (THF-d_8, 25 °C): δ = 26.2 (s, $C(CH_3)_3$), 29.6 (s, CH_3), 70.6 (s, $C_{12}H_{24}O_6$).

IR (KBr): $\tilde{\nu}$ = 2936 (s, CH), 2894 (s, CH), 2866 (s, CH), 2825 (m, CH), 2796 (w), 2746 (vw), 2711 (vw), 2689 (vw), 2353 (s, BH), 2274 (m, PH), 2055 (m, AsH), 1976 (vw), 1622 (vw), 1476 (s), 1457 (m), 1435 (w), 1391 (vw), 1353 (s), 1286 (m), 1251 (m), 1194 (vw), 1109 (vs), 1026 (vw), 966 (vs), 868 (w), 840 (m), 821 (w), 713 (vw), 669 (vw), 640 (vw), 526 (vw).

ESI-MS (THF): anion: *m/z* = 225.0 (100%, $[H_2P\text{-}BH_2\text{-}^t BuPH\text{-}BH_2\text{-}AsH_2]^-$).

Elemental analysis (%) calculated for $C_{16}H_{42}AsB_2NaO_6P_2$ (**5**): C: 37.53, H: 8.27; found: C: 37.59, H: 8.11.

6.5.2 X-ray Diffraction Analysis

The X-ray diffraction experiments were performed on a GV50 diffractometer with TitanS2 detector (**3**, **4**, **5**) or a Gemini R Ultra with Atlas detector (**2**) from Rigaku Oxford Diffraction (formerly Agilent Technologies) applying Cu-$K\alpha$ radiation (λ = 1.54178 Å). The measurements were performed at 123 K (**2**, **4**, **5**) or at 139 K (**3**). Crystallographic data together with the details of the experiments are given in Table S 6.1 and Table S 6.2 (see below).

A Numerical absorption correction based on gaussian integration was performed over a multifaceted crystal model (**3**, **4**, **5**), an analytical numeric absorption correction using a multifaceted crystal model based on expressions derived by *Clark and Reid*[3] (**2**) or an empirical absorption correction using spherical harmonics as implemented in SCALE3/ ABSPACK (CrysAlisPro software by Rigaku Oxford Diffraction).[4]

All structures were solved using SIR97[5], SHELXT[6] and OLEX2[7]. Least square refinements against F^2 in anisotropic approximation were done using SHELXL[8].

All non-hydrogen atoms were refined anisotropically. The hydrogen positions of the methyl groups were located geometrically and refined riding on the carbon atoms. Hydrogen atoms belonging to BH_2, PH_2 and AsH_2 groups were located from the difference Fourier map and refined without constraints (**3**) or with restrained X–H (X = B, P, As) distances (**2**, **4**, **5**).

6.5.3 Solid State Structures

$[Na(C_{12}H_{24}O_6)(thf)_2][H_2P\text{-}BH_2\text{-}PPh_2\text{-}BH_2\text{-}PH_2]$ $(2(thf)_2)$:

2$(thf)_2$ crystallizes from a saturated THF/ *n*-hexane mixture at -28 °C as colourless blocks in the monoclinic space group *C2/c*. Figure S 6.1 shows the molecular structure of **2**$(thf)_2$ in solid state.

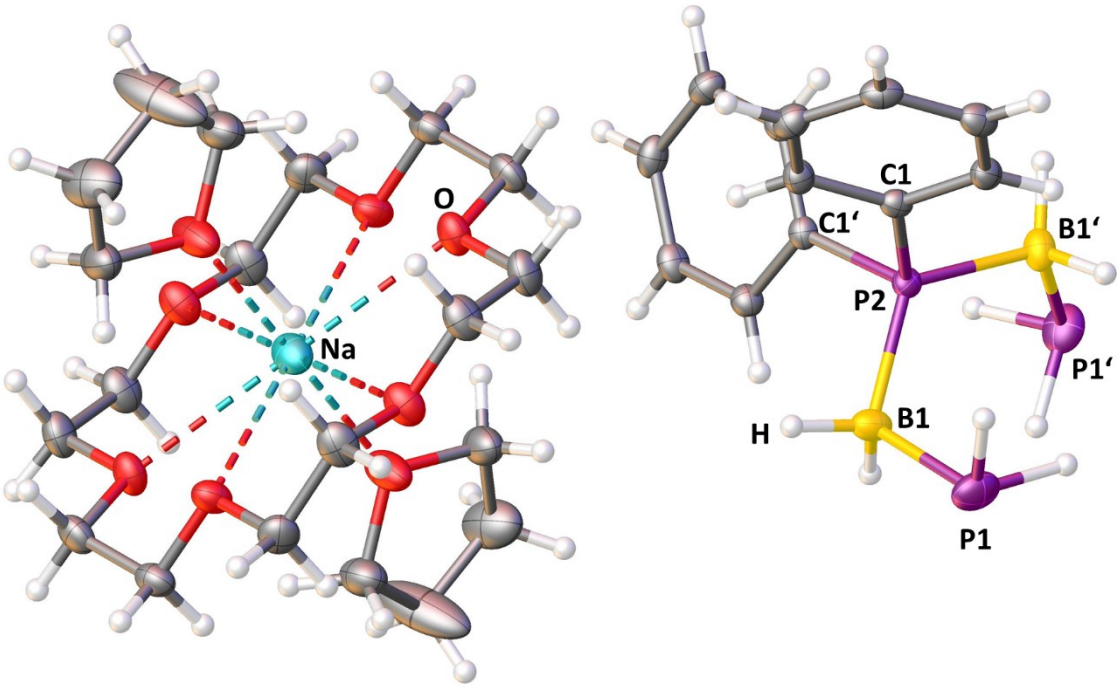

Figure S 6.1. Molecular structure of **2**$(thf)_2$ in solid state. Thermal ellipsoids are drawn with 50% probability. Atoms labeled with ‘ are generated by symmetrical operations. Selected bond length [Å] and angles [°]: P1-B1: 1.965(2), P2-B1: 1.940(2), P1-C1: 1.825(2), ∠(P1-B1-P2): 113.1(1), ∠(B1-P2-B1’): 121.124, ∠(B1-P2-C1): 107.44(8).

$[Na(C_{12}H_{24}O_6)(thf)_2][H_2As\text{-}BH_2\text{-}PPh_2\text{-}BH_2\text{-}AsH_2]$ $(3(thf)_2)$:

3$(thf)_2$ crystallizes from a saturated THF solution at -28 °C as colourless blocks in the monoclinic space group *C2/c*. Figure S 6.2 shows the molecular structure of **3**$(thf)_2$ in solid state.

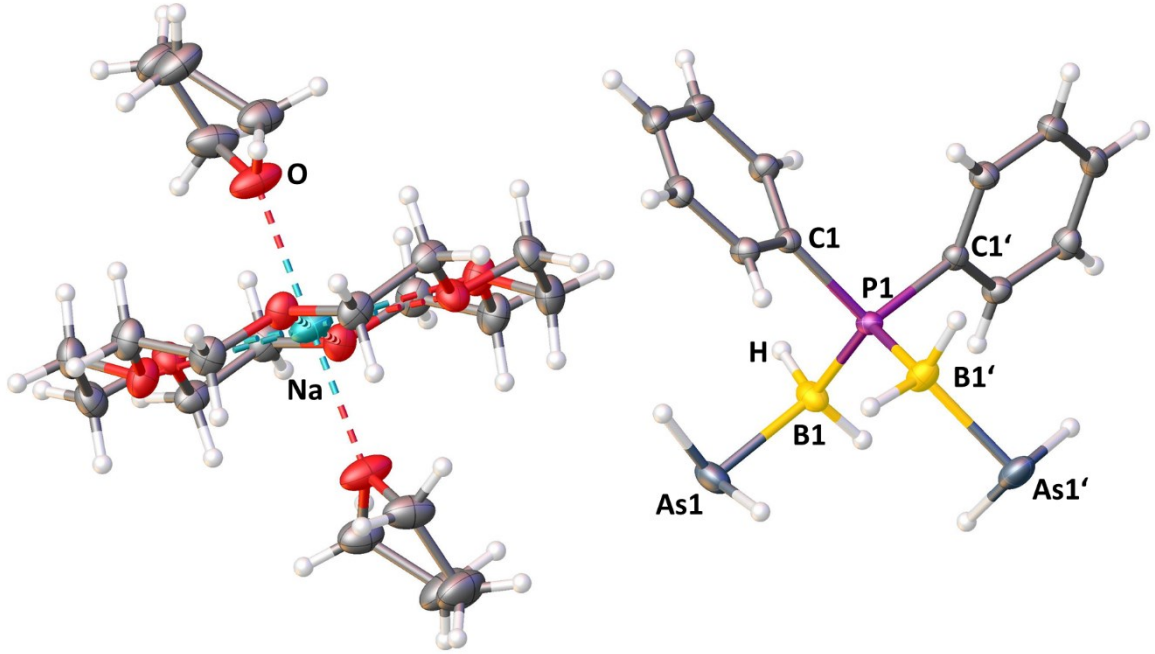

Figure S 6.2. Molecular structure of **3**$(thf)_2$ in solid state. Thermal ellipsoids are drawn with 50% probability. Atoms labeled with ' are generated by symmetrical operations. Selected bond length [Å] and angles [°]: As1-B1: 2.071(2), P1-B1: 1.940(2), P1-C1: 1.828(1), ∠(As1-B1-P1): 113.08(8), ∠(B1-P1-B1'): 121.332, ∠(B1-P1-C1): 107.73(7).

$[Na(C_{12}H_{24}O_6)(thf)_2][H_2P\text{-}BH_2\text{-}PPh_2\text{-}BH_2\text{-}AsH_2]$ $(4(thf)_2)$:

4$(thf)_2$ crystallizes from a THF solution layered by the 3-4-fold amount of *n*-hexane at -28 °C as colourless blocks in the monoclinic space group *C2/c*. Figure S 6.3 shows the molecular structure of **4**$(thf)_2$ in solid state.

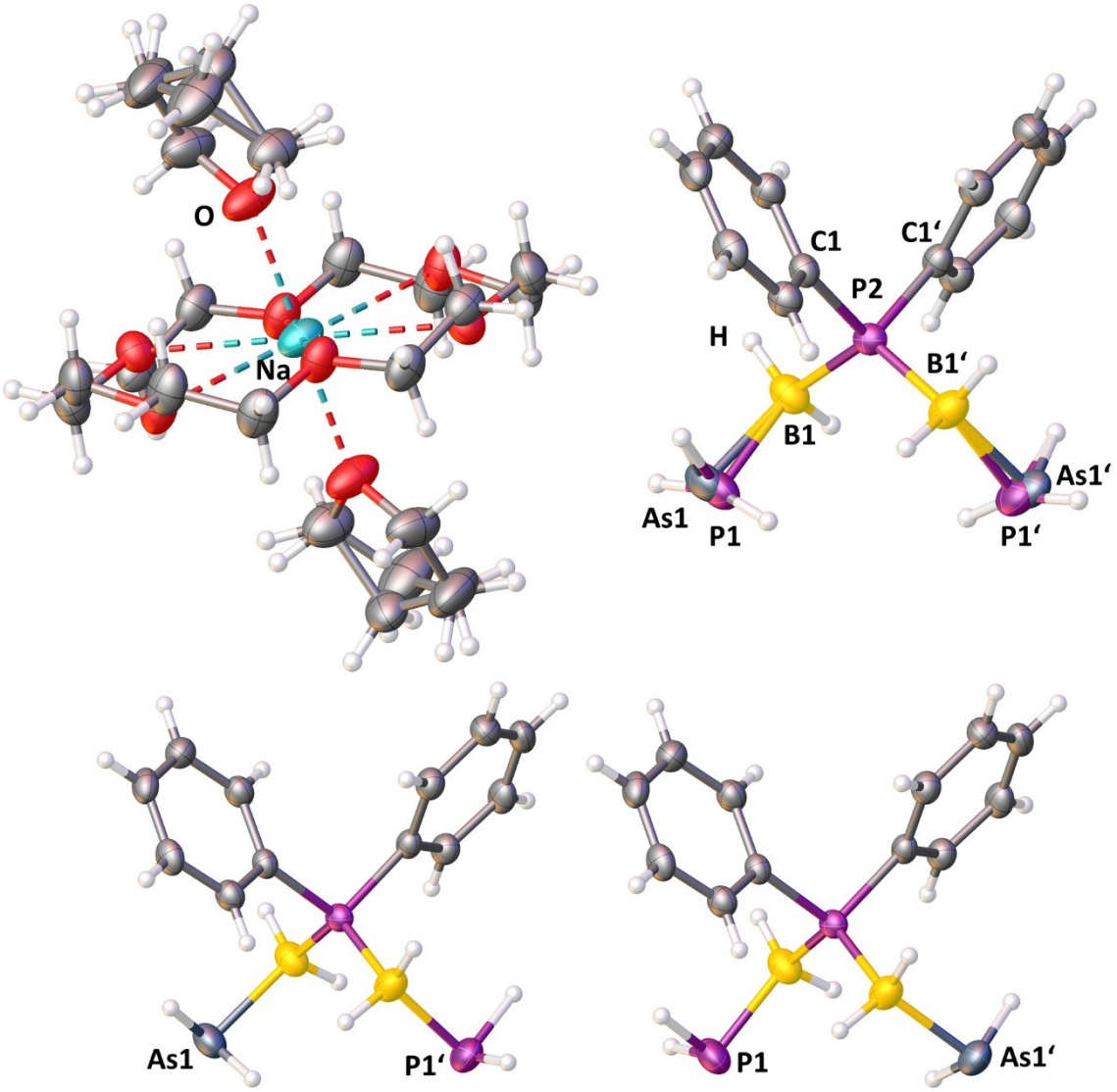

Figure S 6.3. Molecular structure of **4**$(thf)_2$ in solid state. Thermal ellipsoids are drawn with 50% probability. Atoms labeled with ' are generated by symmetrical operations. Selected bond length [Å] and angles [°]: P1-B1: 1.99(1), As1-B1: 2.032(6), P2-B1: 1.944(3), P2-C1: 1.827(2), ∠(P1-B1-P2): 112.2(5), ∠(As1-B1-P2): 114.3(2), ∠(B1 P2-B1'): 120.902, ∠(B1-P2-C1): 107.5(1). Top: disordered solid state structure of **4**$(thf)_2$; bottom: separated disorder of the anionic part of **4**$(thf)_2$.

$[Na(C_{12}H_{24}O_6)(thf)_2][H_2P\text{-}BH_2\text{-}^tBuPH\text{-}BH_2\text{-}AsH_2]$ (**5**(thf)$_2$):

5(thf)$_2$ crystallizes from a THF solution layered by the 3-4-fold amount of *n*-hexane at -28 °C as light brown blocks in the monoclinic space group *C2/c*. Figure S 6.4 shows the molecular structure of **5**(thf)$_2$ in solid state.

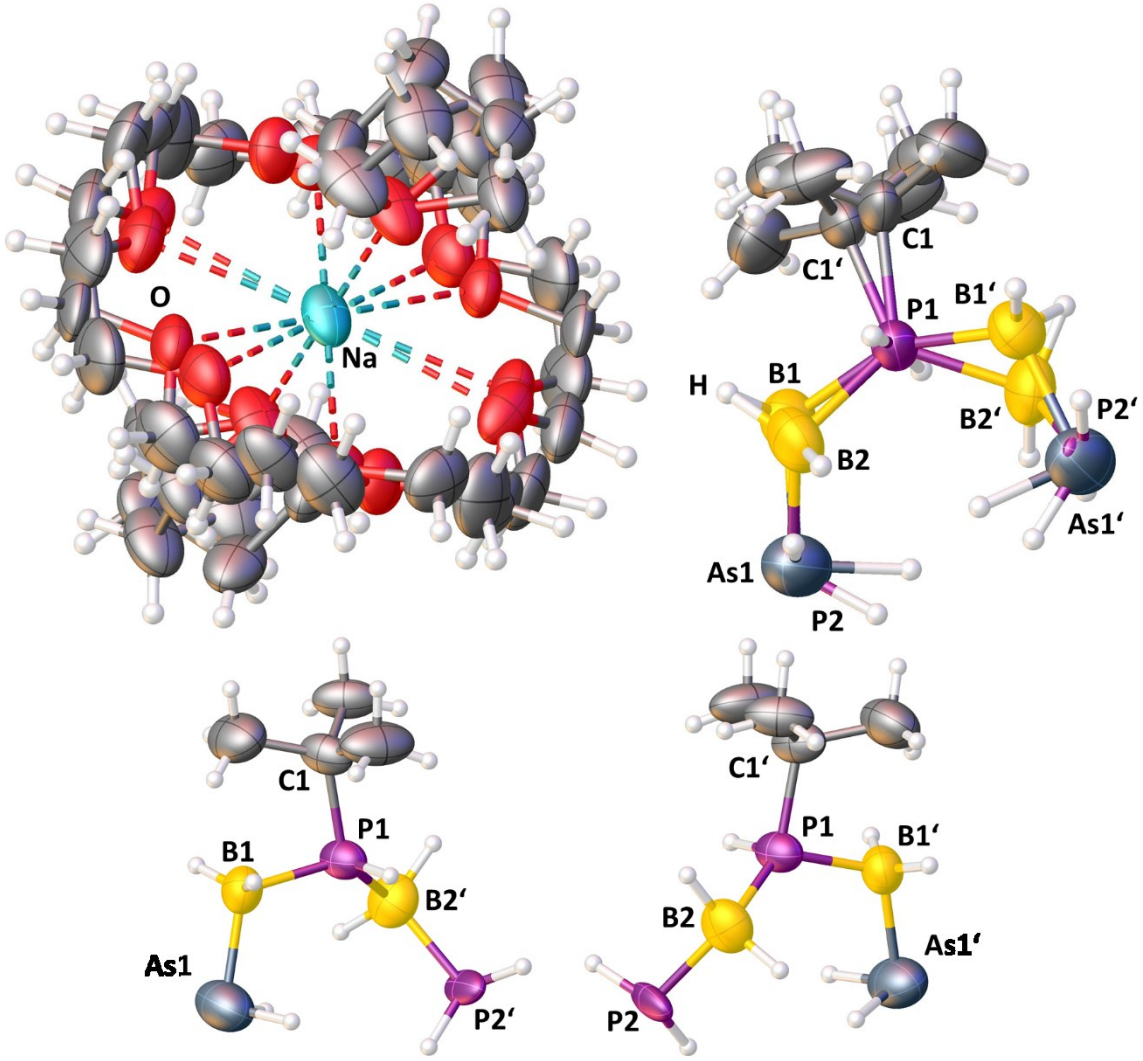

Figure S 6.4. Molecular structure of **5**(thf)$_2$ in solid state. Thermal ellipsoids are drawn with 50% probability. Atoms labeled with ‘ are generated by symmetrical operations. Selected bond length [Å] and angles [°]: As1-B1: 1.995(8), P2-B2: 1.909(5), P1-B1: 1.902(5), P1-B2: 1.908(5), P1-C1: 1.874(6), ∠(As1-B1-P1): 112.5(4), ∠(P2-B2-P1): 119.7(4), ∠(B1-P1-B2): 122.998, ∠(B1-P1-C1): 112.6(3), ∠(B2-P1-C1’):114.169. Top: disordered solid state structure of **5**(thf)$_2$; bottom: separated disorder of the anionic part of **5**(thf)$_2$.

6.5.4 Crystallographic Information

Table S 6.1. Crystallographic data for compounds **2**$(thf)_2$ and **3**$(thf)_2$.

	2$(thf)_2$	**3**$(thf)_2$
Emipirical formula	$C_{32}H_{58}B_2NaO_8P_3$	$C_{32}H_{58}As_2B_2NaO_8P$
Formula weight *M*	708.30 g/mol	796.20 g/mol
Crystal	clear colourless block	clear colourless block
Crystal size [mm³]	0.1278 x 0.1732 x 0.3264	0.143 x 0.184 x 0.24
Temperature *T*	122.8(6) K	139.08(10) K
Cristal system	monoclinic	monoclinic
Space group	*C2/c*	*C2/c*
Unit cell dimensions	*a* = 18.1267(4) Å *b* = 9.14215(14) Å *c* = 26.0012(6) Å *α* = 90° *β* = 115.213(3)° *γ* = 90°	*a* = 18.2132(6) Å *b* = 9.2419(2) Å *c* = 24.5646(8) Å *α* = 90° *β* = 106.719(4)° *γ* = 90°
Volume *V*	3898.34(15) Å^3	3960.0(2) Å^3
Formula units *Z*	4	4
Absorption coefficient $\mu_{Cu\text{-}K\alpha}$	1.868 mm^{-1}	2.932 mm^{-1}
Density (calculated) ρ_{calc}	1.207 g/cm^3	1.335 g/cm^3
F(000)	1520	1664
Theta range θ_{min} / θ_{max} / θ_{full}	3.758 / 66.920 / 66.920°	3.758 / 74.160 / 67.684°
Absorption correction	analytical	gaussian
Index ranges	-21 < *h* < 20 -10 < *k* < 8 -31 < *l* < 30	22 < *h* < 22 -6 < *k* < 11 -30 < *l* < 30
Reflections collected	8588	7393
Independent reflections [$I > 2\sigma(I)$]	3120 (R_{int} = 0.0219)	3664 (R_{int} = 0.0141)
Completeness to full θ	0.984	0.990
Transmission T_{min} / T_{max}	0.692 / 0.824	0.636 / 0.730
Data / restraints / parameters	3421 / 4 / 226	3864 / 0 / 341
Goodness-of-fit on F^2 *S*	1.028	1.054
Diffractometer type	Gemini R Ultra	GV50
Radiation type (λ)	CuK_α (1.54184 Å)	CuK_α (1.54184 Å)
Final *R*-values [$I > 2\sigma(I)$]	R_1 = 0.0361 wR_2 = 0.0941	R_1 = 0.0270 wR_2 = 0.0717
Final *R*-values (all data)	R_1 = 0.0400 wR_2 = 0.0976	R_1 = 0.0285 wR_2 = 0.0728
Largest difference hole and peak $\Delta\rho$	-0.347 0.370 eÅ^{-3}	-0.598 0.275 eÅ^{-3}

Table S 6.2. Crystallographic data for compounds **4**$(thf)_2$ and **5**$(thf)_2$.

	4$(thf)_2$	**5**$(thf)_2$
Emipirical formula	$C_{32}H_{58}AsB_2NaO_8P_2$	$C_{24}H_{58}AsB_2NaO_8P_2$
Formula weight *M*	752.25 g/mol	656.17 g/mol
Crystal	clear colourless block	clear light brown block
Crystal size [mm³]	0.112 x 0.127 x 0.273	0.139 x 0.166 x 0.227
Temperature *T*	122.96(17) K	123.00(10) K
Cristal system	monoclinic	monoclinic
Space group	*C2/c*	*C2/c*
Unit cell dimensions	*a* = 18.1956(7) Å	*a* = 20.4271(7) Å
	b = 9.2295(2) Å	*b* = 8.6437(2) Å
	c = 26.1256(10) Å	*c* = 20.0745(6) Å
	α = 90°	*α* = 90°
	β = 115.231(5)°	*β* = 93.972(3)°
	γ = 90°	*γ* = 90°
Volume *V*	3968.9(3) Å^3	3535.95(18) Å^3
Formula units *Z*	4	4
Absorption coefficient $\mu_{Cu\text{-}K\alpha}$	2.381 mm^{-1}	2.591 mm^{-1}
Density (calculated) ρ_{calc}	1.259 g/cm^3	1.233 g/cm^3
F(000)	1592	1400
Theta range θ_{min} / θ_{max} / θ_{full}	3.741 / 74.184 / 67.684°	4.339 / 74.197 / 67.684°
Absorption correction	gaussian	gaussian
Index ranges	-21 < *h* < 22	-25 < *h* < 22
	-11 < *k* < 11	-10 < *k* < 10
	-32 < *l* < 32	-23 < *l* < 24
Reflections collected	11146	13139
Independent reflections [$I > 2\sigma(I)$]	3628 (R_{int} = 0.0212)	3107 (R_{int} = 0.0368)
Completeness to full θ	0.998	0.996
Transmission T_{min} / T_{max}	0.878 / 0.938	0.657 / 0.765
Data / restraints / parameters	3928 / 2 / 241	3502 / 218 / 349
Goodness-of-fit on F^2 *S*	1.102	1.036
Diffractometer type	GV50	GV50
Radiation type (λ)	CuK_α (1.54184 Å)	CuK_α (1.54184 Å)
Final *R*-values [$I > 2\sigma(I)$]	R_1 = 0.0484	R_1 = 0.0663
	wR_2 = 0.1305	wR_2 = 0.1931
Final *R*-values (all data)	R_1 = 0.0519	R_1 = 0.0717
	wR_2 = 0.1338	wR_2 = 0.2008
Largest difference hole	-0.509	-0.370
and peak $\Delta\rho$	0.586 eÅ^{-3}	0.913 eÅ^{-3}

6.5.5 NMR Spectroscopy

$[Na(C_{12}H_{24}O_6)(thf)_2][H_2P\text{-}BH_2\text{-}PPh_2\text{-}BH_2\text{-}PH_2]$ $(2(thf)_2)$:

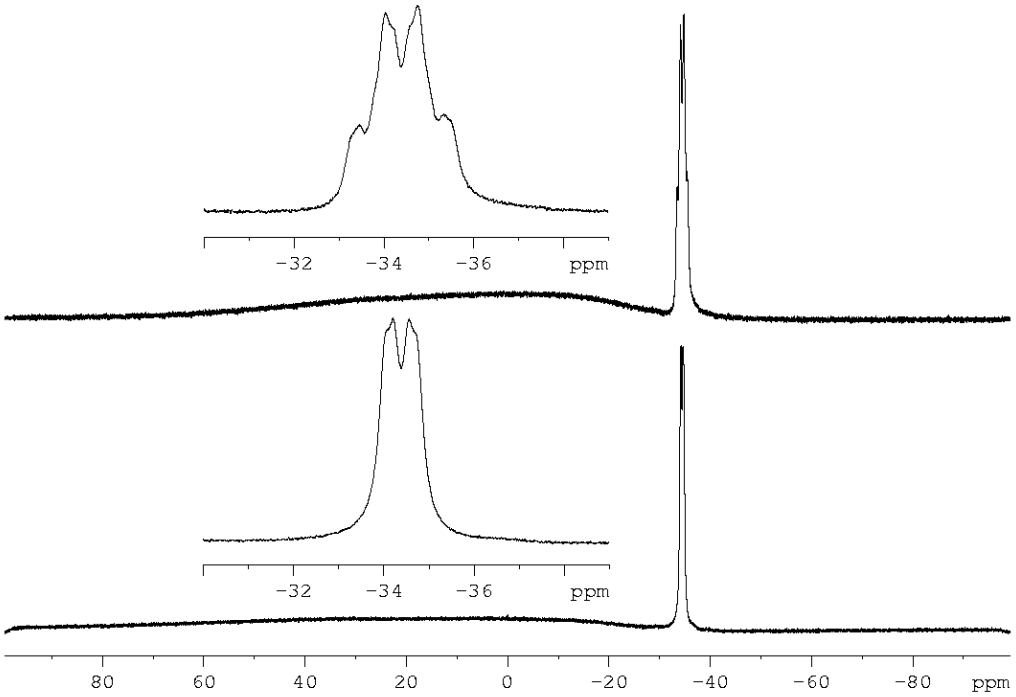

Figure S 6.5. $^{11}B\{^1H\}$ (bottom) and ^{11}B NMR spectrum (top) of **2** in THF-d_8.

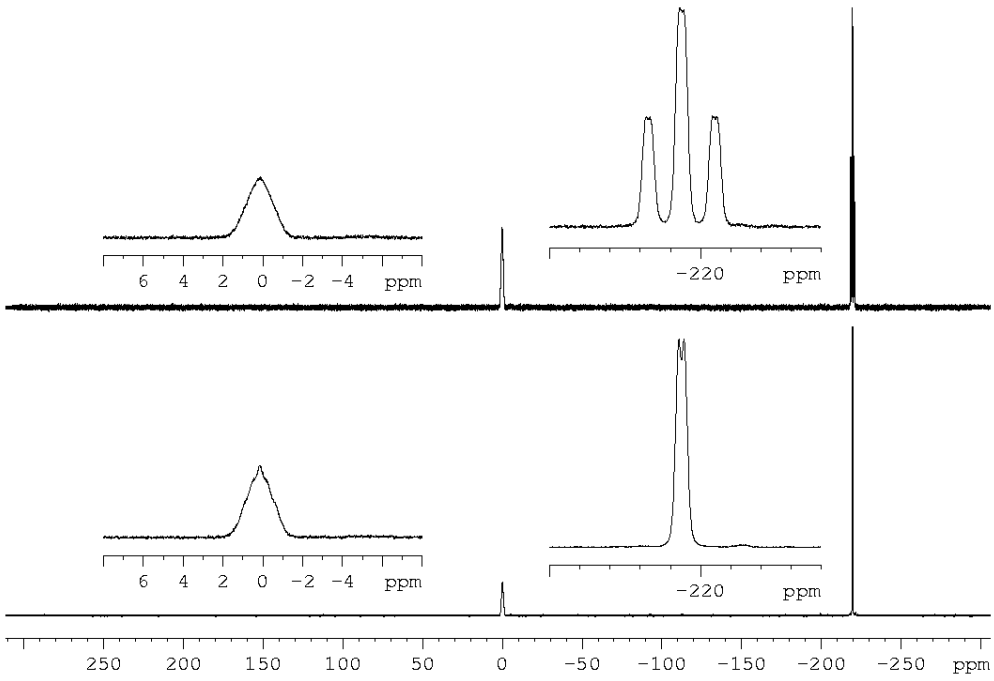

Figure S 6.6. $^{31}P\{^1H\}$ (bottom) and ^{31}P NMR spectrum (top) of **2** in THF-d_8.

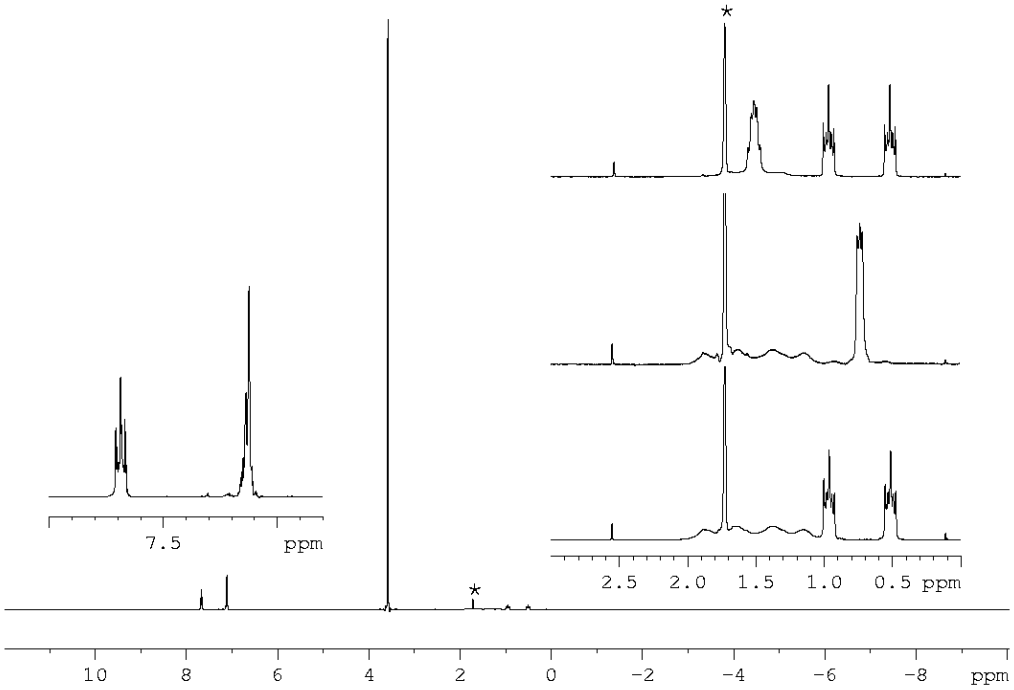

Figure S 6.7. ^{1}H NMR spectrum of **2** in THF-d_8. * = solvent (THF-d_8).
Magnified part shows ^{1}H, ^{1}H{^{31}P}, ^{1}H{^{11}B}, NMR (from bottom to top) of the anion**.**

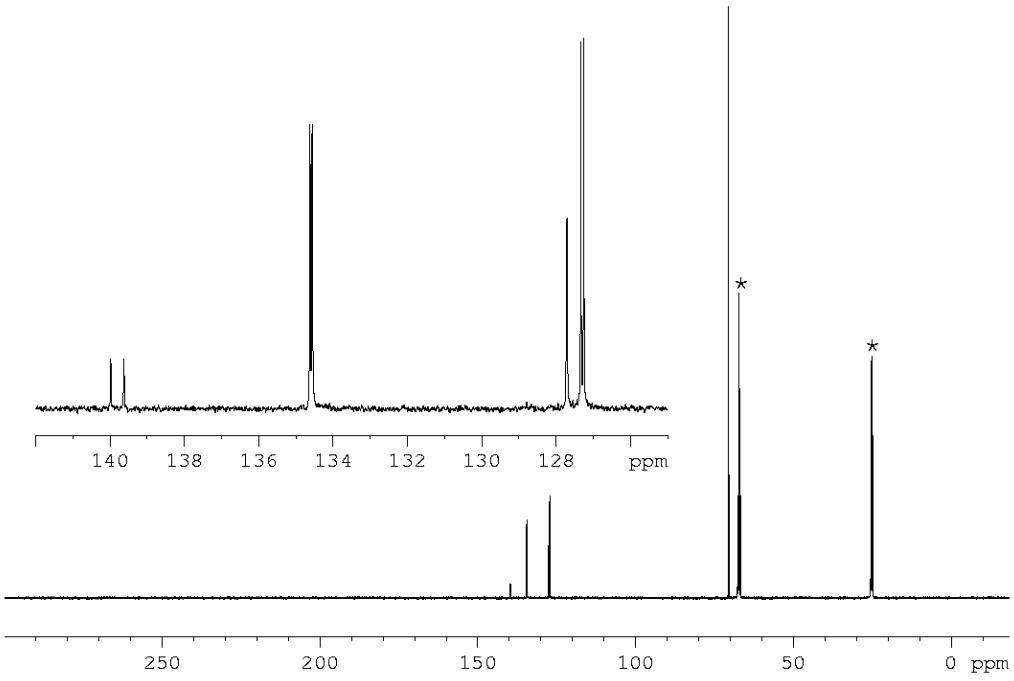

Figure S 6.8. ^{13}C NMR spectrum of **2** in THF-d_8. * = solvent (THF-d_8).

$[Na(C_{12}H_{24}O_6)(thf)_2][H_2As\text{-}BH_2\text{-}PPh_2\text{-}BH_2\text{-}AsH_2]$ $(3(thf)_2)$:

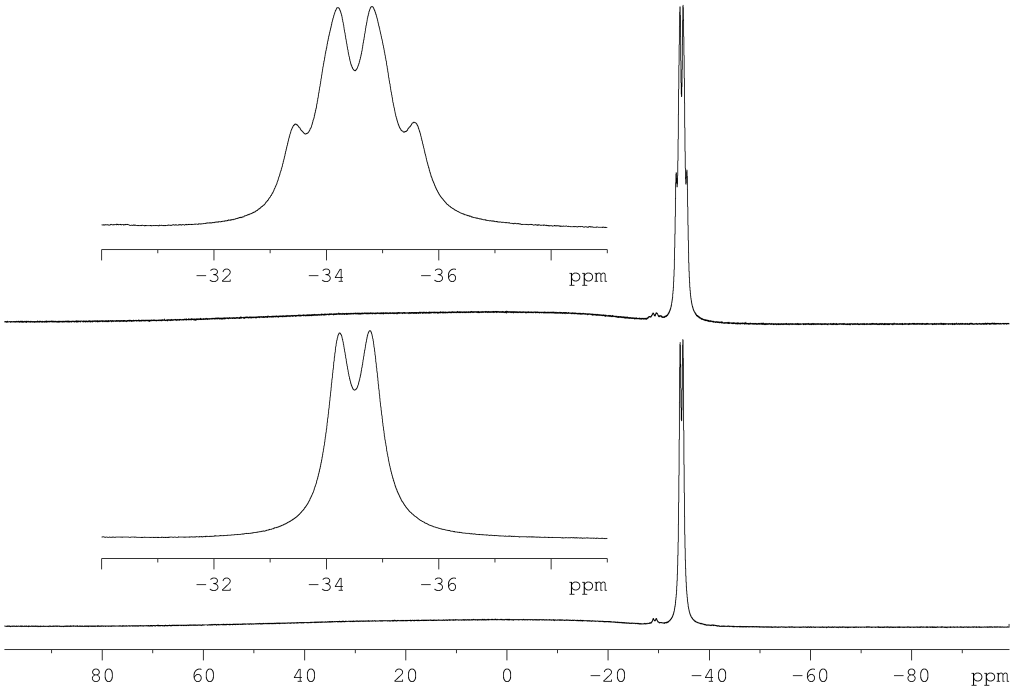

Figure S 6.9. $^{11}B\{^1H\}$ (bottom) and ^{11}B NMR spectrum (top) of **3** in THF-d_8.

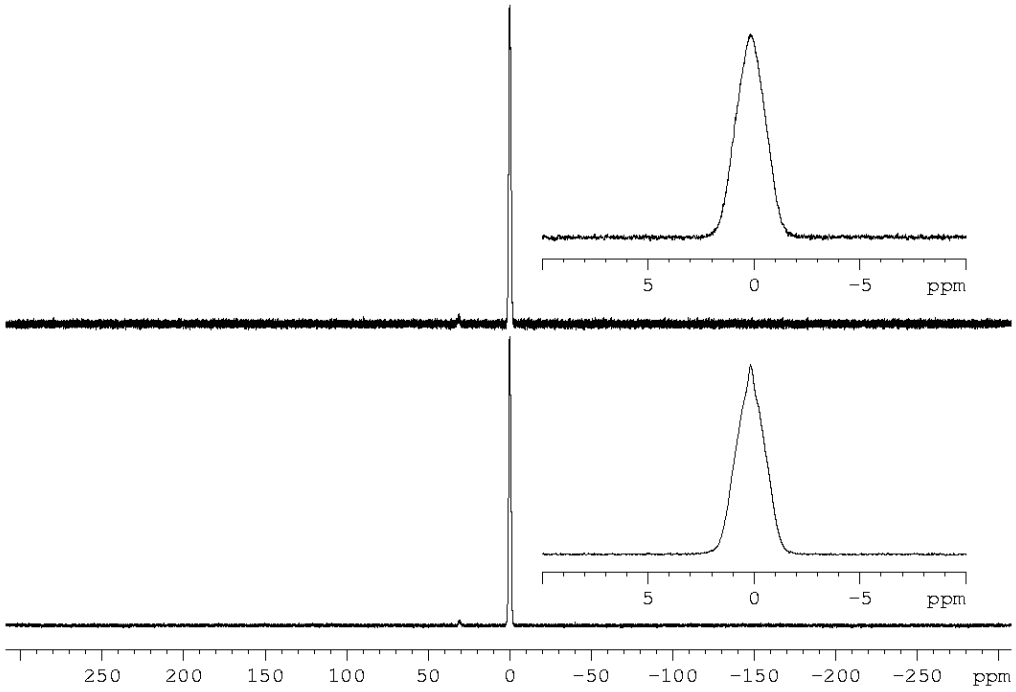

Figure S 6.10. $^{31}P\{^1H\}$ (bottom) and ^{31}P NMR spectrum (top) of **3** in THF-d_8.

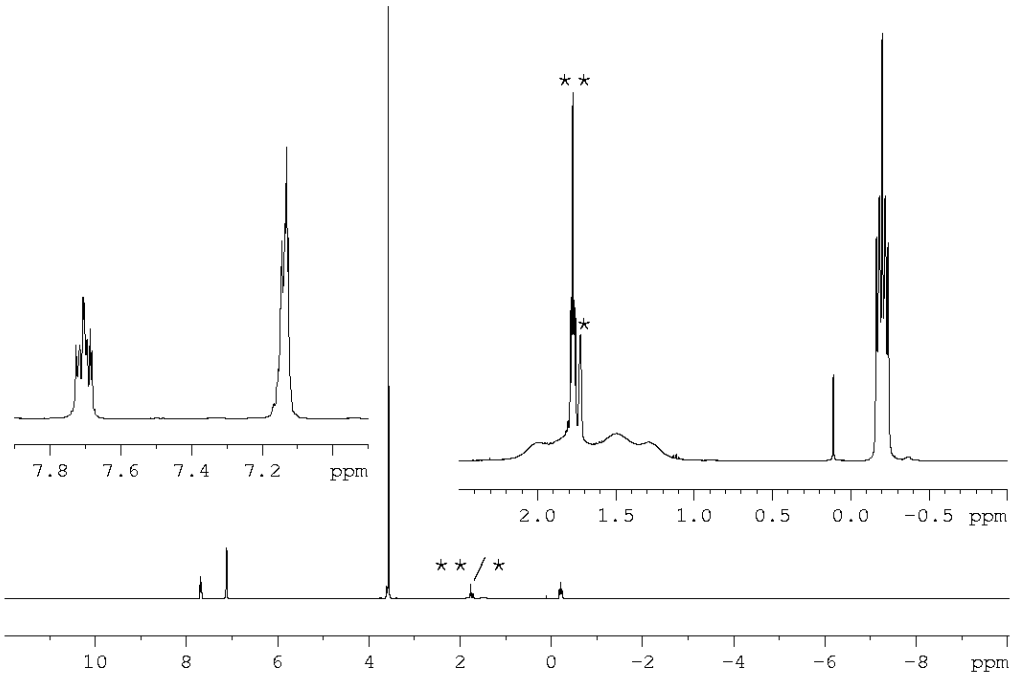

Figure S 6.11. ^{1}H NMR spectrum of **3** in THF-d_8. * = solvent (THF-d_8).

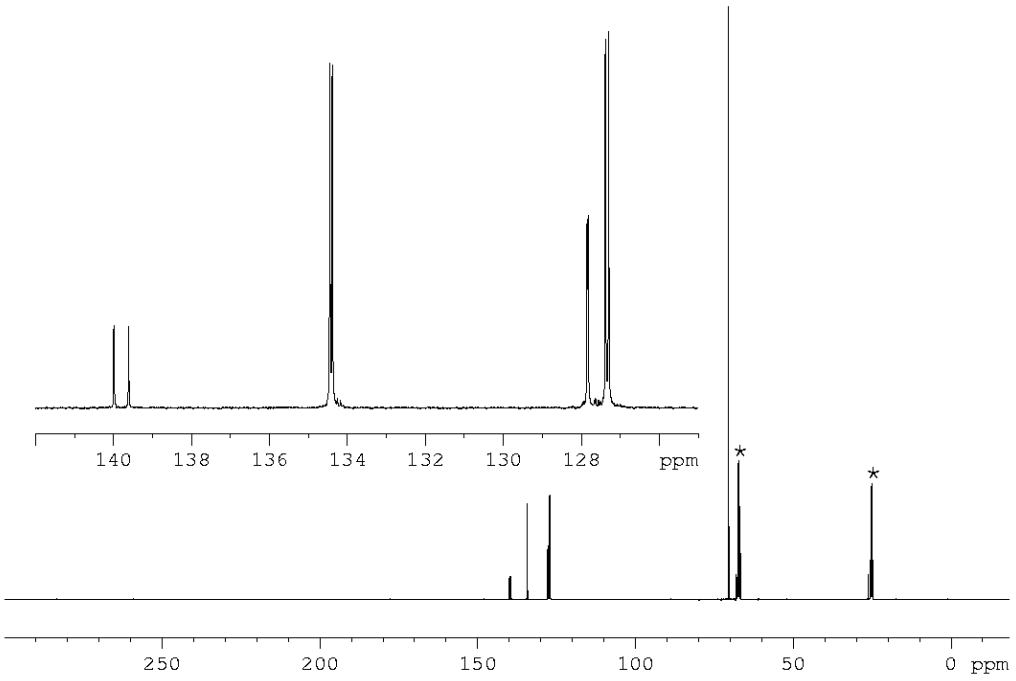

Figure S 6.12. ^{13}C NMR spectrum of **3** in THF-d_8. * = solvent (THF-d_8).

$[Na(C_{12}H_{24}O_6)(thf)_2][H_2P\text{-}BH_2\text{-}PPh_2\text{-}BH_2\text{-}AsH_2]$ $(4(thf)_2)$:

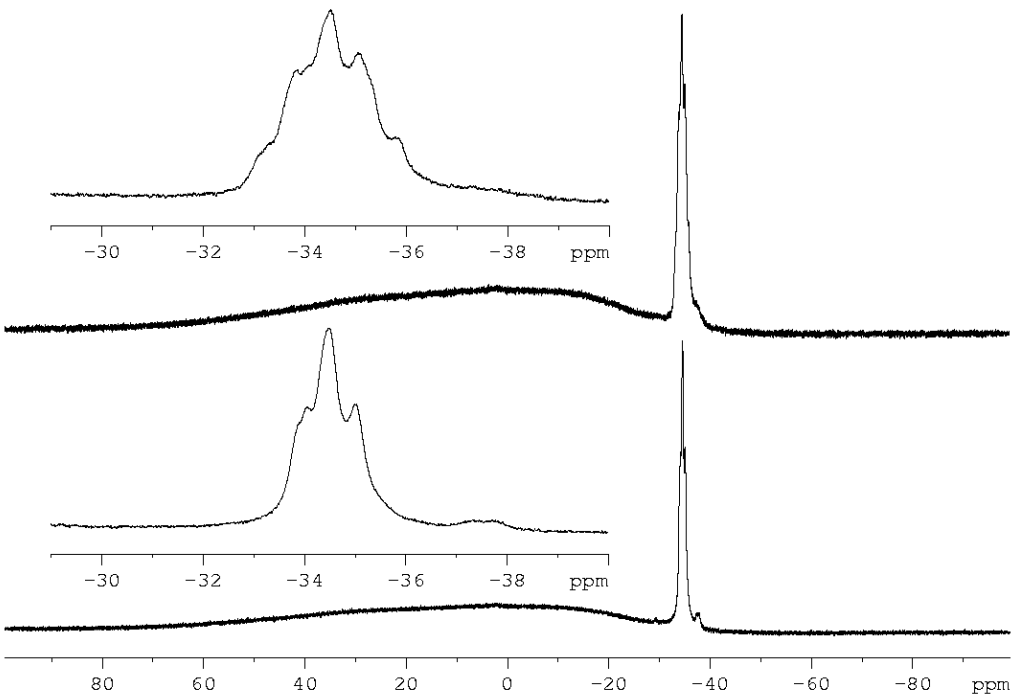

Figure S 6.13. $^{11}B\{^1H\}$ (bottom) and ^{11}B NMR spectrum (top) of **4** in THF-d_8.

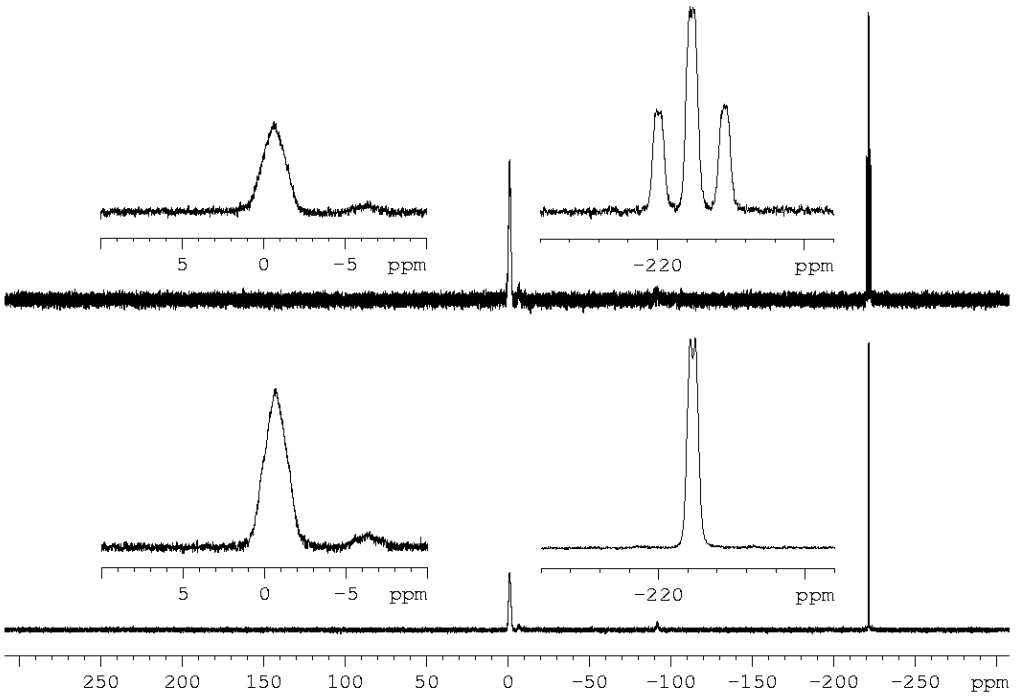

Figure S 6.14. $^{31}P\{^1H\}$ (bottom) and ^{31}P NMR spectrum (top) of **4** in THF-d_8.

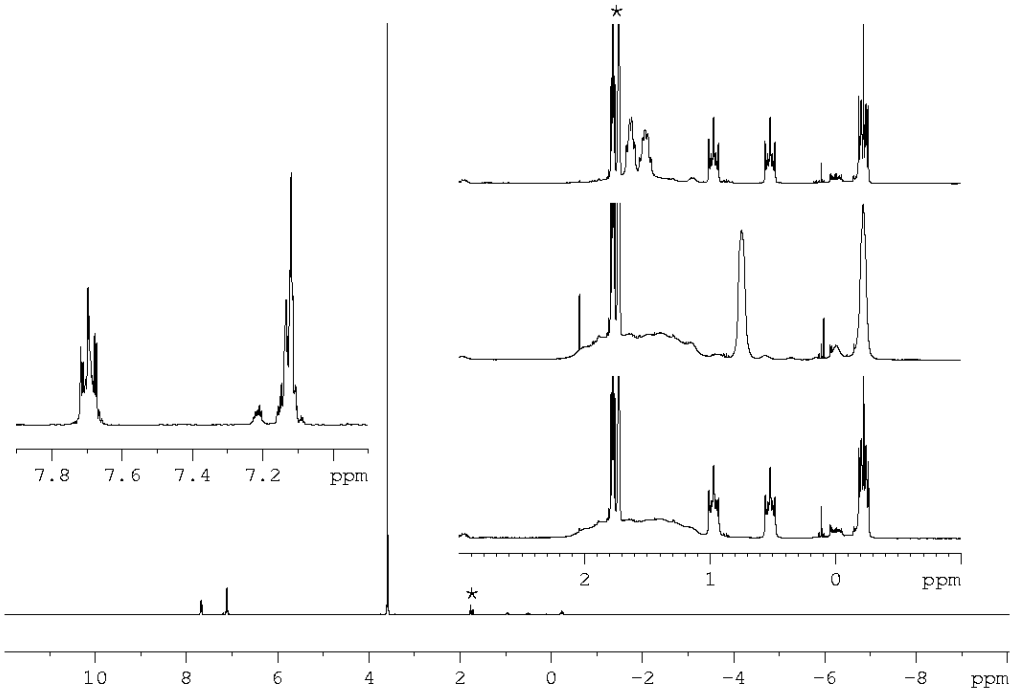

Figure S 6.15. ^{1}H NMR spectrum of **4** in THF-d_8. * = solvent (THF-d_8).
Magnified part shows ^{1}H, $^{1}H\{^{31}P\}$, $^{1}H\{^{11}B\}$, NMR (from bottom to top) of the anion**.**

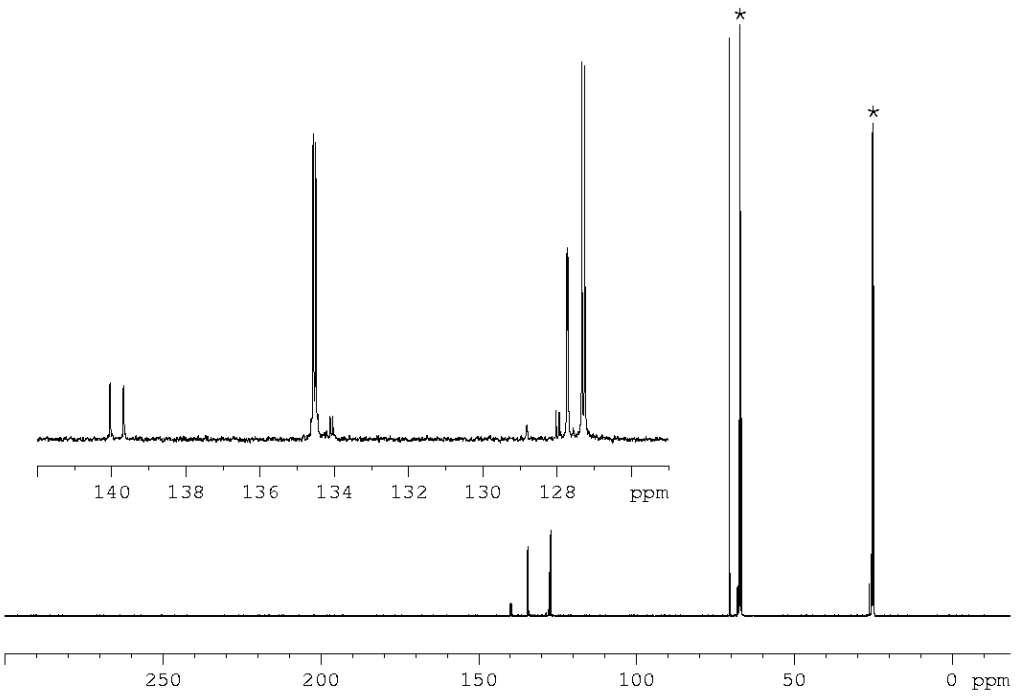

Figure S 6.16. ^{13}C NMR spectrum of **4** in THF-d_8. * = solvent (THF-d_8).

$[Na(C_{12}H_{24}O_6)(thf)_2][H_2P\text{-}BH_2\text{-}^tBuPH\text{-}BH_2\text{-}AsH_2]$ $(5(thf)_2)$:

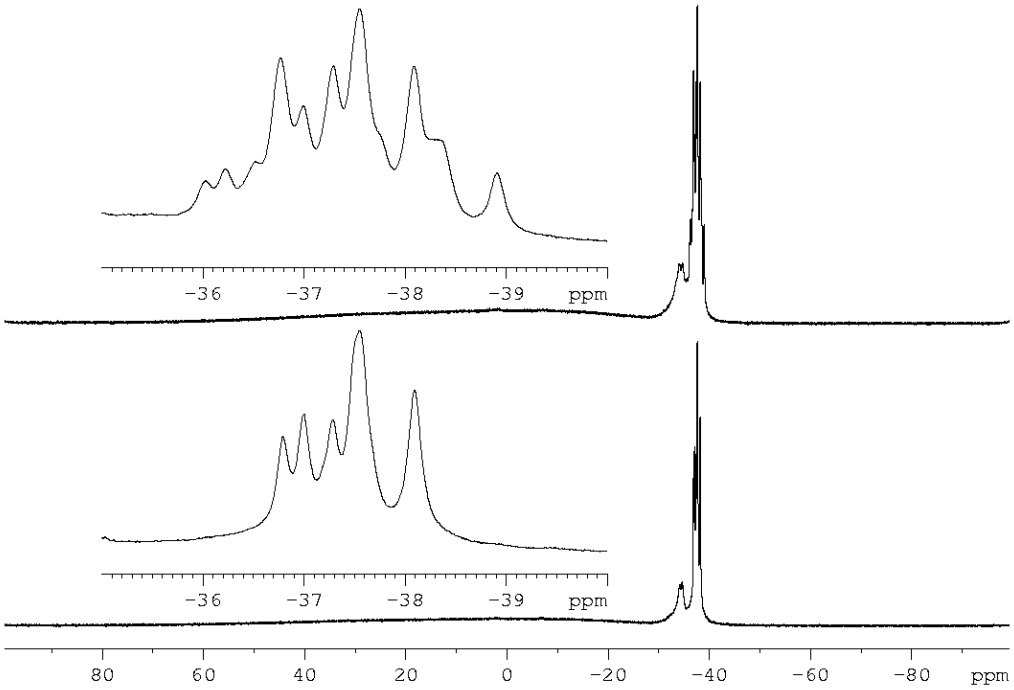

Figure S 6.17. $^{11}B\{^1H\}$ (bottom) and ^{11}B NMR spectrum (top) of **5** in THF-d_8.

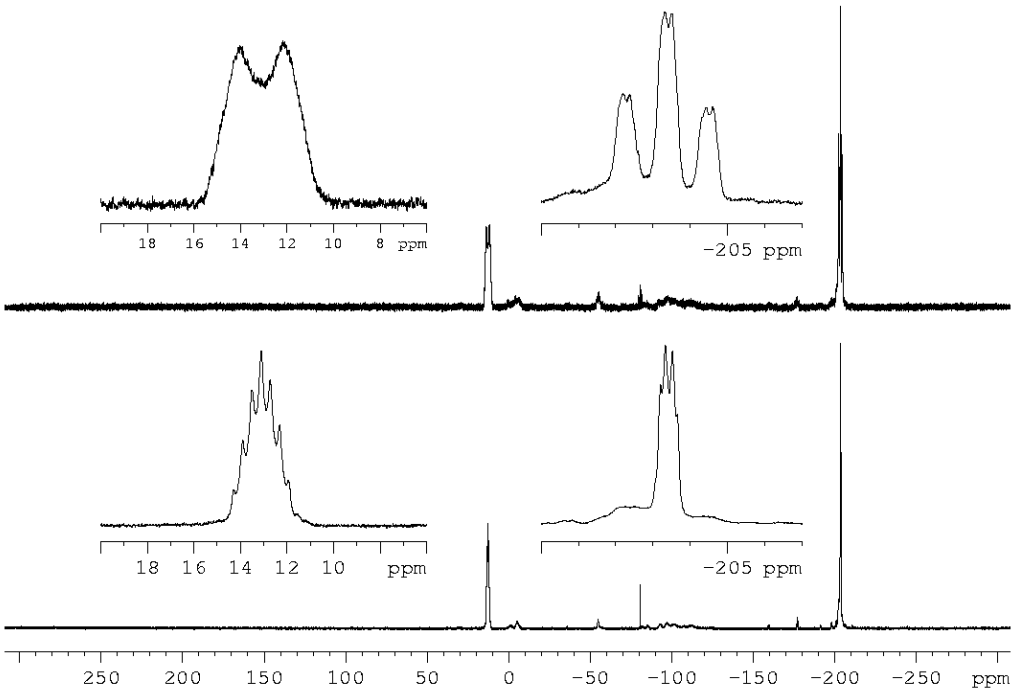

Figure S 6.18. $^{31}P\{^1H\}$ (bottom) and ^{31}P NMR spectrum (top) of **5** in THF-d_8.

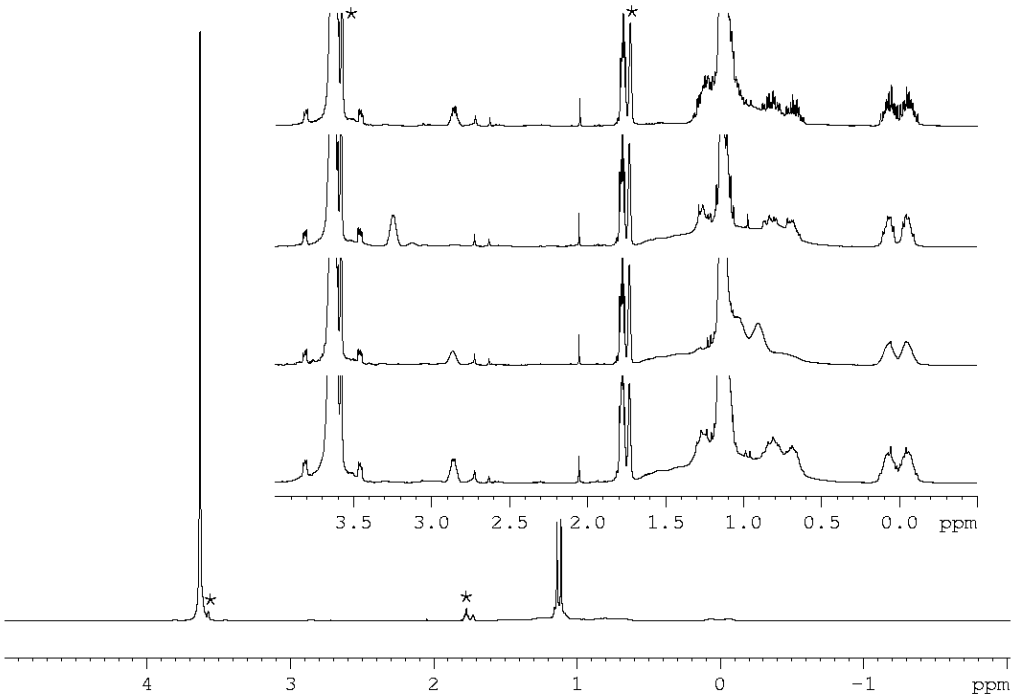

Figure S 6.19. ^{1}H NMR spectrum of **5** in THF-d_8. * = solvent (THF-d_8 / THF).
Magnified part shows ^{1}H, ^{1}H{^{31}P} (P<u>H</u>$_2$), ^{1}H{^{31}P} (^{t}BuP<u>H</u>), ^{1}H{^{11}B}, NMR (from bottom to top) of the anion.

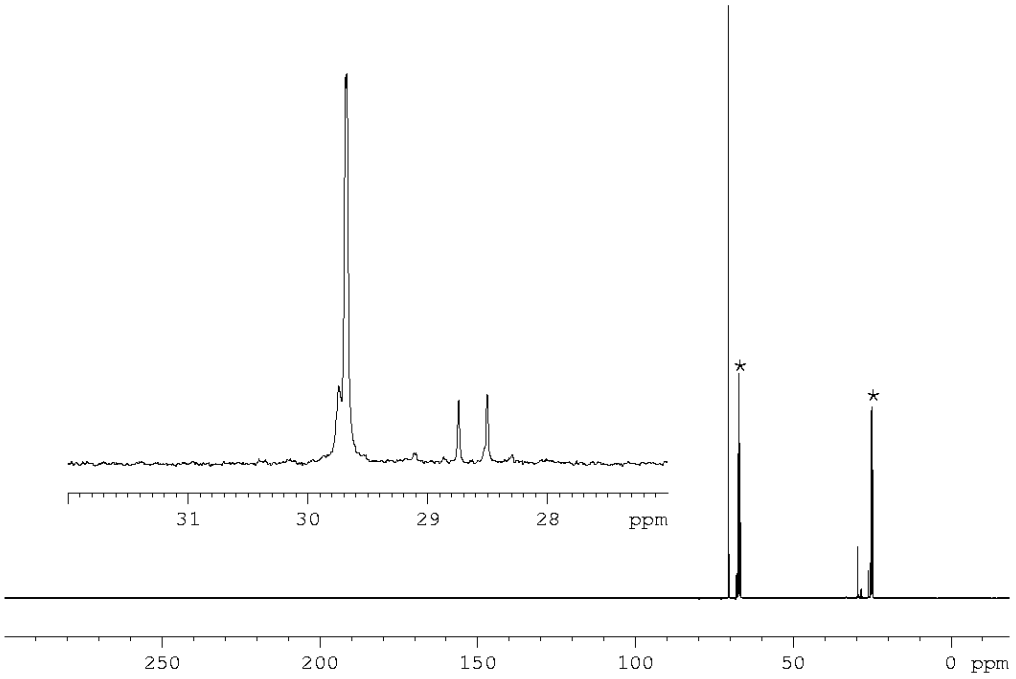

Figure S 6.20. ^{13}C NMR spectrum of **5** in THF-d_8. * = solvent (THF-d_8).

6.5.6 Computational Details

For all computations Gaussian 09 program package[9] was used throughout. Density functional theory (DFT) in form of Becke's three-parameter hybrid functional B3LYP[10] with 6-311++G** all electron basis set was employed. Basis sets were obtained from the EMSL basis set exchange database.[11] The geometries of the compounds have been fully optimized and verified to be true minima on their respective potential energy surface (PES).

Table S 6.3. Gas phase reaction energies ΔE^{o}_{0}, standard reaction enthalpies ΔH^{o}_{298}, Gibbs energies ΔG^{o}_{298} in kJ mol^{-1}, and standard reaction entropies ΔS^{o}_{298}, J mol^{-1} K^{-1}. B3LYP/6-311++G** level of theory.

Reaction	**ΔE^{o}_{0}**	**ΔH^{o}_{298}**	**ΔS^{o}_{298}**	**ΔG^{o}_{298}**
$[PH_2\text{-}BH_2\text{-}^{t}BuPH]^{-}$ + $PH_2\text{-}BH_2\text{-}NMe_3$ = $[PH_2\text{-}BH_2\text{-}^{t}BuPH\text{-}BH_2\text{-}PH_2]^{-}$ + NMe_3	-53.3	-56.5	-4.3	-55.2
$[PH_2\text{-}BH_2\text{-}^{t}BuPH]^{-}$ + $AsH_2\text{-}BH_2\text{-}NMe_3$ = $[PH_2\text{-}BH_2\text{-}^{t}BuPH\text{-}BH_2\text{-}AsH_2]^{-}$ (**5**) +NMe_3	-56.9	-59.6	-9.8	-56.7

Table S 6.4. Total energies E^{o}_{0}, sum of electronic and thermal enthalpies H^{o}_{298} (Hartree) and standard entropies S^{o}_{298} (cal·mol^{-1}·K^{-1}) for studied compounds. B3LYP/6-311++G** level of theory.

Compound	**Point Group**	**E^{o}_{0}**	**H^{o}_{298}**	**S^{o}_{298}**
NMe_3	C_{3v}	-174.5277593	-174.401711	68.834
$PH_2\text{-}BH_2\text{-}NMe_3$	C_s	-543.1864873	-543.012836	88.909
$AsH_2\text{-}BH_2\text{-}NMe_3$	C_s	-2437.688332	-2437.516475	94.775
$[PH_2\text{-}BH_2\text{-}tBuPH]^{-}$	C_1	-868.5802614	-868.399538	103.033
$[PH_2\text{-}BH_2\text{-}^{t}BuPH\text{-}BH_2\text{-}PH_2]^{-}$	C_1	-1237.259299	-1237.0322	122.069
$[PH_2\text{-}BH_2\text{-}^{t}BuPH\text{-}BH_2\text{-}AsH_2]^{-}$ (**5**)	C_1	-3131.76249	-3131.536995	126.639

Table S 6.5. Optimized xyz coordinates (in Angstroms) for studied compounds B3LYP/6-311++G** level of theory.

NMe_3

Atom	**x**	**y**	**z**
N	0.000000000	0.000000000	0.367467000
C	0.000000000	1.391145000	-0.059957000
H	0.000000000	1.502833000	-1.161580000
H	-0.884565000	1.899384000	0.331951000
H	0.884565000	1.899384000	0.331951000
C	-1.204767000	-0.695572000	-0.059957000
H	-1.202632000	-1.715748000	0.331951000
H	-2.087198000	-0.183636000	0.331951000
H	-1.301492000	-0.751417000	-1.161580000

C	1.204767000	-0.695572000	-0.059957000
H	1.202632000	-1.715748000	0.331951000
H	1.301492000	-0.751417000	-1.161580000
H	2.087198000	-0.183636000	0.331951000

PH_2-BH_2-NMe_3

Atom	x	y	z
P	-1.968522000	-1.143581000	0.000000000
B	-0.945248000	0.546654000	0.000000000
N	0.722203000	0.462761000	0.000000000
H	-1.217018000	1.158325000	1.004099000
H	-1.217018000	1.158325000	-1.004099000
C	1.232069000	-0.231054000	1.214957000
H	2.325415000	-0.208258000	1.229998000
H	0.836952000	0.271798000	2.096341000
H	0.883556000	-1.261587000	1.209356000
C	1.232069000	1.864466000	0.000000000
H	0.856527000	2.374363000	-0.885309000
H	0.856527000	2.374363000	0.885309000
H	2.326008000	1.868299000	0.000000000
C	1.232069000	-0.231054000	-1.214957000
H	0.836952000	0.271798000	-2.096341000
H	2.325415000	-0.208258000	-1.229998000
H	0.883556000	-1.261587000	-1.209356000
H	-1.337737000	-1.885301000	1.043729000
H	-1.337737000	-1.885301000	-1.043729000

AsH_2-BH_2-NMe_3

Atom	x	y	z
As	-1.788881000	0.167310000	0.000000000
B	0.156486000	0.957854000	0.000000000
N	1.441160000	-0.090999000	0.000000000
H	0.283622000	1.611249000	1.005083000
H	0.283622000	1.611249000	-1.005083000
C	1.441160000	-0.952488000	1.215659000
H	2.328021000	-1.592163000	1.221830000
H	1.436768000	-0.313149000	2.097118000
H	0.540641000	-1.562361000	1.217251000
C	2.683915000	0.735963000	0.000000000
H	2.684015000	1.368957000	-0.885432000
H	2.684015000	1.368957000	0.885432000
H	3.566698000	0.090113000	0.000000000
C	1.441160000	-0.952488000	-1.215659000
H	1.436768000	-0.313149000	-2.097118000
H	2.328021000	-1.592163000	-1.221830000
H	0.540641000	-1.562361000	-1.217251000
H	-1.673853000	-0.887313000	1.104622000
H	-1.673853000	-0.887313000	-1.104622000

$[H_2P\text{-}BH_2\text{-}^tBuPH]^-$

Atom	x	y	z
P	-0.111859000	-0.745775000	-0.228660000
P	-3.307255000	0.046281000	0.052905000
B	-1.435134000	0.741023000	-0.082008000
H	-3.190995000	-0.898755000	1.123523000
H	-3.318995000	-0.979810000	-0.945766000
H	-1.388185000	1.388406000	-1.111059000
H	-1.267585000	1.450814000	0.890754000
H	-0.193060000	-1.302235000	1.088663000
C	1.632251000	0.038244000	0.024264000
C	2.675180000	-1.092186000	0.053951000
H	2.497211000	-1.771548000	0.894347000
H	2.638887000	-1.685779000	-0.864459000
H	3.692736000	-0.685537000	0.161126000
C	1.912593000	0.952948000	-1.180497000
H	2.921522000	1.385391000	-1.111839000
H	1.846847000	0.397013000	-2.121754000
H	1.190330000	1.771862000	-1.227866000
C	1.736336000	0.856219000	1.320809000
H	0.984683000	1.647375000	1.347256000
H	1.578263000	0.220972000	2.198417000
H	2.732551000	1.317775000	1.413876000

$[H_2P\text{-}BH_2\text{-}^tBuPH\text{-}BH_2\text{-}PH_2]^-$

Atom	x	y	z
P	3.087302000	-1.556434000	-0.280819000
P	0.000000000	-0.249805000	0.169283000
P	-3.087304000	-1.556432000	-0.280820000
B	1.718318000	-0.842393000	0.979907000
B	-1.718319000	-0.842390000	0.979907000
H	2.303391000	-2.473726000	-1.047024000
H	3.088690000	-0.575322000	-1.321735000
H	1.445341000	-1.731854000	1.748654000
H	2.198949000	0.102634000	1.566005000
H	-0.000003000	-0.645219000	-1.192567000
H	-2.198951000	0.102638000	1.566002000
H	-1.445344000	-1.731848000	1.748658000
H	-3.088680000	-0.575324000	-1.321741000
H	-2.303390000	-2.473731000	-1.047017000
C	0.000001000	1.634141000	-0.085116000
C	-1.256669000	2.054122000	-0.865829000
H	-1.283696000	1.595399000	-1.858783000
H	-2.168312000	1.766979000	-0.338528000
H	-1.265855000	3.144447000	-0.999024000
C	-0.000004000	2.317526000	1.294575000
H	-0.000005000	3.407817000	1.166777000
H	-0.885137000	2.042394000	1.873018000
H	0.885125000	2.042395000	1.873022000

C	1.256675000	2.054124000	-0.865820000
H	1.265859000	3.144447000	-0.999019000
H	2.168315000	1.766985000	-0.338510000
H	1.283712000	1.595396000	-1.858772000

$[H_2P\text{-}BH_2\text{-}^tBuPH\text{-}BH_2\text{-}AsH_2]^-$ (5)

Atom	x	y	z
P	3.016497000	-2.297233000	-0.291254000
P	0.481894000	-0.111359000	0.211929000
As	-2.944236000	-0.545551000	-0.140858000
B	1.951136000	-1.202116000	0.989806000
B	-1.289386000	-0.115918000	1.102424000
H	1.976577000	-2.951471000	-1.021553000
H	3.277051000	-1.371899000	-1.349802000
H	1.431893000	-1.969189000	1.763521000
H	2.703079000	-0.449037000	1.568306000
H	0.304744000	-0.511723000	-1.135606000
H	-1.487197000	0.974382000	1.587761000
H	-1.264976000	-0.977985000	1.944322000
H	-2.656987000	0.384112000	-1.327417000
H	-2.391247000	-1.756362000	-0.900423000
C	1.058077000	1.672725000	-0.102840000
C	-0.028943000	2.438063000	-0.876588000
H	-0.224465000	1.980227000	-1.850806000
H	-0.969859000	2.464712000	-0.323679000
H	0.296781000	3.472630000	-1.050283000
C	1.308299000	2.360425000	1.251370000
H	1.639704000	3.393650000	1.085378000
H	0.398858000	2.387892000	1.856095000
H	2.082785000	1.842356000	1.821927000
C	2.360344000	1.662492000	-0.921465000
H	2.691556000	2.693428000	-1.105733000
H	3.159628000	1.136805000	-0.395682000
H	2.220600000	1.177476000	-1.892153000

6.5.7 References

[1] C. Marquardt, A. Adolf, A. Stauber, M. Bodensteiner, A. V. Virovets, A. Y. Timoshkin, M. Scheer, *Chem. Eur. J.* **2013***,* 19, 11887-11891.

[2] See **chapter 5**; compounds $[Na(C_{12}H_{24}O_6)][H_2P\text{-}BH_2\text{-}PPh_2]$ (**7**), $[Na(C_{12}H_{24}O_6)][H_2As\text{-}BH_2\text{-}PPh_2]$ (**9**), $[Na(C_{12}H_{24}O_6)][H_2P\text{-}BH_2\text{-}^tBuPH]$ (**3**), $[Na(C_{12}H_{24}O_6)][H_2As\text{-}BH_2\text{-}^tBuPH\text{-}BH_3]$ (**6**).

[3] R. C. Clark, J. S. Reid, *Acta Cryst.* **1995**, *A51*, 887-897.

[4] CrysAlisPro Software System, Rigaku Oxford Diffraction, (**2017**).

[5] A. Altomare, M. C.Burla, M. Camalli, G. L. Cascarano, C. Giacovazzo, A. Guagliardi, A.G. G. Moliterni, G. Polidori, R. Spagna, J. Appl. Cryst. **1999**, *32*, 115-119.

[6] Sheldrick, G.M., ShelXT-Integrated space-group and crystal-structure determination, *Acta Cryst.* **2015**, *A71*, 3-8.

[7] O. V. Dolomanov and L.J. Bourhis and R.J. Gildea and J.A.K. Howard and H. Puschmann, Olex2: A complete structure solution, refinement and analysis program, *J. Appl. Cryst.* **2009**, *42*, 339-341.

[8] Sheldrick, G. M., Crystal structure refinement with ShelXL, *Acta Cryst.* **2015**, *C71*, 3-8.

[9] M. J. Frisch, G. W. Trucks, H. B. Schlegel, G. E. Scuseria, M. A. Robb, J. R. Cheeseman, G. Scalmani, V. Barone, B. Mennucci, G. A. Petersson, H. Nakatsuji, M. Caricato, X. Li, H. P. Hratchian, A. F. Izmaylov, J. Bloino, G. Zheng, J. L. Sonnenberg, M. Hada, M. Ehara, K. Toyota, R. Fukuda, J. Hasegawa, M. Ishida, T. Nakajima, Y. Honda, O. Kitao, H. Nakai, T. Vreven, J. A. Montgomery, Jr., J. E. Peralta, F. Ogliaro, M. Bearpark, J. J. Heyd, E. Brothers, K. N. Kudin, V. N. Staroverov, T. Keith, R. Kobayashi, J. Normand, K. Raghavachari, A. Rendell, J. C. Burant, S. S. Iyengar, J. Tomasi, M. Cossi, N. Rega, J. M. Millam, M. Klene, J. E. Knox, J. B. Cross, V. Bakken, C. Adamo, J. Jaramillo, R. Gomperts, R. E. Stratmann, O. Yazyev, A. J. Austin, R. Cammi, C. Pomelli, J. W. Ochterski, R. L. Martin, K. Morokuma, V. G. Zakrzewski, G. A. Voth, P. Salvador, J. J. Dannenberg, S. Dapprich, A. D. Daniels, O. Farkas, J. B. Foresman, J. V. Ortiz, J. Cioslowski, and D. J. Fox, Gaussian 09, Revision E.01, Gaussian, Inc., Wallingford CT, **2013**.

[10] a) A. D. Becke, *J. Chem. Phys.* **1993**, *98*, 5648. b) C. Lee, W. Yang, R. G. Parr, *Phys. Rev. B.* **1988**, *37*,785.

[11] (a) D. Feller, *J. Comp. Chem.* **1996**, *17*, 1571-1586; (b) K. L. Schuchardt, B. T. Didier, T. Elsethagen, L. Sun, V. Gurumoorthi, J. Chase, J. Li, T. L. Windus, *J. Chem. Inf. Model.* **2007**, *47*, 1045-1052.

7 Conclusion

7.1 Parent anionic derivatives of Pnictogenylboranes

High molecular inorganic polymers bearing a group 13/15 backbone are mainly obtained by dehydrocoupling reactions of saturated pnictogen-boron adducts using transition metal catalysts. A catalyst free linkage of monomers is achievable by thermal treatment of Lewis base stabilized pnictogenylboranes undergoing a head-to-tail polymerization, under release of the Lewis base. To investigate the catenation of unsaturated group 13/15 adducts and to get deeper insight into the head-to-tail polymerization reaction steps, the phosphorus based nucleophile $NaPH_2$ was reacted with the Lewis base stabilized parent phosphanylborane $H_2P\text{-}BH_2\text{-}NMe_3$ (**C1**). Substitution of the Lewis base NMe_3 by the nucleophile leads to the formation of the anionic chain like compound $[Na(C_{12}H_{24}O_6)][H_2P\text{-}BH_2\text{-}PH_2]$ (**C3**) in the presence of 18-crown-6 ($C_{12}H_{24}O_6$) (Scheme 7.1).

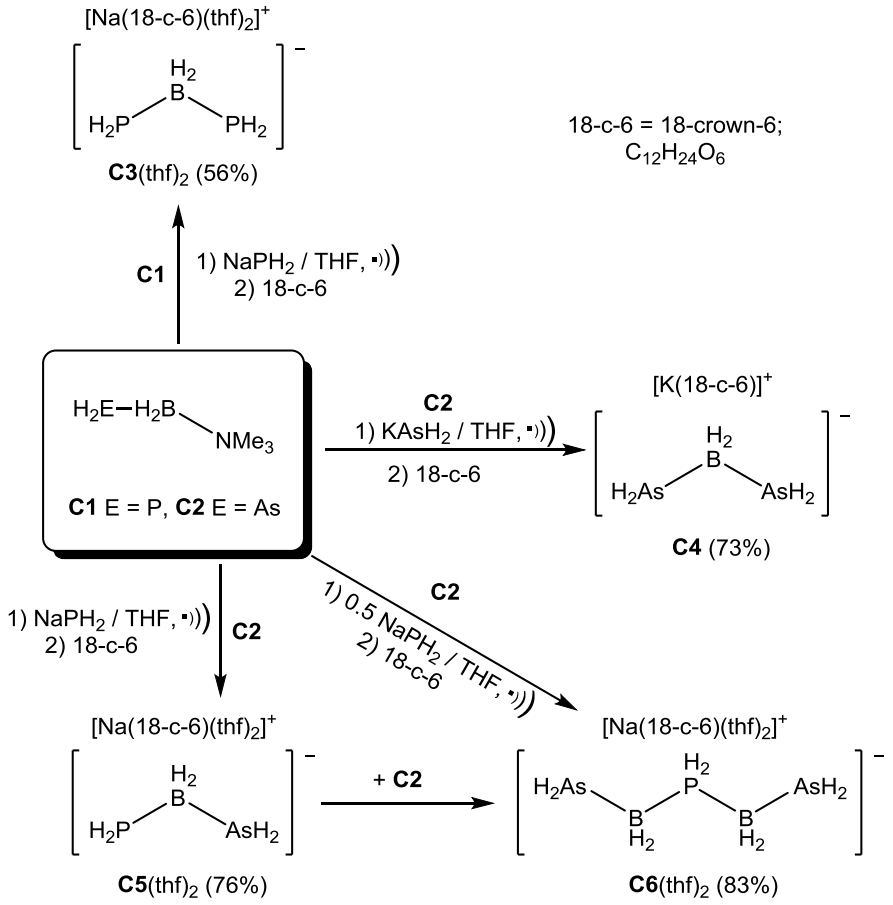

Scheme 7.1. Reaction of **C1** and **C2** with phosphorus and arsenic centered nucleophiles. Isolated yields are given in parentheses.

The analog reaction with corresponding arsenic containing starting materials $KAsH_2$ and $H_2As\text{-}BH_2\text{-}NMe_3$ (**C2**) results in the three membered chain like compound $[K(C_{12}H_{24}O_6)][H_2As\text{-}BH_2\text{-}AsH_2]$ (**C4**, Scheme 7.1). The phosphorus and arsenic mixed compound $[Na(C_{12}H_{24}O_6)][H_2P\text{-}BH_2\text{-}AsH_2]$ (**C5**) is accessible by the reaction of arsanylborane (**C2**) with $NaPH_2$ (Scheme 7.1). Reaction of **C5** with a second equivalent of arsanylborane (**C2**) leads to elongation of the group 13/15 backbone under formation of $[Na(C_{12}H_{24}O_6)][H_2As\text{-}BH_2\text{-}PH_2\text{-}BH_2\text{-}AsH_2]$ (**C6**, Scheme 7.1). This compound is also accessible by reacting **C2** with $NaPH_2$ in a two to one stochiometry, representing an alternative and more straight forward synthetic pathway.

The reaction of phosphanylborane (**C1**) with NHC^{dipp} (NHC = N-heterocyclic carbene) instead of pnictogen based nucleophiles and subsequent refluxing in toluene leads to the formation of the cyclic compound $[NHC^{dipp}\text{-}BH_2\text{-}PH_2\text{-}BH_2\text{-}NHC^{dipp}][P_5B_5H_{19}]$ (**C7**) containing a *n*-butylcyclohexane-like anion (Scheme 7.2).

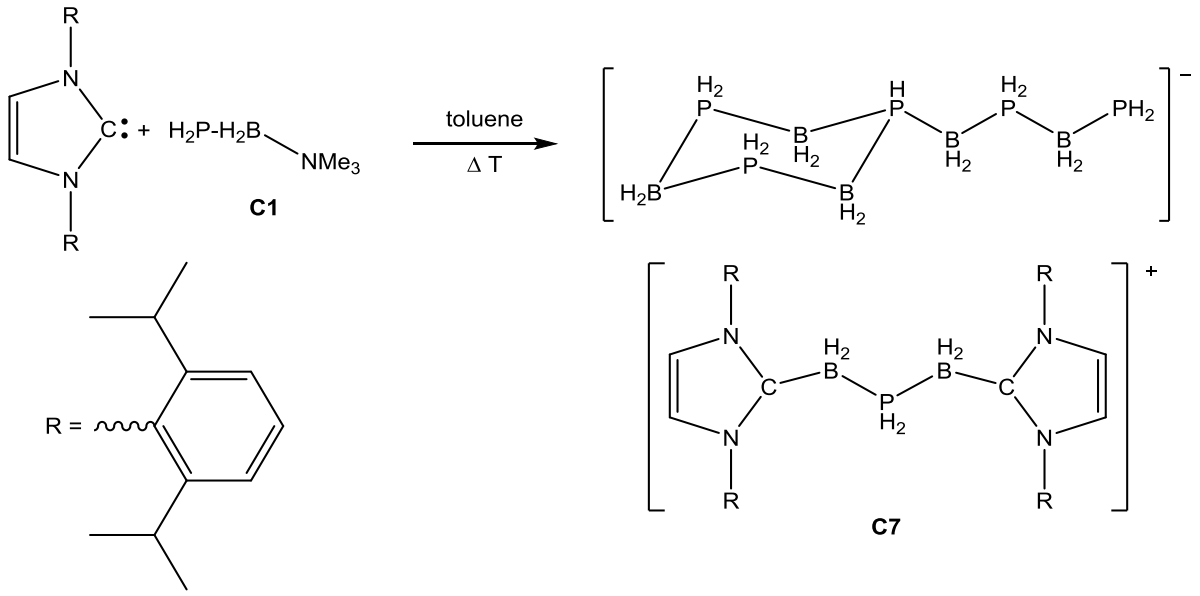

Scheme 7.2. Synthesis of **C7**.

The results show that the parent phosphanylborane (**C1**) and arsanylborane (**C2**) are valuable starting materials for the generation of mixed anionic group 13/15 chain like compounds. For the first time a rational synthetic approach was achieved for 3- and 5-membered chain like compounds, which could be structurally characterized. Furthermore, the first examples of parent compounds of anionic pnictogenylborane derivatives **C3**-**C6** have been synthesized. Overall, this unique class of compounds can be seen as stable intermediates representing the nucleophilic attack at the boron of the head-to-tail polymerization of unsaturated group 13/15 adducts. Furthermore, they represent promising starting materials for the preparation of extended mixed group 13/15 element chain compounds, cycles and polymers.

7.2 Coordination Chemistry of Anionic Pnictogenylborane Derivatives

Since their first synthesis, the chemistry of trimethyl amine stabilized pnictogenylboranes has been investigated in detail. Beside polymerization and oxidation with chalcogens their coordination behavior towards boron centered Lewis acids as well as transition metal fragments has been investigated. Bearing a terminal EH_2 group (E = P, As), these compounds are proven to be suitable candidates serving as complex ligands. The reactions of pnictogenylboranes (**C1**, **C2**) with pnictogenbased nucleophiles lead to the formation of anionic chain like compounds (**C3**-**C6**) bearing two terminal EH_2 groups. Similar approaches with *tert*-butyl substituted pnictogenylboranes (**C8**, **C9**) and pnictogenides of the type Na^{t}BuEH, lead to the corresponding three membered anionic derivatives [Na($C_{12}H_{24}O_6$)][^{t}BuEH-BH_2-^{t}BuEH] (**C10**: E = P, **C11**: E = As; Scheme 7.3) after subsequent addition of equivmolar amounts of 18-crown-6 ($C_{12}H_{24}O_6$).

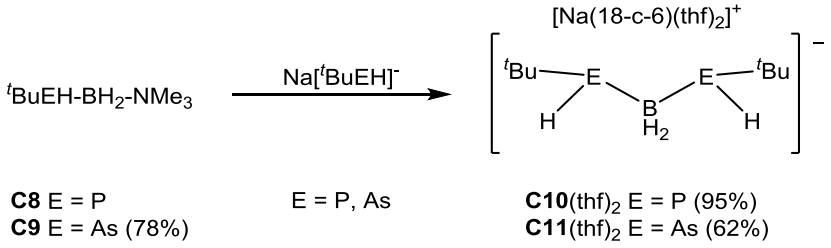

Scheme 7.3. Synthesis of [^{t}BuEH-BH_2-^{t}BuEH]$^-$ (**C10**: E = P, **C11**: E = As). Isolated yields are given in parentheses. 18-c-6 = 18-crown-6 ($C_{12}H_{24}O_6$).

To investigate the coordination behavior of three membered anionic chain like compounds **C3**, **C4**, **C10** and **C11** as well as the five membered derivative **C6** are reacted with [$W(CO)_4$(nbd)] (nbd = bicyclo[2.2.1]hepta-2,5-diene). Under substitution of the nbd ligand the corresponding coordination products are formed, revealing anions with cyclic structural motifs of different ring size. The resulting compounds [Na($C_{12}H_{24}O_6$)][$(CO)_4W(H_2P\text{-}BH_2\text{-}PH_2)$] (**C12**), [Na($C_{12}H_{24}O_6$)][$(CO)_4W(^t$BuPH-$BH_2$-^{t}BuPH)] (**C15**) and [Na($C_{12}H_{24}O_6$)][$(CO)_4W(^t$BuAsH-BH_2-^{t}BuAsH)] (**C16**) bear a four membered heterocycle. Compound [Na($C_{12}H_{24}O_6$)][$(CO)_4W(H_2As\text{-}BH_2\text{-}PH_2\text{-}BH_2\text{-}AsH_2)$] (**C14**) reveal a six membered and ([K($C_{12}H_{24}O_6$)][$(CO)_4W(H_2As\text{-}BH_2\text{-}AsH_2)$])$_2$ (**C13**) an eight membered ring, respectively. In all cases the anionic chain like compounds serve as chelating ligands except of compound **C13** in which the two [$H_2As\text{-}BH_2\text{-}AsH_2$]$^-$ units serve as a linker connecting two $W(CO)_4$ fragments (Scheme 7.4).

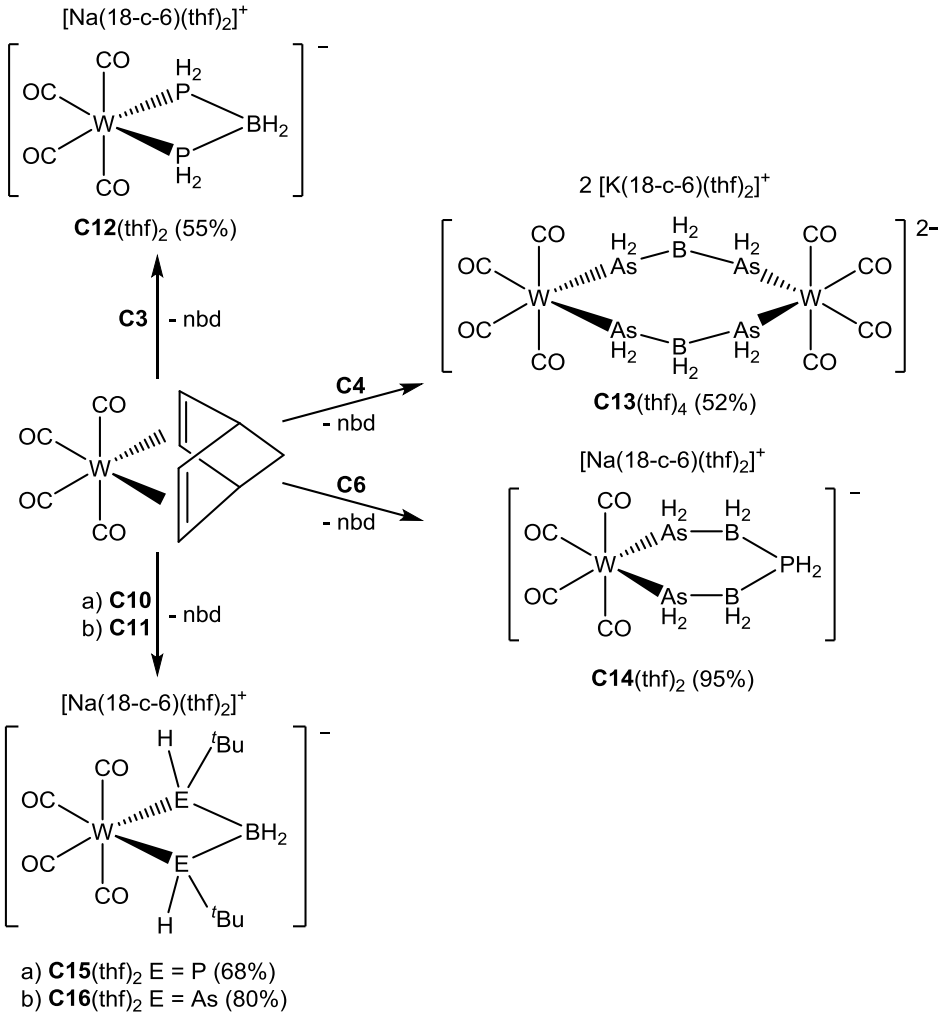

Scheme 7.4. Synthetis of the compounds **C12**-**C16**. Isolated yields are given in parentheses. 18-c-6 = 18-crown-6 ($C_{12}H_{24}O_6$).

Reaction of two equivalents of Na[H_2P-BH_2-PH_2] (**C3**) with one equivalent of [Cu(MeCN)$_4$][BF_4] in THF leads to the coordination product [Cu_2Na_2(thf)$_4$(H_2P-BH_2-PH_2)$_4$] (**C17**). The corresponding derivatives [Cu_2Na_2(thf)$_4$(^{t}BuPH-BH_2-^{t}BuPH)$_4$] (**C19**), [Cu_2Na_2(thf)$_4$(^{t}BuAsH-BH_2-^{t}BuAsH)$_4$] (**C20**) are accessible under analog reactions conditions using Na[^{t}BuPH-BH_2-^{t}BuPH] (**C10**) and Na[^{t}BuAsH-BH_2-^{t}BuAsH] (**C11**) as starting materials (Scheme 7.5).

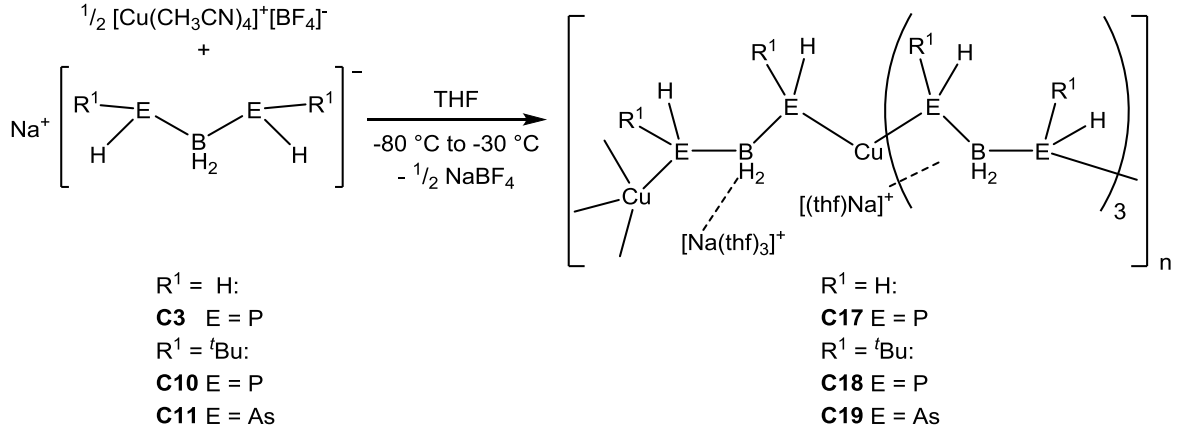

R^1 = H:
C3 E = P
R^1 = ^{t}Bu:
C10 E = P
C11 E = As

R^1 = H:
C17 E = P
R^1 = ^{t}Bu:
C18 E = P
C19 E = As

Scheme 7.5. Reaction of **C3**, **C10** and **C11** with $[Cu(CH_3CN)_4][BF_4]$.

Beside characterization by multinuclear NMR spectroscopy, the compounds **C17**, **C18** and **C19** have been characterized by mass spectrometry. For each compound, a respective peak for a $[Cu_2(L)_3]^-$ fragment (L = anion of compound **C3**, **C10**, **C11**) can be detected. Compound **C17** was additionally characterized by single crystal X-ray diffraction revealing a three dimensional scaffold structure with a distorted adamantane like repeating unit (Scheme 7.6).

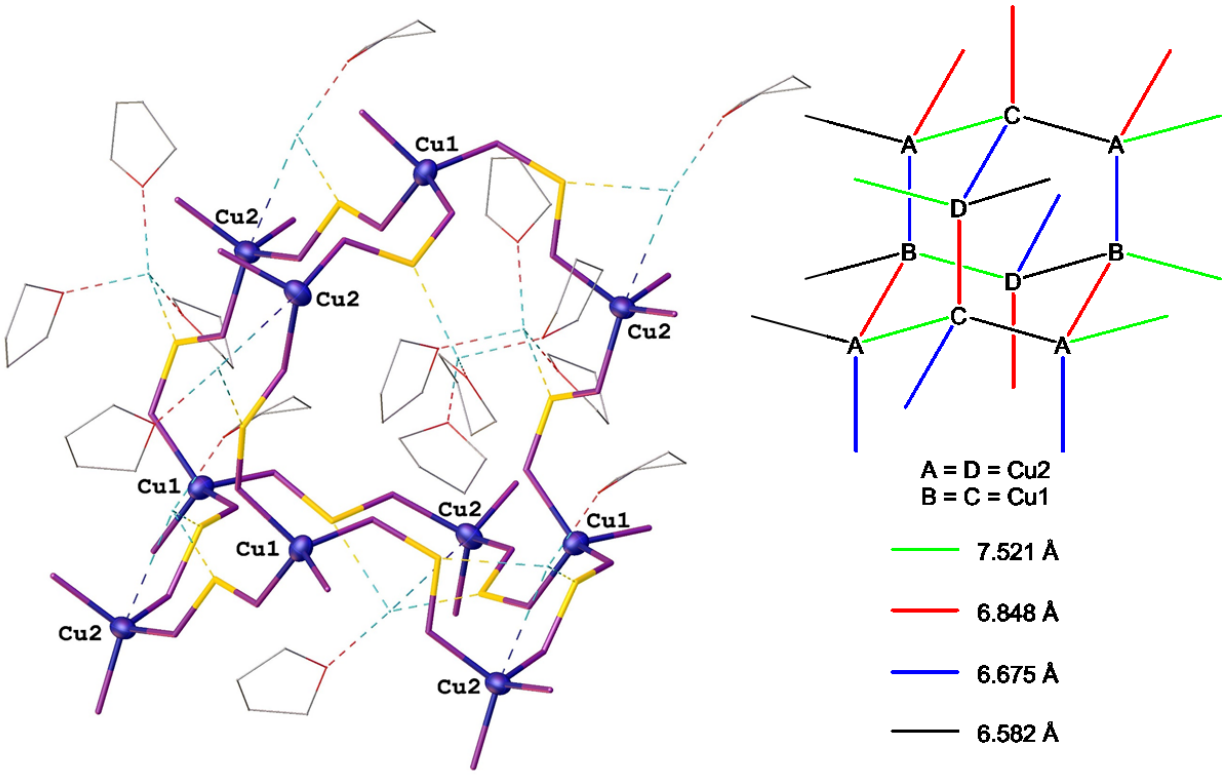

Scheme 7.6. Adamantane like repeating unit with Cu-Cu distances within the three dimensional scaffold of compound **C17**.

The results show that anionic derivatives of the parent as well as the substituted pnictogenylboranes are suitable building blocks in coordination chemistry. They can serve as chelating ligands in transition metal based complexes as well as linkers between copper(I) ions, leading to a novel three dimensional inorganic MOF like scaffold.

7.3 Three and Five Membered Substituted Anionic Derivatives of Parent Pnictogenylboranes

The number of anionic linear substituted 13/15 oligomers is limited to few examples which are solely characterized by NMR spectroscopy. An uncomplicated way to obtain linear three and five membered anionic 13/15 oligomers in good to excellent yields is presented here. The parent anionic chain like compounds $[M(C_{12}H_{24}O_6)][H_2E\text{-}BH_2\text{-}EH_2]$ (**C3**: E = P, M = Na; **C4**: E = As, M = K) are accessible by reacting trimethyl amine stabilized pnictogenylboranes $H_2E\text{-}BH_2\text{-}NMe_3$ (**C1**: E = P; **C2**: E = As) with MEH_2 (E = P, As; M = Na, K). Using substituted pnictogenides of the type Na^{t}BuEH (**C20**: E = P; **C21**: E = As;) (**A**, Scheme 7.7) and $[EPh_2]^-$ (**C22**: E = P; **C23**: E = As) (**C**, Scheme 7.7) instead, leads to the formation of the corresponding anionic organosubstituted asymmetrical pnictogenylborane derivatives $[Na(C_{12}H_{24}O_6)][H_2P\text{-}BH_2\text{-}^t\text{BuPH}]$ (**C24**), $[Na(C_{12}H_{24}O_6)][H_2As\text{-}BH_2\text{-}^t\text{BuAsH}]$ (**C25**), $[Na(C_{12}H_{24}O_6)][H_2P\text{-}BH_2\text{-}^t\text{BuAsH}]$ (**C26**), $[Na(C_{12}H_{24}O_6)][H_2P\text{-}BH_2\text{-}PPh_2]$ (**C28**), $[K(C_{18}H_{36}N_2O_6)][H_2As\text{-}BH_2\text{-}AsPh_2]$ (**C29**), $[Na(C_{18}H_{36}N_2O_6)][H_2As\text{-}BH_2\text{-}PPh_2]$ (**C30**) and $[K(C_{18}H_{36}N_2O_6)][H_2P\text{-}BH_2\text{-}AsPh_2]$ (**C31**) after adding stoichiometric amounts of 18-crown-6 ($C_{12}H_{24}O_6$) (**C24**-**C26**, **C28**) or [2.2.2]cryptand ($C_{18}H_{36}N_2O_6$) (**C29**-**C31**). Compound $Na[H_2As\text{-}BH_2\text{-}^t\text{BuPH}]$ is not accessible via the reaction of Na^{t}BuPH (**C20**) with $H_2As\text{-}BH_2\text{-}NMe_3$ (**C2**). The decompostion of the starting material is observed instead. Using the nucleophile $Na[^t\text{BuPH-}BH_3]$ alternatively to **C20**, the formation of $[Na(C_{12}H_{24}O_6)][H_2As\text{-}BH_2\text{-}^t\text{BuPH-}BH_3]$ (**C27**) can be observed, after addition of equivalent amounts of 18-crown-6 (**B**, Scheme 7.7). The compounds $Na[Ph_2E\text{-}BH_2\text{-}EPh_2]$ (E = P, As) are accessible by salt metathesis reaction of $NaEPh_2$ (**C22**: E = P; **C23**: E = As) with $IBH_2\text{-}SMe_2$ in a two to one stochiometrie. Subsequent addition of stoichiometric amounts of 18-crown-6 leads to the isolable compounds 1,1-Bis(diphenylphosphino)borate (dppb) (**C32**) and 1,1-Bis(diphenylarsino)borate (dpab) (**C33**) (**D**, Scheme 7.7).

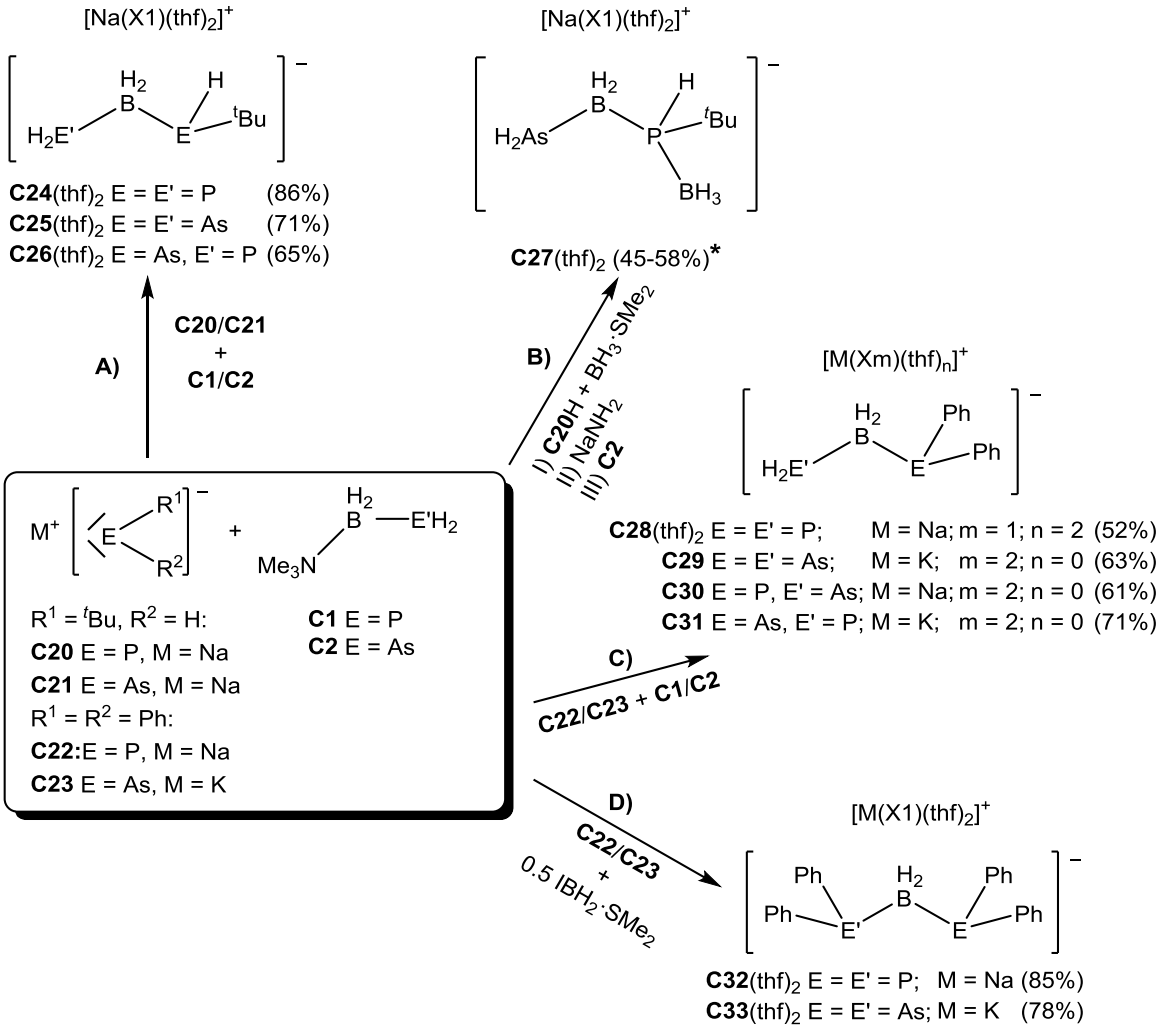

Scheme 7.7. Synthesis of asymmetric (**A**-**C**) and symmetric (**D**) anionic chain like compounds; * variable content of THF. Yields are given in parentheses. X1 = 18-crown-6 ($C_{12}H_{24}O_6$); X2 = [2.2.2]cryptand ($C_{18}H_{36}N_2O_6$).

For compound **C5** an elongation of the pnictogen boron backbone can be achieved by the reaction with equivalent amounts of arsanylborane resulting in compound $[Na(C_{12}H_{24}O_6)][H_2As\text{-}BH_2\text{-}PH_2\text{-}BH_2\text{-}AsH_2]$ (**C6**, Scheme 7.1). Analog reaction with anionic chain like compounds of the type $[M(C_{12}H_{24}O_6)][H_2E\text{-}BH_2\text{-}ER^1R^2]$ (E = P, As; $R^1 = R^2$ = H, Ph; R^1 = H, $R^2 = {}^t$Bu; M = Na, K) only works in selected cases. Using $H_2P\text{-}BH_2\text{-}NMe_3$ (**C1**) as reactant an elongation of the 13/15 backbone only occurs in combination with compound **C28** resulting in the product $[Na(C_{12}H_{24}O_6)][H_2P\text{-}BH_2\text{-}PPh_2\text{-}BH_2\text{-}PH_2]$ (**C34**, Scheme 7.8). Starting from other compounds no formation of desired products can be observed. Further five membered anionic chain like compounds are accessible by the reaction of arsanylborane (**C2**) with compounds **C30**, **C28** and **C24**. The elongation of the 13/15 chain only occur at the terminal substituted phosphorus atoms under formation of $[Na(C_{12}H_{24}O_6)][H_2As\text{-}BH_2\text{-}PPh_2\text{-}BH_2\text{-}AsH_2]$ (**C35**), $[Na(C_{12}H_{24}O_6)][H_2P\text{-}BH_2\text{-}PPh_2\text{-}BH_2\text{-}AsH_2]$ (**C36**) and $[Na(C_{12}H_{24}O_6)][H_2P\text{-}BH_2\text{-}{}^t\text{BuPH}\text{-}BH_2\text{-}AsH_2]$ (**C37**) (Scheme 7.8).

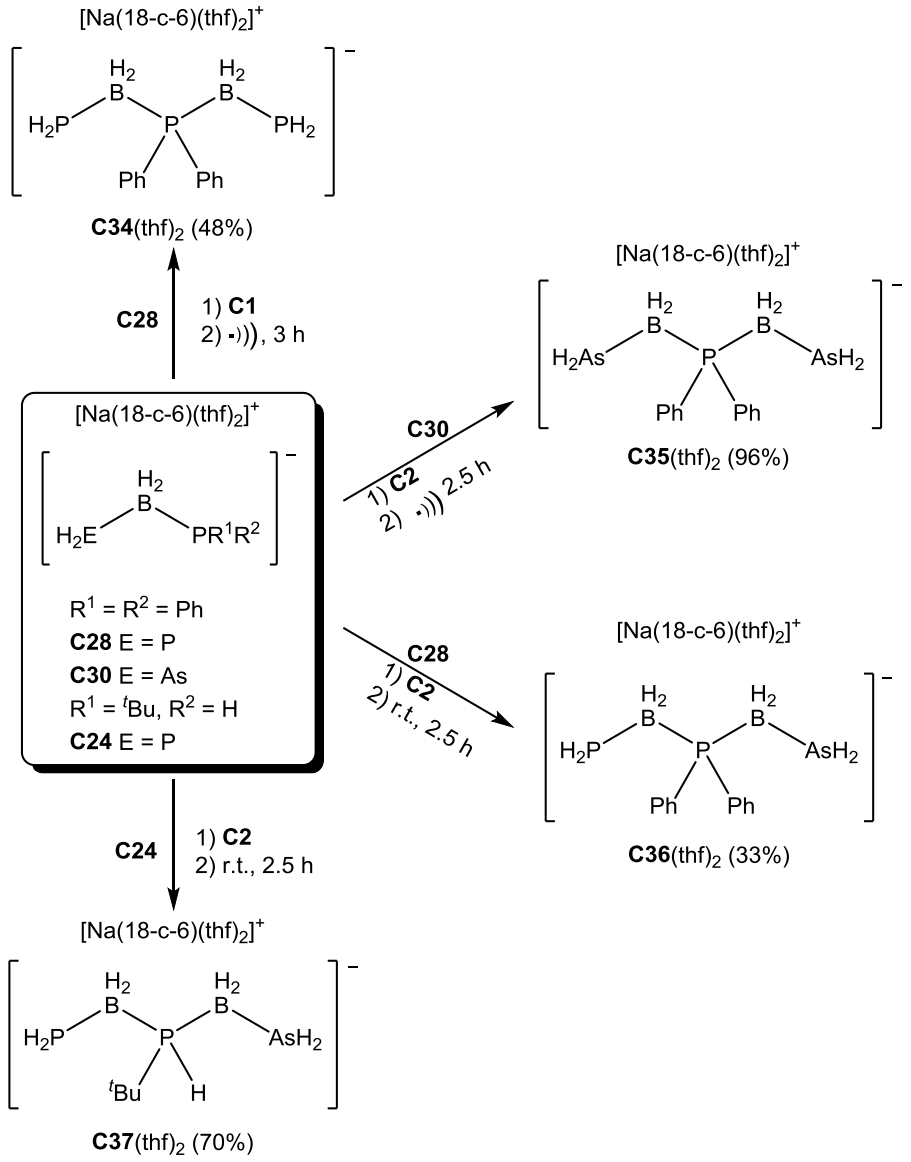

Scheme 7.8. Reaction of substituted three membered chain like compounds with pnictogenylboranes. Isolated yields are given in parentheses. 18-c-6 = 18-crown-6 ($C_{12}H_{24}O_6$).

Beside the three membered asymmetric compounds also the five membered derivatives are interesting substrates for coordination chemistry. Further the presented compounds substantially enlarge the number of linear arsenic containing oligomers bearing a 13/15 backbone. Additionally the synthesis of the first 1,1-Bis(diphenylphosphino)borate (dppb) and 1,1-Bis(diphenylarsino)borate (dpab) is achieved. As isostructural but negatively charged derivatives of dppm (1,1-Bis(diphenylphosphino)methane) and dpam (1,1-Bis(diphenylarsino)methane) they are promising alternatives as complex ligands.

8 Appendices

8.1 List of Abbreviations

∠	angle
‘	arcmin, 1’ = $\frac{1}{60}$ degree
°	degree
18-c-6	18-crown-6, $C_{12}H_{24}O_6$
Å	Angstroem, 1 Å = $1 \cdot 10^{-10}$ meter
BN	boron nitride
btmsa	bis(trimethylsilyl)acetylene
Cp	cyclopentadienyl, C_5H_5
Cy	cyclohexyl, C_6H_{11}
°C	degree Celsius
δ	chemical shift
DFT	density functional theory
dipp	2,6-diisopropylphenyl, $C_{12}H_{18}$
EI MS	electron impact mass spectrometry
ESI MS	electron spray ionization mass spectrometry
Et	ethyl, C_2H_5
e^-	electron, elemental charge
FD MS	field desorption ionization mass spectrometry
FLP	frustrated Lewis pair
h	hour
Hz	Hertz
IR	infrared spectroscopy
^{i}Pr	*iso*-propyl, C_3H_7
K	kelvin
kJ	kilojoule, 1 kJ = $1 \cdot 10^3$ joule
LA	Lewis acid
LB	Lewis base

Me	methyl, CH_3
mg	milligram, 1 mg = $1 \cdot 10^{-3}$ gram
MHz	megahertz, 1 MHz = $1 \cdot 10^{3}$ hertz
ml	milliliter, 1 ml = $1 \cdot 10^{-3}$ liter
mmol	millimol, 1 mmol = $1 \cdot 10^{-3}$ mol
MOF	metal organic framework
Mw	molecular weight
m/z	mass to charge ration
nbd	bicyclo[2.2.1]hepta-2,5-diene, C_7H_8
NHC	N-heterocyclic carbene
nm	nanometer, $1 \cdot 10^{-9}$ meter
NMR	nuclear magnetic resonance
NPA	natural population analysis
Ph	phenyl, C_6H_5
ppm	parts per million
R	organic substitutent
r.t.	room temperature
^{t}Bu	*tert*-butyl, C_4H_9
THF	tetrahydrofuran, C_4H_8O
$\tilde{\nu}$	frequency/ wavenumber
vdW	van der Waals
VE	valence electron
wt-%	mass fraction

br(NMR)	broad
d(NMR)	doublet
J(NMR)	coupling constant
m(NMR)	multiplett
s(NMR)	singulett
t(NMR)	triplett
q(NMR)	quartett

m(IR)	medium
s(IR)	strong
vs(IR)	very strong
vw(IR)	very weak
w(IR)	weak

E^{o}_{0}	reaction energy
H^{o}_{298}	standard reaction enthalpy
G^{o}_{298}	standard Gibbs reaction energy
S^{o}_{298}	standard reaction entropy

8.2 Acknowledgments

Finally I would like to thank…

- Prof. Dr. Manfred Scheer for giving me the opportunity to be part of his working group, enabling researches under excellent working conditions and the possibility to freely develop and pursue my own ideas.
- Dr. Gábor Balázs for the uncountable hours he spended in discussions, giving helpful advices, searching for problem solutions, proof-reading and for his patience and friendliness.
- Prof. Dr. Alexey Timoshkin for many DFT calculations, interesting thinking approaches and his commitment as our goal keeper at ChemCup.
- Dr. Michael Bodensteiner for his kind and informative support during X-ray diffraction analysis, solving crystallographic problems and showing helpful Olex² commands.
- All the employees and co-workers of the Central Analytical Services of the University of Regensburg: X-ray (Dr. Michael Bodensteiner, Sabine Stempfhuber, Katharina Beier), mass spectrometry department (Josef Kiermaier, Wolfgang Söllner), elementary analysis department (Helmut Schüller, Barbara Baumann, Wilhelmina Krutina) and in particular the NMR Department (Dr. Ilya Shenderovich, Anette Schramm, especially Georgine Stühler and Fritz Kastner) for recording countless spectra and satisfying all special requests.
- Our secretary Barbara Bauer, for your kindness, your patience and your steady helpfulness.
- Our technical employees Petra, Martina, Matthias, Schotti, Julian, Barbara and Walter.
- My great current 13/15 lab colleagues Felix and Matthias and already graduated colleagues Jens, Christian and Oliver for a great time, funny discussions and helping each other during depressing periods of daily research work.
- The motivating lunch therapy sessions with Dani, Felix, Claudia, Helena and Maria. You are a decisive reason for the success of this work. I really enjoyed the time I spent with you.
- All present and former members of the Scheer group.
- All my friends and family for your support.
- My great and beloved wife Melli, for your comprehension, your patience, your support and your love during this work (1000 :*)